Techno-Economic and Life Cycle Assessment of Jet Fuel Production through various Fischer-Tropsch Pathways

By:

Maria Fernanda Rojas Michaga

The University of Sheffield

Faculty of Engineering

Department of Mechanical Engineering

A thesis submitted in fulfilment of the requirements for the degree of Doctor of Philosophy.

September 2023

DECLARATION

The candidate confirms that the work submitted is his own and that appropriate credit has been given where reference has been made to the work of others.

RESEARCH OUTPUTS

List of publications:

1. M. F. Rojas-Michaga, S. Michailos, K. J. Hughes, D. Ingham, and M. Pourkashanian, **"Techno-economic and life cycle assessment review of sustainable aviation fuel produced via biomass gasification,"** in Sustainable Biofuels, 2021. doi: 10.1016/b978-0-12-820297-5.00012-8.
2. M. F. Rojas Michaga, S. Michailos, M. Akram, E. Cardozo, K. J. Hughes, D. Ingham, and M. Pourkashanian, **"Bioenergy with carbon capture and storage (BECCS) potential in jet fuel production from forestry residues: A combined Techno-Economic and Life Cycle Assessment approach,"** Energy Convers Manag, vol. 255, no. November 2021, p. 115346, 2022, doi: 10.1016/j.enconman.2022.115346.
3. L. Jiang, W. Liu, R. Q. Wang, A. Gonzalez-diaz, M. F. Rojas-michaga, S. Michailos, M. Pourkashanian, X. J. Zhang, and C. Font-palma, "**Sorption direct air capture with CO_2 utilization,**" Prog Energy Combust Sci, vol. 95, no. January, p. 101069, 2023, doi: 10.1016/j.pecs.2022.101069.
4. M. F. Rojas-Michaga, S. Michailos, E. Cardozo, M. Akram, K. J. Hughes, D. Ingham, and M. Pourkashanian, "**Sustainable aviation fuel (SAF) production through power-to-liquid (PtL): A combined techno-economic and life cycle assessment,**" Energy Convers Manag, vol. 292, p. 117427, Sep. 2023, doi: 10.1016/j.enconman.2023.117427..
5. M. F. Rojas-Michaga, S. Michailos, E. Cardozo, K. J. Hughes, D. Ingham, and M. Pourkashanian, **"A combined techno-economic and environmental assessment of novel Power and Biomass to Liquids (PBtL) configurations with negative emissions for the production of Sustainable Aviation Fuel (SAF),"** Submitted to the Journal Energy Conversion and Management on September 2023.

Poster/presentations in academic events:

1. M. F. Rojas-Michaga, S. Michailos, M. Akram, and M. Pourkashanian. **Demonstration of BECCS for Sustainable Aviation Fuels production (BECCS-4-SAF)**, Supergen Bioenergy Annual Assembly. November 16th, 2020, Online.
2. M. F. Rojas-Michaga, Stavros Michailos, Muhammad Akram, Evelyn Cardozo, Kevin J. Hughes, Derek Ingham, Mohamed Pourkashanian. **BECCS potential in jet fuel production from forestry residues: From a TEA and LCA approach**, Supergen Bioenergy Hub SHARE Lecture Series: Seminar 2. June 15th, 2021, Online

3. M. F. Rojas-Michaga, S. Michailos, K. J. Hughes, Derek Ingham, and M. Pourkashanian. **Techno-Economic and Life Cycle Assessment of jet fuel production through various Fischer-Tropsch pathways**. MEC PhD Students Poster Presentations. June, 2021, Online.
4. M. F. Rojas-Michaga, S. Michailos, K. J. Hughes, Derek Ingham, and M. Pourkashanian. **BECCS-To-SAF/H2**, Optionality and Flexibility. IDRIC, MIP session. April 28th, 2022.
5. M. F. Rojas-Michaga, S. Michailos, E. Cardozo, M. Akram, K. J. Hughes, D. Ingham, and M. Pourkashanian, **"Sustainable aviation fuel (SAF) production through power-to-liquid (PtL): A combined techno-economic and life cycle assessment"**. Postgraduates Sheffield poster presentation Sheffield, UK. June, 2023.
6. M. F. Rojas-Michaga, S. Michailos, E. Cardozo, M. Akram, K. J. Hughes, D. Ingham, and M. Pourkashanian, **"Sustainable aviation fuel (SAF) production through power-to-liquid (PtL): A combined techno-economic and life cycle assessment"**. 20th International Conference on Carbon Dioxide Utilization. Bari, Italy. June, 2023.
7. M. F. Rojas-Michaga, S. Michailos, E. Cardozo, M. Akram, K. J. Hughes, D. Ingham, and M. Pourkashanian, **"Sustainable aviation fuel (SAF) production through power-to-liquid (PtL): A combined techno-economic and life cycle assessment"**. 2nd Feria Conference. Sheffield, UK. September, 2023.

ACKNOWLEDGEMENTS

First and foremost, I would like to express my heartfelt gratitude to the Almighty God for granting me the strength and resilience to reach this significant milestone despite the numerous challenges encountered along the way.

Special thanks are due to my supervisors Prof. Mohamed Pourkashanian, Prof. Derek Ingham, Dr. Stavros Michailos, and Dr. Kevin J. Hughes. Their guidance and assistance were instrumental in making this journey a reality. I particularly want to single out Dr. Stavros for his constant support; he has not only been a supervisor but also a true friend.

I extend my deepest gratitude to my parents for their unconditional love and support, and the sacrifices they made, without which none of this would have been possible. I also wish to thank my friends and family in Bolivia, whose prayers and good wishes have been a constant source of encouragement.

I am immensely grateful to my colleagues in the Energy 2050 group. Their support, countless conversations, tea time, and camaraderie in the office have made this experience truly memorable. To all my friends in Sheffield and the individuals I have met along this path, who have imparted invaluable lessons and offered support, I offer my heartfelt thanks.

I would like to express my gratitude to the Ministry of Education of Bolivia for their financial support, without which this experience would not have been possible.

Thank you all for being a part of this significant chapter in my life. Your contributions and support have played an indispensable role in my journey.

ABSTRACT

The activity of the aviation sector accounts for at least 2% of the worldwide anthropogenic Green-House-Gas (GHG) emissions, while in the UK it represents 7%. Several practises have been proposed in order to diminish these emissions, among them, the use of sustainable aviation fuels (SAF) appears to be the most relevant global warming mitigation strategy for the aviation industry. However, the choice of feedstock and conversion technology have a direct impact on the economic, and environmental performance of the SAF. There is a great variety of processes for the production of SAF, from which the Fischer-Tropsch (FT) technology has achieved high maturity. Despite its level of development, the production and use of SAF will not be fully deployed until technical, economic and environmental constraints are properly addressed.

An extensive and critical literature review of techno-economic assessment (TEA) and/or life cycle assessment (LCA) studies for FT-derived SAF identified some important research gaps. Although some studies evaluated the production of SAF, there exists a lack of combined TEA and LCA approach. Furthermore, most of these studies did not include the synthetic crude oil processing steps within the boundaries of the system, which results in different economic and environmental estimates. Additionally, this is the first study to include CCS for the production of SAF. Consequently, to tackle the techno-economic and environmental uncertainties, this project aimed at evaluating the production of SAF through three scenarios based on the FT pathway, with different feedstocks and/or process configurations: i) Biomass to liquids, with and without carbon capture and storage (CCS); ii) Power to Liquids; iii) Power and Biomass to Liquids without and with CCS. For each scenario, detailed Aspen Plus process models and deterministic and probabilistic TEA and LCA estimated technical, economic and environmental indicators. Additionally, this study also included an evaluation of the effect of the "UK SAF mandate" on the SAF's economic feasibility, making it the first study to apply this policy.

The results suggest that, regardless the scenario, the minimum jet fuel selling price (MJSP) of the SAF produced through the investigated processes cannot break even the gate price of the fossil jet fuel. Each pathway could achieve significant cost reductions through the reduction of CAPEX and/or lower feedstock and energy costs. The estimated global warming potential (GWP) demonstrated considerable emissions reductions for all scenarios when compared to fossil jet fuel, and even negative emissions were obtained for the scenarios with CCS. The water footprint, on the other hand, reflected larger water consumptions than those required for the production of conventional jet fuel. Given that policies such as the SAF mandate is a function of the GWP, the produced SAFs could benefit from economic incentives that could boost their economic feasibility and aid their MJSPs to break even on the fossil jet fuel gate price.

NOMENCLATURE

AACE	Association for the Advancement of Cost Engineering
AC	Alternating Current
AE	Alkaline Electrolyser
AEA	Aspen Energy Analyzer
ar	As received
ASTM	American Standard for Testing and Materials
ASF	Anderson-Schulz-Flory
ASU	Air Separation Unit
ATAG	Air Transport Action Group
ATJ	Alcohol-to-Jet fuel
ATR	Auto Thermal Reformer
BECCS	Bioenergy with Carbon Capture and Storage
Bio-GtL	Biogas to liquids
BoL	Begin of Life
BP	British Petroleum
BtL	Biomass-to-Liquid
CAAFI	Commercial Aviation Alternative Fuels Initiative
CAPEX	Capital Expenditures
CCS	Carbon Capture and Storage
CCU	Carbon capture and utilisation
CDR	Carbon Dioxide Removal
CEPCI	Chemical Engineering Plant Cost Index
CFD	Computational Fluid Dynamics
CH_4	Methane
CHP	Combined Heat and Power
CO	Carbon monoxide
Co	Cobalt
CO_2	Carbon Dioxide
CO_{2eq}	Carbon dioxide equivalent
Cr	Chromium
DAC	Direct Air Capture
db	Dry basis
DC	Direct Current
DCFA	Discounted Cash Flow Analysis
DFBG	Dual Fluidised Bed Gasifier
EDF	Électricité de France
EFTA	European Free Trade Association
FCI	Fixed Capital Investment
Fe	Iron
FOM	Fixed Operating and Maintenance costs
FR	Forest residues
FRL	Fuel Readiness Level
FT	Fischer-Tropsch
GAB	Guggenheim–Anderson–de Boer
GB	Great Britain

GHG	Green-House-Gas
GTG	Gate-to-Gate
GWP	Global Warming Potential
Gt	Giga tonnes
H_2	Hydrogen
H_2O	Water
HEFA	Hydro processed Fatty Acid Esters and Free Fatty Acids
HFS	Hydroprocessing of Fermented Sugars
HHV	High Heating Value
HP	High Pressure
HT	High temperature
HTFT	High temperature Fischer-Tropsch
HYD	Hydrocracker
IATA	International Air Transport Association
IC	Indirect Cost
ICAO	International Civil Aviation Organization
IDC	Installed direct costs
IEA	International Energy Agency
IPCC	Intergovernmental Panel on Climate Change
IRR	Internal rate of return
ISO	International Organization for Standardization
kJ	kilojoules
KPI	Key performance indicator
LCA	Life Cycle Assessment
LCI	Life Cycle Inventory
LCOE	Levelised cost of Electricity
LHV	Low Heating Value
LP	Low Pressure
LT	Low temperature
LTFT	Low Temperature Fischer-Tropsch
LUC	Land use change
MD	Medium Distillates
MEA	Methyl Ethyl Amine
MJ	Mega-joules
MJel	Megajoules of electricity
MJSP	Minimum Jet Fuel Selling Price
MJth	Megajoules of thermal energy
MM	Millions
MM£	Millions of pounds
MP	Medium Pressure
MSW	Municipal solid waste
Mt	Millions of metric tonnes
Ni	Nickel
NIDC	Non-installed direct costs
NOx	Nitrogen oxides
NPC	Net Present Cost
NPV	Net Present Value

NREL	National Renewable Energy Laboratory
NRMM	Non-road mobile machinery
O_2	Oxygen
OPEX	Operating Expenses
PBtL	Power-and-Biomass to liquids
PEC	Purchase Equipment Cost
PEM	Proton Exchange Membrane
PFR	Plug Flow Reactor
PM	Particulate Matter
PSA	Pressure Swing Adsorption
PSD	Particle Size Distribution
PtL	Power-to-Liquids
PTX	Power to any chemical compound
PV	Photovoltaic
RDF	Refuse derived fuel
RED II	Renewable Energy Directive II
RFS	Renewable Fuels Standard
RH	Relative Humidity
RKS-BM	Redlich Kwong Soave Boston Mathias
RoW	Rest of the World
RTFO	Renewable Fuel Transport Obligation
Ru	Ruthenium
RWGS	Reverse Water Gas Shift
SAF	Sustainable aviation fuels
SAM	System Advisor Model
SNG	Synthetic Natural Gas
SOEC	Solid Oxide Electrolysis Cell
SOx	Sulphur oxides
SPK	Synthetic Paraffinic Kerosene
STR	Stirred Tank Reactor
Syngas	Synthetic gas
T&S	Transport and storage
TCI	Total capital investment
TCR	Total Capital Requirement
TDC	Total Direct Costs
TDS	Total dissolved solids
TEA	Techno-economic Assessment
TIC	Total Installation Cost
TRL	Technology Readiness Level
UNFCC	United Nations Framework Convention on Climate Change
VC	Variable Operating Costs
VTSA	Vacuum and Temperature Swing Adsorption
w/w	Weight to weight
WC	Working Capital
WGS	Water Gas Shift
WT	Wind Turbine
WtWa	Well-to-Wake

CONTENTS

LIST OF FIGURES

LIST OF TABLES

1. INTRODUCTION

This introductory chapter seeks to provide a comprehensive overview of the various aspects that have motivated the selection of the research topic for this thesis. At the same time, it outlines the objectives to be completed in this research in order to address the research gaps identified in Chapter 2. This chapter begins by providing an overview of the aviation industry and its contribution to global warming. Following, there is a summary of the global and UK-specific decarbonisation strategies for the aviation sector. The subsequent sections focus on different aspects of sustainable aviation fuels, including production technologies and their level of development, feedstock, and an overview of production and deployment limitations. Concluding this chapter, the purpose and specific objectives of this work are presented, while also outlining how this thesis is structured in the following chapters.

1.1 Overview of the aviation sector

The development of the aviation industry has brought significant benefits since it offers the fastest interconnected network worldwide, which is a key factor for the development of business and tourism globally [1]. Nevertheless, the constant growth of air travel has raised awareness about several inherent environmental impacts, such as the rise of aviation GHG emissions, discomfort from aircraft noise, and concern for local air quality [2], [3]. Aviation emissions mostly originate from the combustion of jet fuel within the aircraft engines and are mainly composed of carbon dioxide (CO_2) (around 70%) and water vapour (H_2O) (around 30%); additionally, minor constituents are also produced (less than 1%), such as nitrogen oxides (NO_X), sulphur oxides (SO_X), unburned hydrocarbons, carbon monoxide (CO) and particulate matter [3], [4]. CO_2 emissions accumulate in the atmosphere for hundreds to thousands of years, thereby increasing its CO_2 concentration and causing global temperature to increase [5].

In 2019, aviation activities were responsible for the release of 1.2 Gt CO_{2eq}, which represented around 2% of the anthropogenic GHG emissions [1], [6], and 3.5% of the anthropogenic climate impact (radiative forcing) [7]. Based on the departure location, the three countries accounting for the largest CO_2 emissions from transport of passengers in 2019 were the United States (US) with 23% of the total, followed by China and the United Kingdom (UK) with 13% and 4.1%, respectively [6]. Furthermore, of the total emissions registered within the UK, 95% were attributed to international aviation [6]. Figure 1-1 illustrates the yearly evolution of the GHG emissions from the UK's international aviation, highlighting the peak in 2019 prior to the COVID-19 pandemic [8]. Predictions indicate that air travel could return to pre-pandemic demand levels by 2024; however, if mitigation actions were not implemented, aviation could be responsible for 22% of the global GHG emissions by 2050 [7].

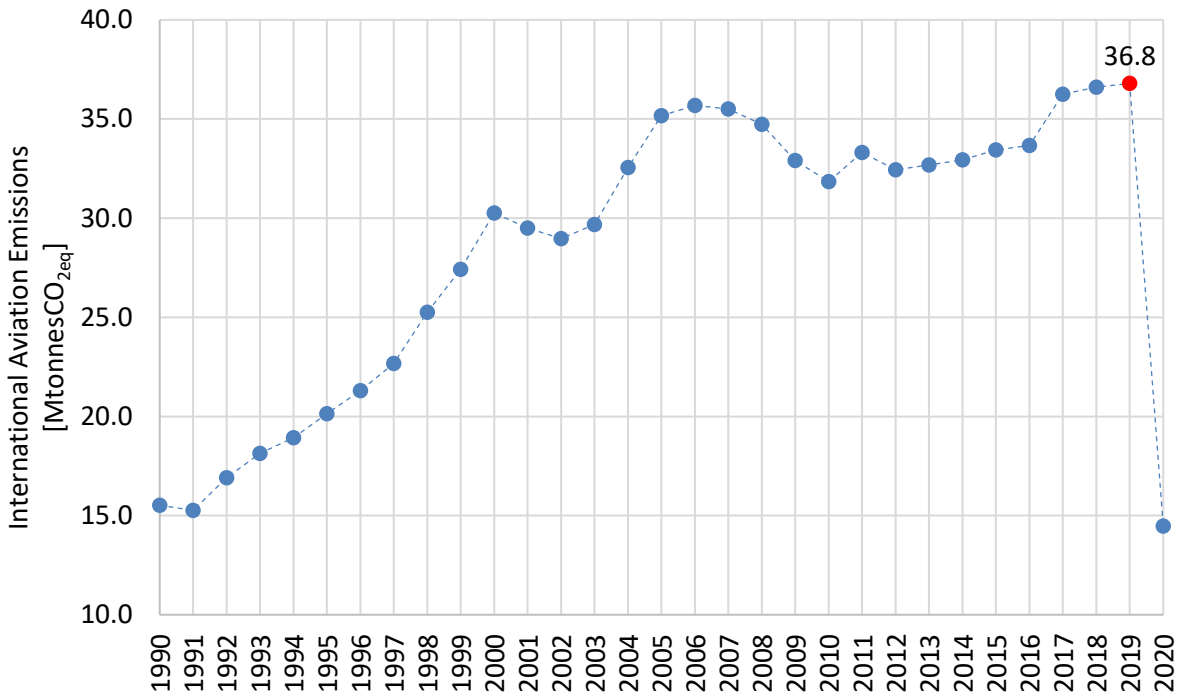

Figure 1-1: Green-House-Gas emissions from international aviation (UK) [8]**.**

1.2 Reduction of aviation GHG emissions in the aviation sector

The Paris Agreement of 2015 outlined the actions that countries needed to undertake in order to tackle climate change together and achieve net-zero GHG emissions by 2050 [4]. However, this agreement does not specifically mention international aviation emissions, since national borders do not enclose them. For this reason, in the course of the last decades, the aviation sector has set its own targets for the reduction of its GHG emissions. The 66th IATA annual general meeting held in 2010 established three ambitious targets; among them, the most important was the reduction in net aviation emissions of 50% of the value registered in 2005 by 2050 [9]. However, in order to align with the Paris Agreement, the 77th IATA meeting of 2020 decided to strengthen their previous target of achieving a net-zero aviation industry by 2050 [10].

Figure 1-2 depicts the emissions reduction roadmap for CO_2 mitigation strategies to achieve the IATA's target. This will require the adoption of various actions, which, in order of relevance, are: 1) the development and use of SAF; 2) offsets and carbon capture; 3) the development of new technologies (electric and hydrogen-powered aircraft); and 4) the improvement of infrastructure and operational efficiencies [11] as shown in Figure 1-3. Evidently, considerable CO_2 emissions reductions could be achieved by the replacement of fossil fuels by SAF [9]. However, SAF alone cannot be sufficient to completely eliminate GHG emissions since the past LCA estimated that the GWP of SAF is lower than

that of fossil jet fuel but still positive. Therefore, carbon offsets and CCS become relevant to compensate for residual emissions that might still exist after the deployment of SAF [11].

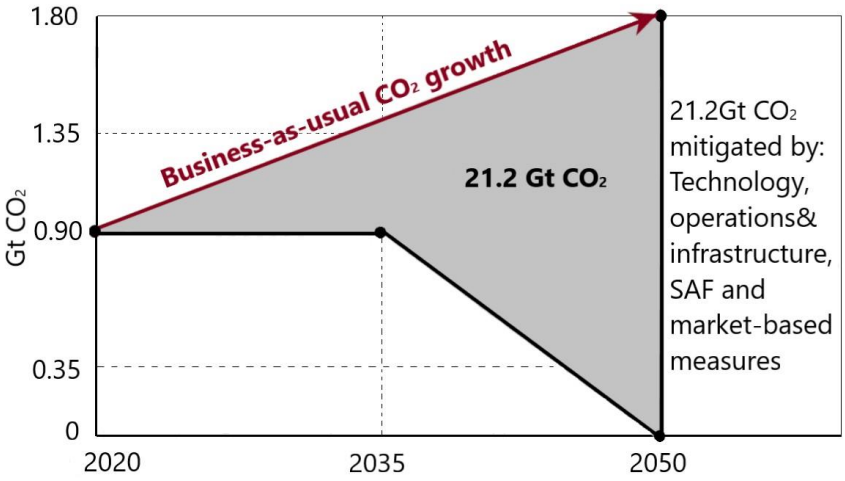

Figure 1-2: Emissions reduction roadmap ('No-action' scenario and emissions reduction strategies set by the aviation industry) [12].

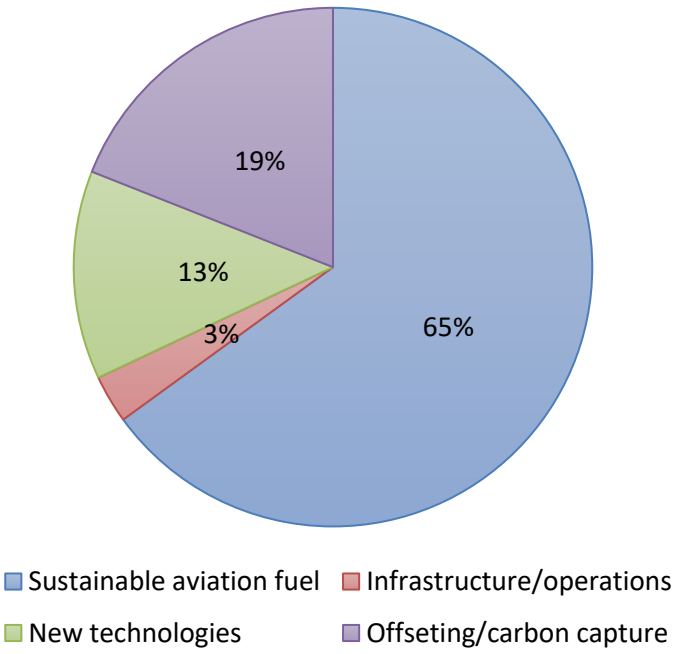

Figure 1-3: Contribution of mitigation actions to net-zero in 2050 [12].

1.3 UK SAF mandate

Individual commitment and actions undertaken by airlines are not sufficient to achieve the environmental targets set by the aviation industry. Therefore, it is necessary that governments outline

standalone aviation emissions reduction goals that are in line with the Paris agreement, while also putting in place robust policies that not only support the development of innovative technologies for SAF production but also provide economic incentives for producers [13]. In 2019, the UK government set a stringent target to achieve carbon neutrality by 2050 [14]. Consequently, within the aviation sector, the UK has also set its own objectives to provide significant and cost-effective support in reducing GHG emissions, aligning with different institutions such as ICAO, the United Nations, and the European Union [15]. The government recognised SAF as a key technology and therefore included it in the UK renewable transport fuel obligation [16]. Later on, it was identified the need for a dedicated policy that accelerates SAF demand and provides incentives to the producers, thereby making SAF production profitable [17].

The SAF mandate is currently under formulation and will be finalised and implemented by 2025 [18]. To accomplish carbon neutrality in the aviation sector by 2050, the Jet Zero Strategy was launched by the UK government. One of the proposed action plans within this strategy is to replace 10% of fossil jet fuel use by 2030 with the intention of achieving a 50% SAF uptake by 2050 [19]. Within the SAF mandate, SAF is defined as a drop-in fuel that could be used in existing aircraft without modification while exhibiting a 50% reduction in the life cycle emissions of conventional jet fuel. Furthermore, these SAFs must be obtained from sustainable feedstocks that are non-competitive with human consumption and that do not create deforestation [17], [19], [20]. The last statement translates into the use of all kinds of waste, residues, and low-carbon footprint energy. The economic support offered by the SAF mandate could benefit SAF producers through a scheme of tradable certificates that will have a monetary value. The value of these certificates will be determined by the market in order to close the gap between SAF and jet fuel prices [23].

1.4 Sustainable aviation fuels (SAF): Potentials and barriers

Much effort was employed during the last decade for the development of SAF coming from bio-based feedstocks with low carbon intensity since they are expected to reduce the environmental impact of the aviation sector [3]. There is not an agreed definition for SAF; however, according to the European Environmental Agency, SAF are “bio-based aviation fuels that reduce GHG emissions relative to conventional aviation fuel while avoiding other adverse sustainability impacts” [3]. “Biofuel” is the term used to refer to fuels of biological origin, such as biomass. However, the evolution of conversion technologies has allowed the use of other types of feedstock, such as waste and other renewable sources. In this sense, the use of the term SAF is more convenient since it refers to the entire range of fuels with a renewable origin [21]. These fuels must be “drop-in fuels”, because their use should not imply any change in engine or aircraft configuration or airport fuel distribution system [22], [23].

In the current context, the use of SAF is uneconomical for airlines; if aviation companies used them regularly, they would double their present-day fuel expenses [22]. As a result, the main challenge to the development of SAF is ensuring an ample production volume at a price that can compete with regional fossil fuel pricing [4]. The production cost of SAF is directly linked to various factors, including feedstock price, feedstock availability and composition, electricity price, capital investments, feedstock conversion efficiency, operating charges, and quality and composition of the final product, among others [24]. Evidently, the gap between the price of conventional aviation fuel and that of SAF is substantial, leading to low market demand. As a consequence, the allocation of investments towards the scale-up of SAF production facilities or the construction of new ones is limited, which sustains an elevated production cost [2], [3]. Another factor holding back large-scale production is low biomass availability, particularly in the context of biogenic SAF [24]; nevertheless, there are other production pathways that are not restricted by feedstock availability, such as the power-to-liquids technology, which, on the other hand, depends on the provision of substantial amounts of renewable electricity [25]. Therefore, having a handful of SAF production options could potentially fulfil the target of replacing a significant portion of the fossil jet fuel demand [7].

1.5 SAF production technologies

Given that aviation is a worldwide trade, the compatibility of SAF is an important characteristic. This means that airlines should be able to supply their fuel needs at any international airport and expect their aircraft fleet to operate normally [4]. In this sense, different certifications have been established to guarantee the quality of the new SAFs and their production processes. The “Technology Readiness Level” (TRL) is a certification with a scale ranging from 1 to 9, to establish the maturity of the fuel production technology, while the Fuel Readiness Level (FRL) is used to specify the level of development of different conversion pathways with a scale that also ranges from 1 to 9 [3].

Furthermore, the American Society for Testing and Materials (ASTM) has developed the standard ASTM D-7566 to certify that synthetic kerosene produced through various SAF pathways can be blended with fossil jet fuel in order to produce a fuel that can be safely used in airplanes. Up to the writing of this thesis, nine technologies were certified by this standard. These technologies are listed in Table 1-1, along with their maturity level (TRL and FRL levels), required feedstocks, and synthetic kerosene blending limits. Among these processes, HEFA-SPK and co-processing have achieved technological maturity at the commercial level. Besides these pathways, ATJ and FT-SPK are recently attracting the interest of the industry, which is reflected in the investment towards the construction of first-of-a-kind commercial plants based on these technologies [26].

Table 1-1: SAF production processes certified by ASTM D 7566 [3], [13], [21], [27], [28].

SAF production process	TRL	FRL	Feedstock	Blending Limit
Fischer-Tropsch Synthetic Paraffinic Kerosene (FT-SPK)	7-8	7	Biomass (forestry residues, grasses, municipal solid waste)	50%
Fischer-Tropsch Synthetic Paraffinic Kerosene with Aromatics (FT-SPK/A)	6-7	7	Biomass (forestry residues, grasses, municipal solid waste)	50%
Hydroprocessed Esters & Fatty Acids-Synthetic Paraffinic Kerosene (HEFA-SPK)	9	9	Oil-bearing biomass (e.g. algae, jatropha, camelina, carinata)	50%
Hydroprocessed Esters & Fatty Acids-Synthetic Paraffinic Kerosene from algae (HEFA-SPK)	5	-	Microalgae oils	10%
Hydroprocessing of Fermented Sugars-Synthetic Iso-Paraffinic Kerosene (SIP)	7-8	5-7	Microbial conversion of sugars to hydrocarbons	10%
Alcohol-to-Jet Synthetic Paraffinic Kerosene (ATJ-SPK)	7-8	7	Agricultural wastes products (stover grasses, forestry slash, crop straws)	50%
Co-processing biocrude up to 5% by volume of lipidic feedstock in petroleum refinery processes	7-8	6-7	Oil-bearing biomass (e.g. algae, jatropha, camelina, carinata)	5% (refinery input)
Catalytic Hydrothermolysis Jet (CHJ)	6	-	Vegetable and animal fat	50%
FOG Co-processing	-	-	Fat, oils, and greases	FOG (up to 5%)

Fuels derived from sources such as starch, sugar, animal fats, and vegetable oil are known as first-generation biofuels. Nowadays, around 85% of SAF is produced through the HEFA process, which uses oleo-chemical feedstocks, including animal fats, used cooking oil, or vegetable oil [13]. Nonetheless, various factors such as price, availability, and sustainability restrict an increase in their production and use. At the same time, the food versus fuel conflict is heightened since some of the aforementioned raw materials could be used at the same time as food [9], [29]. Alternatively, lignocellulosic biomass is regarded as a potential feedstock. Its utilisation for biogas or bio-oil does not compromise the world's nourishment supply since lignocellulosic biomass is not part of the human food chain [30].

After coal and oil, biomass is ranked as the third most abundant energy source [31]. Besides being used as a source of energy, its utilisation as a gasification feedstock has gained attention [32]. Because lignocellulosic and cellulosic feedstocks are cheap and abundant, they have the potential to produce sustainable fuels at a low cost [4], [29], [33]. Lignocellulosic material is converted into second-generation sustainable fuels through thermochemical processes, mainly via gasification coupled to a FT unit, which emerges as a promising and high-performance synthesis process to turn syngas into hydrocarbons [34]–[36].

The use of biomass has promising benefits such as sustainability, reduction of greenhouse gas emissions, stable energy supply, and regional, economic, and social development, in a context where stringent regulations and policies are trying to modify the current energy matrix [31]. Biomass derives from different sources, which include plants and plant-derived materials. They can be grouped into two main categories: waste and virgin biomass. Municipal waste, sewage, human and animal wastes, landfill-derived gases, and agricultural wastes are categorised as wastes. On the other hand, virgin biomass includes crops and vegetables, mainly containing carbohydrates, and wood, plants, and leaves, which are the main source of lignocellulose [30].

The pathway, called "Power-to-Liquids" (PtL), appears as a long-term alternative to achieve the aviation targets of GHG emissions reduction [37]. PtL is a process that converts hydrogen (H_2), usually obtained from water electrolysis, and carbon dioxide into liquid fuels. Several pathways are included under this denomination; however, the most important processes are Fischer-Tropsch and methanol synthesis and conversion [38]. Combining renewable electricity and carbon dioxide capture may lead to the production of low-carbon emissions fuels. Another great advantage is that water and land demand for PtL are much lower than for biofuels [37], [38]. Furthermore, the combination of the PtL and BtL pathways could result in a process that concurrently enhances the BtL production capacity and the PtL economic performance while also providing a fuel with emissions reduction potential [39].

1.6 Research aim and objectives of the thesis

The motivation of this work arises from the importance of the development of SAF for the aviation industry as a response to emissions reduction targets. Although some techno-economic and environmental assessments of SAF production have been found in the literature, they are either solely TEA or LCA evaluations. Combined TEA and LCA evaluations provide the opportunity for systematic exploration of technical, economic, and environmental performance indicators while identifying relationships and trade-offs among them [40]. Based on the absence of this type of holistic study, the aim of this thesis is to use this combined TEA and LCA approach for assessing various FT-based configurations for the production of SAF. This technology was chosen due to its level of development and its flexibility in treating various carbonaceous feedstocks. In this sense, the thesis is divided into three main sections. The first part evaluates the production of SAF from a BtL configuration with and without CCS. The second main section is focused on the PtL pathway, while the third section analyses the hybrid PBtL process with and without CCS. To achieve the main goal of this research, the following specific objectives are proposed:

1. Create detailed models representing SAF production from the BtL, PtL, and PBtL processes, based on the Fischer-Tropsch synthesis, in Aspen Plus® and Matlab softwares.
2. Determine relevant mass and energy efficiency indicators based on the mass and energy balances obtained from the process modelling.
3. Develop deterministic techno-economic assessments for each case study for the estimation of important economic indicators, such as the minimum jet fuel selling price (MJSP), the CAPEX, and the OPEX. Additionally, apply a probabilistic approach for the estimation of the uncertainty of the MJSP.
4. Perform deterministic life cycle assessments to estimate various environmental impacts, and develop a probabilistic estimation of the global warming potential (GWP) for each scenario.
5. Evaluate the difference between the economic and environmental performances of the analysed SAF and conventional fossil jet fuel.
6. Create a reliable database of economic and environmental metrics that can support decision-making and policy elaboration.
7. Assess the impact of the UK SAF mandate on the final performance of the produced SAF for the different scenarios.

1.7 Thesis structure

This thesis is organised into seven chapters and is structured as follows:

Chapter 1 provides an introduction that describes the importance of the study, the motivation behind the selection of the research topic, and the main aim and objectives of the research. Additionally, it provides a brief overview of the thesis structure.

Chapter 2 explains the essential concepts necessary for a better understanding of the evaluated scenarios. These technical concepts are related to the various operating units of the proposed process configuration. Further, the chapter devolves to the critical discussion of the existing techno-economic and environmental studies found in the literature, which are based on the proposed processes. Finally, the chapter outlines the identified research gaps and emphasises the importance of the study.

Chapter 3 explains the approach applied for the development of the process models as well as for the economic and environmental assessments. Considering the common nature of the evaluations, the methodology explained in this chapter is the one applied for the evaluation of the three BtL, PtL, and

PBtL configurations. When more specific methods were used, this methodology was described in their corresponding research chapters.

Chapter 4 presents the outcomes of the evaluation of the BtL scenario that was assessed in the publication authored from this research and named "Bioenergy with carbon capture and storage (BECCS) potential in jet fuel production from forestry residues: A combined Techno-Economic and Life Cycle Assessment approach". This chapter explores the techno-economic and environmental performance of the BtL-CCS scenario for the production of SAF and outlines the impact of adding CCS to the technical, economic, and environmental performance of a normal BtL scenario. Furthermore, this chapter explores the effect of policies that provide economic incentives to the SAF based on the estimated GWP.

Chapter 5 presents the outcomes of the evaluation of a PtL configuration that consists of a Direct Air Capture unit and an alkaline electrolyser for the supply of CO_2 and H_2, respectively. These outcomes are presented in the author's publication entitled "Sustainable aviation fuel (SAF) production through power-to-liquid (PtL): A combined techno-economic and life cycle assessment". The study focuses on the development of a process that is integrated in order to reduce water and energy requirements. Furthermore, an off-shore wind farm is designed for the supply of power to the system. This chapter explores the techno-economic and environmental performance and outlines the influence of electricity sources, H_2, and CO_2 sources on the final performance indicators. Furthermore, the results explore the effect of the proposed UK SAF mandate and the cost of the certificates for the PtL-SAF in order to break even the gate price of conventional jet fuel.

Chapter 6 evaluates Power-and-Biomass-to-SAF with CCS scenarios which are able to achieve negative emissions. The evaluation is presented in the publication "A combined techno-economic and environmental assessment of novel Power and Biomass to Liquids (PBtL) configurations with negative emissions for the production of Sustainable Aviation Fuel (SAF)". The study aims at evaluating the production of PBtL SAF from an integrated economic and environmental perspective. Furthermore, the effect of integrating CCS into this configuration is evaluated. Various scenarios based on the amount of CO_2 sent for storage are assessed. Furthermore, the effect of the UK SAF mandate is evaluated based on the calculated GWPs for each scenario.

Chapter 7 lists the overall conclusions and key findings of the thesis. It also addresses the main limitations and the recommendations for future research. To finalise, the main outcomes of the policy analysis draw some key points that could be useful for the final version of the UK SAF mandate.

2. LITERATURE REVIEW

The imminent consequences of global warming have caused concern in the aviation sector. The reduction of its GHG emissions can only be achieved by the production and use of SAF, which leads to the following questions: i) What feedstocks could be used for FT for SAF production? ii) Does FT SAF fulfil the criteria of sustainability? iii) What is the effect of adding CCS to the production of SAF? iv) What are the trade-offs between the technical, economic, and environmental indicators of various SAF production scenarios? v) What actions should be taken for a more sustainable production of SAF from the FT process?

There are many uncertainties around the production of SAFs, which may be clarified by answering the questions mentioned above. To this end, this chapter will develop the concepts related to the FT conversion technology, and at the same time, it will review the different TEA and LCA studies for the process configurations that are assessed in this research. Based on the identified findings and limitations of the existing literature, the research gaps are narrowed down. Consequently, the specific gaps are outlined so that this study can address them throughout the development of this research.

2.1 Gasification

Gasification is a technology with high potential for the conversion of carbonaceous feedstocks. It operates in an atmosphere of low oxygen and high temperature for the production of significant products such as H_2, electricity, and syngas [41], [42]. Syngas, or synthesis gas, is the name of the gasification product whose impurities have been removed [42]. Consequently, it could be used for different purposes, e.g., the production of fuels and wax through the well-known Fischer-Tropsch process [43]. Nowadays, various biomass gasification technologies at different development levels exist [44]. Therefore, different feedstocks could be gasified, and due to their distinct characteristics, specific pre-treatment steps are required for their processing in a particular gasification technology [44]. Mainly, these steps include size reduction, drying, densification, torrefaction, and steam explosion, among others [45], [46].

Biomass composition is represented by proximate and ultimate analyses. The ultimate analysis shows the elemental basic composition of the raw material, except for its moisture and its inorganic constituents that are not taken into account (Equation 2-1). On the other hand, the proximate analysis characterises the biomass in terms of gross components such as fixed carbon, volatile matter, ash, and moisture [30].

$$C + H + O + N + S + Ash + M = 100\% \quad \textbf{(2-1)}$$

2.1.1 Gasification chemistry

The gasification process is composed of the following stages [30]:

1. Drying: Normally, biomass moisture content ranges between 5 to 35%, for most of the gasification technologies available, the moisture content of the biomass should be reduced to 10-20% [32]. Drying requires huge amounts of energy, which affects negatively on the overall process energy efficiency [30], [45].
2. Devolatilisation: Also known as pyrolysis, is the process when biomass is thermally decomposed under an oxygen-free environment [32]. This process results in products such as char and volatiles, which are composed of long-chain liquid hydrocarbons and a small amount of gases [45]. However, in this process also tars are produced, which are complex mixtures of condensable hydrocarbons. Tars include single-ring to five-ring aromatic compounds, alongside other oxygenated, and complex polyaromatic hydrocarbons. These tars represent a significant challenge for the deployment of gasifiers at industrial level since they have the potential to clog downstream equipment [30].
3. Oxidation: In this step occurs the oxidation of the pyrolysis-derived char, which results in the production of CO_2, H_2O, and considerable amounts of heat. When oxygen is provided below the stoichiometric amount, CO is also produced [32].
4. Reduction: During this stage, various chemical reactions take place at high temperatures. These reactions occur without oxygen and are mostly endothermic. The average reaction temperature ranges between 800 °C and 1,000 °C, and the products obtained are mainly CO, CH_4 and H_2 [32], [47].

The main chemical reactions that are associated to the gasification process are presented in Table 2-1 [47]–[49]:

Table 2-1: Major chemical reactions of the gasification process [48]**.**

Gasification Step	Reaction
Pyrolysis	$Biomass \rightarrow CO + H_2 + CO_2 + CH_4 + H_2O + Tar + Char$
Oxidation	$Char + O_2 \rightarrow CO_2\ (Char\ oxidation)$
	$C + \frac{1}{2}O_2 \rightarrow CO\ (Partial\ Oxidation)$
	$H_2 + \frac{1}{2}O_2 \rightarrow H_2O\ (Hydrogen\ Oxidation)$
Reduction	$C + CO_2 \leftrightarrow 2CO\ (Boudouard\ Reaction)$
	$C + H_2O \leftrightarrow CO + H_2\ (Reforming\ of\ Char)$
	$CO + H_2O \leftrightarrow CO_2 + H_2\ (Water\ Gas\ Shift\ WGS\ Reaction)$
	$C + 2H_2 \leftrightarrow CH_4\ (Methanation\ Reaction)$
	$CH_4 + H_2O \leftrightarrow CO + 3H_2\ (Steam\ Reforming\ of\ Methane)$
	$CH_4 + CO_2 \leftrightarrow 2CO + 2H_2\ (Dry\ Reforming\ of\ Methane)$
Tar Reforming	$Tar + H_2O \rightarrow H_2 + CO_2 + CO + C_xH_y\ (Steam\ Reforming\ of\ Tar)$

2.1.2 Types of gasifiers

The performance of the gasifier relies on a number of interdependent variables, such as the properties of the feedstock, the reactor design, and operating parameters [50]. Gasifiers are classified according to various parameters. According to the operating pressure, gasifiers could be atmospheric or pressurised. If the gasifier needs an external source of energy, it is called allothermal, and if it is energy autonomous, it is known as autothermal [30]. Depending on the gasification agent, gasifiers could be air-blown, oxygen-blown, or steam-blown [32]. Based on gas-solid phase contact, gasifiers are divided into fixed bed, fluidised bed, and entrained bed [30], [50]:

1. **Fixed bed gasifier:** Inside this type of reactor, a bed of fixed fuel particles is crossed by the gasifying agent and the gas produced, both moving up (updraft), down (downdraft), or from one side to the other (cross-draft) [32]. Because they are easily constructed, there are many small-scale fixed-bed gasifiers around the world [30]. Normally, they operate with high carbon conversion efficiency, a long solid residence time, low ash carry-over, and low gas speed [32]. Poor mixing and heat transfer inside the reactor are the major operational drawbacks; thus, the cross-section does not have a uniform distribution of fuel, temperature, and gas composition [30].
2. **Fluidised bed gasifier:** Within this unit, the gasifying agent moves a bed composed of fuel and inert particles. Silica is commonly used as inert bed material; however, other particles such as olivine, sand, dolomite, etc. have gained attention due to their catalytic power to discompose tars

[47]. Their efficient gas-solid mixing and heat transfer enable operation in nearly isothermal conditions [30], [47]. Nevertheless, the melting point of the inert material limits the increase in the operating temperature, which normally ranges between 800 °C and 900 °C. Unless a catalyst is added, this low temperature and short residence time do not allow gasification reactions to reach chemical equilibrium. On the other hand, carbon conversion efficiency is high and could be up to 95% [51]. Fluidised bed gasifiers are subdivided as bubbling, circulating, and dual fluidized bed gasifier (DFBG).

3. **Entrained bed gasifier:** This type of gasifier is the most suitable for large-scale applications; however, several technical difficulties are associated with its operation. Due to its short residence time, the feedstock must be supplied in very small particle sizes; reducing biomass into small particles is very difficult and high-energy-demanding due to its fibrous nature. For this reason, this gasifier is not suitable for biomass conversion; nevertheless, it is important to highlight that the syngas produced is almost free of tar since its operating temperature could go up to 1,000 °C or more [30], [51].

In addition to these traditional gasifiers, there are novel technologies that have been developed, including plasma gasification and gasification in supercritical water [41]. The plasma gasification technology treats hazardous waste because the feedstock reacting within the gasifier is completely decomposed into clean syngas [52]. The main part of the gasifier is a plasma torch where an electric arc is generated between two separate electrodes, which are located in a closed container through which an inert gas circulates and is converted into plasma [30]. Gasification with supercritical water uses water over its critical point (647.10 K and 22.12 MPa), and it is used for biomass with high moisture without the need for pre-treatment steps [41].

2.1.2.1 Dual Fluidised Bed Gasifier (DFBG)

DFBG consists of two separated compartments, as depicted in Figure 2-1. The feedstock enters the first compartment, which is a bubbling fluidised bed, for its gasification with steam, resulting in raw syngas and char; the residual char is sent to the second reactor, which is a circulating fluidized bed or fast fluidized bed, for its combustion in the presence of an oxidising or fluidising agent. The produced heat is recirculated to the first compartment by the inert particles for the endothermic gasification reactions [32].

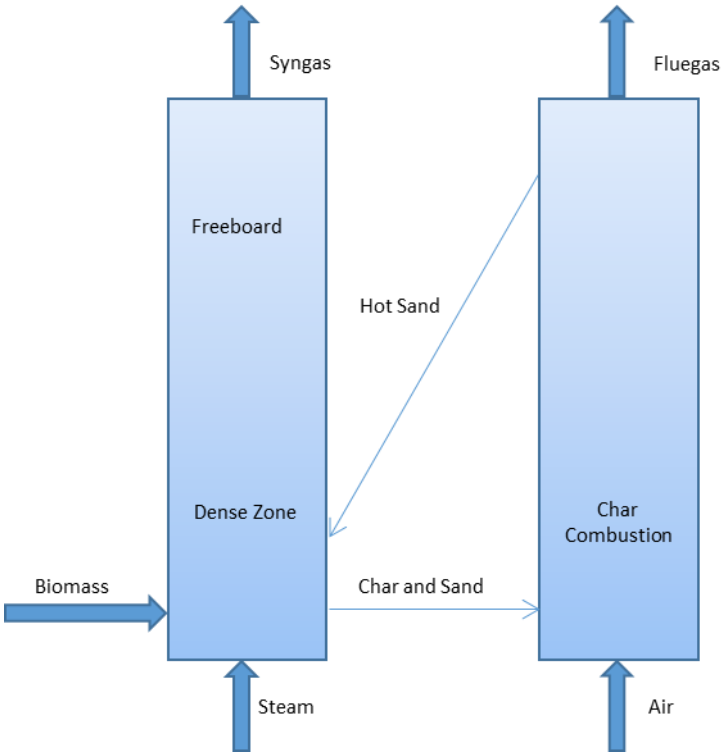

Figure 2-1: Dual fluidized bed gasifier [53]**.**

2.1.3 Gasification modelling

Experimental and computational aspects of biomass gasification have been widely studied. Different mathematical models effectively depict chemical and physical phenomena occurring inside a gasifier. Computational tools play a crucial role in determining optimal gasifier conditions, eliminating the need for costly and time-consuming experiments [50]. Mostly, kinetic approaches, equilibrium, and artificial neural networks are used [32]. The kinetic modelling approach encompasses the kinetic expressions of the main reactions that occurred in the gasification process. The advantage of kinetic models is that they are comprehensive and accurate; however, they are computationally intensive [50]. Furthermore, these models are useful for fluidized bed gasifiers because their chemical reactions are limited by their kinetics [53].

2.2 Fischer-Tropsch

Fischer-Tropsch (FT) is a well-developed technology used for the production of hydrocarbons, oxygenated compounds, H_2O, and CO_2, by hydrogenating carbon monoxide. Its importance is reflected in the capability to obtain heavy hydrocarbon mixtures that can be used as synthetic fuels that accomplish the most stringent environmental regulations for the ever-increasing energy demand [34], [54]. An important advantage linked to the use of these liquid fuels is the fact that their properties are similar to those of petroleum-derived fuels, which means that no further conversion is necessary [54].

Currently, coal, oil, or natural gas are the main sources for the production of syngas. However, the growing need to minimise dependency on fossil fuels has increased the importance of using syngas derived from renewable sources as feedstock for the FT process [55].

The parameters affecting the quality and yield of the formation of hydrocarbons with a specific chain length, are mainly the operating conditions, the design of the reactor, and the choice of catalyst [54]. Normally, the FT reactions occur in the presence of a catalyst under a pressure of 1×10^6 Pa to 6×10^6 Pa (10 bar to 60 bar), and a temperature of 200 °C to 300 °C [56]. The reactions taking place over the FT catalyst use a polymerization mechanism. The catalyst adsorbs H_2 and CO for their reaction and production of a chain initiator. Then, next steps are chain propagation, chain termination and product desorption from the catalyst surface [54]. The FT conversion is an exothermic process mainly represented by two reactions. Equation (2-2) represents the formation of alkanes and Equation (2-3) represents the production of alkenes [34]:

$$nCO + (2n+1)H_2 \overset{cat}{\leftrightarrow} C_nH_{2n+2} + nH_2O \quad \textbf{(2-2)}$$

$$nCO + 2nH_2 \overset{cat}{\leftrightarrow} C_nH_{2n} + nH_2O \quad \textbf{(2-3)}$$

The main characteristic that a FT catalyst should have for the synthesis of fuels is a high capacity for hydrogenation of CO into higher hydrocarbons [54]. According to this, the most active metals for FT conversion are Co, Fe, Ru, and Ni. Nevertheless, due to availability and economic constraints, Fe and Co are mainly used [34], [57]. Table 2-2 presents and contrasts the main properties of these two main catalysts. Additionally, the selection of the catalyst is complemented by two operation modes: high-temperature Fischer-Tropsch (HTFT), which uses a catalyst based on Fe at around 320 °C, and low-temperature Fischer-Tropsch (LTFT), which employs either a Fe-based or Co-based catalyst at temperatures ranging from approximately 170 °C to 270 °C. The main characteristics of the products derived from these operating modes are detailed in Table 2-3. LTFT using a Fe-based catalyst produces a synthetic crude (syncrude) that contains more alkenes than a Co-based catalyst [29]. In this sense, to enhance kerosene and diesel production through FT, Co as a catalyst and LTFT are the preferred choices [58]–[60].

Table 2-2: Comparison of some salient features of cobalt and iron FT catalysts [54].

Parameter	Co catalyst	Fe catalyst
Operating temperature	190-240 °C Used only in LTFT reactors High temperature increases CH_4 selectivity and causes catalyst deactivation	200-350 °C Operates both in HTFT and LTFT reactors
Feed gas	Syngas with H_2:CO ratio in the range of 2.0-2.3, due to very low WGS activity	Flexible H_2:CO ratio in the range 0.5-2.5, due to high WGS activity
Activity	More active at higher CO conversions i.e., lower space velocities	More active than Co at higher space velocities
Product spectrum	Primary products are n-paraffins with marginal production of α-olefins Higher paraffin/olefin ration α=0.85-0.92	Primary products are n-paraffins with considerable production of α-olefins Lower paraffin/olefin ration α=0.65-0.92
Operating plants	Shell Middle Distillate Synthesis, Oryx-GTL facility-Sasol	Sasol Slurry process (LTFT), Sasol-SAS (HTFT), Mossgass facility
Promoters	Noble metals (Ru, Rh, Pt, Pd)	Alkali metals (Li, Na, K, Rb, Ca)
Life & cost	Longer life time, more expensive	Lower life time, less expensive

Table 2-3: Main Product Types Produced of different Fischer-Tropsch Operation Modes [29]**.**

Product Property	HTFT	LTFT
Carbon number range	C_1-C_{30}	C_1-C_{120}
Compound Classes		
Alkanes (paraffins)	20-30%	Major product (>70%)
Cycloalkanes (naphthenes)	<1%	<1%
Alkenes (olefins)	Major product (>50%)	15 to 20%
Aromatics	1-5%	<1%
Oxygenates	10-15%	~5%
HTFT using Fe-based catalyst LTFT using Fe or Co-based catalysts		

2.2.1 Fischer-Tropsch modelling

The mathematical representation of the FT reactions plays an important role in the design and operation of processes based on this technology. Furthermore, these models facilitate an insight into reaction kinetics, product distribution, and catalyst performance. There are several mathematical models, each with a different level of complexity and assumptions [61]. Studies on the FT synthesis

proposed different mechanisms, e.g., carbide, enol, CO-insertion, and hydrogen-assisted CO activation mechanisms. The carbide mechanism suggests that CHx species originate from the breakdown of C-O bonds on the surface of the catalyst [62].

Furthermore, the kinetic modelling of the FT synthesis encompasses three crucial steps: i) selection of a possible mechanism; ii) formulation of the CO consumption rate; and iii) description of the product distribution. The most common kinetic approaches are simple power-law expressions, or the Langmuir–Hinshelwood–Hougen–Watson kinetic rate expressions [62]. Normally, most of the kinetic studies approach the product distribution through the probabilistic Anderson-Schulz-Flory (ASF) [63].

The ideal ASF model mathematically describes the product distribution of n-alkanes [34], [57]. Equation (2-4) and (2-5) express this distribution in terms of mole fraction ($y_{N_c,n}$), and mass fraction ($y_{N_c,m}$) for n-alkane compounds with a carbon number (N_c). Equation (2-6) defines α, which is known as the chain growth probability factor, which depends of the rate of propagation (r_p) and the rate of termination (r_t), but it is independent of the Carbon-number (N_c) [34], [57]. The value of α depends on several parameters, such as temperature, pressure, catalyst, and CO to H_2 ratio; to maximise the yield of liquid transportation fuels α should range between 0.82 to 0.95 [34], [54]. Figure 2-2 reflects the product distribution for different α values, between 0 and 1.

$$y_{N_c,n} = (1-\alpha)\cdot\alpha^{N_c-1} \quad \textbf{(2-4)}$$

$$y_{N_c,m} = N_c\cdot(1-\alpha)^2\cdot\alpha^{N_c-1} \quad \textbf{(2-5)}$$

$$\alpha = \frac{r_p}{r_p + r_t} \quad \textbf{(2-6)}$$

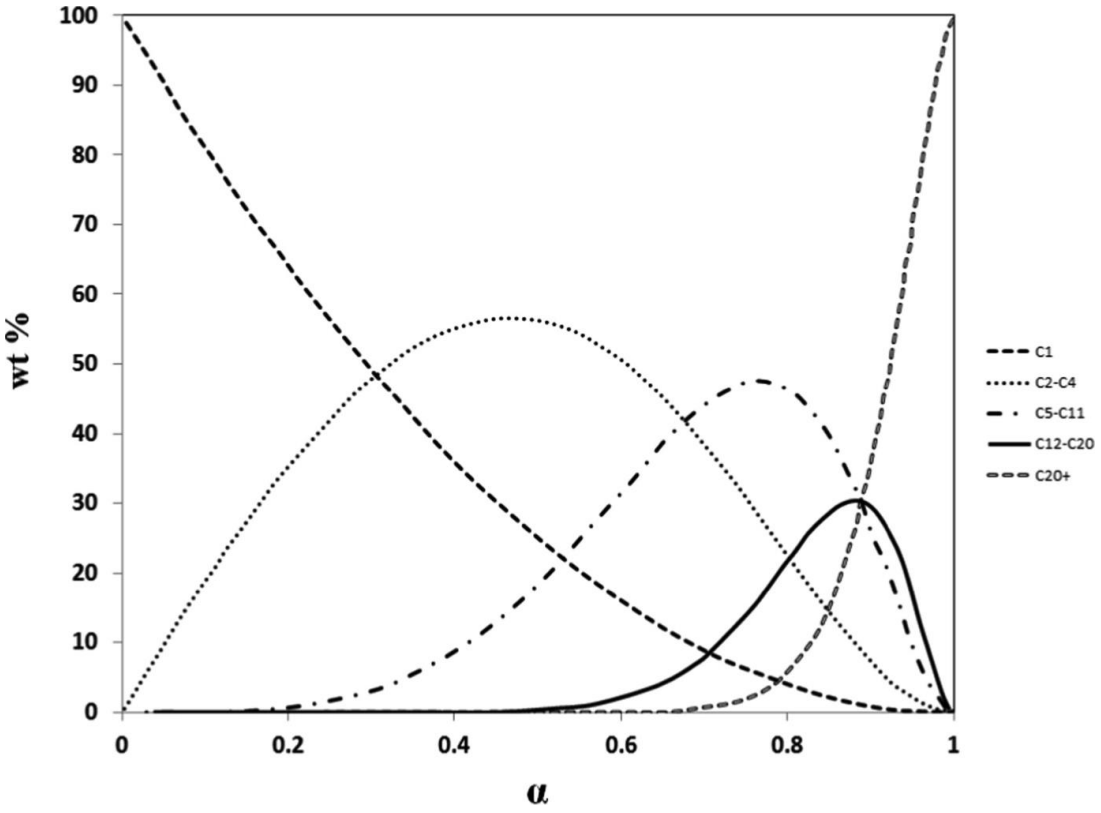

Figure 2-2: Product distribution [57]**.**

To improve the product distribution prediction, the deviations from the ASF model should be accounted for. The selectivity of hydrocarbons is affected by local factors such as temperature, pressure, and species concentrations (mainly CO and H_2, but also the synthesised water) [63], [64], but also by the inherent deviations of the FT synthesis, such as higher methane yield, lower ethylene yield [62], and olefin production [64]. Therefore, for an enhanced FT representation, it is crucial to integrate models that properly account for the deviations from the ASF models. An example of such improved models is the one proposed by Marchese et al. [64], with its predicted product distribution represented in Figure 2-3. The figure on the left displays the capability of the model to estimate paraffin and olefin production. The black and red lines, on the other hand, depict the higher methane yield and lower ethylene yield, respectively, which the ideal ASF model fails to represent.

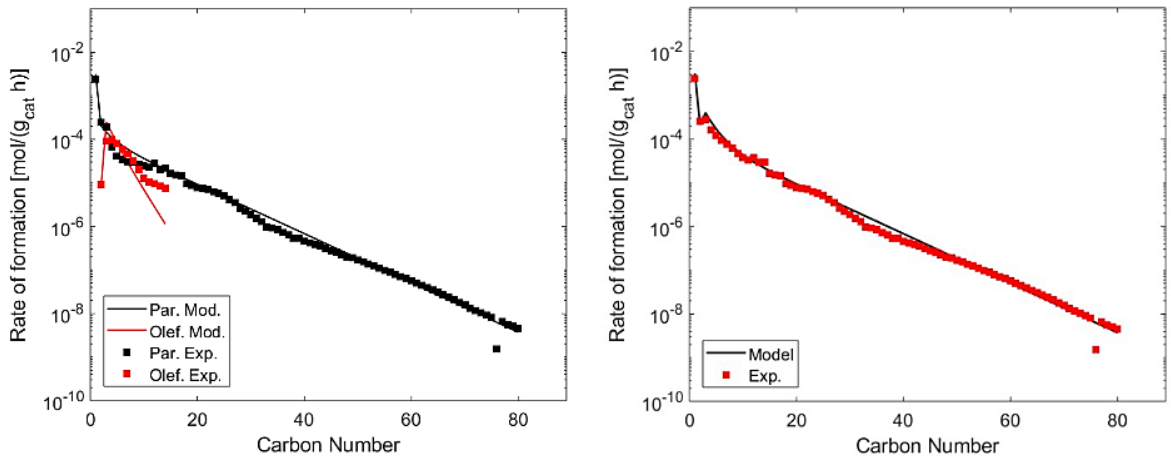

Figure 2-3: Experimental and calculated FTS distribution comparison for paraffins and olefins (left column) and total distribution (right column), at T=482 K, p=2×10^6 Pa (20 bar), H_2/CO=2.08 (adapted from [64]).

2.3 Biomass to Liquid (BtL) for SAF production through Fischer-Tropsch

A generic representation of the bio-based FT process is presented in Figure 2-4. In accordance with this diagram, five main sections are distinguished: pre-treatment of feedstock, gasification section, syngas conditioning and cleaning section, and FT synthesis and refining of FT syncrude (synthetic crude) [65].

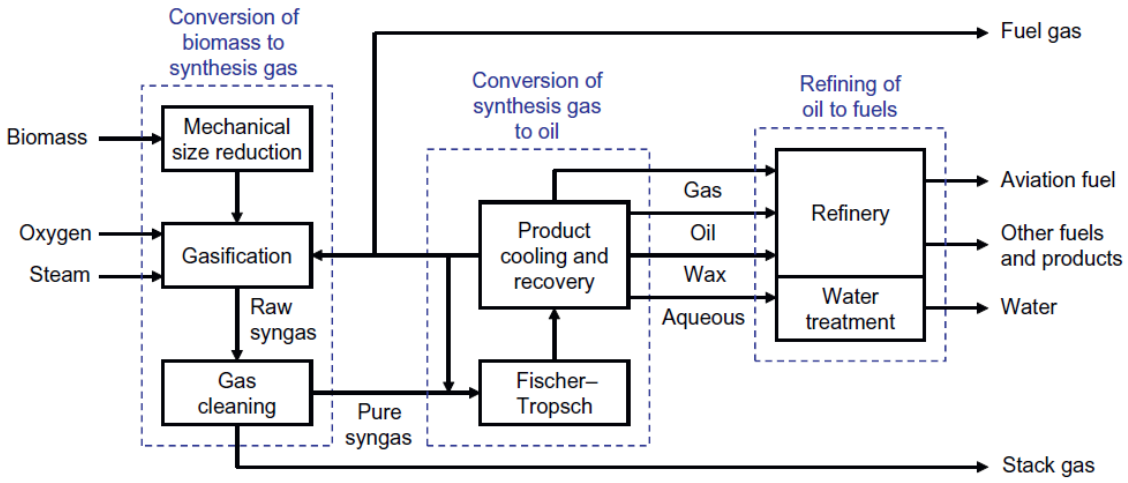

Figure 2-4: Diagram of the FT process for the production of synthetic fuels [29]**.**

Initially, the feedstock is pre-treated via different processes such as drying and grinding, among others [60]. Subsequently, the pre-treated biomass is sent to the gasification process, which depends on many parameters, such as feedstock characteristics (particle size, biomass composition), operating

parameters (pressure, temperature, type of gasifying agent, heating rate, equivalence ratio), catalyst addition, and reactor configuration, all of which will impact the yield and composition of syngas [65].

Raw syngas has various impurities that must be separated to avoid problems with the FT catalyst. In this sense, several cleaning-up technologies exist. Similarly, it is imperative to adjust the ratio H_2/CO to a value of 2.1 [30]. Once the syngas is purified and adjusted, it is directed to the Water-Gas-Shift (WGS) reactor. This catalytic reaction, Equation 2–7, could be conducted either over Fe or Cr catalysts at high temperatures (650–700 K) or in Cu-ZnO-Al2O3 at low temperatures (450–500 K) [66].

$$CO + H_2O \rightarrow CO_2 + H_2 \ (\Delta H = -41 kJmol^{-1}) \quad \textbf{(2-7)}$$

Purified and adjusted syngas is then introduced into the FT reactor, where parameters such as catalyst and temperature will determine the properties and composition of the FT-syncrude produced. As mentioned before, to maximise the production of middle distillates via FT, Co-based catalysts and LTFT are selected [58]–[60]. Once the hydrocarbon product leaves the FT unit, it is upgraded to final liquid fuels using common oil refinery processes. In order for the products to achieve the required properties, it is necessary to convert the long chains into smaller units inside a hydrocracking reactor and rearrange some of the atoms in an isomerization unit. The production of middle distillates is maximised, while naphtha and diesel are also produced [36], [67].

2.3.1 Techno-economic assessment for BtL SAF

The preferred method for determining the economic feasibility of a SAF production pathway is through the minimum jet fuel selling price (MJSP). The MJSP of SAF is the price at a net present value (NPV) of zero and at a minimum acceptable internal rate of return (IRR) [35], [68]. A number of existing TEA studies tried to be more transparent by considering a "pioneer plant analysis", while others preferred not to take into account the risks associated with the immaturity level of development and considered the "nth plant" approach.

A considerable number of techno-economic studies analysing biomass conversion through gasification and FT have been published. Generally, there are more studies for the production of middle distillates (jet fuel and diesel) [69]–[71] rather than only jet fuel [35], [60], [72]. These past TEA studies identified that bio-based FT projects are not financially feasible, but economic parameters could be improved by increasing the production capacity of the proposed configurations. However, commercial-scale plants are associated with a high level of uncertainty, due mainly to the high capital investment, the scarce and seasonal availability of biomass, and also its handling logistics [73].

The cost of transportation fuels obtained through the FT process is higher for biomass derived fuels, than coal or natural gas derived fuels. This could be as a consequence of the long distance for the transport of the biomass and to its low energy density. In this sense, Hileman et al. [74] found that the MJSP for SAF from biomass is around 20% higher than the production cost of aviation fuel derived from coal.

Typically, the economic performance of these FT configurations are found to be CAPEX and feedstock intensive [35], [60], [65], [69]–[71]. In the FT pathway, the feedstock and syngas production and conditioning have a significant effect on the cost of the fuel. Tijmensen et al. [69] studied the conversion of poplar via gasification coupled with FT; the economic analysis showed that biomass pretreatment, oxygasification and cold gas clean-up account for 75% of total capital cost, while biomass represents 30% of total production cost. Similarly, Anex et al. [71] determined higher CAPEX with the use of gasifiers at low temperature, since high temperature gasification leads to less complex FT process due to a cleaner syngas and faster gasification kinetics. In the study of Atsonios et al. [72] on the conversion of wood into jet fuel through FT; the TEA determined that the most expensive section of the process is the syngas cleaning and conditioning section, representing near to 30% of the Total Installation Cost (TIC). Additionally, the choice of oxygen as the gasifying agent increased the TIC due to the need for an Air Separation Unit (ASU).

Among various SAF production pathways, the FT process stands out for having one of the highest CAPEX [65]. Diederichs et al. [35] compared biochemical, thermochemical, and hybrid pathways for the production of SAF from lignocellulosic biomass and first-generation feedstocks. The TEA results for the investigated processes determined that the FT process has the highest capital investment, while processes with first-generation feedstocks have lower values. Similarly, Neuling et al. [60] compared four different conversion pathways; among HEFA, FT, biogas to liquids, and ATJ, FT had the highest total investment costs.

Table 2-4 summarises some of the MJSP for the FT scenarios of the aforementioned studies.

Table 2-4: MJSP of FT jet fuel.

Pathway	Feedstock	Plant size (based on feedstock input) (kg/h)	MJSP (£/L)	Reference
FT	Wheat Straw	875,000	1.12	[60]
	Wood Chips	650,000	0.70	[60]
	Wood	864,000	1.10	[72]
	Lignocellulose feedstock	77,800	1.45	[35]

2.3.2 Life Cycle Assessment for BtL-SAF

LCA produced through FT has been broadly studied for middle distillate liquids, with more processes focusing on diesel production [75], [76], rather than kerosene [77], [78]. While analyses of on-road diesel are similar to those of kerosene, differences in product yields and changes in energy inputs, as well as end-of-life applications, could lead to different estimations of the environmental impacts [79].

Compared with other SAF production pathways, FT achieves high GHG emission reductions. This is mainly explained by the energy self-sufficiency of the process and the excess power production [60], [80]. De Jong et al. [80] compared relative mature technologies, i.e., FT, HEFA, and ATJ, with a well-to-wake (WtWa) approach. All of them have demonstrated high GHG emissions reductions compared to fossil jet fuel; among them, FT is the one that performs better (86–104% of reductions). Similarly, Neuling et al. [60] found that FT outperformed other processes in terms of GHG emissions reductions.

The analysis of the whole life cycle of FT-SAF led to the conclusion that stages associated with feedstock production (e.g., biomass cultivation and fertiliser utilisation for cropped feedstock) and transport have an important contribution to the GHG emissions [80]–[82]. Neuling et al. [60] analysed the FT-derived SAF for two different feedstocks, including wood chips and wheat straw. The biomass provision and transport contributed from 30 to 50% of the total GHG emissions. In a similar way, De Jong et al. [80] determined that the major GHG contributor is the feedstock production. Furthermore, they emphasized that this contribution becomes even more important for crops that are associated with emissions from land use change.

It is also important to highlight that, in general, the choice of the method for addressing the multifunctionality of a system significantly affects the estimated environmental performance. [79], [83], [84]. De Jong et al. [80] analysed the FT pathway for SAF production using both an energy allocation and a hybrid (energy allocation/system expansion) method. Their findings reported important differences in the results of these two methodologies due to the high amount of co-products derive from the FT pathway. For this reason, de Jong et al. recommended the energy and economic (for non-energy products) allocation method to avoid the uncertainty introduced by the system expansion.

Some results from the aforementioned studies are summarised in Table 2-5:

Table 2-5: Green-House-Gas emissions of jet fuel production pathways.

Pathway	Feedstock	GHG emissions (gCO_{2eq}/MJ)	Reference
FT	Wheat Straw	38.2	[60]
FT	Wood Chips	32.4	[60]
Bio-GtL	Biomethane	38	[60]
Bio-GtL	Natural Gas	75.3	[60]
FT	Wood Chips	6	[80]
FT	Willow	9	[80]
FT	Poplar	10	[80]

2.3.3 Bioenergy with carbon capture and storage (BECCS) for biofuels production

In recent years, there has been an increased interest in Carbon Dioxide Removal technologies (CDR) since estimations claim that they have the potential to remove between 100 and 1,000 Gt of CO_2 in the 21st century, and thus they are included in all strategies that intend to limit global warming to 1.5 °C, with limited or no overshoot. There are several CDR technologies, such as afforestation and reforestation, land restoration and soil carbon sequestration, bioenergy with carbon capture and storage (BECCS), direct air capture (DAC), enhanced weathering, and ocean alkalization [5]. Among them, BECCS is a promising technology for carbon removal whose process stages have been independently demonstrated at scale, such as bioenergy plants and the capture, transport, and storage of CO_2 [85].

BECCS processes for energy production are more carbon-efficient (amount of carbon coming from biomass that is reported as negative emissions) than BECCS processes for biofuel production. However, the latter option has the ability to create negative-emissions alternatives to decarbonise the transport sector, which lacks options to reduce its carbon footprint compared to power generation [86]. Despite this, the literature abounds with case studies related to power production through BECCS [87]–[93].

Few studies are available in the literature for CCS coupled with biofuel production plants. Generally, the major benefit of this process configuration is the improvement of GHG emissions performance with an increase in fuel production costs. Tagomori et al. [94] analysed the techno-economic performance of biodiesel production via gasification and FT. The difference in the levelised cost between the plant without and with CCS is almost negligible. From an environmental point of view, important savings on GHG emissions are highlighted for the plants with CCS. A report of the IEA [73] analysed the implementation of two different plants for the production of biofuels integrated with CCS. For both cases, it was determined that the application of the CCS has a positive impact in the sense that it halves the CO_2 emissions; however, it increases the biofuel production cost by 10%–14%.

2.3.4 Summary of the findings and research gaps of the TEA and LCA of biomass-to-SAF through the FT pathway

In this section, the key points and research gaps identified in the literature review are listed:

1. **Need for more detailed process models:** The production of FT-derived fuels is still not well implemented at commercial scale. Therefore, it is necessary to have detailed process models to more accurately represent the mass and energy interactions within the production pathway. For example, it has been found that for the reviewed studies, the most common practice is to model the gasification process using a thermodynamic-equilibrium approach. Although this methodology is reliable, it lacks accuracy. Few researchers have used the kinetic approach, which is an accurate modelling method.

2. **Biomass-to-liquids (BtL) process design for SAF production:** Most studies found in the literature analysed the FT process for diesel production, but the production of SAF may require additional processing units as well as specific operating conditions for some important sections of the process. In this sense, creating process models that contain more specific processes and operating conditions for SAF production is important.

3. **UK-based TEA and LCA studies for SAF production:** The choice of location for conducting TEA and LCA studies is an important parameter that can significantly impact the results. Despite the increased interest in SAF production in the UK, there is a lack of studies focused on this location. Region-specific parameters for feedstock availability, economic and environmental conditions, and regulatory frameworks should be considered.

4. **More comprehensive LCA:** While there are many environmental studies for the production of SAF, most of them involve simple carbon accounting. A comprehensive LCA is important as it offers a deeper understanding of the stages within the process. Furthermore, this offers the opportunity to identify the most polluting steps but also to estimate other environmental impacts beyond just the GWP.

5. **Need for the assessment of the Biomass to SAF with BECCS:** While there are limited studies analysing the BECCS concept for fuel production, none were found for SAF. Therefore, there is a research gap due to the lack of comprehensive TEA and LCA studies addressing the scenario of BECCS linked with FT for SAF production. It is critical to investigate the economic and environmental implications of this configuration in order to determine its feasibility and sustainability.

Addressing the aforementioned gaps will advance our understanding of SAF production. Clearly, there is a scarcity in TEA and LCA studies for the production of SAF through the BtL-CCS concept. To address this research gap in a more comprehensive way including key points 1, 2, 3, and 4 in a single study is important. Furthermore, while separate TEA and LCA studies are available, there is a crucial need for combined evaluations that systematically examine technical, economic, and environmental performance indicators for the identification of potential trade-offs between them.

2.4 Power-to-Liquids (PtL) for SAF production

The process of Carbon Capture and Storage (CCS) is a well-studied technology. Despite having been developed for almost three decades within the scientific community, its high investment and operation costs render its expansion and industrial implementation difficult. Thus, research is also focusing on the field of Carbon Capture and Utilisation (CCU), as an alternative to justify the high capital inversion of CO_2 capture, which is regarded as a feedstock for the synthesis of chemicals and fuels [95]. CCU takes the name of Power-to-Liquids (PtL) for the process that aims to obtain liquid hydrocarbons (Figure 2-5). The PtL is made up of three basic steps: i) Water electrolysis for H_2 production, ii) Provision of CO_2 and iii) Synthesis of hydrocarbons that need to be upgraded or converted to attain some specific properties [38].

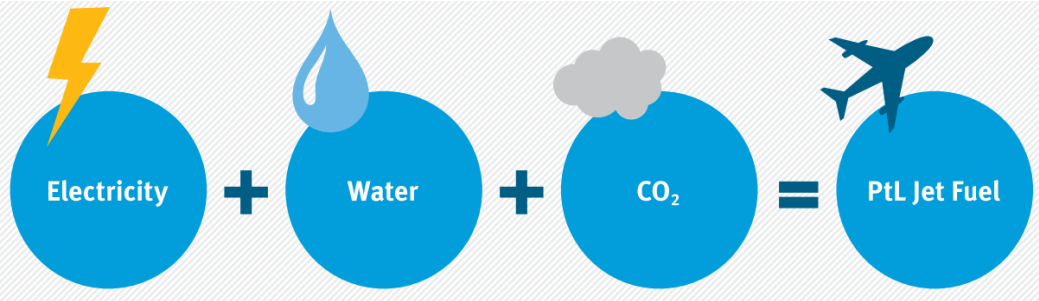

Figure 2-5: Schematic of power-to-liquids concept [38]**.**

There are two main PtL processes for the production of jet fuel: FT synthesis and upgrading, and Methanol synthesis and conversion [38], [96]. Although individual steps of these conversion pathways are in a mature state of development (TRL between 8 and 9), full integrated systems for the selective production of jet fuel from power are not commercially available [38], [97]. CCU conversion technologies have a very low degree of maturity. Thus, research related with process configuration and integration, process equipment design, catalyst, LCA, and policy analysis is in its early stages of development [95].

FT has been widely explained in Section 2.3. To prepare CO for the conventional FT process, CO_2 sourced from renewable or atmospheric capture undergoes conversion through a reverse water gas

shift (RWGS) unit. This resultant CO is then blended with H_2 to generate syngas, which is subsequently fed into the FT unit (Figure 2-6) [38]. FT synthetic jet fuel is ASTM approved to be mixed up to 50% with conventional jet fuel [98].

Diverse methods for the production of hydrogen from renewable and non-renewable sources are available [99]. Among them, electrolysis appears as the focus of interest of many researchers since it could be easily coupled to renewable energy sources, producing hydrogen with minimum emissions. Nevertheless, this immature technology needs more development to attain higher efficiencies and consequently, lower H_2 production costs [99]. Three kind of electrolysers are mainly used, alkaline water electrolysis (AE), proton exchange membrane water electrolysis (PEM) and solid oxide electrolysis cell (SOEC) [97], [100]–[102]. The AE is the technology that has the largest TRL (8 or 9), as it is found in industrial applications [103].

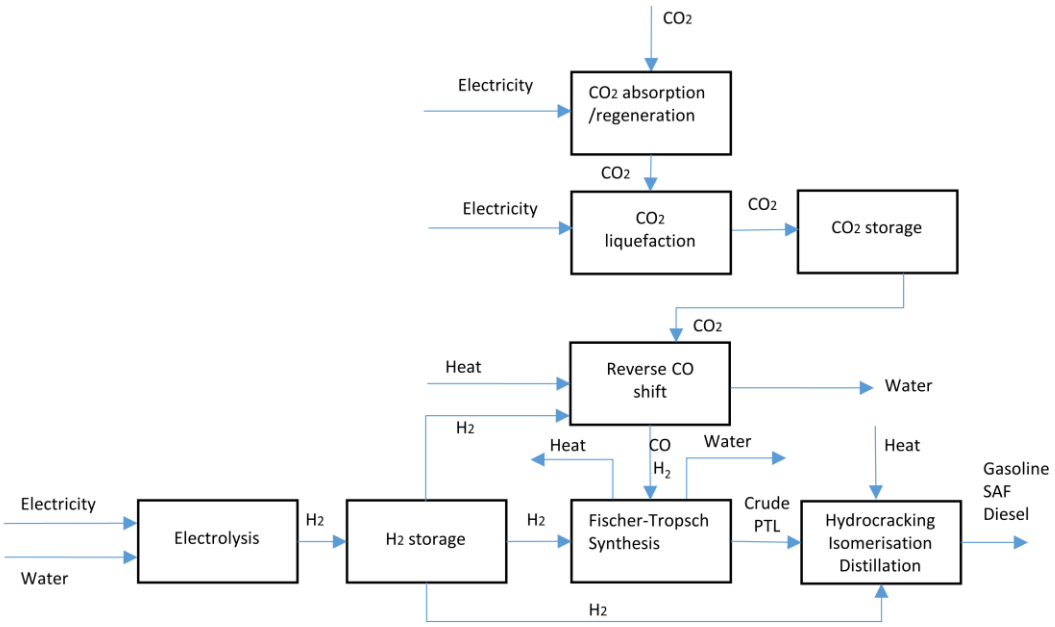

Figure 2-6: Process diagram of the Fischer-Tropsch pathway for power-to-liquids [104].

2.4.1 Techno-economic assessments for PtL SAF

Depending on the specific product of interest, CCU could be referred to in the literature or different databases as “electrofuels”, “PtL”, “CCU”, “Power-to-Aviation” and so on. Gathering these names with additional keywords, such as “techno-economic analysis”, “environmental analysis” or LCA, different search engines propose a variety of publications and reports whose number increases year after year. The state-of-the-art of Power-to-X TEA and LCA research is developing around three main applications: i) storing of intermittent electricity generation (as wind or PV) [105], [106], ii) production of

transportation fuels [38], [39], [59], [97], [107]–[112], and iii) production of chemical substances [95], [97], [111]. It is also important to highlight the large availability of bibliography for the production of methane [113]–[115] and hydrogen production [97], [115].

The PtL concept for the production of FT-derived fuels is a relatively new alternative pathway. As for now, only a few demonstration plants have been constructed [116], [117], and more studies are required to fully understand the performance of the scenario for a larger commercial scale plant. Some studies have focused on the technical aspect of the scenario through process modelling [118]–[121], while others further proceeded to economic assessments [38], [39], [121], [122] to find the levelised cost at which these fuels could be feasible. Similarly, there are other studies focusing on the environmental performance of this production pathway, from which most of them focused on the estimation of the global warming potential (GWP) [38], [123]–[125].

Some research towards technical and experimental [109], [126] performances of the PtL process or bottleneck sections of the process, is currently under development. Through process modelling, König et al. [110] found that the PtL process attained a carbon conversion rate of 73.7% and an efficiency of 43.3%. High costs of PtX (Power to any product) are associated with high capital costs and high H_2 production cost (mainly influenced by the electricity cost and capital cost of the electrolyser). Tremel et al. [108] compared different fuel/chemical synthesis technologies in terms of technology, economics and acceptance; FT public acceptance is high due to its product similarity to conventional fossil products. Additionally, they found that high cost of H_2 produced by water electrolysis is the main reason for the high cost of PTX fuels and chemicals.

There has been only a little research that specifically analyses the production of SAF from a PtL process that is available. Economic assessments are typically conducted to evaluate the cost and economic feasibility of such a process, taking into account the cost of the feedstock, energy, and capital investments needed. Three different reports produced by Batteiger et al.[127], Schmidt et al. [104], and Fasihi et al. [128] assessed the economic and environmental performance of PtL-derived SAF. By analysing short- and long-term scenarios, these reports determined whether this method was economically viable. Furthermore, the estimated minimum jet fuel selling price of the SAF is much higher when compared to the gate price of conventional jet fuel.

2.4.2 Life Cycle Assessments for PtL-SAF

The methodology of the LCA is relatively new. Many assumptions have to be undertaken during its elaboration and for this reason, similarities between different case studies either do not exist or are scarce. Consequently, there are many critical reviews on CCU studies [129]. As a measure to avoid the

increasing cases of disparities between different LCA studies, some authors have elaborated assessment guidelines [130]–[134], in order to highlight the typical misunderstandings that many researchers incurred and to give concise methodological guidelines to avoid them.

Many studies were developed around Power-to-gas, especially for H_2 and CH_4 production [113], [135]; however, literature on LCA for PtL for SAF production is scarce. The three aforementioned reports by Batteiger et al. [127], Schmidt et al. [104], and Fasihi et al. [128] assessed the environmental performance of PtL-derived SAF. Generally, these assessments conclude that PtL is a more sustainable option than other SAF production technologies, with significantly lower GWP. Key environmental performance indicators for the PtL jet fuel is improved when compared with conventional jet fuel or jet fuel from biomass. In the current situation, the PtL jet fuel has a reduction of GHG emissions of about 70% compared to conventional fossil jet fuel. However, taking into account that the energy matrix of the following years will be based on renewable energy, the reductions in GHG emissions will be higher (>95%). It is also important to say that the combustion of PTL jet fuel is cleaner since less volatile and non-volatile particulate matter is observed. Concerning water, the amount consumed in the production of PTL jet fuel is 400 to 15,000 times lower than jet fuel from biomass. Finally, the yield of fuel per land surface is higher than biomass jet fuel, and in terms of food competition, PtL does not need arable land [96].

Although the information provided by the aforementioned reports is very informative, it lacks accuracy as there are no process models and/or comprehensive LCAs. In this sense, the only study registered for the LCA of Power-to-jet fuel is the one performed by Micheli et al. [136], who studied the environmental assessment of various PtL SAF process configurations and calculated the GWP alongside other environmental factors such as the water footprint and land use. The foreground data used in the LCA of this study, which is solely an environmental assessment, derives from previous available studies related to the production of PtL fuels and not from industrial data or detailed process models.

2.4.3 Summary of the findings and research gaps of the TEA and LCA studies on PtL for SAF production

The keys points identified in the literature review dedicated to this topic are as follows:

1. **Limited understanding of the CCU processes:** CCU is a developing discipline with a great need of further research in a variety of related topics, such as catalysis, unit and process configuration design, performance of commercial scale integrated plants, economic optimisation, life cycle assessment, policy development, etc.

2. **Limited understanding of the PtL to SAF process:** Few technical reports concerning the power-to-aviation process exist. It is important to analyse the influence of various operating parameters in order to maximise the overall efficiency of the process and maximise the jet fuel yield through a detailed process design. Furthermore, detailed mass and energy balances are useful for identifying opportunities for synergies between the different process sections. For instance, the heat generated in the process could be used in the DAC section, or the water captured in the DAC could be integrated to cover the system's requirements.
3. **UK-based TEA and LCA studies for PtL-SAF production:** As stated in Section 2.3.4, the choice of location for conducting TEA and LCA studies is an important parameter that can significantly impact the results. Despite the increased interest in SAF production in the UK, there is a lack of studies focused on this location. Region-specific parameters for electricity availability, economic and environmental conditions, and regulatory frameworks should be considered. For example, understanding how the UK SAF mandate impacts the economic feasibility of this production pathway, which is a key part of the UK aviation net-zero strategy, is essential.
4. **Assessment of the intermittent supply of electricity to the PtL-SAF system:** Due to the high electricity demand of PtL systems, most studies assumed that the energy requirements are met with a dedicated renewable electricity source. Since this supply is often intermittent, it is important to evaluate options for ensuring a consistent electricity supply, such as using battery banks or a connection to the grid (as a virtual storage). TEA and LCA should incorporate these considerations to assess their impact on the economic and environmental performances.
5. **Need for TEA and LCA assessment of the PtL to SAF process:** While limited studies few technical reports have conducted general TEA and LCA studies of Power-to-jet fuel scenario; however, it is necessary to analyse the influence of technical and economic parameters such as CO_2 source, CO_2 price, type of electrolyser, electricity source and price, FT operating conditions and location, on the feasibility of jet fuel production through a detailed TEA and LCA study. Furthermore, while separate TEA and LCA studies are available, it is important to elaborate combined evaluations that systematically examine technical, economic, and environmental performance indicators while identifying potential trade-offs between them.

An exhaustive literature review revealed the lack of a comprehensive study on SAF production via the PtL pathway. As a result, the goal of this research project is to fill this gap by doing a full process simulation, developing a UK-specific framework, accounting for intermittent renewable electricity supplies, and conducting a combined TEA and LCA. As a result, uncertainties about the feasibility, efficiency, and sustainability of PtL-SAF production could be answered. Additionally, the effect of the UK SAF mandate in this production pathway will be explored.

2.5 Power-and-Biomass-to-Liquids for SAF production

The PBtL is a hybrid configuration that combines the original BtL and PtL technologies while also producing drop-in SAF. This process is performed through various integrated stages, including water electrolysis, biomass gasification, and liquid fuel synthesis and separation units, as shown in Figure 2-7. The synthesis of hydrocarbons typically occurs in a FT reactor; prior to FT, syngas production step is achieved via the RWGS reactor or by the direct injection of H_2 [39], [137]. Several studies that evaluated the PBtL technology exist in the literature [39], [137]–[149]. A summary of the technical findings indicates that the PBtL process enhances the BtL carbon conversion efficiency, therefore increasing fuel productivity. Moreover, when compared to the PtL configuration, the PBtL scenario requires less energy per unit of fuel, therefore achieving higher energy efficiency.

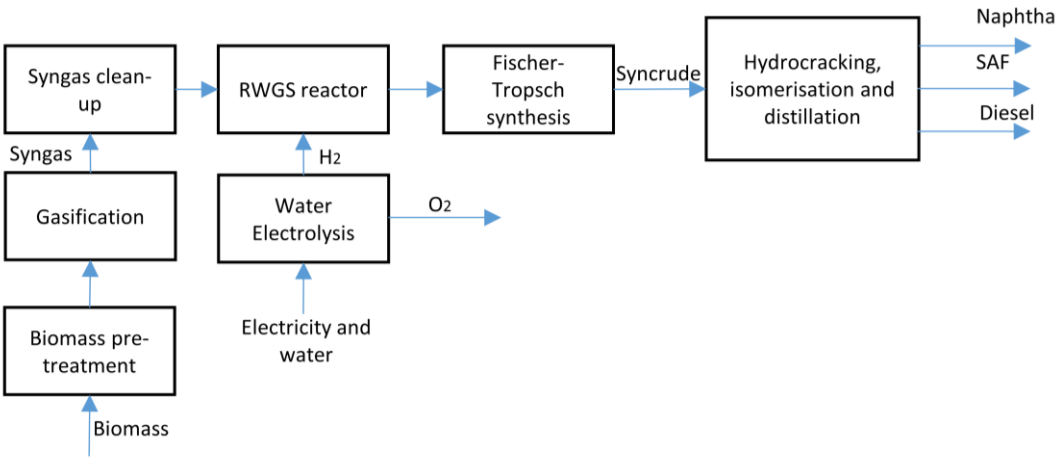

Figure 2-7: Schematic of the Power-and-Biomass-to-Liquid.

2.5.1 Techno-economic assessment for PBtL SAF

Extensive research has focused on the techno-economic (TEA) for BtL SAF production, and the number of PtL SAF studies is also increasing. However, TEA of PBtL for SAF production remains limited, with only a handful of studies exploring this configuration [137], [146]. Hillestad et al. [138] found that PBtL diesel is more profitable than the one produced through the BtL process. In contrast, the net present costs (NPC) estimated by Dietrich et al. [39] reflected that the BtL liquid fuel was less expensive than the one produced through the PBtL route, while the PtL-derived fuel was the least profitable. Habermeyer et al. [147] evaluated a PBtL small-scale experimental facility for FT fuel production with an integrated TEA and LCA approach. The conceptual design of this facility includes a water scrubber for the separation of the CO_2 from the syngas, which is further recycled to the gasifier to substitute the steam as gasification medium. This setup eliminated the need for a RWGS reactor, resulting in H_2 injection occurring prior to the FT reactor, but downstream purification and separation units were

excluded from the assessment. The resulting NPC of the PBtL C5+ hydrocarbons was estimated at 0.029 £2020/l [147], while for a large-scale plant, the same authors estimated a NPC equal to 0.036 £2020/MJ [137].

Other studies contrast the PtL process against scenarios such as BtL and PBtL. Generally, the scenario of PBtL has higher carbon conversion efficiency than BtL, but its total capital investment increases, since the cost of the gasifier is added to the high cost of the electrolyser. Dietrich et al. [39] compare these three technologies for the production of liquid hydrocarbons; as a result of the process modelling and TEA, Dietrich et al. determined that the total capital investment of the PBtL is lower than BtL, but higher than a simple PtL process; in respect to the technical performance, they found that carbon conversion efficiencies for BtL, PBtL and PtL were 26.9%, 97.7% and 98.9% respectively. Similarly, other authors as König et al. [107] Hillestad et al. [138] arrived to results that agreed with Dietrich et al. [39].

2.5.2 Life Cycle Assessments for PBtL-SAF

There are few LCA of PBtL configurations in the literature [137], [146], [147], [149], mostly focusing on the global warming potential (GWP) impact. These studies concluded that the major contributor to the GWP is the consumed electricity. When compared to analogous BtL or PtL scenarios, the GWP of the PBtL process was lower or higher, [147], [149] depending on the energy source that was used [149]. Habermeyer et al. [137], [147] performed the only SAF-oriented LCA; [8], [21] the boundaries of this LCA did not include the post-FT separation processes and hence it was a well-to-refinery gate assessment. Their results briefly explored several environmental impacts in addition to the GWP; the latter resulted in a positive value regardless of the source of electricity used. However, due to the missing separation section, the estimated environmental impacts would be different to a WtWa scenario since the various hydrocarbon fractions that are produced in the process plant imply the presence of a multifunctional system.

2.5.3 Summary of the findings and research gaps of the TEA and LCA studies on PBtL for SAF production

The keys points identified in the literature review dedicated to this topic are as follows:

1. **Lack of Comprehensive Life Cycle Assessments (LCAs) for PBtL-SAF:** There are limited LCA studies focusing on PBtL SAF configurations. Given that these studies did not include the post-FT separation processes, they are incomplete. Furthermore, more comprehensive LCAs are needed to evaluate other environmental impacts of this process.

2. **Need for TEA and LCA assessment of the PBtL to SAF process:** While separate TEA and scarce LCA studies are available for the PBtL for SAF production, there is a crucial need for combined evaluations that systematically examine technical, economic, and environmental performance indicators while identifying potential trade-offs between them.
3. **UK-based TEA and LCA studies for SAF production:** As expressed in previous sections, it is relevant to evaluate the feasibility of SAF production within a specific location. In this sense, there is the need of PBtL-SAF assessment that can capture the UK conditions in the economic and environmental performance. Furthermore, because the UK context affects the feedstock production and electricity generation potential for the process, it is important to consider this when evaluating PBtL scenario.
4. **Need for the assessment of the PBtL with BECCS:** While BECCS integration with BtL scenarios has been proposed and limited studies are available in the literature, the PBtL process is also promising for integration with CCS due to the presence of pure CO_2 streams. Therefore, a comprehensive combined TEA and LCA of the PBtL-CCS configuration could revealed the feasibility and sustainability of this novel process configuration, which has not been previously explored.

An exhaustive literature review revealed the lack of a comprehensive study on SAF production via the PBtL pathway. As a result, this research aims at filling this gap by doing a full process simulation, based in the UK, accounting for intermittent renewable electricity supplies, and conducting integrated TEA and LCA. As a result, uncertainties about the feasibility, efficiency, and sustainability of PBtL-SAF production could be answered. Additionally, the potential benefits of integrating CCS into the PBtL process will be explored, offering the aviation industry the flexibility to choose a negative emissions approach for SAF production via this pathway. Consequently, this research will assess various PBtL and PBtL-CCS scenarios with a combined TEA and LCA approach.

3. METHODOLOGY

The evaluation of the BtL, PtL and PBtL scenarios requires detailed models that can comprehensively represent the mass and energy interactions of the various sections of the systems. Subsequently, the resulting mass and energy balances, along with additional required data available in the literature, are used for the economic and life cycle assessments. Based on these steps, this chapter is structured into three main sections:

i. Process modelling: The first section explains the steps and resources needed for the construction of the process models in each case study. Moreover, the equations for calculating the mass and energy efficiencies are explained.

ii. Economic assessment: This section depicts the methodology for the economic assessment, which is further subdivided into OPEX and CAPEX estimations.

iii. Life Cycle Assessment: The last main section describes the methodology and resources that are needed to perform the LCA.

Additionally, each scenario is subjected to sensitivity and uncertainty evaluations for both economic and environmental performances. Given the specificity of the analysed parameters, these assessments will be explained within the dedicated research chapter for each scenario. Similarly, the development of some other scenario-specific models and the policy assessments are described in their respective research chapters.

3.1 Process modelling

A model is the representation of a system by using a group of mathematical equations that are based on fundamental laws of physics and chemistry. The simulation of a process is performed when these equations are solved, resulting in a series of mass and energy outputs that reflect the behaviour of a specific process. Therefore, process modelling and simulation are extremely useful tools for designing, testing, optimising, and integrating existing or new chemical processes, such as the proposed SAF production scenarios. This approach offers a safer, cheaper, and less time-consuming than performing real systems observations [150]. Chemical process plants generally comprise various processing units that are interconnected, and therefore requiring numerous equations for their accurate representation. This model compilation task can be shortened by using process simulation software that are available in the market. These software packages come with built-in models for the representation of the most common chemical operation units.

3.1.1 Aspen Plus models construction

Aspen Plus is a process simulation software that uses a flowsheet simulation approach. This approach quantitatively represents all the stages of the process, from the transformation of the raw material to the production of the final product. The methodology required to build the model of any chemical process within this software encompasses the following steps [151]:

i. Select the required chemical components and a suitable thermodynamic model from the Aspen Plus databanks.

ii. Set up the flowsheet for the process: To start, the operating units of the process are identified within the available models of the Aspen Plus library. Then, these models are placed on the flowsheet and connected to each other through inlet/outlet mass and/or energy streams.

iii. Define the stream's characteristics (such as flowrates and physical properties) and operating conditions for the process units.

Three scenarios for the production of SAF are developed in the present research project; all these pathways are modelled utilising the process simulation tool Aspen PlusV10. This software is the main tool to represent most of the processes since, due to the nature of the processes, they are suitably represented through the available chemical databanks and thermodynamic packages. All these characteristics are important for the design and process optimisation in a steady-state regime. The required data to be input in the model construction is gathered from a rigorous literature review. More details on the models are provided in the respective research chapter for each scenario.

3.1.2 Aspen Plus-Matlab interface

Despite the wide range of available models in the Aspen Plus library, there are more specific new technologies that are not included. This brings the need for programming softwares that can handle more elaborate and complex mathematical models. Thus, Matlab could be used to develop user models that can be integrated into the Aspen Plus interface so that they can continue to take advantage of the capabilities of this process simulation software. The protocol of this connection was explained in detail in the study of Fontalvo [152], and is summarised in Figure 3-1. To start, a "user model" from the Aspen Plus library is connected to the flowsheet in representation of the specific operating unit. Within this module, one defines the names and values of the input parameters of the model, and at the same time, they specify the name of the Excel file that serves as a bridge to Matlab. This Excel file contains some VBA routines that allow the reception of information of the "user model" inlet streams and parameters. Subsequently, another VBA routine sends the received information to the Matlab routine, which contains the mathematical models representing the operating unit. Then,

the code in Matlab calculates the properties of the outlet streams and, if defined, some additional outlet parameters. This information returns to the Excel file, which subsequently sends it to the Aspen Plus model. Finally, Aspen Plus translates it as the user model's parameters and output streams, adjusting for these latter thermodynamic properties based on the information received.

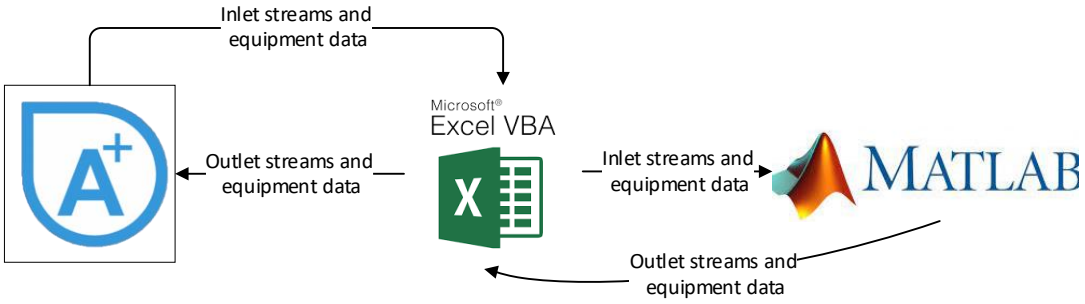

Figure 3-1: Data exchange framework within the Aspen-Excel-Matlab interface (Adapted from Fontalvo [152]).

3.1.3 Technical performance indicators

To quantify the performance of the proposed process configuration, the following mass and energy performance indicators were calculated:

i. Carbon fixation (η_C), or carbon conversion efficiency, is the indicator that accounts for the level of conversion of the feedstock into the product. This indicator is determined by Equation 3-1, which relates the moles of carbon ($\dot{n}_{C,products}$ in kmol/h) in the products with the moles of carbon in the feedstock ($\dot{n}_{C,feedstock}$ in kmol/h) [153], [154].

$$\eta_C = \frac{\dot{n}_{C,products}}{\dot{n}_{C,feedstock}} \quad \textbf{(3-1)}$$

ii. Hydrogen conversion efficiency (η_H), as calculated by Equation 3-2, indicates the conversion of hydrogen entering the system's boundaries into the desired fuel products. This is determined by the ratio of the hydrogen content of the hydrocarbon to the hydrogen content of the feedstock [122].

$$\eta_H = \frac{\dot{n}_{H,hydrocarbons}}{\dot{n}_{H,feedstock}} \quad \textbf{(3-2)}$$

iii. Energy ratio (η_e) of a process is identified as the ratio between the energy of the produced hydrocarbons and the energy content of the feedstock, as presented in Equation 3-3. Where η_e is the energy ratio of the conversion process, m_{fuel} is the mass of the jet fuel obtained, $m_{feedstock}$ is the mass of the feedstock converted in the process, LHV_{fuel} and $LHV_{feedstock}$ are the lower heating value (LHV) of the fuel and feedstock [35].

$$\eta_e = \frac{\left|\dot{m_{fuel}} \cdot LHV_{fuel}\right|}{\left|\dot{m_{feedstock}} \cdot LHV_{feedstock}\right|}$$

(3-3)

iv. The overall energy efficiency ($\eta_{overall}$) establishes the global efficiency of the process, by taking into account the energy in the products, such as fuels and electrical power produced (P_{El}), and the energy content the feedstocks, which is expressed as follows [35]:

$$\eta_{e\ overall} = \frac{\left|\dot{m_{fuel}} \cdot LHV_{fuel}\right| + P_{El}}{\left|\dot{m_{feedstock}} \cdot LHV_{feedstock}\right|}$$

(3-4)

v. For the PtL scenario, the overall energy efficiency, or Power-to-Liquid efficiency (η_{PtL}), is the ratio of the energy content of the produced hydrocarbons to the electrical energy input of the process (Equation 3-5). The electrical energy input represents the electricity consumed by the electrolyser (P_{El}) and the electricity required by the process (P_U) [110].

$$\eta_{PtL} = \frac{\left|\dot{m_{fuel}} \cdot LHV_{fuel}\right|}{|P_{El} + P_U|}$$

(3-5)

vi. The Power-and-Biomass-to-Liquid efficiency (η_{PBtL}) is similar to the η_{PtL} efficiency, but additionally it includes the energy content of the biomass in the denominator (Equation 3-6) [110]:

$$\eta_{PBtL} = \frac{\left|\dot{m_{fuels}} \cdot LHV_{fuel}\right|}{\left|P_{El} + P_U + \dot{m_{feedstock}} \cdot LHV_{feedstock}\right|}$$

(3-6)

LHV_{fuel} is equivalent to the low heating value of the synthesized commercial hydrocarbon fractions, being 42.6 MJ/kg [155], 44.9 MJ/kg [155] and 42.8 MJ/kg [156], for naphtha, diesel and kerosene respectively. The LHV of the FR on a dry basis (db) is equal to 19.54 MJ/kg [157], and this value is

recalculated at different moisture contents (MC) as received (ar) in accordance with Equation 3-7 [157].

$$LHV\ \left[\frac{MJ}{kg}a.r.\right] = \left(1 - \frac{MC(w/w\%)}{100}\right) * LHV_{db} + -\frac{MC(w/w\%)}{100} * 2.44 \quad \textbf{(3-7)}$$

3.2 Economic assessment

The main purpose of the economic assessment is to estimate relevant economic indicators, such as CAPEX, OPEX and MJSP. Uncertainty about the future price of SAF is significant; thus, the preferred method for determining the economic feasibility of a specific production pathway is through the MJSP. This latter is defined as the SAF selling price at which the net present value (NPV) is equal to zero for an internal rate of return (IRR) of 10% [35], [68]. A discounted cash flow analysis (DCFA) is used to determine the MJSP, whose financial parameters and assumptions are detailed for each scenario and presented in its corresponding research chapter. Furthermore, the TEA of all the SAF production scenarios adopted the "nth plant" approach, as recommended by Humbird et al. [158]. The key assumption of the "nth plant" is that the analysed technology is not a pioneering plant but that it has been successfully scaled to a commercial level, with several plants operating at an industrial level [68], [158]. Given that the main objective of the TEAs is to evaluate the economic performance of new SAF production configurations, this adopted approach avoids unnecessary artificial inflation of project costs related to uncertain characteristics of pioneer plants, such as risk financing, longer start-ups, and overdesign of the equipment, among others.

3.2.1 CAPEX estimation

The CAPEX is estimated based on the expenditures for the acquisition of the equipment, which is also known as “purchased equipment cost” (PEC). The purchased equipment cost (PEC) of the various common process units, such as heat exchangers and pumps, absorbers, and strippers, was estimated using the Aspen Plus Economic Evaluator tool. For other more specific equipment (e.g., gasifiers, catalytic reactors, among others), bibliographic research was conducted to find baseline costs from vendor quotes or past studies. Equation 3-8 [68], [159] was used to adjust the PEC for units at different capacities. C denotes the cost of the unit at the actual capacity S, while C_0 is the base cost at a specific base size S_0 or capacity. The scaling capacity factor f has different values depending on the type of process equipment, and its goal is to reflect the effect of the economies of scale [68].

$$C = C_0 \left(\frac{S}{S_0}\right)^f \quad \textbf{(3-8)}$$

Equation 3-9 is used to adjust the calculated PEC at different economic base year. $C_{base\ year}$ and $index_{base\ year}$ correspond to the base year of the study, while the other variables, C_0 and $index_0$, refer to the year in which the original cost was obtained. The indices were taken from the "Chemical Engineering Plant Cost Index (CEPCI)" that serves as an important tool for chemical-process-industry projects in the adjustment of equipment prices from one year to another. When the original prices of the equipment were not reported in GBP (£), a conversion factor was applied, corresponding to the year where this equipment price was detailed [160].

$$C_{base\ year} = C_0 \left(\frac{index_{base\ year}}{index_0} \right) \quad \textbf{(3-9)}$$

Following the calculation of the PEC, the Indirect Costs and Total Direct Costs were calculated as depicted in Table 3-1. To include the cost of installation, the PEC is multiplied by a factor, which represents the cost of auxiliary equipment, the cost of labour for installation, the cost of engineering, and the cost of contingencies [161]. Subsequently, the FCI is estimated as the sum of Indirect Costs and Total Direct Costs. The interest during construction is calculated considering that the investments during the first, second, and third years are 10%, 50%, and 40%, respectively, at an interest rate of 10%. Finally, the CAPEX was estimated by adding the start-up cost and the interest during construction. The working capital was considered to be 5% of the CAPEX.

Table 3-1: Methodology for the calculation of the CAPEX [162]–[164].

Component	**Cost, MM £**
Installed direct costs (IDC)	**PEC+(A+B+C+D)**
A) Purchased equipment installation	0.39*PEC
B) Instrumentation and controls	0.26*PEC
C) Piping	0.31*PEC
D) Electrical systems	0.10*PEC
Non-installed direct costs (NIDC)	**E+F+G**
E) Buildings	0.55*PEC
F) Yard improvements	0.12*PEC
G) Land	0.06*PEC
1) Total direct costs (TDC)	**IDC+NIDC**
2) Indirect costs (IC)	**0.255*PEC**
3) Fixed Capital Investment (FCI)	**TDC+IC**
4) Start-up costs	**0.05*FCI**
5) Interest during construction	**Calculated**
Total Capital Requirement (TCR) or CAPEX	**3+4+5**
Working Capital	**0.05*FCI**

3.2.2 OPEX estimation

The OPEX (operating expenditures) or manufacturing costs were calculated by adding up the estimated values of fixed operating and maintenance costs (FOM), variable operating costs (VC), and plant overhead costs, as shown in Table 3-2. VC were calculated by adding the cost of raw materials, utilities, and catalysts (that are replaced every three years). In turn, the labour, which is included within the FOM, is calculated using an empirical relationship (Equation 3-10) proposed by Peters et al. [165]. In this correlation, "plant capacity" refers to the amount of SAF produced, expressed in kg/h, "$n_{process\ steps}$" or the number of process steps, refers to the number of sections within the process where significant chemical and/or physical changes occur. In addition, "$h_{plant\ operation}$", refers to the annual operating hours of the plant, which is considered as 8,000 h/year. Once the hours of labour "h_{labour}" were estimated, the cost of the labour was calculated by considering that the price of one hour of labour is equal to 15 £/h [166], [167].

$$h_{labour}\left[\frac{h}{year}\right] = 2.13 \times plant\ capacity\left[\frac{kg_{fuel\ output}}{h}\right]^{0.242} \times n_{process\_steps} \times \frac{h_{plant\ operation}}{24} \quad \textbf{(3-10)}$$

Table 3-2: Fixed Operating and Maintenance cost, and Variable Cost [161]–[164].

Fixed Operating and Maintenance (FOM)	Value
Labour	(Equation 3-10) * 15 £/h
Supervision	0.25*A
Direct overhead	0.5*(A+B)
General overhead	0.5*(A+B+C)
Maintenance Labour	0.015*FCI
Maintenance materials	0.015*FCI
Insurance and tax	0.010*FCI
Financing WC	0.1*Working Capital
FOM	A+B+C+D+E+F+G+H
Variable Cost (VC)	
OPEX	FOM+VC

3.3 Life Cycle Assessment (LCA)

The LCA is a methodology used to determine the environmental impacts associated with the production of a good or service, by analysing the whole production system [79]. The concept of the life cycle of a product can be understood as the monitoring of a product from its "cradle" where raw materials are obtained from natural resources through production and use until its "grave", the elimination [168]. Applied to the SAF production processes, these system boundaries are also referred

to as well-to-wake (WtWa). In turn, the WtWa analysis is divided into two stages: well-to-tank and tank-to-wake [67].

To ensure consistency and transparency of the LCA estimations and assumptions, the standardised approach outlined in the standards ISO 14040 and 14044 was adopted [168]. According to this methodology, the LCA of the scenarios was divided into four main stages: Goal and scope definition, life cycle inventories, environmental impact, and interpretation [169].

3.3.1 Goal and scope definition

According to the ISO standard, the goal of the LCA should clearly state the goal of the assessment, the reasons behind its elaboration, and to whom the results will be communicated [170]. The scope of the study is defined such that the profundity and extent of the study are enough to respond to the specified objective. The establishment of a clear and detailed LCA scope requires the definition of a variety of elements, including: the functional unit, system boundaries, allocation procedures, impact categories (methodology of impact assessment and subsequent interpretation to be used), level of detail in the study, data requirements, and limitations of the study, among others [168], [170].

LCA studies are structured around a functional unit, which basically defines what is being studied. Therefore, subsequent analysis, as well as the inputs and outputs of the system, are correlated with the functional unit [170]. For energy products such as SAF, the functional unit is usually referred to as "unit of delivered energy" (e.g., a litre or a megajoule (MJ) of SAF). The purpose of this choice is to easily compare fuels of different origins when they have the same end use (e.g., combustion in the same aircraft) [81]. The boundaries for the LCA of BtL-derived SAF include the cultivation, harvesting, and transportation of the feedstocks, as well as the associated land use change (direct and indirect); it also includes the production and transportation of the auxiliary chemicals, the conversion process, and the storage, distribution, and combustion of the SAF [65]. The system boundaries of the PtL pathway do not include the stages associated with the feedstock; instead, they comprise CO_2 capture, electricity generation, and H_2 production.

3.3.2 Multi-functionality

When multiple products and by-products are produced within the studied system, the attribution of environmental impacts between products and co-products is done through allocation or substitution methods. The choice of attribution procedure is challenging, as each method leads to results with significant differences [79]. The substitution methodology (also known as system expansion or displacement method) evaluates the effects of co-products by deducting from the LCA the impacts avoided by substituting the co-products for other products that have the same purpose [79]. On the

other hand, the allocation method assigns emissions to products according to their flow properties, such as the content of carbon, energy, exergy, mass, or economic value [130].

Initially, ISO 14040 guidelines advice tackling a multifunctional system by applying subdivision or "system expansion." However, in specific situations when this approach is not applicable, the subsequent recommendation is the allocation based on any physical relationship. Lastly, when neither of the approaches is deemed suitable, the economic allocation is advised by the guidelines [170]. Nevertheless, past LCA studies for the production of sustainable fuels observed a tendency of this approach on calculating lower GWP since in most cases, the co-products were substituting analogous goods with high emissions intensities, such as those of fossil origin [80], [171], [172]. In relation to SAF production, de Jong et al. [80] found that the choice of allocation method has an effect on those processes producing high proportions of co-products or generating co-products that are able to displace carbon-intensive products (e.g., fossil fuels-derived electricity). Therefore, the authors recommended using energy and economic allocation, as this hybrid method values both energy and non-energy co-products. For his part, Suresh et al. [43] chose an energy allocation for energy products, while the system expansion was used for the allocation of non-energy products.

3.3.3 Life cycle inventory (LCI)

The elaboration of the inventory implies the collection of data and the definition of calculation procedures in order to quantify inputs and outputs of the system [170], which can be divided in the following steps: Elaboration of the flowchart, assemble of data, and determination of the environmental loads [168]. The construction of the flowchart model is based on the boundaries determined in the goal and scope sections. The model is basically a material and energy balance accounting for the environmentally relevant flows only [168]. The flowchart illustrates the process through a combination of quantitative and qualitative data that must be collected. Numerical data can be broadly classified as: energy inputs, raw materials, ancillary inputs, and other physical inputs; products, co-products, and waste; as well as emissions to air, water, and soil. Qualitative data encompasses the description of the process, temporal and geographical frames of inputs, outputs, and emissions, and any other relevant information [168], [170]. Once de data are collected, calculations are performed, including the following steps: data validation, and association of these data to operating processes, and to the reference flow of the chosen functional unit [170].

Generally, the elaboration of the life cycle inventory is a time-demanding step [170]. Data collection is a resource-intensive process, and its availability depends on many factors, such as the openness of industries and companies to share process-related information. On the other hand, it is common that

LCIs manage large amounts of data, which at the same time makes calculation procedures difficult. For this reason, it is advisable to use LCA software tools, which generally come with built-in databases containing LCIs of numerous processes. These softwares also have calculation methods, making this task less cumbersome [131], [168], [170]. Among the most known commercial LCA software, GaBi, SimaPro, and Umberto could be mentioned [131]. For this research, SimaPro was used, given that it comes with the Ecoinvent database. LCA practitioners point out that the advantages of using this database are the completeness and transparency of their LCI datasets that are available for numerous sectors.

For the LCAs of this research, the data sources are distinguished as foreground and background data. The foreground LCIs of the different scenarios were mainly built upon the resulting mass and energy balances from the Aspen Plus models. The LCI Ecoinvent 3.6 database, as well as any other external sources, are used to generate the LCI of the background data as well as to complete any information missing for the foreground LCI. From the system models available, the "allocation, cut-off by classification-system" was chosen, as recommended by Ecoinvent [173]. Given the chosen location for the SAF production plant, preferably, UK LCIs were selected, but in the absence of this geographical coverage, Europe, Global, or Rest of the World databases were used instead, in order of preference.

3.3.4 Impact assessment and interpretation

The impact assessment process consists of associating inventory data with particular health and environmental impact categories [170]. In every LCA, it is important to establish which environmental impacts are of interest for the study. There are several suggestions for complete sets of impact assessment methods in the LCA literature [168], among them, the ReCiPe method was selected for this research. This method calculates 18 midpoint indicators and 3 endpoint indicators. The main difference between the midpoint and endpoint indicators is that the formers focus on single environmental problems, while the others group these impacts in three aggregation levels: 1) effect on human health, 2) biodiversity and 3) resource scarcity. The use of endpoint impacts makes the interpretation of the LCA simpler but increases the uncertainty of the results. Instead, the midpoint approach provides more insights on the emissions by breaking them down at each stage of the SAF production pathway.

For this study, the chosen impact assessment is the "Recipe 2016 midpoint (H)", which calculates several environmental impact indicators. The main focus was placed on the GWP, which is estimated for a 100-year time horizon. The relevance of this environmental impact lies in the fact that it is used as a sustainability criteria that allows comparison with existing SAF production pathways as well as

with regulating standards, such as the U.S. Renewable Fuels Standard (RFS) and the European Renewable Energy Directive II (RED II). These standards establish the required threshold for CO_{2eq} emissions reduction compared to those of conventional jet fuel, which is equal to 89 gCO_{2eq}/MJ and 94 gCO_{2eq}/MJ, for the RFS and the RED II, respectively [174], [175]. Synthesized jet fuel can be considered SAF when its inherent GWP achieves at least 50% and 70% GHG emissions savings when compared to fossil jet fuel, in compliance with the RFS [176] and the RED II [175], respectively. On the other hand, the UK government is planning that for SAF to receive credits under the SAF mandate, it will be required to achieve a 50% GHG saving compared to a fossil fuel benchmark of 89 gCO_{2e}/MJ [17]. In addition, for some scenarios, dedicated attention was paid to the estimated water footprint, although there is currently no regulation on this specific environmental impact.

3.4 Sensitivity and uncertainty analysis

The sensitivity analysis is of the type of "scenario analysis" and was performed for both the economic and the life cycle assessment. The main goal of this analysis is to provide insight on how economic or environmental outputs are affected by the change of important parameters that are varied one at a time within reasonable and realistic ranges while keeping the others unchanged [177]. Therefore, the results of these optional scenarios can be compared with those of the baseline scenarios. The effects of uncertain economic variables were studied for the MJSP, and depending on the SAF production scenario, different parameters were considered, such as raw material costs, fixed capital investment, internal rate of return, and so on. For the LCA, the sensitivity analysis focused on the GWP, for which, depending on the scenario, different variables were considered, such as feedstock transport distance, carbon footprint of some stages of the system, and GWP of the electricity generation, among others.

Understanding the effect of varying the uncertain parameters at the same time is also important; therefore, a stochastic, probabilistic, or uncertainty analysis was performed for the MJSP and GWP estimations. The sensitivity analysis varies one parameter at a time, whereas the interaction of varying them simultaneously requires a statistical method such as the well-known Monte Carlo analysis. This analysis was considered for the same economic and environmental parameters used in the sensitivity analysis of each scenario. It was assumed that all of them follow a triangular distribution. A Monte Carlo analysis was performed in Matlab, where a code randomly varied these parameters and recalculated the MJSP and GWP of the system in 10,000 trials. The results are presented as a histogram of frequency, for which the mean value ($\bar{x}$) and the standard deviation (were calculated. Finally, for each MJSP and GWP, the 95% confidence interval ($95\%\ CI$) was determined based on Equation 3-11.

$$95\%\ CI = \bar{x} \pm 1.96 \times \sigma \quad \textbf{(3-11)}$$

4. Bioenergy with carbon capture and storage (BECCS) potential in jet fuel production from forestry residues: A combined Techno-Economic and Life Cycle Assessment approach

Abstract

In this chapter, the economic and environmental feasibility of a process configuration based on the Bioenergy and Carbon Capture and Storage (BECCS) concept is assessed. The research analyses the production of jet fuel from forestry residues-derived syngas via the Fischer-Tropsch (FT) technology. Further, the CO_2 removed in the syngas cleaning section is not released to the environment, instead it is permanently sequestrated. The produced Sustainable Aviation Fuel (SAF) has the potential to achieve negative emissions. The present research is a one-of-a-kind study for the jet fuel production within the BECCS concept. The process was modelled within the Aspen Plus and Matlab software to obtain detailed and realistic mass and energy balances. Based on these balances, the technical, economic, and environmental parameters were calculated. Based on a plant that treats 20 dry-t/h of forest residues, 1.91 t/h of jet fuel are produced, while 11.26 t/h of CO_2 are permanently stored. The inclusion of the CCS chain in the biorefinery increases the minimum jet fuel selling price from 3.03 £/kg to 3.27 £/kg. The LCA results for global warming show a favourable reduction in the BECCS case, in which negative emissions of -121.83 gCO_2eq/MJ of jet fuel are achieved, while without CCS case exhibits GHG emissions equal to 15.51 gCO_2eq/MJ; in both cases, the multi-functionality is faced with an energy allocation approach. It is, then, evident the significant environmental advantages of the BECCS process configuration. Nevertheless, financial feasibility can only be attained through the implementation of existing policy schemes and the formulation of new strategies that would reward negative emissions. The application of the UK's policy "Renewable Transport Fuel Obligation" and a hypothetical scheme that rewards negative CO_2 emissions, breaks-even the MJSP at 1.49 £/kg for a certificate and carbon price of 0.20 £/certificate and 246.64 £/tonne of CO_2.

Keywords: Sustainable Aviation Fuels (SAF); Fischer-Tropsch (FT) synthesis; Bioenergy and Carbon Capture and Storage (BECCS); Techno-economic analysis (TEA); Life-cycle assessment (LCA); Greenhouse gas emissions.

4.1 Introduction

In recent years, there has been an important development of SAF production technologies; therefore, the American Society for Testing and Materials (ASTM) has developed the standard ASTMD 7566 to validate the safe use of SAF without the need to modify the airplanes engines. Out of all the certified

processes, the Fischer-Tropsch (FT) pathway has one of the highest TRL (6 to 8) and FRL (7) [3]. The FT process is a well-established technology for the conversion of coal or natural gas-derived syngas to long-chain hydrocarbons, such as liquid transportation fuels. On the contrary, the conversion of biomass through FT requires overcoming some drawbacks, especially those related to the handling of the biomass feedstock and the syngas cleaning-up steps [178]. However, the capacity to treat a wide range of cheap feedstocks increases the attractiveness of the FT pathway [179]. As a consequence, the use of residual lignocellulosic-based biomass, such as agricultural or forestry residues, is promising. Apart from their ability to reduce GHG emissions, these "second generation" fuels avoid the controversy over food versus fuel [4], [29], [30].

The critical literature review of BtL SAF production in Chapter 2 pointed out that techno-economic studies on biomass conversion through gasification and FT have focused on the production of middle distillates rather than just kerosene. FT processes were mostly found to be CAPEX and feedstock intensive, making commercial-scale plants associated with high uncertainty. Environmental analysis through LCA for FT fuels has also been assessed in previous studies, but mostly focused on diesel production. It was found that FT achieves high GHG emission reductions due to energy self-sufficiency and excess power production.

Carbon Dioxide Removal technologies (CDR) have gained interest due to their potential to remove considerable amounts of atmospheric CO_2. BECCS is a promising technology for carbon removal, with applications and studies mostly focused on power generation. However, there is limited discussion about the techno-economic and environmental performances of SAF production within the BECCS concept, as demonstrated in the critical literature review of Chapter 2.

From the literature review, it is evident that there are a plethora of studies assessing the economic and environmental feasibility of liquid fuels produced through the FT process. Nevertheless, few studies have explored the feasibility of FT fuels production from a BECCS perspective. It seems evident that the economic performance of the process is not dramatically affected by the incorporation of the CCS. However, previous studies have failed to provide a detailed LCA that would provide a robust accounting of emissions and a better understanding of the contribution of the different stages of the life cycle of the fuel. At the same time, it is important to state that jet fuel is not the main product of any of the aforementioned studies [73], [94]. Considering this gap in knowledge and the growing importance of both CDR and SAF production technologies, the research in the current chapter seeks to determine the economic and environmental performance of producing SAF from forest residues-derived syngas coupled with CCS. To the best of our knowledge, this is the first attempt to assess comprehensively the economic and environmental performance of a bio-CCS jet fuel production route. The assessments are developed for two scenarios: the baseline scenario (referred to as BECCS)

and the scenario without CCS (referred to as BE). The outputs of these analyses will establish a clear contrast between the advantages and disadvantages of the BECCS configuration for the production of aviation fuels and can provide meaningful insights to a wide range of audiences, including policymakers and researchers.

4.2 Outline of the research

4.2.1 Goal and scope of the study

The main objective of this chapter is to evaluate the process, economic, and environmental performance of the production of SAF from forest residues using the FT process under the BECCS concept. To this end, a detailed process model is developed in Aspen Plus V10 to obtain accurate mass and energy balances and, therefore, increase the reliability of the TEA and LCA outcomes. A cradle-to-gate economic evaluation for the proposed scenarios, encompassing upstream costs for feedstock production and distribution, is carried out in order to calculate relevant economic indicators, such as the MJSP. Likewise, a WtWa LCA is performed in the software SimaPro. These assessments are developed for both the baseline "BECCS" and the "BE" scenarios in order to estimate trade-offs due to the incorporation of the CCS. Moreover, a sensitivity analysis is applied to determine the parameters with the greatest impact on economic and environmental performances. Finally, the impact of relevant policies on the viability of the proposed process is also investigated.

4.2.2 Capacity of the plant and description of the process

Biomass is identified as an important constituent of the future UK energy grid, and forest residues (FR) are highlighted as one of the main sources of biomass supply [180], [181]. Therefore, this scenario considers FR as the main feedstock for the SAF production process, assuming that it is supplied entirely by the UK's forestry industry. Consequently, the capacity of the plant is fixed by the country's availability of this feedstock. FR originate from the unutilized remaining parts of felled trees, which are generally left in the forest and that include tops and limbs. The below-ground part of stumps and a percentage of the branches and stem tips are left on-site due to sustainability reasons, performing a major role with their anti-erosion effect, their capability of avoiding loss of soil carbon and nutrients, as well as providing habitats [181], [182]. The major advantage of considering FR as the feedstock is that they are not related to any land use change, like some energy crops [94].

In the report elaborated by E4tech [183] for the total availability of sustainable forest residues in the UK, it was determined that 1.35 Mtonnes/year are available, of which 0.8 Mtonnes/year originate in Scotland. The same report proposed three potential locations for an advanced biofuel production

plant, all of them placed in Scotland due to its high forest residue production capacity as well as the short transport distance between feedstock collection points and potential conversion plants. Therefore, it is assumed that the biorefinery is located in the Solway Firth area owing to its short distance to two of the largest forests of public ownership in the UK (approximately 50km) [183]. Based on this information, the capacity of the SAF production plant is fixed at 20 dry tonnes per hour (0.16 million dry tonnes per year) of FR, a feedstock requirement that could be supplied by the local production.

The UK potential for the storage of CO_2 has been assessed in the past years, reaching the conclusion that the available capacity for at least 600 potential storage sites could go as high as 78 Gt of CO_2 [184], [185]. Most of the storage options are found in offshore saline aquifers, while some depleted hydrocarbon fields are also available; both options are primarily located in Scotland [186]. A major disadvantage of the facilities that are most suitable for CCS projects is their large size, which makes their usage less likely to be quickly expanded for strategic projects. In this sense, the Hamilton store (with a storage capacity of 5 Mtonnes/y of CO_2) located in the East Irish Sea has been proposed as the best candidate for relatively small-scale CCS projects [184] such as the proposed SAF scenario. Another advantage of this location is the distance to the process plant, as it is below 200 km and no additional electricity for recompression is needed [187].

4.3 Methods

4.3.1 Process design and modelling

4.3.1.1 Basis for process design

Aspen Plus V10 was used to create the process models of the proposed scenarios with the aim of obtaining detailed mass and energy balances. The main thermodynamic property package "Redlich-Kwong-Soave-Boston-Mathias (RKS-BM)" was assigned to the overall process plant as this method is widely applied for gas processing, refinery, and petrochemical applications [188]. Nevertheless, the CO_2 capture plant used a different thermodynamic package, i.e., "ELECNRTL", in order to represent the ionic interactions of the electrolytic species associated with the amine solvent [188]. Ash and biomass were considered non-conventional solids without particle size distribution (PSD), while char was modelled as a conventional solid. The ultimate and proximate analysis of the feedstock can be found in Table 4-1.

Table 4-1: Proximate and ultimate analysis of forestry residues [189].

Proximate analysis (mass %)	**Wood**
Moisture (as received)	30.00
Fixed carbon (dry basis)	17.16
Volatile matter (dry basis)	82.29
Ash (dry basis)	0.55
Ultimate analysis (mass %)	
Carbon	50.54
Hydrogen	7.08
Nitrogen	0.15
Sulphur	0.57
Oxygen	41.11
Ash	0.55

Most of the reactors were modelled based on operating conditions and efficiencies obtained from experimental and pilot plants documented in previous studies. However, the pyrolysis and gasification sections were modelled in a more comprehensive way. Experimental correlations and kinetic expressions were used with the intention of producing mass and energy balances that can accurately reflect the operation of a dual fluidised bed gasifier (DFBG) at industrial level.

4.3.1.2 Process design

Figure 4-1 depicts the boundaries that were considered for the process modelling and the economic analysis of the BECCS scenario. A more comprehensive description of the approaches used in the Aspen Plus modelling, the operating conditions, and detailed process flow diagrams are explained in the following sections. The BE scenario has a similar process configuration, with the only difference being that it does not include a CO_2 compression section.

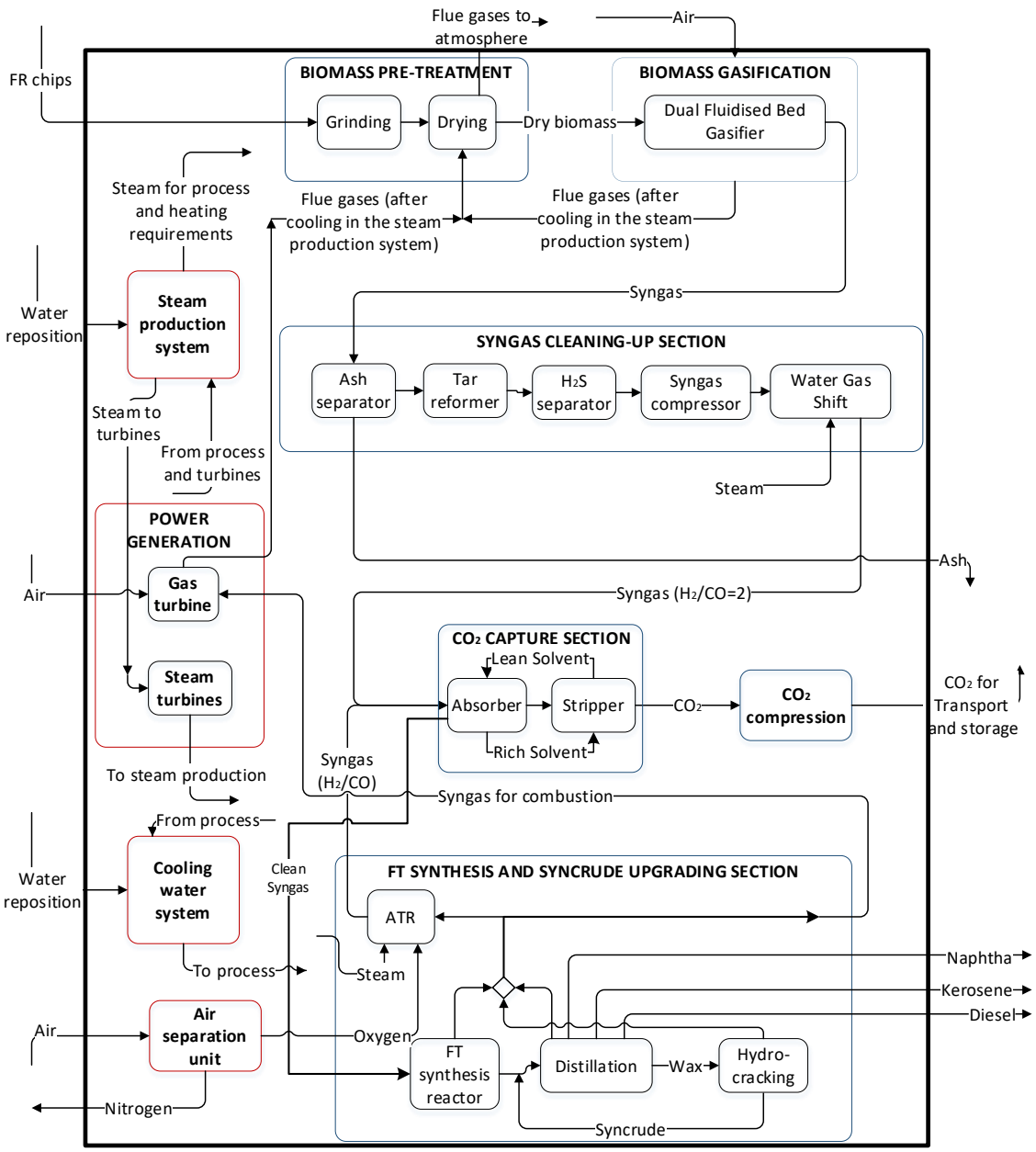

Figure 4-1: Block flow diagram of the BECCS scenario. The boundaries include the units that have been modelled in Aspen Plus. Also, the same boundaries have been used for the economic assessment.

1. **Biomass pre-treatment:** This section aims to adjust the feedstock properties so that they are suitable for the normal operation of the gasifier. The process starts with the mechanical particle-size reduction of the FR chips in a hammer mill, for which the associated work for attaining a 2 mm particle size is determined by using Equation 4-1 [190]. Subsequently, the biomass is dried in order to reduce its water content from 30% to 10% (w/w) [51]. The Aspen Plus model of the dryer

consists of a calculator that controls the conversion of the biomass moisture content to water in a RSTOIC reactor; the drying agent is the flue gases coming from the CHP unit at 120 °C [191].

$$Energy\left[\frac{kWh}{ton}\right] = 5.31 * size^2 - 30.86 * size + 55.45$$

(4-1)

2. **Gasification section:** The DFBG consists of two separate compartments, as explained before. The pre-treated FR enter the first compartment for gasification with steam, while the unreacted char is sent to the second bed for combustion. Heat is transferred to the first compartment (for the endothermic reactions) by circulating the inert bed particles [32]. Due to the absence of a DFBG in the library of Aspen Plus, the pyrolysis, gasification, and combustion sections were decoupled for modelling purposes [53], [192], as depicted in Figure 4-2. Ash and biomass were considered non-conventional solids without particle size distribution (PSD), while char was modelled as a conventional solid.

   The pyrolysis chemistry was modelled in accordance with the correlations depicted by Arora et al. and Abdelouahed et al. [53], [192]. Complete biomass pyrolysis was assumed inside a conversion reactor, in which the dried particles are in contact with the inert bed particles and the reactions are held at a constant temperature, i.e., 870 °C [192]. Generally, the equilibrium Gibbs minimization approach is used to predict the pyrolysis products yield; however, this model uses Equation 4-2 [193], in which the parameters a, b, and c for each component were obtained from relevant experimental studies [193]. The values of these parameters are shown in Table A-1 of APPENDIX A-1, along with the Fortran code (APPENDIX A-2) containing these correlations, which is coupled to the Aspen Plus conversion reactor.

$$Y_i = aT^2 + bT + c$$

(4-2)

   Where Y_i is the mass yield (based on anhydrous ash-free biomass) of each pyrolysis product, and T is the sand temperature (in Kelvin) in the pyrolysis zone. Ash is considered inert, biomass water moisture is added to the amount predicted with the above equation, and char mass yield is calculated by difference in order to perfectly close the mass balance. Ten tar species are produced; however, the developed model grouped them into four groups, including “benzene” (benzene), “phenol” (phenol and cresols), “toluene” (toluene, xylene, and indene), and “naphthalene” (naphthalene, 1+2methylnaphthalene, acenaphthylene, and phenanthrene) [192].

   A cyclone is used to split the char produced in the pyrolysis section [53], of which 5% is sent to the gasifier bed and the rest to the combustion chamber, where it is burnt with excess air at a constant

temperature of 965 °C [53]. The combustion chamber was modelled using an equilibrium Gibbs reactor where the exit products are fixed as CO_2 and H_2O, mainly [191]. It is important to mention that the heat generated in this section is enough to be provided to the endothermic sections of the gasifier.

The pyrolysis products and an appropriate amount of steam are then fed into the gasification bed, which is modelled as a plug-flow reactor (PFR) (represented by a user model unit in Aspen Plus). The selected gasification reactions, along with their kinetic expressions, are detailed in Table A-2 of APPENDIX A-1 [53]. The mass balance of the gasification section is then obtained by solving a system of differential equations representing the gasification kinetics. This was performed through the Aspen-Excel-Matlab interface that was explained in the methodology chapter. The Matlab code is attached to the APPENDIX A-3. It was assumed that the PFR operates at a constant temperature of 891 °C with a steam-to-fuel ratio (kg of steam per kg of dry biomass) equal to 0.4 [53]. Figure 4-2 summarizes the mass and energy interactions described in this section and shows the gasifier's configuration for modelling purposes in Aspen Plus.

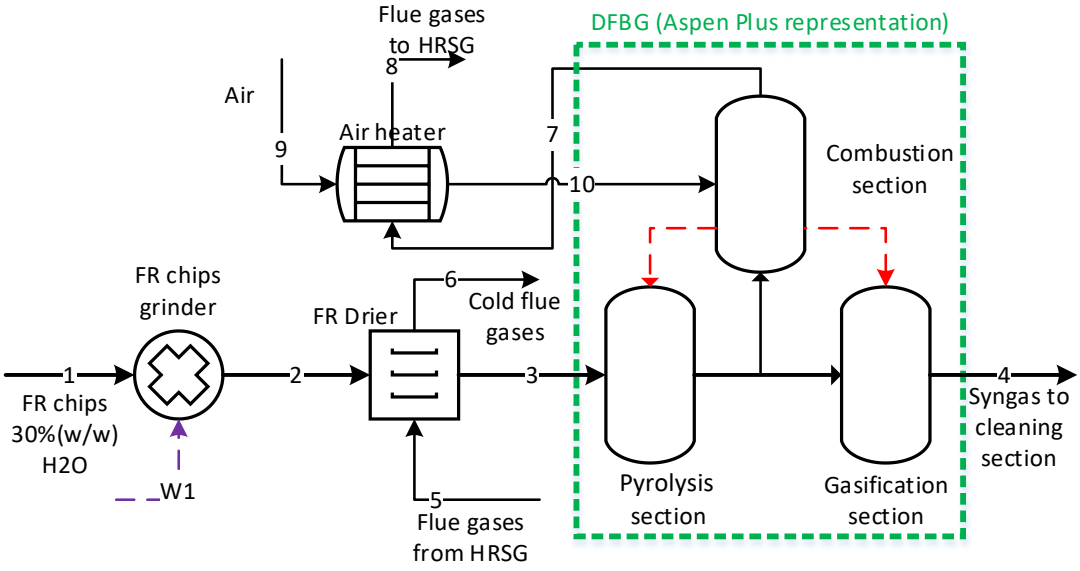

Figure 4-2: PFD for the biomass pre-treatment and gasification sections.

3. **Syngas cleaning-up and upgrading sections**: The goal of the cleaning section is to reduce the pollutant content that could have major effects on downstream catalytic units, such as the RWGS and FT reactors. The advantage of using wood-derived biomass is that the level of contaminants is relatively low when compared to other biogenic residues, and therefore pollutants such as NH_3, H_2S, HCl, and sulphur-containing compounds are most probably found in low concentrations [194]. Nevertheless, regardless of the feedstock quality, tars are unavoidably produced, especially due

to the relatively low operating temperature of the DFBG [195]. Considering the potential damage to downstream applications, particular interest must be paid to the selection of the tar removal technology [194]. The syngas cleaning section includes the following operating units: 1) Ash separator; 2) Tar and methane reformer [196], [197]; 3) ZnO bed for H_2S removal [166], [198]; 4) WGS reactor, to adjust the ratio H_2/CO to 2.1 [30]. Once the syngas is free of pollutants, it is compressed from atmospheric pressure to 2.5×10^6 Pa (25 bar) [70], [199].

Initially, the ash is removed by a cyclone represented by a "component separator" from the models available in Aspen Plus, assuming that all the ash is separated. For the tar removal, a high-temperature tar cleaning technology is selected since it can improve the energy efficiency of the system by avoiding unnecessary energy losses derived from cooling and reheating [200], [201]. For instance, the chosen technology is based on the catalytic reforming principle [197], in which the tars are converted to CO and H_2, while some methane reformation (50% of it) and ammonia decomposition occur at the same time. The reformer operates at constant temperature and is represented by an RStoic block. Due to the endothermicity of the reactions taking place inside this reformer, 10% of the syngas is burnt in order to provide the heat. Finally, hydrogen sulphide (H_2S) is removed in a zinc oxide adsorption unit with a ZnO bed, in which a reaction of desulphurisation takes place ($ZnO + H_2S \rightarrow ZnS + H_2O$) [166], [198]. It is assumed that 100% of H_2S is removed.

At the exit of the cleaning section, the ratio H_2/CO is adjusted to a value of 2.1 [30]. For this purpose, the process proposed by Scott et al. [199] was adapted herein. Syngas free of pollutants is compressed and fed to a water gas shift (WGS) reactor, which is modelled by using three adiabatic equilibrium reactors in series. Steam enters the first reactor, and its mass flow is regulated by a manipulator in order to obtain the desired H_2/CO ratio, i.e., 2.1 [199]. This process section is described in Figure 4-3.

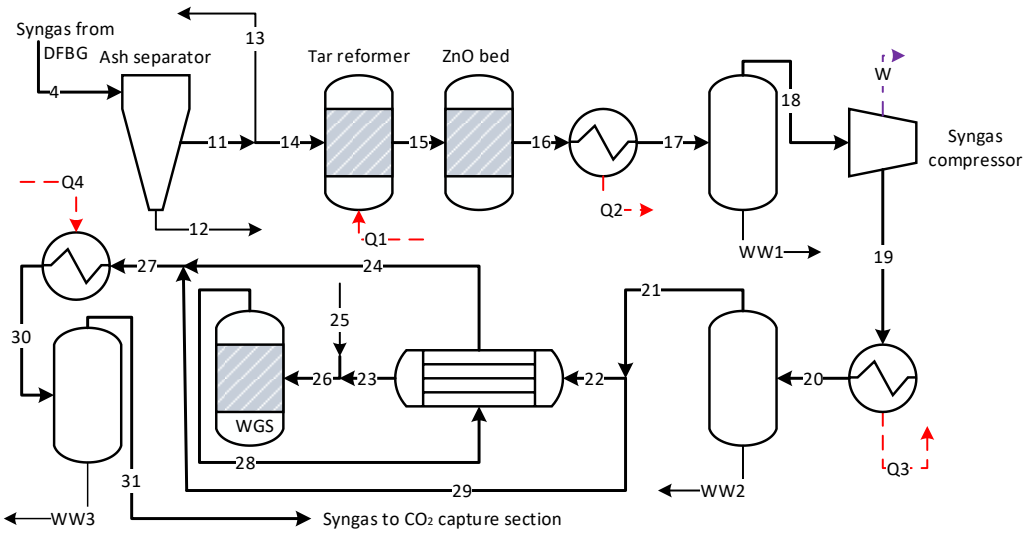

Figure 4-3: PFD for the syngas pre-treatment section.

4. **CO_2 capture plant:** The CO_2 capture process is mainly comprised of a CO_2 absorption column and a MEA regenerative stripper, throughout which circulates a solution of monoethanolamine (MEA). The absorption column operates at high pressure (2.5×10^6 Pa pressure at the feed inlet), while the stripper column operates at low pressure (2.5×10^5 Pa), and therefore the pump work is higher than in an atmospheric process configuration [202].

   A rate-based absorption model was implemented on Aspen Plus for the modelling of the CO_2 capture section [203], while considering the ELECNRTL as the thermodynamic property package. It is assumed that the capture plant separates 90% of the available CO_2 [70], [199], [204], [205] since a higher capture level could compromise the energy efficiency of the plant [205]. The process described in this section is shown in Figure 4-4.

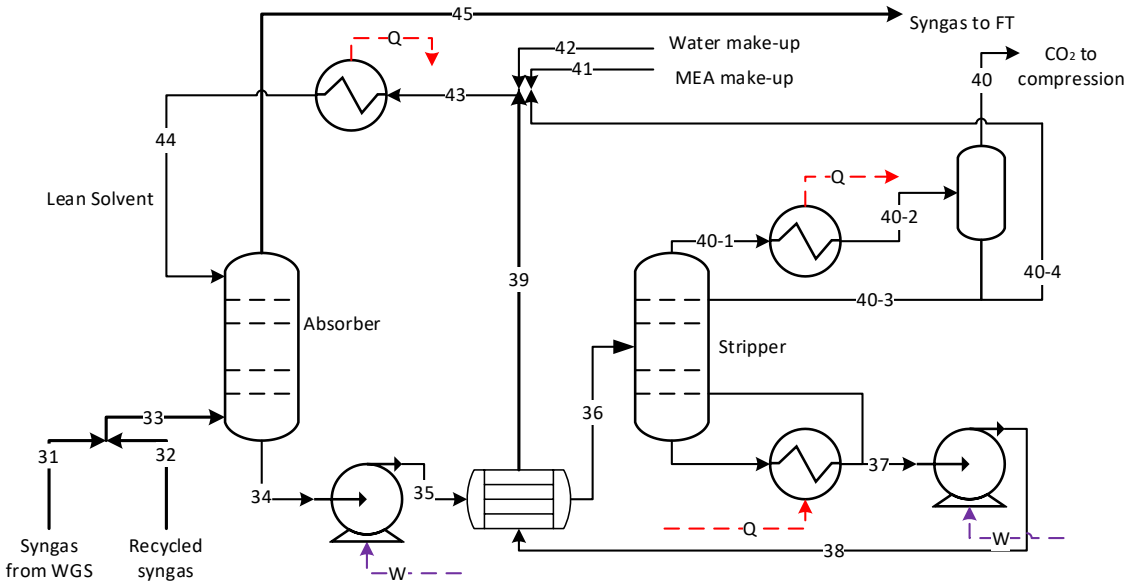

Figure 4-4: PFD for the CO_2 separation process.

5. **CO_2 compression section:** As depicted in Figure 4-5, this section aims to adjust some properties, such as pressure or moisture content, of the captured CO_2 so that it can be safely transported and stored. For this purpose, the CO_2 passes through a series of operating units, as depicted in Figure 4-5. Initially, the CO_2 goes through a multi-stage compressor with intercooling stages that help in keeping the temperature at 80 °C and reducing the moisture content (since the condensed water is separated from the gas stream) [196], [199]. Later, in another multistage compressor, the CO_2 is compressed to 8×10^6 Pa (80 bar), which is already above its critical pressure of 7.38×10^6 Pa (73.8 bar). Finally, this stream is cooled to 30 °C so that it is in a liquid state, and immediately afterwards, a pump increases the pressure of this liquid CO_2 until it reaches 1.53×10^7 Pa (153 bar), which is the required pressure for transport by pipeline [187], [199].

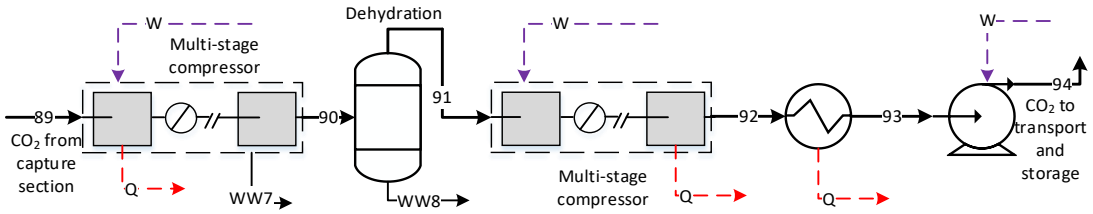

Figure 4-5: PFD for the CO_2 compression section.

6. **FT synthesis:** As explained in Chapter 2, in order to obtain long-chain hydrocarbons, the operating conditions of the synthesis reactor were selected as 240 °C and 2.5×10^6 Pa (25 bar), using a cobalt-based catalyst [54]. The reactor of slurry type was selected for the process due to its advantages in terms of simple configuration, and ease of temperature control, since the heat of the

exothermic reactions is removed by generating medium pressure steam [70], [206]. The model assumes that the CO conversion per pass is equal to 40% and that only alkanes are produced [70]. The product distribution (in mole fraction of each hydrocarbon $y_{N_C,n}$) is estimated by the ASF correlation (Equation 4-3). In this expression, alpha (α) represents the chain growth probability and assuming the value of 0.9 the synthesis reactions are oriented towards jet fuel production [70]. This model was implemented in Aspen Plus by using a conversion reactor linked to a calculator in which C_1 to C_{20} are defined as independent chemical compounds, while C_{30} is used to represent long-chain hydrocarbons [70], [199].

$$y_{N_C,n} = (1-\alpha)\alpha^{N_c-1}$$

(4-3)

7. **Syncrude upgrading section:** The FT product is sent to a series of separators, where three phases are obtained: gaseous hydrocarbons (C_1, C_2, C_3, mainly), liquid hydrocarbons (C_5-C_{30}) and water. The liquid hydrocarbons head to the upgrading section, while a portion of the unreacted syngas is sent to a combined heat and power (CHP) unit; in this way, the accumulation of inert gases in the recycling loop is avoided. A value of 15% has been chosen as this amount of gas can raise electricity that can match the power demand of the biorefinery. The remaining unreacted syngas fraction is treated in an autothermal reforming reactor (ATR) and then recirculated to the CO_2 separation section, where it is treated before being sent back to the FT reactor; as a consequence of the recirculation, the global conversion of CO increases.

   The liquid fraction of FT products, also known as syncrude, enters the atmospheric distillation column with the aim of being split into different hydrocarbon commercial mixtures of different boiling points. The partial condenser located at the top of the column produces a gaseous and a liquid distillate. The gas stream, consisting mainly of C_1, C_2, C_3, and some C_{4+}, is recycled into the process along with the unreacted syngas exiting the FT reactor. The liquid distillate is equivalent to the gasoline fraction, which is mainly made up of C_5 to C_7. A few stages below the top of the column, the jet fuel fraction (C_8 to C_{16}) is recovered, and, further down, the diesel fraction (C_{17} to C_{20}). Finally, heavy hydrocarbons (C_{21+}) or waxes are extracted from the bottom of the column. The atmospheric distillation column in Aspen Plus was modelled by using a series of "RadFrac" distillation columns, where light and heavy keys are fixed along with their recovery fractions.

   For the proposed SAF production scenario, wax is not a desired product, and to maximise jet fuel production, a hydrocracking unit is incorporated into the process. The aim of the hydrocracker is to break down long hydrocarbon chains in order to obtain smaller hydrocarbons. The operating conditions, such as temperature, pressure, and H_2 inlet flow, define the severity of the

hydrocracking reactions and, therefore, the product distribution. This work adopts the operating conditions proposed by Teles et al. [207], i.e., 5×10^6 Pa (50 bar), 277 °C, and 1.5% of H_2 in the reactor inlet stream, in order to favour mild hydrocracking that leads to the production of middle distillates. Theoretically, this operation mode allows a complete conversion of the waxes with an assumed average product distribution of 50% of jet fuel, 30% of diesel, 15% of gasoline, and 5% of light gases (all on a mass basis) [58], [69], [70], [207], [208]. The necessary hydrogen for the reactor is recovered from a fraction of the syngas stream that is directed to the FT synthesis reactor [199] through a pressure swing absorption unit (PSA). In Aspen Plus, the hydrocracking reactor was modelled using a stoichiometric reactor, where the product distribution defines the fractional conversion of the hydrocracking reactions. For the PSA, a common separator was used with a H_2 recovery efficiency of 70% [209]. The liquid stream produced in the hydrocracking reactor is recirculated to the atmospheric distillation column, where it is mixed with the syncrude before entering the column.

The mixture resulting from the combination of the unreacted syngas and gaseous hydrocarbon fractions obtained from the hydrocracker and the distillation column contains high amounts of CH_4 and other volatile hydrocarbons that have to be treated prior to recycling to the FT unit. To this purpose, an ATR reactor is in charge of converting light hydrocarbons into CO and H_2. Compared with steam reforming, ATR has a simpler design and is able to prevent carbon deposition. The differences in the impact of the various syngas reforming technologies on the H_2/CO ratio are small. [210]. In the ATR process, the ratio H_2/CO is adjusted by the flows of steam and oxygen [211]; the latter is produced in an air separation unit (ASU). In Aspen Plus, the ATR reactor is modelled using a Gibbs reactor operating at 950 °C. The heat for the endothermic reforming reactions is provided by the combustion of a fraction of the gases. Therefore, the amount of O_2 will be set by the amount of heat needed. The vapour mass flow is calculated in Aspen Plus by determining a design specification so that the H_2/CO ratio equals 2.1. Finally, the product of the ATR is mixed with the fresh syngas before the CO_2 capture plant, where the excess CO_2 is extracted. The process diagram for this section is presented in Figure 4-6.

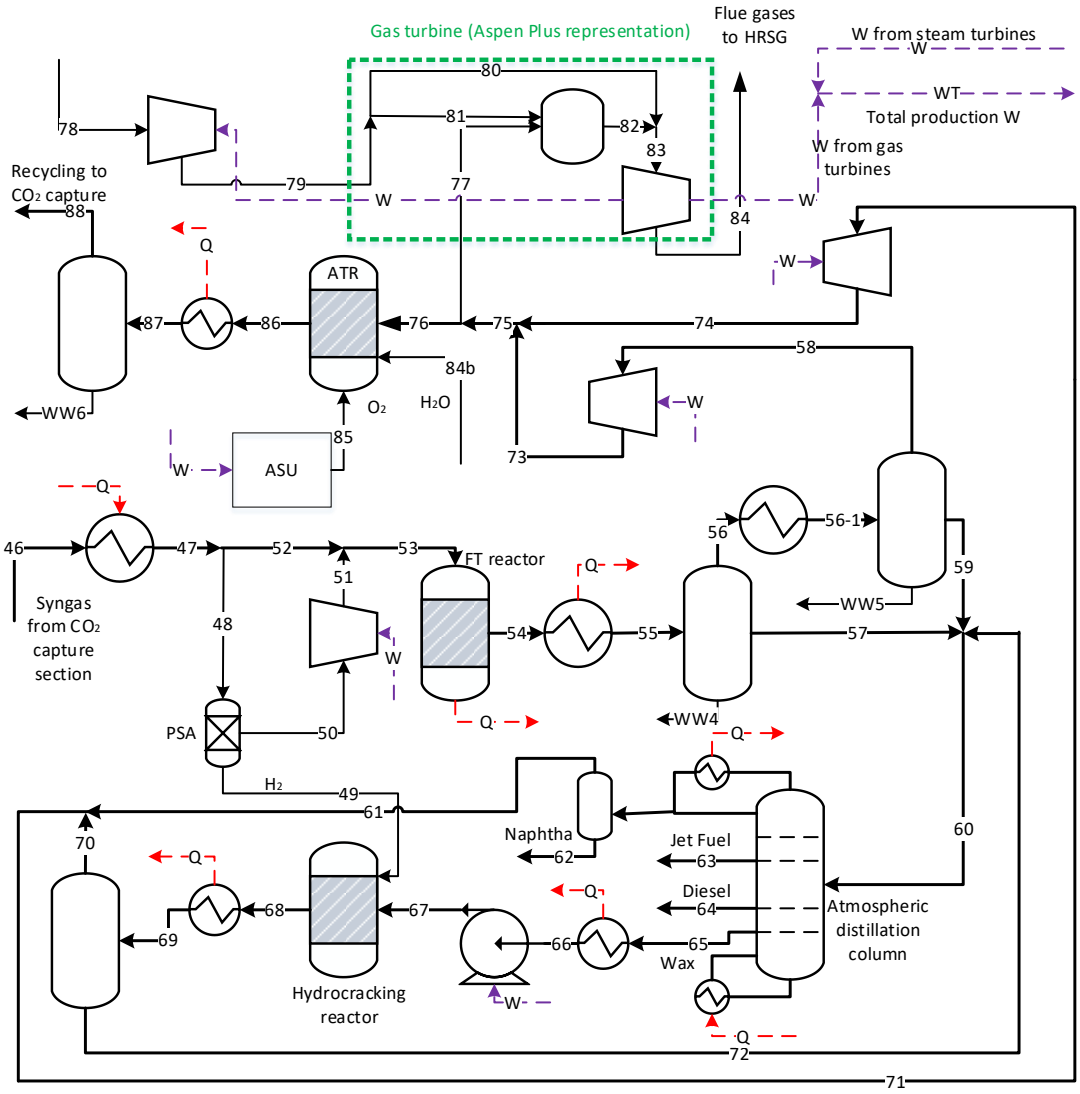

Figure 4-6: PFD for the Fischer-Tropsch synthesis, syncrude upgrading and gas turbine sections.

8. **Combined heat and power (CHP) and cooling water system:** The design of the biorefinery aims to achieve energy autonomy in terms of both electricity and heat requirements. The process is energy integrated since the high-temperature process streams are cooled in heat exchangers, where steam at different conditions is produced, namely superheated steam (500 °C and 5×10^6 Pa), steam saturated at high pressure (215 °C and 2×10^6 Pa), medium pressure (177 °C and 1×10^6 Pa), and low pressure (135 °C and 3×10^5 Pa). Additionally, for further cooling, cooling water is used. The cooling water system is designed by fixing the exit temperature of the water at 25 °C. The system includes a cooling tower to decrease the temperature of the returning cooling water. A 5% water loss is assumed to account for drift, evaporation, and blow-down losses [212]. Subsequently, the steam generated in the different processes is sent to the plant to cover the heat

requirements (distillation columns, heat exchangers, e.g.). The remaining steam fraction is used in low, medium, and high pressure steam turbines to generate extra electricity.

As mentioned in the previous section, a gas turbine is coupled to the process, where 15% of the recycling gas is combusted [70]. Air is compressed and split into two streams: the first fraction, containing 9 to 10% of stoichiometric O_2 excess, is sent to the combustion chamber, which is modelled using an adiabatic Gibbs reactor [213]. The second air fraction aims to cool down the hot gases coming from the combustion chamber until they attain the operating temperature of the gas turbine. It is assumed that the gas turbine technology is normally used for natural gas (GE 7FB) but adapted for syngas combustion. The recommended operating conditions for this turbine are a ratio of mass flow of air through the compressor to mass flow of gas ($\dot{m}_{air\ compressor}/\dot{m}_{gas\ turbine}$) of around 0.91, and an inlet temperature of 1370 °C [214]. Due to the difference in composition between the syngas and the natural gas, the ratio is slightly different and equal to 0.94. However, this value allows the gas turbine inlet temperature to remain below the recommended temperature of 1370 °C.

Furthermore, mechanical, polytropic, and isentropic efficiencies for compressors, turbines, expanders, and pumps assumed in all the explained Aspen models are presented in the following Table 4-2:

Table 4-2: Assumed efficiencies for mechanical unit operations in the Aspen Plus models used in this work.

Unit Operation	Isentropic Efficiency	Polytropic Efficiency	Mechanical Efficiency
Compressors	-	0.850	0.940
Gas Turbines	0.898	-	0.988
Expanders	0.898	-	0.988
Steam Turbines	0.875	-	0.983
Pumps	-	-	0.800

4.3.2 Economic Evaluation

4.3.2.1 System boundaries of the economic assessment

This section delivers a cradle-to-gate analysis, which is also represented by the boundaries of the block diagram in Figure 4-1, which includes the following sections: 1) biomass pre-treatment; 2) biomass gasification; 3) syngas conditioning and cleaning section; 4) CO_2 capture and compression; and 5) gas and steam turbines. It is important to mention that the production of the forest residue chips has not been modelled; however, the associated costs of harvesting, chipping, and transporting them to the

processing plant are included in the price of biomass "as received". The cost of transport and storage of CO_2 is considered part of the VC for the OPEX calculation.

4.3.2.2 Basis for the Economic Evaluation

The main purpose of the economic assessment is to estimate economic indicators of great importance, such as CAPEX, OPEX and MJSP. The MJSP of SAF is the selling cost at which the NPV is equal to zero, at an IRR of 10% [35], [68]. A typical discounted cash flow analysis (DCFA) is used to determine the MJSP, whose financial parameters and assumptions, such as the discount rate, depreciation method, income tax rates, plant life, and construction start-up period and so on, are detailed in Table 4-3. The methodology followed for the economic assessment is described in more detail in Section 3.2. The PEC for the components of the process plant of the BECCS and BE scenarios are detail in Table 4-4. Similarly, the variable costs for the OPEX estimation are presented in Table 4-5.

Table 4-3: Parameters for conducting the discounted cash flow analysis [70], [196].

Location	United Kingdom
Plant life	20 years
Currency	£
Base year	2019
Plant capacity	20 dry-tonnes of FR/h
Discount rate	10%
Tax rate	30%
Construction period	3 years
First 12 months' expenditures	10%
Next 12 months' expenditure	50%
Last 12 months' expenditures	40%
Depreciation method	Straight line
Depreciation period	10 years
Working capital	5% of FCI
Start-up time	6 months

Table 4-4: Purchased equipment costs at base capacity and year of reference.

Equipment	Base cost [MM £]	Base capacity	Unit	Scaling factor	Base year	Reference
ASU	147.535	145	kg/s O_2	0.50	2014	[215]
ATR	13.028	12.2	kg/s total feed	0.67	2014	[215]
Biomass receive and unload	1.751	198.1	wet t/h	0.62	2007	[216]
Biomass storage, preparation, feeding to atmospheric gasifier	1.294	64.6	wet t/h	0.77	1999	[217]
Compressor	0.395	413	kW	0.68	2014	[218]
Cooling tower	2.422	4530.3	kg/s	0.78	2014	[215]
Cyclone	0.040	1	m^3/s total gas	0.70	2014	[218]
DFBG	9.184	100	$MW_{th,LHV}$ at moisture content of 20%	0.72	2010	[157]
Drier	5.064	1	air or hot gas m^3/h	0.8	2003	[157]
FT-REACT	153.607	2,420	MW of fuels produced	0.75	2011	[216]
Hydrocracker	6.233	1.13	kg/s (feed mass flow)	0.70	2014	[218]
Isomerization	16,288	1	t product/year	0.62	2015	[219]
PSA	4.710	0.294	kmol/s purge gas	0.74	2014	[218]
Steam turbine	0.274	10.5	MW	0.44	2014	[218]
TAR-REF	0.682	12	Nm^3/s	0.6	2010	[157]
WGS reactor	2.224	150	kg/s total feed	0.67	2014	[218]
ZnO guard bed	0.016	8	m^3/s total gas	1.00	2014	[218]

Table 4-5: Variable Costs for the OPEX estimation.

Variable Operating Costs	Value		
A) Feedstock			
	Price		Reference
Chips of FR	58.53 £/t		[220]
B) Utilities			
	Price		Reference
Ash disposal	20.218 £/t		[58]
CO_2 T,S&M	19 £/t		[196]
Waste water treatment	0.415 £/t		[58]
Cooling water	0.025 £/t		[196]
Feed boiler water	0.784 £/t		[58]
C) Catalysts			
	Price	Lifetime [years]	Reference
FT synthesis	16 £/kg	3	[221]
Tar Reformer	3% of VC	3	[196]
Wax hydrocracking	18 £/kg	3	[221]
WGS	13,836 £/m3	3	[221]
PSA	0.85 £/kg	3	[166]
ATR	42,452 £/m3	3	[222]

4.3.3 Life Cycle Assessment (LCA)

The LCA is constructed by the sequence of four main steps, following the standardized methodology of ISO 14040 and 14044 [168], as explained in Section 3.3.

4.3.3.1 Goal and scope definition, functional unit

The goal of the LCA of this study is to assess the environmental sustainability of processing forest residues for jet fuel production via gasification and Fischer-Tropsch coupled with CCS. To quantify the global warming potential (GWP) of the whole supply chain of these processes, a WtWa LCA was performed. The impact of adding CCS was measured by analysing the same scenario but without the capture of CO_2 (BE scenario), and finally, the results of both analyses are compared against the GWP of conventional jet fuel. The selected functional unit is 1 MJ of SAF while the LHV of the SAF is considered to be 42.8 MJ/kg [98]. It is assumed that the process plant is located in the UK.

4.3.3.2 System boundaries for the LCA

The boundaries of the LCA section are broader than those of the techno-economic analyses (TEA), and this is because the latter only focuses on the conversion process. Figure 4-7 shows in detail the stages considered in this environmental assessment: i) Production and chipping of forest residues through

sustainable forest management; ii) Transport of feedstock to the process plant; iii) Conversion of forest residues into SAF (gasification and FT); iv) Compression, transport, and storage (T&S) of CO_2; v) Transport and distribution of SAF, and vi) Combustion of SAF. At the same time, these limits also expand towards the production and transport of the secondary material inputs and energy required by some stages of the life cycle. Since the LCA of this SAF production process considers the emissions from the field where the feedstock is collected until the wake of the aircraft, this analysis is of the WtWa kind [67].

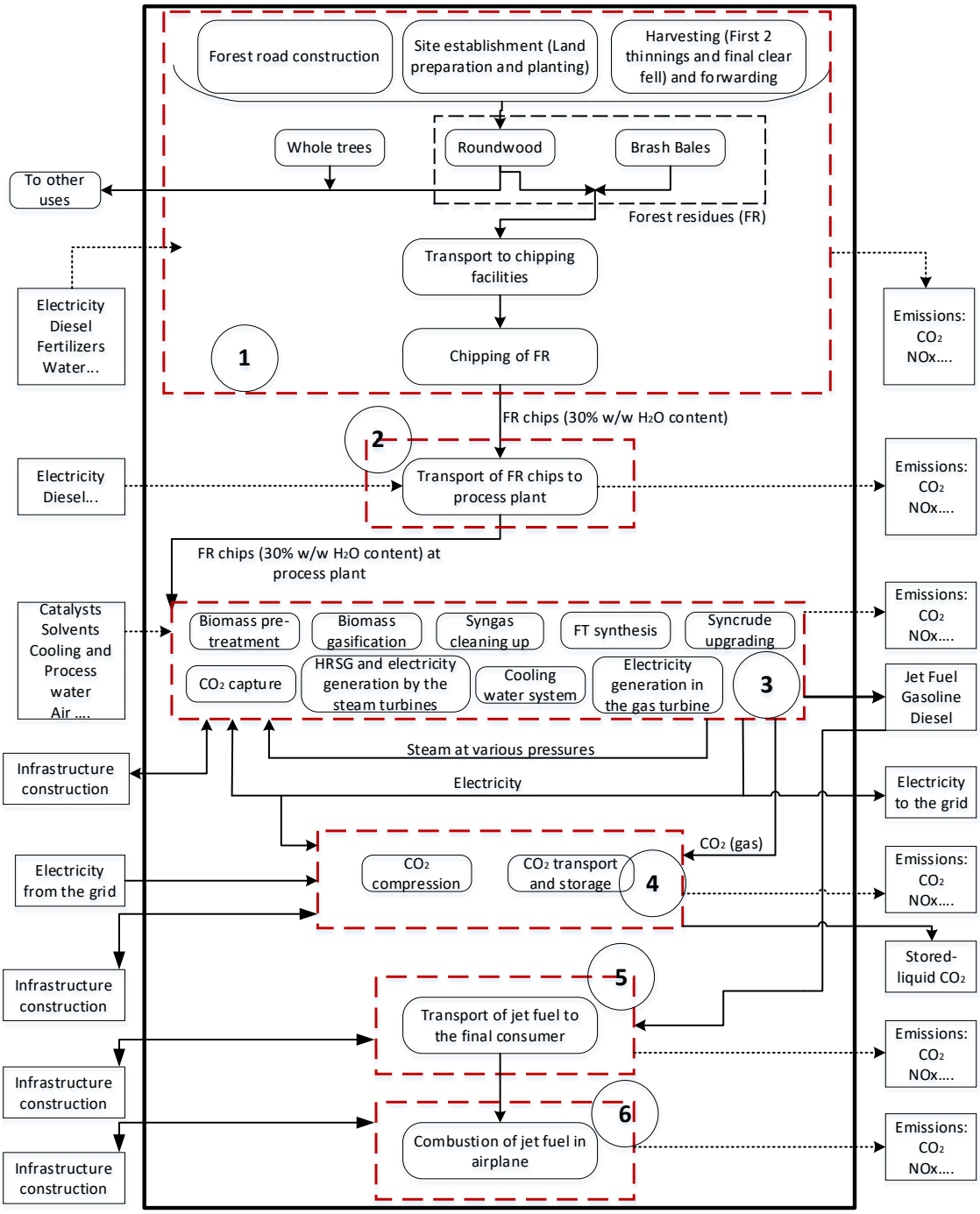

Figure 4-7: The System Boundary Diagram for the LCA of the BECCS scenario.

4.3.3.3 Life cycle inventory (LCI) and description of the life cycle stages

The elaboration of the LCI for this study is based on two main sources. The first data source, as depicted in previous sections, is the mass and energy balances, resulting from the process modelling in Aspen Plus. This data includes the normalized values (for 1 MJ of jet fuel) for the conversion of the main feedstock into jet fuel and the secondary products (gasoline, diesel and electricity). Seemingly, the data contains information about the different emissions and waste streams generated in the conversion process. The second data source is the inventories of the "Ecoinvent-3" database. The inventories of the system stages depicted in Figure 4-7 are detailed in the APPENDIX A-4, however, their construction are explained as follows:

Stage 1 of the life cycle in Figure 4-7 depicts the production of FR chips, which are mainly composed of whole tree early thinning, small roundwood, stem tips, and branches. The FR chips are considered co-products of the timber production process [180], [223]. To achieve more complete and reliable mass and energy balances, the life cycle inventory of this stage is taken from Ecoinvent 3.6 [224], [225]. The generic sustainable forest management database analyses the production of different wood products over one stand's rotation period, including site preparation and all processes associated with forest management such as clearing, tending, pruning, thinnings, harvesting operations, and the maintenance of forest roads [226]. The three produced assortments, which are sawlogs, industrial wood, and wood fuel (which is further processed into chips and cleft timber), are allocated according to the environmental load of the aforementioned activities, according to their economic values [224]–[226]. Ecoinvent offers regional and tree-species-adjusted databases since the assortment distribution varies depending on the tree species and the regional markets. For more processed assortments, such as wood chips, the database "Wood chips, wet, measured as dry mass {RoW}| sustainable forest management | Cut-off, U" is chosen. Apart from including the production of the basic wood assortments, this database also includes the processes for further processing wood fuel into chips. The wood chips production stage ends with their natural drying on the forest road before transportation to the process plant [226].

It is also important to mention that a fraction of branches and stem tips should remain in the forest site due to sustainability reasons [180], [182], [227]. However, there is no existing threshold that determines the FR percentage that should be left on-site in the UK [227]. Therefore, the data presented in the selected Ecoinvent inventory for wood chips is also adopted in this study. The chosen database does not present this information as the amount of FR that are left on-site, instead, it provides the amount of wood assortments harvested per hectare of stand over one rotation period (in accordance with the prevailing principles of sustainable forest management practices in Europe)

[226]. As mentioned before, the environmental loads of the stand establishment, management, and harvesting steps are distributed among the wood assortments, therefore, FR left onsite are not attributed with any environmental impact [224]–[226]. Because the wood chips production databases are elaborated according to the sustainable forest practices of Germany [226], [228], [229], the assortment distribution and the amount harvested could fail to exactly represent the UK's practices, and the environmental load of the FR chips could be slightly different. For this reason, the GWP of the stage of wood chips production is included in the sensitivity and uncertainty analysis of the LCA.

Finally, in this study, the tree species that give origin to the forest residues were chosen according to the data on wood production presented by the UK's Forestry Commission estimation for 2018 [230]. In agreement with this source, 93.2% of the roundwood comes from stands of softwood, while 6.8% comes from hardwood; herein, the same share is considered for the wood chips. Sitka Spruce and Oak are the tree species representing softwood and hardwood, respectively, since they represent a higher proportion of the stands found in the UK [231].

Stage 2: The second phase of the life cycle consists of transporting the chips to the process plant by road, since this is the most common mode for the carriage of commodities in the UK [232]. Similarly to stage 1, the transport of forest residues is taken from the database presented by Ecoinvent [233] but slightly modified to fit the conditions of this study. Originally, this database considered that each kg on a dry basis of forest residue chips contained 1.4 kg of H_2O, and the transport distance to the processing plant was 50 km. In this study, it is considered that the chips are left in their place of production until their moisture content naturally reduces to 30% (0.43 kg of H_2O for each kg of dry biomass) [223], [234]. The average transport distance of the forest residues is considered to be 50 km [183]. In addition, if the requirements of the plant could not be satisfied by the regional provision of forest residues, the transport distance is another parameter to consider for the sensitivity analysis.

Stage 3: The third stage of the life cycle begins with the reception of forest residue chips and ends with the final production of fuels and electricity. In this section, the inventory is built from the mass and energy balances resulting from the modelling of the process. However, not all the material inputs are obtained from Aspen Plus and therefore, some rough estimations have been made. The amount of catalyst required for the different catalytic reactors is calculated according to data from the literature, and it is considered that they will be changed every 3 years. There are no life-cycle inventories for the production of the catalysts, but they are represented in the inventory by considering the production of the main constituent of the catalyst, and therefore, the amount of this material is equal to the total mass of its catalyst. In regards to the operation of the gasifier, the fluidising medium is sand, and its reposition ratio is taken from a database of wood gasification in a

fluidised gasifier found in Ecoinvent [235]. The construction of the process plant is represented by the inventory related to a generic "Chemical factory organics" that can be found in Ecoinvent. For this plant, the capacity is about 50,000 t/year (PC_1) with a lifetime of 50 years. To adjust to the process plant, a six-tenths factor rule was applied (Equation 4-4) [236] in order to find the fraction of the original Ecoinvent plant (PU_1) that is needed for this process (PU_2), considering the capacity (PC_2) equal to the sum of the gasoline, diesel, and jet fuel mass flows and a plant's lifetime of 20 years.

$$PU_2 = PU_1 \left(\frac{PC_2}{PC_1}\right)^{0.6} \quad \textbf{(4-4)}$$

Stage 4 represents the compression of the CO_2 coming from the capture section of stage 3 and its transport & storage. The compression section uses electricity produced by the plant, and for the infrastructure, the inventory for "Air compressor screw type of 300kW" available in Ecoinvent is used [237]. In line to the infrastructure considerations of stage 3, Equation 4-4 is used to adjust this database according to the energy requirements (instead of capacity) of each compressor.

In regards to the CO_2 transport & storage subsection, the life-cycle inventory is developed as proposed by Wildbolz (Figure 4-8) [187]. The inventory of the "Transport infrastructure" considers the construction of the pipeline by considering the materials needed, the construction and land use, the dismantling and disposal at the end of the lifetime of the pipeline, as well as the monitoring of the operating pipeline by helicopter. Wildbolz [187] also considered an overpressure of 3×10^6 Pa (30 bar) with respect to the place of injection (gas field or aquifer). According to their calculations, the operation of the pipeline, considering a distance of 200 km, does not need a recompression station since the CO_2 stream arriving at the injection point meets the overpressure requirement. Therefore, the inventory of the operation section only considers the infrastructure construction and the leakage, which is 0.026% per 1000 km. Another important section is the "Deep Drilling and Well infrastructure". Wildbolz [187] considers the establishment of a double well with the option of occupying an aquifer or a depleted gas field. In the UK, saline aquifers have the highest storage option, but the understanding of their properties is highly uncertain; thus, gas fields are preferred [238]. Figure 4-8 depicts the life cycle of the stored CO_2:

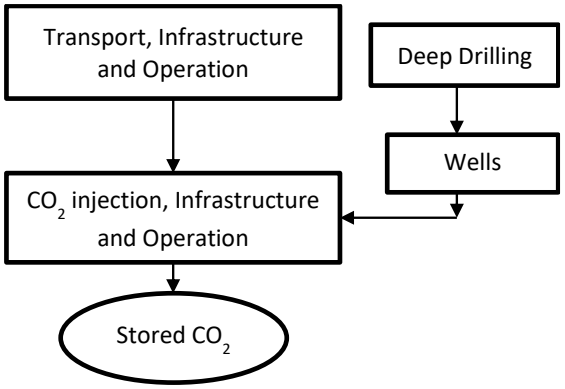

Figure 4-8: Scheme of the transport and storage chain [187].

Stage 5: This stage encompasses all the processes related to the transport of the fuel from the process plant to the final user and is represented by the database for "Market for kerosene" in Ecoinvent [239]. This database includes the transportation of the fuel, the operation of the storage tanks, and the emissions due to the evaporation and treatment of the effluents.

Stage 6: The last stage of the life cycle is the use of jet fuel in the airplane. The emissions from the combustion of SAF are taken from the database of Ecoinvent for medium-haul aircraft for passengers without considering the incurred environmental impact of the aircraft and airport construction. This assumption is considered valid since the chemical properties of SAF are similar to those of jet fuel [80]. In this stage, it is also important to mention that the carbon neutrality [240] of CO_2 emissions from the combustion of SAF is assumed, which means that biogenic CO_2 emissions are considered to be zero.

4.3.3.4 Multi-functionality

The SAF and the by-products of the process plant are all used for energy purposes; therefore, energy allocation was the main method to be considered in this assessment [79], [83]. Even though there is associated uncertainty, the system expansion or substitution method is also recommended since it considers the environmental impacts of the displaced by-products [79]. In this sense, this method was also applied herein in order to determine the effect of the choice of the attribution methodology on this environmental assessment.

4.3.3.5 Negative emissions

The benefit of using the BECCS concept in a process design is the potential of achieving negative emissions. The negative emissions claimed by the BECCS scenario need to be demonstrated and supported by a LCA. Conventional LCA of systems with biogenic inputs considers that the consumed atmospheric CO_2 is released at the end of the product's life cycle [241]. Therefore, the LCA impact

methods assign a Global Warming Potential (GWP) of zero to biogenic CO_2 emissions. Time plays an important role in the definition of "negative emissions", since CO_2 removed from the atmosphere and the biosphere to storage, is transferred from a short-term cycle to a long-term pool (geological) [242]. According to the 2006 IPCC Guidelines, the calculation and report of the emissions associated with CCS in the energy of industrial sector do not consider any particular difference between CO_2 from fossil or biogenic sources. In this sense, the emissions of the processes using biomass will be zero, while the captured biogenic CO_2 will be subtracted resulting in negative emissions. Emissions from transport, injection and storage of CO_2 are accounted regardless of its fossil or biogenic origin [243].

4.3.4 Sensitivity analysis

The sensitivity analysis was performed according to the methodology described in Section 3.4 and applied only to the BECCS scenario. The following sections explain the parameters that were considered for both the MJSP and the GWP:

4.3.4.1 Sensitivity analysis on the MJSP

Table 4-6 presents the parameters with high uncertainty that were considered for the sensitivity analysis of the MJSP. The CAPEX was changed between a low and a high value of -30% and +50%, according to the recommendations of the classification of the AACE International, for plants of low level of maturity, as in the case of a biomass to liquid fuels process plant [244]. The feedstock price was changed by ±50% with respect to the nominal value in order to reflect the market volatility and uncertainties related to the commercialization logistics of the forest residues [196]. Different values for important economic parameters such as tax and discount rates were also analysed. The discount rate is associated with the risk of investing in a particular project. An optimistic value of 8% was proposed for biorefinery investments [245], whereas the pessimistic discount rate was proposed at 12%. The optimistic tax rate value was set at 0% to reflect a scenario in which the biorefinery may be eligible for tax exemptions, while the higher value was set at 40%.

Regarding the CO_2 T&S, low and high costs of 8 and 31 £/t CO_2 were considered [246]. For a better interpretation, these values are adjusted to include the cost of the CO_2 compression. The cost of the CCS is then obtained by adding the cost of the T&S and the annualised CAPEX of the capture section (see Equation 4-5 [196], where i_d is the internal rate of return and *n* the lifetime of the plant); it should be noted that the electricity for the CO_2 compression is generated on-site, and as such, it is not included in the CCS cost, and the respective energy penalty is captured in the electricity exported to the grid.

$$ACAPEX = CAPEX \cdot \frac{i_d \cdot (1 + i_d)^n}{-1 + (1 + i_d)^n}$$

(4-5)

Table 4-6: Parameters for the sensitivity analysis.

Parameter	Low Value	Nominal	High value	Unit
CAPEX	130.38	186.25	279.38	MM £
Feedstock cost	29.26	58.53	87.79	£/t
CCS cost	13.38	24.38	36.38	£/t CO_2
tax rate	0	30	40	%
Discount rate	8	10	12	%

4.3.4.2 Sensitivity analysis on the GWP

A sensitivity analysis was also conducted for the LCA results to identify the process sections with the greater influence on the GWP of the BECCS scenario. When uncertainty data is not available for life-cycle stages, reasonable ranges have been chosen (see Table 4-7).

Table 4-7: Variables used for the sensitivity and uncertainty analyses.

Parameter	Nominal Value	Units	Variation (%)
Share Jet Fuel (Energy basis)	58.35	%	±10*
FR Chips production	6.04	gCO_2e/MJ SAF	±30
Transport FR Chips	1.30		-30, +200
Biorefinery	3.40		±30
CO_2 compression-T&S (operation + infrastructure)	0.22		±10
CO_2 stored	90	%	-15, +5*
SAF distribution	0.69	gCO_2eq/MJ SAF	±30
SAF combustion	4.36		±10

* percentage points

The share of the jet fuel could be slightly different due to different process conditions and the uncertainty associated (e.g., a different product distribution of the hydrocracker). Therefore, a deviation of ±10% was considered. According to the proposed plant location, the transport distance for the FR chips is 50 km. However, in the event that the required feedstock could not be supplied by the surrounding forests, the possibility of getting it from the northern region of Scotland (a travel distance of about 150 km) was also analysed [183]. An increase in the efficiency of the CO_2 capture plant was also examined through different percentages of CO_2 that could be separated from the

syngas and subsequently stored. Finally, concerning the other parameters of Table 4-7, as explained in the LCA section, they were associated with some level of uncertainty. This decision is based on the fact that their inventories were adapted from existing databases for similar processes and/or for different geographic locations. Therefore, their GWP is also changed between ±30% and ±10%, depending on whether this uncertainty is high or moderate.

4.3.4.3 Monte Carlo Uncertainty analysis

Based on the uncertain parameters considered for the sensitivity of the GWP, a Monte Carlo analysis was performed in Matlab; a code randomly varied these parameters and recalculated the GWP of the system in 10,000 trials. The results are presented as a histogram of frequency, for which the mean value is calculated as well as the standard deviation; finally, it is possible to determine the 95% confidence interval.

4.4 Results and discussions

This section reports in detail the TEA and LCA results for both the BECCS and BE scenarios. Firstly, the technical parameters in conjunction with the mass and energy balances are presented. Subsequently, the economic and environmental performance indicators are presented. Finally, a sensitivity analysis determines the impact of different parameters on the economic and environmental results of the BECCS scenario, as well as the effect of the plant capacity (economies of scale). Additionally, the effect of policy schemes on the feasibility of the SAF produced through the BECCS scenario is investigated.

4.4.1 Process modelling

4.4.1.1 Gasification and pyrolysis section

The predicted composition of the syngas obtained through the modelling methodology described for the gasifier and pyrolysis sections is presented and compared with the experimental data, found in a report of E4Tech [247], in Table 4-8. From these results, it can be inferred that there is a good agreement between the results obtained from the model and the pilot plant outputs [247], especially concerning the major components of the syngas (H_2, CO, CO_2 and CH_4).

Table 4-8: Modelling results of the DFBG compared to experimental data [247].

Composition (dry basis)	**Experimental** [247]	**This model**
H_2	41.50%	33.35%
CO	22.50%	24.07%
CO_2	21.50%	23.56%
CH_4	10.50%	12.69%
C_2H_4	2.50%	3.74%
C_2H_6	0.50%	0.09%
C_6H_6	8.00 g/Nm^3	18.66 g/Nm^3
C_7H_8	0.50 g/Nm^3	3.00 g/Nm^3
$C_{10}H_8$	2.00 g/Nm^3	3.40 g/Nm^3

4.4.1.2 Carbon distribution

The mass and energy balances of the process were obtained from the process models. Based on the ultimate analysis of the feedstock, and the resulting mass balances of both processes, it is possible to calculate the carbon efficiency. The input of 20 dry-tonnes/h of forest residues resulted in the production of 0.31 tonnes/h of gasoline, 1.91 tonnes/h of jet fuel, and 0.93 tonnes/h of diesel, for both scenarios. In reference to the BECCS scenario, carbon is lost as CO_2 at different points of the plant, but mainly in the combustion of char at the gasifier (12.32 tonnes/h of CO_2), and in the gas turbine (3.68 tonnes/h of CO_2). In addition, CO_2 is separated from the syngas in the CO_2 capture section and is stored underground (11.26 tonnes/h of CO_2). Therefore, as depicted in Figure 4-9, the carbon balance indicates that 26.26 % of the carbon is found in the products, 43.24% is wasted in the flue gases, and 30.50% is captured and permanently stored. Hence, according to Equation 3-1, the carbon efficiency of the BECCS scenario is equal to 26.26%. The resulting carbon balance of the BE scenario is only different to the baseline scenario only regarding the stored CO_2, which is now included in the share of the flue gases. Hence, the carbon efficiency is equal to the BECCS case. Therefore, the carbon efficiency is not affected by the addition of the CCS.

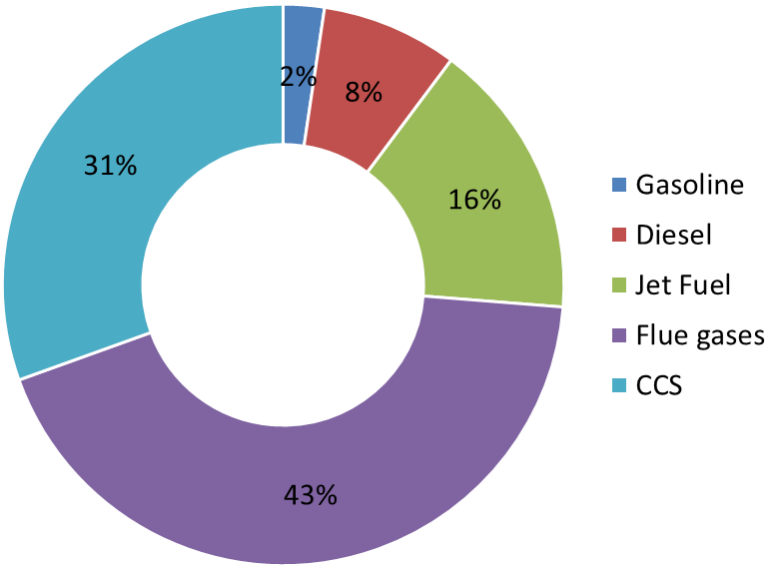

Figure 4-9: Biomass carbon distribution for the BECCS scenario.

The results of both scenarios are in agreement with Swanson et al. [70] who obtained a carbon efficiency of 26.26% for a low temperature gasifier+ FT scenario, and they are slightly different to Marchese et al. [154], i.e. 32%, and Hillestad et al., i.e. 38% [138]; but they considered either different process configuration [154] or gasification technology [138]. The jet fuel mass yield of both scenarios equal 9.6%, agreeing with the 9.7% value obtained by Atsonios et al. [72], while the total fuel mass yield is equal to 0.16, which properly falls in the range of 0.13-0.22 determined by de Jong et al. [248].

4.4.1.3 Energy performance of the process

In terms of energy balance, both cases have been designed to be energy-autonomous, by fixing at 15% the amount of unreacted syngas burnt in the gas turbine. The basis for the design was the BECCS scenario, as it requires additional electricity to compress the captured CO_2. This parameter has been also adopted for the BE, which resulted in higher production of excess electricity. Table 4-9 presents a detail of the power interactions among the plant for both cases. The major consumer of electricity is the syngas compressor due to the difference in operating pressures between the gasifier and the FT reactors, which work at atmospheric and 2.5×10^6 Pa (25 bar) respectively. This huge differential pressure could be avoided by using a gasifier that can operate at higher pressures [70]; however, the drawback of this kind of gasifier, such as the entrained flow gasifiers, is that more power is required to chop the biomass in fine particles, the high capital cost as well as the low H_2 content in the syngas [67].

Table 4-9: Breakdown of power generation and usage.

Power (MW)	BECCS scenario	BE scenario
Total Generation	10.39	10.39
Gas Turbine	5.36	5.36
Steam Turbines	5.02	5.02
Total Usage	8.93	7.93
Grinder	0.43	0.43
Syngas compressor	5.74	5.74
Amine pump	0.12	0.12
CO_2 compression	1.00	0.00
PSA compressor	0.033	0.033
Wax compressor	0.006	0.006
Recirculated syngas compressor	0.027	0.027
ASU+O_2 compressor	1.57	1.57
Net Export	1.46	2.46

Table 4-10 presents a summary of the use and production of steam at different pressures, as well as the amounts that are sent to the steam turbines for power generation for both scenarios. The process streams, from which heat cannot be recovered for steam generation, are cooled down with cooling water; the consumption of which is also reported in Table 4-10. From the data presented, it can be seen that the CCS section does not affect the steam requirements of the process as the CO_2 capture unit is an integral part of both scenarios. The cooling water requirements are minimally increased for the BECCS case.

Table 4-10: Steam generation & utilization and cooling water requirements.

Steam generation and utilization for the BECCS and BE scenarios				
Steam [tonnes/h]	**Generation**	**Consumption in process**	**Use in distillation columns**	**To steam turbines**
Superheated steam;500°C; 4×10^6 Pa	16.33	12.85	1.65	1.83
High pressure steam;210°C; 2×10^6 Pa	23.98	0.00	0.00	25.81
Medium pressure steam;177°C; 9×10^5 Pa	21.35	0.00	0.00	47.16
Low pressure steam; 135°C; 3×10^5Pa	15.27	0.00	15.27	0.00
Cooling water requirement [tonnes/h]				
BECCS scenario			1733.21	
BE scenario			1683.89	

The jet fuel efficiency of the process is calculated as 22.1% for the production of jet fuel (in BECCS and BE scenarios), considering a LHV of 42.8 MJ/kg for the jet fuel [98], and a value of 12.95 MJ/kg for the biomass as received (moisture content equal to 30%). Based on the results of the process modelling, the overall energy efficiency is calculated through Equation 3-4, by taking into account the energy in all the products, such as gasoline, diesel, jet fuel and electricity, as well as the input energy of the forest residues. The overall energy efficiency equals 37.9% and 38.9% for the BECCS and BE scenarios respectively. The efficiency of the BE scenario compares well to the ones obtained in other similar studies [35], [249] and as expected, its overall energy efficiency is higher than in the baseline scenario, due to the higher amount of electricity produced (or equally the more electricity consumed in the BECCS case). Therefore, the CCS section does not compromise the energy efficiency of the process, since the energy penalty is only 2.57%; a value similar to the one reported in [73].

4.4.2 Economic Evaluation

The mass and energy balances are the basis for the economic evaluation since they provide the necessary information for sizing the equipment. Table 4-11 presents the breakdown of the purchased equipment cost according to the main areas of the process plant, for the BECCS and BE scenarios. The total amount of PEC does not have a significant change between both scenarios. In both cases the PEC expenses are dominated by the Biomass Pretreatment+Gasification and the FT synthesis section while the cost of the CO_2 compressors for is relatively small and does not have a significant impact on the total PEC.

Table 4-11: Results for Purchased Equipment Cost, Fixed Capital Investment and Total Capital Requirement.

	Cost [MM £]	
	BECCS Scenario	**BE Scenario**
Biomass Pre-treatment +gasification	12.37 (21.66%)	12.37 (22.09%)
Syngas cleaning up	4.29 (7.51%)	4.29 (7.66%)
CO_2 capture	0.69 (1.21%)	0.69 (1.23%)
Fischer-Tropsch synthesis	28.15 (49.29%)	28.15 (50.28%)
Syncrude upgrading	5.50 (9.63%)	5.50 (9.82%)
CO_2 compression	1.12 (1.96%)	-
HRSG+Gas turbine+Cooling Tower	4.99 (8.74%)	4.99 (8.91%)
PEC	**57.11**	**55.99**
Fixed Capital Investment (FCI)	**173.91**	**170.50**
Total Capital Requirement (TCR) or CAPEX	**186.25**	**182.60**

Table 4-11 also presents the FCI and CAPEX for both scenarios. The obtained results are of the same order of magnitude as in previous studies that evaluated the economic performance of biofuels production through the FT technology [65], [70], [250], [251]. The incorporation of the CO_2 compression section for the BECCS case increases the CAPEX only by around 2%. Similar differences have been also reported in the literature [73], [94]; even if these studies are not oriented to the production of jet fuel, they may serve as a reference to validate the results.

Yearly operating costs or OPEX are presented as £/kg of SAF in Figure 4-10. Among these incurred expenses, the major contributor to the OPEX is the cost of the feedstock (forest residues). Similar results have been found by Tijmensen et al. [69] where the cost of the biomass accounts for at least 30% of the total production cost. Therefore, an increase or decrease in the FR cost could highly influence the value of the MJSP of the BECCS scenario; this is further analysed in the sensitivity analysis section. When comparing both scenarios, the higher OPEX of the BECCS scenario is justified by the cost of CO_2 T&S.

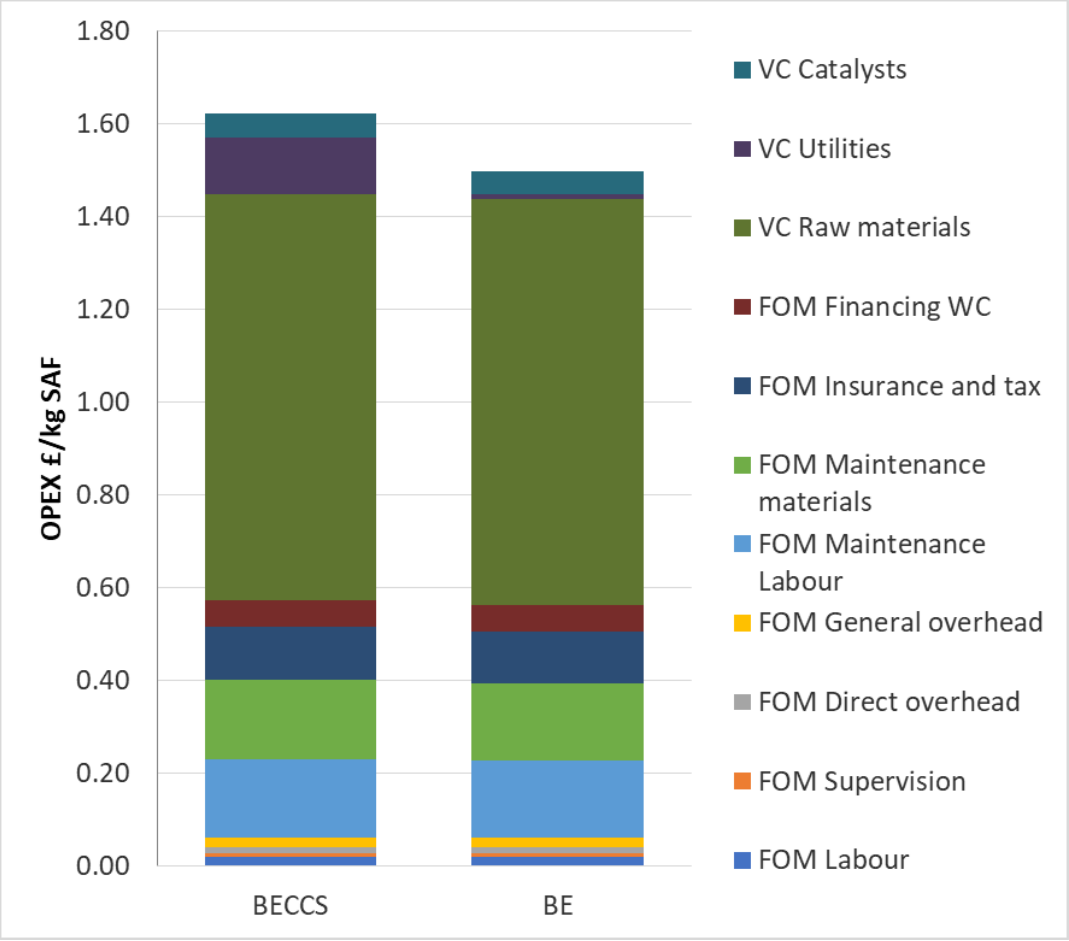

Figure 4-10: Normalized OPEX for the BECSS and BE scenarios.

Finally, a break-even analysis was developed and, by using a DCFA, the MJSP was calculated. The DCFA estimated MJSP of 3.27 £/kg and 3.03 £/kg, for the BECCS and the BE scenarios respectively. The inclusion of the CCS supply chain increased the MJSPs by 7.92%; this figure is in agreement with the results of a previous study available for BECCS, in which the price of the syncrude increases by 10% with the addition of the CCS section [73].

4.4.2.1 Sensitivity analysis on the MJSP

Results from the sensitivity analysis for the alternative scenarios proposed are presented in Figure 4-11. The MJSP is primarily sensitive to CAPEX. If the gasification and FT technologies continue developing, in the upcoming years, equipment prices would drop, which in turn could help improve the economic feasibility of the SAF. In addition, the MJSP exhibits great sensitivity to the feedstock prices; in order to limit volatilities in the feedstock price longstanding procurement deals at ideally fixed costs with forest management corporations are necessary. It is also apparent that the CCS does not have a significant impact on the MJSP and hence future implementations in biorefineries come at relatively low cost and risk. Finally, the discount rate and the tax rate have moderate influence on the MJSP.

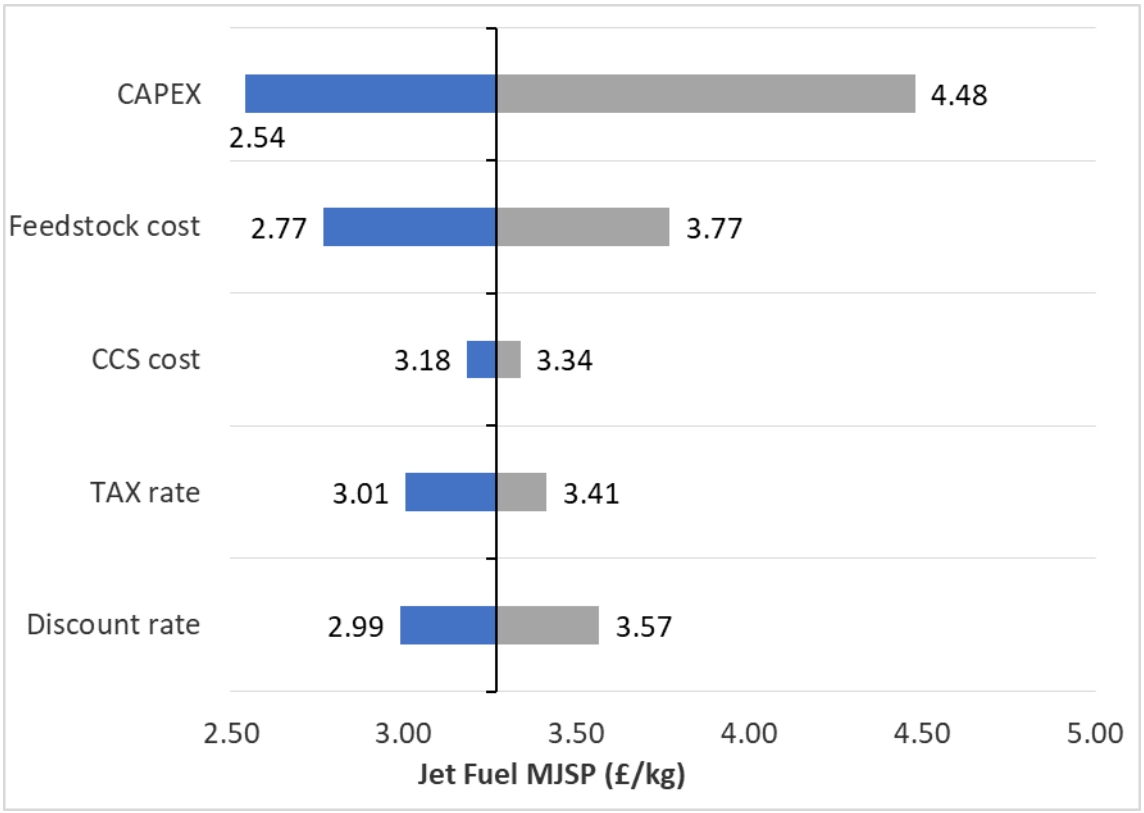

Figure 4-11: Effect of the governing parameters on the MJSP.

4.4.2.2 Effect of the economies of scale

The effect of economies of scale has been also analysed for the BECCS scenario. The CAPEX of the plant is not linearly related to the capacity; therefore, an overall scaling factor of 0.65 was used for upgrading CAPEX [196]. The OPEX (apart from labour) have been assumed proportional to the size of the plant and hence the product yields, waste streams and utilities have been linearly adjusted to the capacity of the plant. In particular, the labour cost has been recalculated for each case by using Equation 3-10. Figure 4-12 shows the MJSP as a function of the plant capacity. The slope for plant's capacities between 20 and 100 dry-tonnes/h is quite steep, and this results in a significant decrease of the MJSP. For a plant size beyond 100 dry-tonnes/h, the MJSP continues to drop but at a slower rate. On the other hand, the increase in the size of the plant implies the need for more feedstock, which availability is limited in the UK. As reported by E4tech [183], 0.8 dry-Mtonnes/year of forest residues are produced in Scotland, where the biorefinery is assumed to be located, meaning that all the available feedstock should be used in a plant treating 100 dry-tonnes/h. This, in turn, will most probably not be a realistic scenario since there exist competing sectors such as CHP.

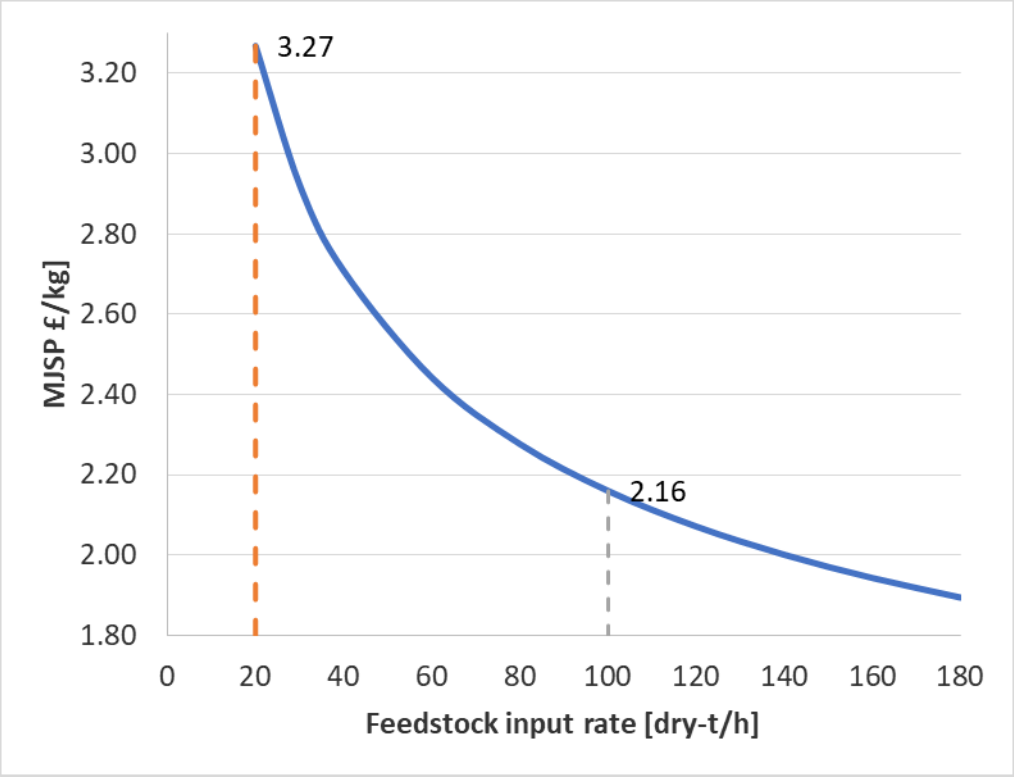

Figure 4-12: Effect of the size of the plant on the MJSP.

4.4.3 Life Cycle Assessment

The inventory of the BECCS and BE scenarios have been developed based on the mass and energy balances, that have been first normalized on a basis of 1 MJ of jet fuel along with the databases of

Ecoinvent 3. In addition, the the ReCiPe 2016 Midpoint (H) impact assessment method has been used. Figure 4-13 presents the results for the GWP (100) for both scenarios at the different life cycle stages (as depicted in Figure 4-7). When the multi-functionality is treated with an Energy Allocation approach, the WtWa results of the GHG emissions for the BECCS and BE, are -121.83 gCO_2eq/MJ and 15.51 gCO_2eq/MJ, respectively, while the system expansion method yields -127.16 gCO_2eq/MJ and 6.02 gCO_2eq/MJ, respectively. In both cases, it can be noticed that the stages that contribute the most to the total GHG emissions are the production of forest residues as well as their transport to the process plant. Regardless the multi-functionality method used, the GWP of the BECCS scenario is negative, due to the characterization factor of -1 for the biogenic CO_2 that is stored. The results for the GWP of the BE scenario (for both multi-functionality methods) are positive, and although it could not approach a net-zero scenario, it still achieves a considerable reduction in emissions when compared to the fossil jet fuel.

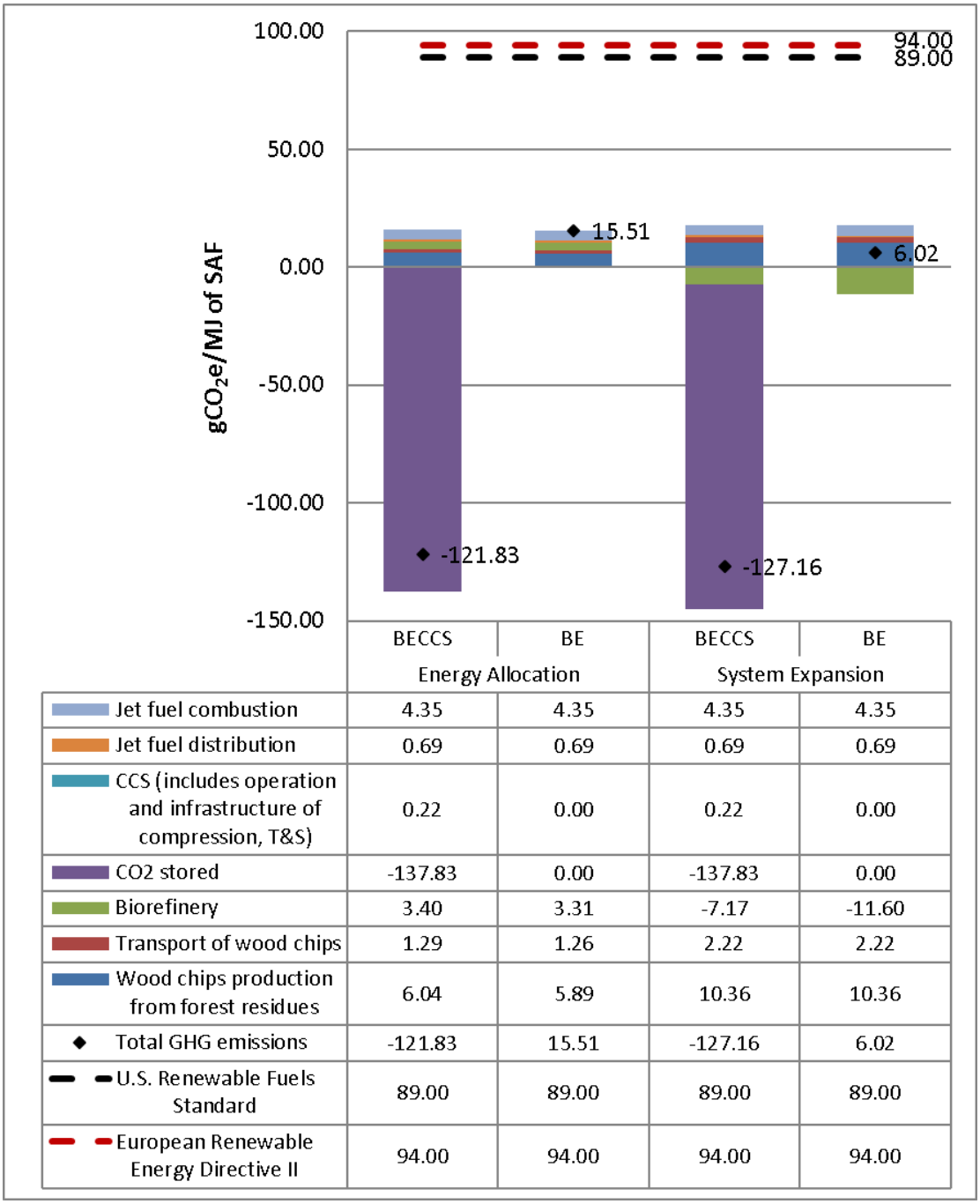

	BECCS	BE	BECCS	BE
	Energy Allocation		System Expansion	
Jet fuel combustion	4.35	4.35	4.35	4.35
Jet fuel distribution	0.69	0.69	0.69	0.69
CCS (includes operation and infrastructure of compression, T&S)	0.22	0.00	0.22	0.00
CO2 stored	-137.83	0.00	-137.83	0.00
Biorefinery	3.40	3.31	-7.17	-11.60
Transport of wood chips	1.29	1.26	2.22	2.22
Wood chips production from forest residues	6.04	5.89	10.36	10.36
Total GHG emissions	-121.83	15.51	-127.16	6.02
U.S. Renewable Fuels Standard	89.00	89.00	89.00	89.00
European Renewable Energy Directive II	94.00	94.00	94.00	94.00

Figure 4-13: Global Warming impact for the BECCS and BE scenarios for displacement and energy allocation.

The results of the GHG emissions for both scenarios are compared against the carbon intensity of conventional jet fuel. Previous studies considered a reference value for the average WtWa GHG emissions equal to 87.50 gCO_2eq/MJ [80], [252]. However, as the GWP depends on several factors, the carbon intensity of fossil aviation fuel varies according to different regulations, such as 89 gCO_2eq/MJ or 94 gCO_2eq/MJ, for the U.S. Renewable Fuels Standard (RFS) [174] and the European

Renewable Energy Directive II [175], respectively. Compared to these values, and in accordance with the sustainability criteria thresholds used for the aforementioned standards (70% of GHG savings for the RED II [175] and a minimum of 50% for the U.S. RFS [176]) the BECCS scenario is way below the GHG emissions reduction targets, while the BE scenario only marginally .

Because of the absence of any study analysing the SAF production within BECCS, the results of both scenarios are compared against FT studies without CCS. In this sense, the GWP for the BE scenario is comparable with similar studies, since its value falls within the range of -1.60 and 18.20 CO_2eq/MJ determined by Wei et al. [65], while it is slightly higher than the value of 6 CO_2eq/MJ determined by de Jong et al. [80]. The low WtWa GHG emissions were explained by de Jong et al. [80] as the result of the self-sufficiency of the process in terms of energy and excess electricity production. In relation to the multi-functionality approach, de Jong et al. [80] found that the system expansion method tends to calculate lower WtWa GHG emissions when the substituted co-products have higher emission intensities than those of the system. This last statement has been also verified in the present work, since the emissions of the substituted fossil gasoline, diesel and electricity are greater than the carbon intensity of the studied system. Therefore, the fact that the displacement method estimates lower GHG emissions than those of the energy allocation method, and as recommended by other authors [80], [83], [253], the results of the energy allocation method are preferred and used for further analyses.

Further, APPENDIX A-5 provides information of the other environmental impact categories calculated by Recipe 2016 Midpoint (H). The fossil jet fuel environmental impacts are taken from the database provided by Ecoinvent3 and compared against the results of the BECCS and BE scenarios analysed by the energy allocation approach.

4.4.3.1 Sensitivity analysis and uncertainty analysis

A parametric analysis was conducted by varying the values of the carbon footprint of each life-cycle stage, as presented in Table 4-7. The ranges of variation for each variable have been roughly defined, either according to the evidence found in the literature or on reasonable assumptions.

As depicted in Figure 4-14, the GWP of the system is very sensitive to the amount of CO_2 that is captured and stored. A 5% increase in the capture capacity of CO_2 has a positive impact on the total emissions of the plant and the GWP diminishes to -129.29 gCO_2e/MJ. On the other hand, a decrease of the capture level by 15% is translated to a higher GWP of -100.50 gCO_2e/MJ. The fact that even in the extreme negative case the GWP value is highly negative, it highlights the importance of storing permanently the captured CO_2 and provides certainty on the sustainability of FT-biofuels production.

In addition, the FR chips production and their transport to the process plant cause relatively significant fluctuations in the GWP of the process. Therefore, ensuring short distance transport for the feedstock is of high importance for the sustainability of the system. Finally, the other process stages appear to have a negligible effect on the GWP.

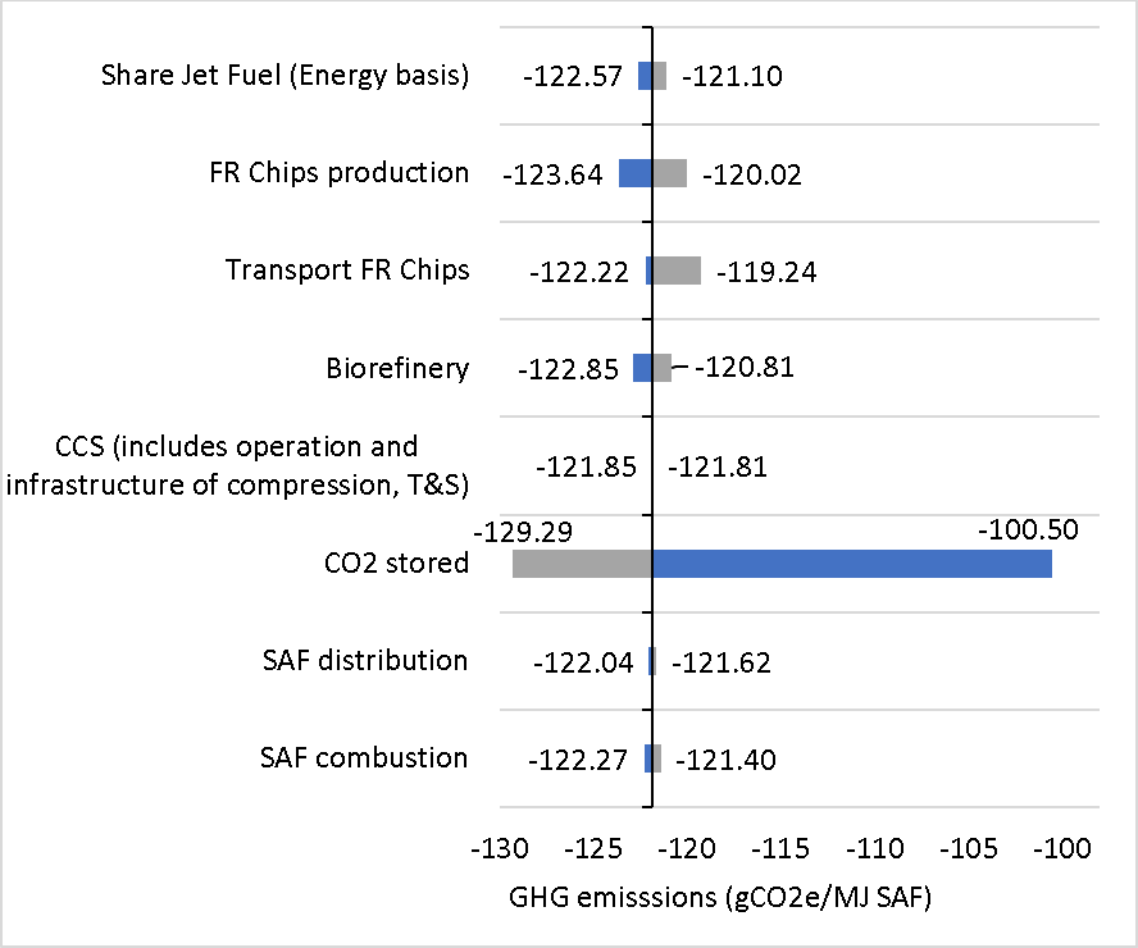

Figure 4-14: Sensitivity analysis on the Global Warming Potential.

4.4.3.2 Monte Carlo analysis

The obtained results for the uncertainty analysis of the BECCS scenario are reflected in the form of histogram in Figure 4-15. The mean value and the GWP's obtained from the simulations is equal to -118.93 gCO_2e/MJ of SAF with a standard deviation of 6.17 gCO_2e/MJ of SAF. In addition, the project has 95% interval for the GWP to be between -131.26 and -106.60 gCO_2e/MJ. Hence, the Monte Carlo simulations revealed that, despite the uncertainty of several parameters, proposed BECCS refinery would most problem achieve highly negative emissions in most cases.

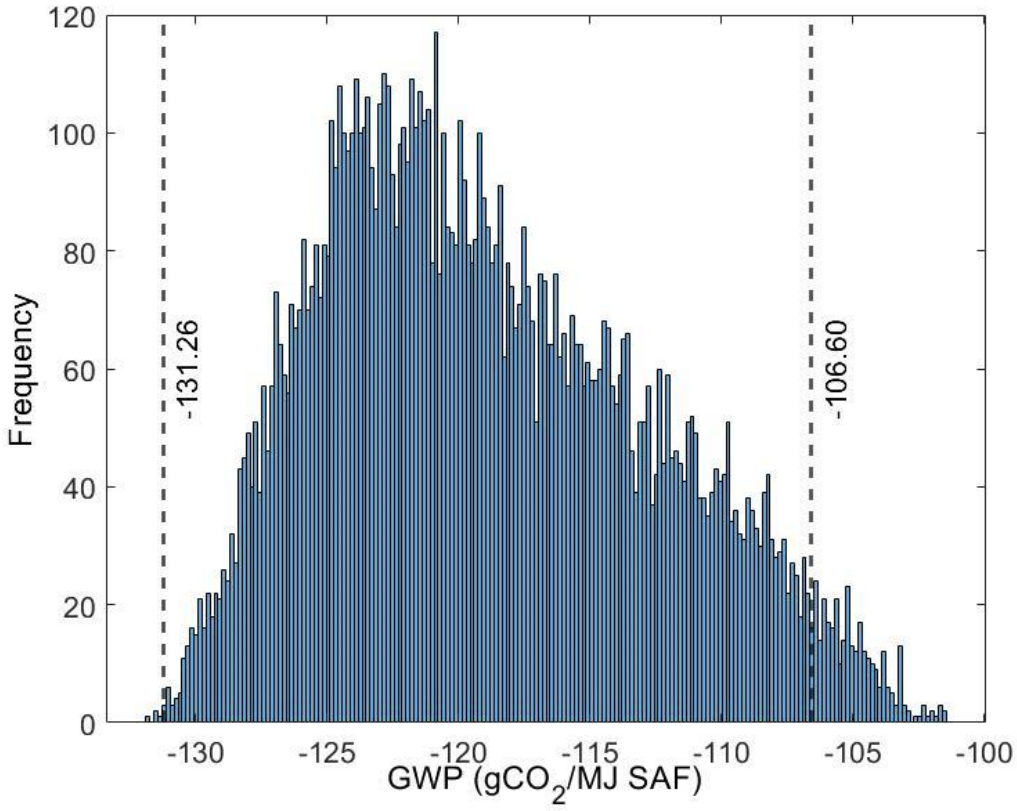

Figure 4-15: Uncertainty analysis on the GWP for the BECCS scenario.

4.5 Policy incentives assessment

This section intends to analyse the effect of existing renewable and potential, that would incentivise negative emissions, support schemes. Therefore, herein the effect of the Renewable Fuel Transport Obligation (RTFO) and the carbon price have been analysed.

The RTFO is a policy of the UK Government that intends to reduce GHG emissions in the transport sector by supporting the production and use of renewable fuels, while imposing an economic obligation to fossil fuel producers. Suppliers that produce more than 450,000 L per year are affected and should pay an amount of 0.50 to 0.80 £ per litre of fossil fuel supplied. On the other hand, this scheme rewards suppliers of sustainable renewable fuels, by granting them one Renewable Transport Fuel Certificates (RTFC) per each litre of fuel produced. If the feedstock for the production of these renewable fuels are wastes or residues, dedicated energy crops, and/or material of non-biological origin, suppliers are awarded two RTFC per litre delivered [254].

Concerning the aviation sector, fossil jet fuel does not have an obligation. However, producers of SAF are rewarded by certificates under the same criteria applied to road-mobile and NRMM [254]. Further, we consider herein the effect of receiving both single and double (as the feedstock is residue from

sustainable forest management) certificates on the economic performance of the process. Since RTFCs can be traded among fuel suppliers [254], it is necessary to determine a price for the certificates in the market. Nevertheless, it is not easy to assign a price to the RTFCs because there is no data published by the government. In the market, an average peak price of 0.30 £/RTFC is provided; however, the prices used for the trading vary from 0.09 to 0.20 £/certificate [255]. As an example, if a price of 0.20 £/certificate is used SAF prices drop from 3.27 £/kg to 3.01 £/kg and 2.76 £/kg when one or two certificates are awarded respectively.

Another support action considered in this study is the price of CO_2, which is a decisive element for the feasibility of CCS projects in the coming years. Theoretically, the CO_2 price may have a double effect on the feasibility of this type of project, since not only additional revenues will be received by the storage of CO_2, but at the same time, the price of conventional jet fuel will be increased. As an example, Figure 4-16 presents the effect of the CO_2 price with and without the effect of the RTFCs, over the MJSP. On considering a CO_2 price of 303.70 £/tonne CO_2, an emission factor of 5.21 kg CO_2/kg for the BECCS-derived SAF (according to the LCA results of -121.83 gCO_{2eq}/MJ), a conventional jet fuel gate price of 0.56 £/kg [256] and an emission factor of the conventional jet fuel of 3.74 kg CO_2/kg (87.5 gCO_{2eq}/MJ) [257], the MJSP of the SAF breaks even the price of the conventional jet fuel at a value of 1.70 £/kg. While, considering both, the CO_2 policy and the RTFCs at a price of 0.20 £/certificate, the MJSP breaks-even the price of the fossil jet fuel at a value of 1.60 and 1.49£/kg, at a CO_2 price of 275.17 and 246.64 £/tCO_2, for a single and double assignation of certificates per kg of SAF produced, respectively.

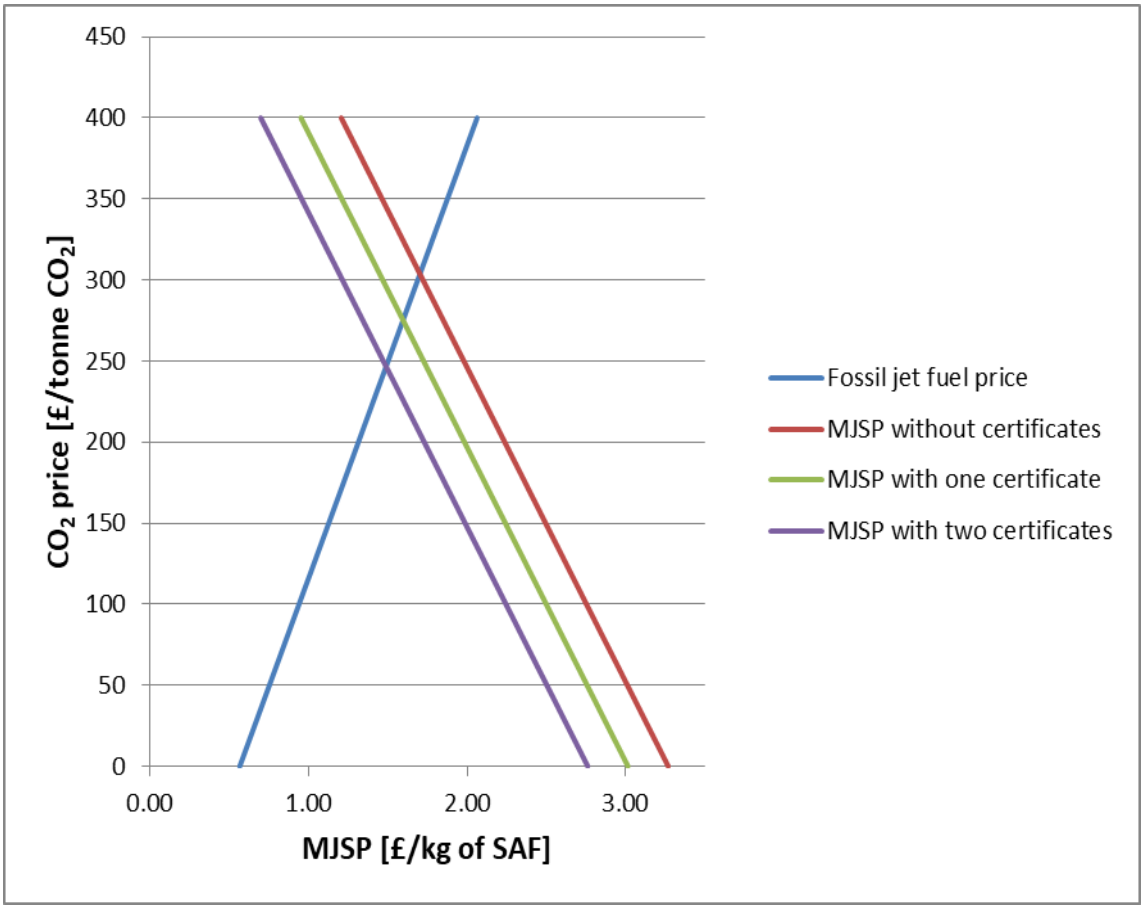

Figure 4-16: MJSP and fossil jet fuel price as a function of CO_2 price and number of RTFC (RTFC=£0.2). Interception points indicate CO_2 prices at which MJSP breaks-even with fossil jet fuel price.

Since the cost of the RTFCs does not have a defined value, as it fluctuates in the market, Figure 4-17 depicts the variation of the MJSP when double certificates are assigned per kg of SAF at different certificates and CO_2 prices. The first thing to notice is that the higher the price of the RTFCs and CO_2, the lower is the value of the MJSP. Similarly, the break-even line indicates that the cost of the SAF could only equal the price of the conventional jet fuel at a range of CO_2 prices between 189.60 and 303.70 £/tonne CO_2, in the price range of the RTFC's between 0 and 0.40 £/certificate. Therefore, the economic feasibility of sustainable fuels has a huge dependence on the incentive policies proposed by the government, which plays the main role for attaining the goal of decarbonizing the country by 2050.

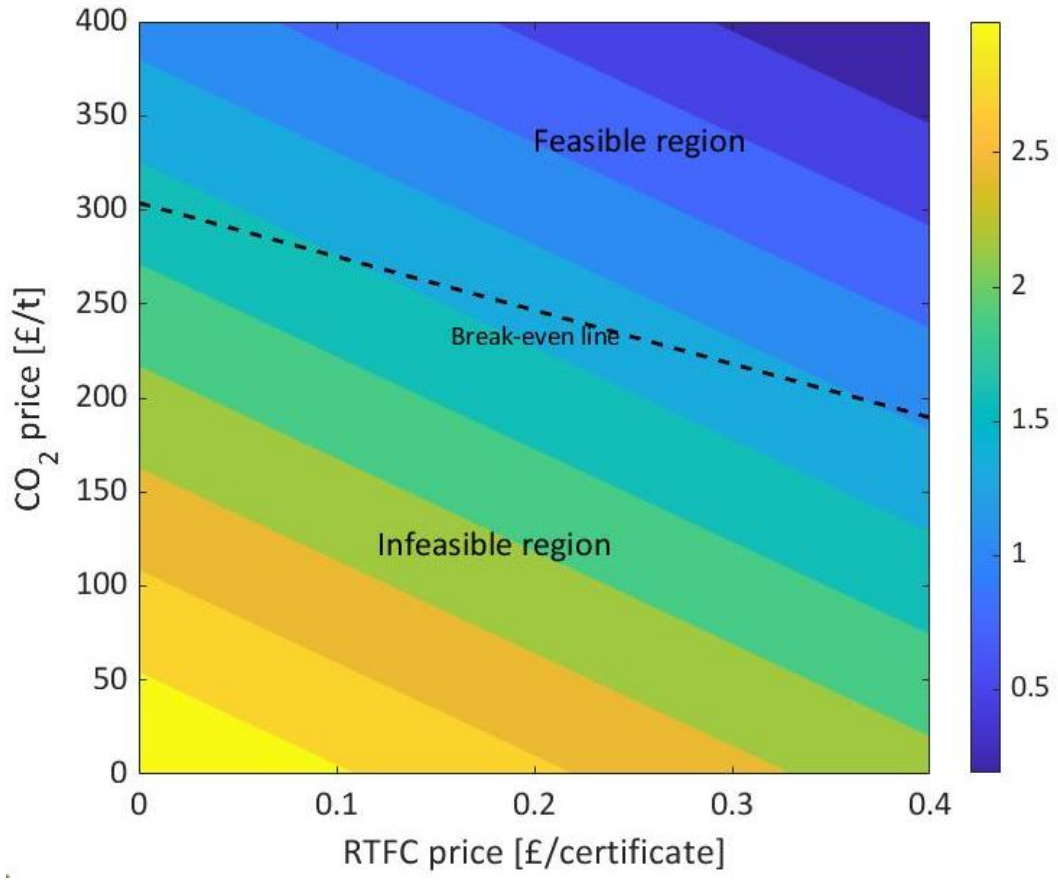

Figure 4-17: Effect of the RTFCs and the CO_2 price on the MJSP. The break-even line indicates pair of CO_2 price and RTFC at which MJSP breaks-even with the fossil jet fuel price.

4.6 Conclusions

This chapter investigated the effect of incorporating CCS on a biorefinery that aims to produce jet fuel from forest residues. The biomass processing capacity of the plant is based on the estimated availability of forest residues in the UK. The purpose of the current study was to evaluate the techno-economic and environmental feasibility of SAF produced through gasification and FT via a BECCS scenario, and this was compared against the same pathway but without the sequestration of carbon dioxide. The CO_2 capture unit is inherent to the process regardless of the provision of permanent CO_2 storage or not and therefore adding the CCS section highly enhance the environmental feasibility of the process while minimally increasing the MJSP. In addition, the on-site generation of heat and electricity generation makes the BECCS-FT attractive since it covers the energy demand of both the CO_2 capture and the compression and hence avoiding the use of external energy loads that may be derived from fossil sources. The LCA results suggest that the BECCS configuration achieves highly negative emissions. The main outcomes of the present study can be summarised as follows:

1. The results of the process modelling in Aspen Plus for the BECCS scenario has revealed that 26.26% of the carbon ends up in the products, 43.24% is wasted in the flue gases, and 30.50% is captured and permanently stored. The BE scenario has a similar carbon balance but in this case the CO_2 captured is released to the atmosphere.
2. The energy balance of the BECCS and BE processes reveal that the electricity production is lower in the former, due to the energy penalty associated with the compression of CO_2. However, in terms of heating and cooling utilities, the requirements of both scenarios are quite similar. As a result, the overall energy efficiency of the BECCS scenario is 37.7%, which is only 2.57% lower than the efficiency of the BE scenario.
3. The economic analysis revealed similar results for the CAPEX for both scenarios. For the BECCS scenario, the CAPEX only increases by 2% due to the cost of the CO_2 compression section. In addition, the addition of CCS increases the OPEX by 8.4%. The calculated MJSP are 3.27 £/kg and 3.03 £/kg, for the BECCS and the BE scenarios respectively. The gap between the MJSPs is about 7.34 %, and hence adding CCS does not have a significant effect on the economic viability of the project. Nevertheless, in both cases, the MJSPs are higher than the gate price of fossil jet fuel (0.56 £/kg [256]).
4. The sensitivity analysis over the MJSP suggest that the BECCS process is CAPEX intensive (MJSP varies from 2.54 to 4.48 £/kg) and hence research and deployment of similar technologies is highly suggested as due to learning effects CAPEX reduction can be achieved. Another important cost factor is the feedstock price. Economies of scale may reduce the MJSP by 33% if the plant size increases to 100 dry-tonnes/h of feedstock. However, this strategy should be carefully analysed in the UK (and elsewhere) due to the restricted availability of FR.
5. The GWP calculated for both BECCS and BE scenarios with the Energy Allocation approach, results in -121.83 gCO_2eq/MJ and 15.51 gCO_2eq/MJ, respectively. According to the sustainability criteria thresholds used for the different investigated standards (70% of GHG savings for the RED II [175] and a minimum of 50% for the U.S. RFS [135]), the BECCS scenario is well below these targets. This result is encouraging since it does not only reflect the potential of the BECSS in reducing the carbon footprint of the aviation sector, but also its suitability as a carbon dioxide removal strategy that could offset the GHG emissions of other sectors that are difficult to decarbonise such as heavy industries.
6. The sensitivity analysis revealed that the GWP of the BECCS scenario is sensitive to the amount of CO_2 to be captured from the syngas, the emission intensity of the FR chips production and the feedstock transport. Despite all the uncertainties associated with the values adopted for the LCA,

the Monte-Carlo analysis demonstrated that the SAF derived from the FT-BECCS configuration would most probably always have a negative GWP, and therefore will act as a CDR technology.

The study demonstrates the importance of coupling the production of value-added products such as jet fuel with CCS since such strategies can achieve negative emissions and facilitate the deployment of next generation CCS/CDR technologies. The current results add to a growing body of literature on the BECCS process configurations, and more studies should be developed to create a robust database to encourage further development and deployment. Similarly, studies that analyse other environmental impacts are highly recommended for a complete environmental evaluation of the BECCS configuration.

5. Sustainable Aviation Fuel (SAF) production through Power-to-Liquid (PtL): A combined techno-economic and life cycle assessment

Abstract

The current chapter critically evaluates the technical, economic, and environmental performance of a Power-to-Liquid (PtL) system for the production of sustainable aviation fuel (SAF). This SAF production system comprises a direct air capture (DAC) unit, an off-shore wind farm, an alkaline electrolyser, and a refinery plant (reverse water gas shift coupled with a Fischer-Tropsch reactor). The calculated carbon conversion efficiency, hydrogen conversion efficiency, and Power-to-liquids efficiency are 88%, 39.16%, and 25.6%, respectively. The heat integration between the refinery and the DAC unit enhances the system's energy performance, while water integration between the DAC and refinery units and the electrolyser reduces the demand for fresh water. The economic assessment estimates a minimum jet fuel selling price (MJSP) of 5.16 £/kg. The process is OPEX intensive due to the electricity requirements, while the CAPEX is dominated by the DAC unit. A Well-to-Wake (WtWa) life cycle assessment (LCA) shows that the global warming potential (GWP) equals 21.43 gCO_{2eq}/MJ_{SAF}, and is highly dependent on the upstream emissions of the off-shore wind electricity. Within a 95% confidence interval, a stochastic Monte Carlo LCA reveals that the GWP of the SAF falls below the UK aviation mandate threshold of 50% emissions reduction compared to fossil jet fuel. Moreover, the resulting WtWa water footprint is 0.480 l/MJ_{SAF}, with the refinery's cooling water requirements and the electricity's water footprint to pose as the main contributors. The study concludes with estimating the required monetary value of SAF certificates for different scenarios under the UK SAF mandate guidelines.

Keywords: Sustainable Aviation Fuels; Power-to-Liquids, process modelling; System integration, Minimum Jet Fuel Selling Price; Global Warming Potential; Water Footprint

5.1 Introduction

Growing concerns over global warming have led to increased awareness among different sectors, including the aviation industry. The Air Transport Action Group (ATAG) has set an ambitious target for 2050 of reducing the net annual emissions to half of what they were in 2005. Achieving this target requires various action plans, including the use of sustainable aviation fuels (SAF) [3]. To support and increase the share of SAF utilization in the total kerosene consumption, some countries such as Germany and the UK are formulating and implementing supporting policies. However, producing SAF on a large scale requires strategies to meet the proposed production targets. The main challenge associated with this is the availability of large quantities of high-quality feedstock, as land-use changes

may have greater environmental consequences than petroleum-based fuels. Therefore, the feedstock selection for SAF production is limited to waste biomass [29]. While some countries have large amounts of residual biomass, others are unable to meet their own needs and must import it from other regions. Given that LCAs have shown that biomass-derived fuels are transport-intensive [257], focusing on the availability is not a sustainable strategy. As a result, having a diverse SAF supply chain is critical in order to meet the aviation market's sustainability criteria.

PtL production has been proposed in this context as a promising and scalable alternative SAF production pathway. This process combines CO_2, water, and renewable energy to produce SAF with properties that are similar to those of fossil jet fuel. The three major steps that comprise this pathway are the CO_2 capture, hydrogen production (generally from water electrolysis), and hydrocarbons synthesis and conditioning process [258]. Hydrocarbons synthesis can be performed through two different pathways: Fischer-Tropsch (FT) synthesis, or methanol to jet fuel; however, the FT process outperforms the methanol pathway since the use of blends containing 50% of FT-derived SAF and 50% of conventional jet fuel is ASTM-certified as drop-in. In terms of CO_2 sources, direct air capture (DAC) is gaining popularity due to its potential for mitigating anthropogenic GHG emissions from dispersed sources while ensuring flexibility in plant location selection [259]. Furthermore, when coupled to low carbon footprint energy, the use of DAC for fuel synthesis may be able to close the carbon cycle and lower CO_2 emissions [260]. More studies that evaluate a suitable integrated Power-to-jet fuel system from a techno-economic and environmental standpoint are thus required to justify this carbon footprint reduction and other economic and environmental claims while providing quantified feasibility data for policymakers or other aviation-related organisations.

The PtL concept for the production of FT-derived fuels is a relatively new alternative pathway. As for now, only a few demonstration plants have been constructed [116], [117], and more studies are required to fully understand large-scale commercial plants. Some past studies focused on the technical aspect through process modelling [118]–[121], while others evaluated the economic feasibility [38], [39], [121], [122], or the environmental performance through the estimation of the GWP of the PtL pathway [38], [123]–[125]. There has been only a little research that specifically analyses the production of SAF from a PtL process that is available, as mentioned in Chapter 2. A commonality between these assessments is that none of them base the economic and environmental assessment on detail process models, and they are not LCAs. The only comprehensive LCA found in the literature was performed by Micheli et al. [136], who studied the environmental assessment of various PtL SAF configurations and calculated the GWP, alongside other environmental factors. Their foreground data

is solely an environmental assessment that derives from previous available studies related to the production of PtL fuels, and not from detail process models.

The research mentioned above is valuable for understanding the economic and environmental performance of PtL-SAF, but they lack a comprehensive process modelling and integration. Without such models, it is difficult to analyse the effect of various parameters, including system design, operation, and energy generation, on the mass and energy performance, as well as the economic and environmental indicators. In particular, these models could improve our understanding of low TRL units, such as the Reverse Water Gas Shift (RWGS) reactor. Moreover, there are few studies that examine SAF production from an integrated techno-economic and environmental perspective, and early studies did not consider the possibility of process integration. By developing detailed models of different sections of the system, it may be possible to achieve synergistic integration that improves technical, economic, and environmental performances [261]. In this regard, given the growing interest in PtL processes, and as for the aforementioned knowledge gaps, to the best of our knowledge, this is the first study of its kind that jointly analyses the technical, economic and environmental performance of the PtL for SAF production, based on comprehensive process models for an integrated DAC-electrolyser-process plant, based in the UK. Furthermore, most studies in the literature concentrate on FT configurations that generate diesel, naphtha, or simply syncrude. Further, the current study focuses on maximising the jet fuel yield that requires the use of additional units, such as hydrocracking and isomerization, as well as higher syngas recycling ratios [257].

5.2 Methodology

5.2.1 Capacity of the plant and potential plant location

The growing interest in producing SAF via the PtL route is reflected in the growing number of studies and projects being developed [262]. For example, a roadmap to support the development of the PtL-derived SAF has been proposed by the German government and industrial leaders targeting an annual production of 200,000 tonnes of SAF for regional utilization by 2030 [263], [264]. In the same context, a public consultation has been released in the UK in order to lay the groundwork for a future SAF mandate [17], [20]. Various SAF uptake scenarios were proposed to replace the UK aviation fuel demand in the short and long term (starting in 2025 until 2050). The UK government has set a target of replacing 10% of fossil jet fuel by 2030. Given the PtL's low GHG emissions and future cost reductions, the government has stated its intention to promote PtL's technological and commercial development. Since the UK consumption of jet fuel estimated by 2030 equals 12.7 Mtonnes [265], and considering that the efuel’s production potential has been estimated as 2.7% of the 2030 jet fuel

demand, an estimated 0.34 Mtonnes/year of PtL-derived SAF could be produced. Considering a coverage of 6% of this SAF target, the production capacity of the plant of the present study is set as 2,500 kg/h of jet fuel [20].

The electricity requirements of PtL systems are significant [258], [266], and this can have a major impact on the GWP of the resulting fuel. Therefore, in this study, the energy for the process is assumed to be supplied by a dedicated offshore wind farm. By 2019, capacities of on-shore and off-shore wind farms in the UK, were 10 GW and 8.5 GW, respectively [267]; furthermore, there is a plan to increase off-shore wind capacity to 40 GW by 2030 [268]. Among the current UK operational off-shore wind farms, the Teesside facility operated by EDF is responsible for producing 62MW of electricity. BP has also announced plans to build a 60 MW facility for electrolysis-based hydrogen production in the same region by 2025, with plans to increase the size to 500 MW by 2030 [269]. Due to the region's high wind potential, the integrated wind farm-electrolyser-DAC-process system of this study has been located in the Teeside region.

5.2.2 System description and modelling

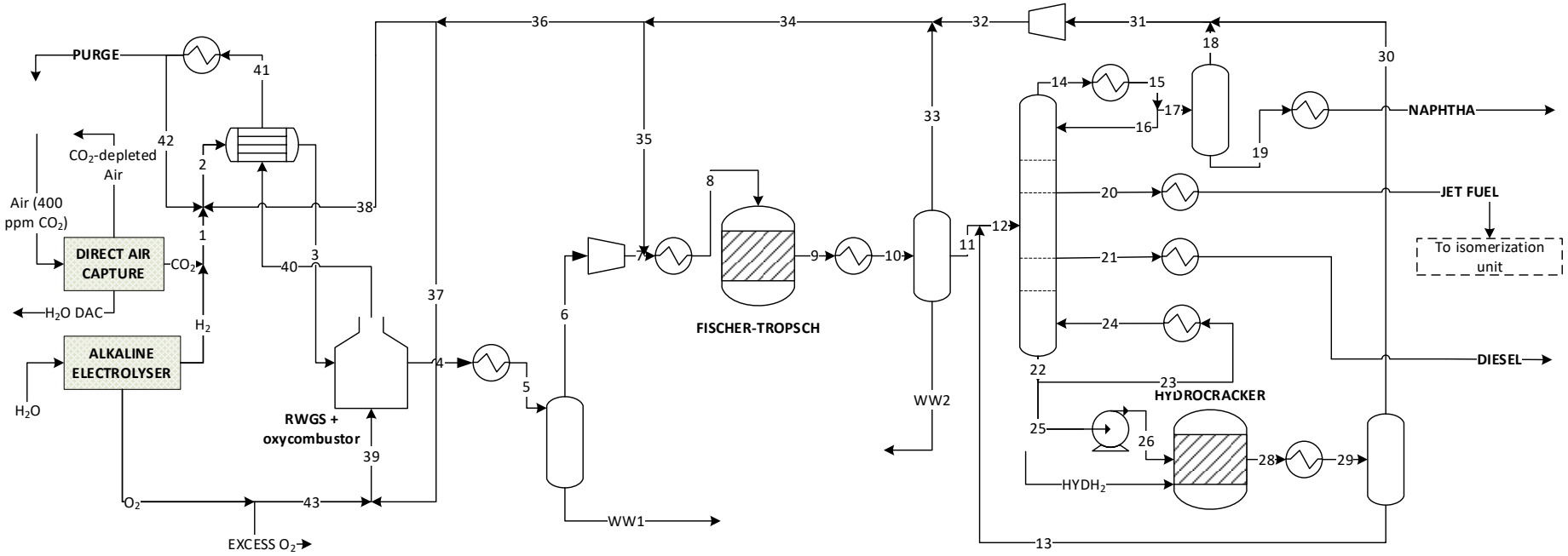

Figure 5-1: Process flow diagram of the investigated PtL process for SAF production.

The system is divided into three major sections, as depicted in Figure 5-1: the DAC unit, water electrolysis, and the refinery plant (syngas and fuel synthesis, as well as conditioning). The process configuration has been set up to favour the production of middle distillates, especially jet fuel range hydrocarbons. The various sections are represented by models at operating conditions that have been determined as optimal [106], [120], [121], [154]. More details of the system are given in the following sections:

5.2.2.1 Direct Air Capture:

Various DAC technologies have been developed, with alkali hydroxide solutions in liquid scrubbing and VTSA (vacuum temperature swing adsorption) on supported sorbents achieving the most advancement [270], [271]. The VTSA technology, also referred to as the low temperature DAC, was chosen for this study because of its modularity that facilitates scaling-up efforts. Another advantage is its ease of operation, as all steps of CO_2 capture occur in the same unit, and bed regeneration occurs at low temperature, allowing low-quality heat generated at different stages of the proposed process to be integrated with the DAC unit [271]–[273]. The sorbent used in low-temperature DAC technology is critical, but the lack of experimental and mathematical models that accurately describe their operation increases the uncertainty of their mass and energy performance [270]. In this study, an amine-functionalized adsorbent, i.e. APDES-NFC, is considered because it has been indicated to be similar to the sorbent used by Climeworks DAC technology [270].

The Toth model is used to represent CO_2 adsorption [270]. The APDES-NFC sorbent behaves by the physisorption mechanism, with chemisorption being ignored [270]. The temperature and partial pressure of CO_2 are the main driving forces in this model: the higher the temperature, the less CO_2 is adsorbed in the bed [274]. Moreover, it has been observed that relative humidity improves CO_2 adsorption; however, few experimental or modelling papers have attempted to investigate its effect on CO_2 adsorption [270], [275]. The methodology proposed by Sabatino et al. [270] is used for this study because it is based on the empirical calculation of the dependence of temperature on relative humidity. Water co-adsorption, on the other hand, is unaffected by factors other than temperature and water content. The temperature-dependent "GAB model" is used to represent water adsorption [270]. The use of the aforementioned models, as well as some ideal gas equations, allows the estimation of the amount of CO_2 and H_2O that are captured after a DAC bed operating cycle. Finally, a carbon capture fraction of 90% (an average value determined at the Hellisheiði and Hinwil Climeworks plants) is assumed [260]. More information on these models can be found in APPENDIX B-1. Finally, the energy consumption encompasses both, heat and electricity requirements. Particularly, energy demands for the APDES-NFC sorbent are assumed to be equal to the data provided by Deutz et al.

[260], and therefore, the process created by Climeworks needs between 1.8 and 2.6 MJ_{el}/kg (electricity requirement) and between 5.4 and 11.9 MJ_{th}/kg (heat requirement) in which the lowest value indicates the future target, and the highest the current consumption.

5.2.2.2 Off-shore Wind Farm and electricity supply

A dedicated offshore wind farm provides electricity to the integrated system. The wind speed profile is not constant and consequently the power generation fluctuates. Hence, to estimate the power generation curve, the hourly wind profile of the selected location, Teeside, was obtained from the NASA/MERRA-2 website [276]. The chosen data is for the year 2021, and the geographic coordinates correspond to the Teeside wind farm operated by EDF. The software SAM was used for the estimation of the hourly energy generation, which was calculated from the adjusted wind speed profile, as well as with the selection of the nominal power generation (by defining the number of wind turbines). The selected wind turbine model is the Senvion 6.2M126 offshore, due to its suitable operation between the speed ranges registered in the chosen location. The wind speed profile (see Figure 5-2) is provided at 10 m above the ground and therefore is adjusted with Equations 5-1 and 5-2 to a height of 80 m. Equation 5-1 estimates α, which is the power law exponent, and is calculated by using the mean wind speed (U_{ref}) and the height at which wind speeds have been collected. Equation 5-2 is the power law profile and finds the new speed values$U(z)$, at a specific height z.

$$\alpha = \frac{0.37 - 0.088\ln\left(U_{ref}\right)}{1 - 0.088ln\left(\frac{z_{ref}}{10}\right)} \quad \textbf{(5-1)}$$

$$\frac{U(z)}{U(z_{ref})} = \left(\frac{z}{z_{ref}}\right)^{\alpha} \quad \textbf{(5-2)}$$

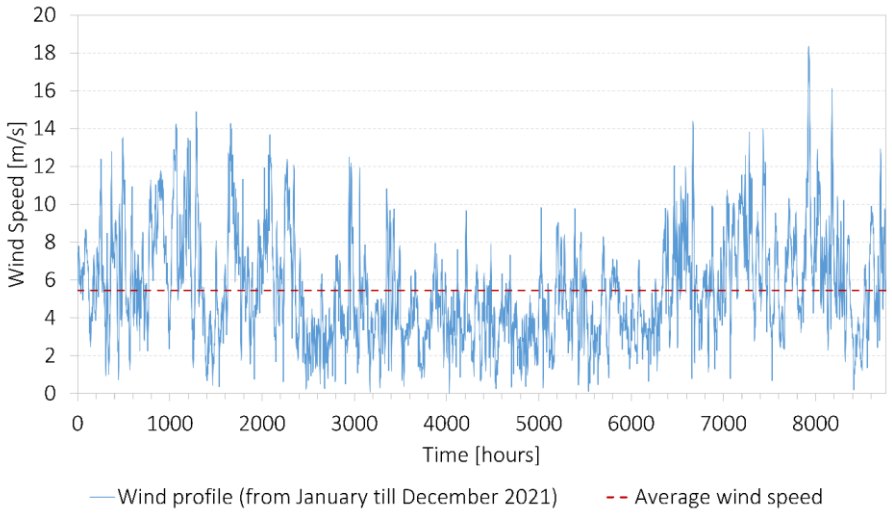

Figure 5-2: The wind speed profile for Teeside.

For an enhanced operating performance, it is important that the electrolyser receives uninterrupted nominal power, which will also maximise its service life [277]. Annexing a battery bank to the wind farm could allow the storage of the excess power, and the supply of energy, when the power generated is lower than the required nominal. Although, few studies have assessed the techno-economic potential of this integrated wind farm-battery bank-electrolyser system for H_2 production [278]–[281]. Moreover, the design of such a system is time consuming since it is a multi-objective optimisation problem, with multiple solutions that have trade-offs between several technical, economic and environmental performance indicators, and due to this reason, this design is out of the scope of this study. Additionally, such hybrid wind farm-battery systems have shown lower energy efficiency and higher capital costs [278], [279]. Therefore, to tackle the energy production fluctuation, the use of the grid network as a "virtual" storage system is proposed: when excess electricity is produced, electricity is injected into the grid, while in the case of lower power generation, the system takes electricity from the grid [278], [282]. The wind farm is sized so that the average annual electricity generation equals the overall electricity demand of the whole PtL system. Further, the grid annual electricity consumption (and its inherent emissions) is offset by the injection of the wind farm excess electricity [282].

5.2.2.3 Electrolyser

Three main water electrolysis technologies can be mentioned: alkaline electrolyser (AE), proton exchange membrane (PEM) and solid oxide electrolysis cell (SOEC). Despite its lower performance, the AE was chosen for this evaluation due to its high TRL and potential for industrial scalability. Equation 5-3 depicts the electrolysis reaction and indicates a requirement of 9 kg of deionised water for the production of 1 kg of H_2. On considering, losses at several sections of the AE operation plant, such as water treatment (ion exchange), condensate, and others, the amount of water required to produce 1 kg of H_2 increases to 9.26 [103]. The ion exchange method of water treatment involves the adsorption of water contaminants into the ion exchange media (resin), which is disposed of or regenerated on a regular basis [283].

$$H_2O \rightarrow H_{2(g)} + \frac{1}{2} O_{2(g)} \quad \textbf{(5-3)}$$

Larger electrolysis capabilities might be accomplished by connecting multiple AE stacks, while also modifying the balance of the plant's elements to the desired size, as commercially available AE stacks have a maximum capacity of 2.5MW [103]. The electrolyser's efficiency is constrained because some of the electricity it receives is converted to heat. This heat must be continuously evacuated in order

to maintain the electrolyser's isothermal operation. Typically, cooling water is utilised for this, and for the sake of increasing the energy efficiency, we assumed that it is also used for district heating at low temperatures. Another additional element of the balance of the plant of the AE electrolyser includes the AC-DC converter, where around 6% of the energy is lost [103]. All the operational parameters and energy and mass balances considered for this study are taken from a 100 MW electrolyser as presented in the work of Holst et al. [103], and adjusted to the required electrolyser capacity. With regards to the operating pressure, it has been found to have low influence in the efficiency of the stack, and it could be set according to the downstream application requirements [284], [285]. Even so, the pressurised AE is described as a system with several operating issues with a larger cost due to the need of resistant to high pressure materials; therefore, it is regarded as rather undesirable, and an atmospheric system with downstream compression is preferred [103].

5.2.2.4 Process plant

The refinery process model was developed in Aspen Plus with the aim of estimating the mass and energy balances of the proposed process configuration. Due to its suitability for gas processing, refinery, and petrochemical plants, the Peng-Robinson-Boston-Mathias was chosen as the thermodynamic property package [188]. In the following sections, the main functional units are explained.

1. **Reverse Water Gas Shift:** In the refinery, the reverse water gas shift reactor is a crucial component since it primarily enables the catalytic conversion of the CO_2/H_2 mixture into syngas. Generally, RWGS reactors operate at a temperature ranging from 700 °C to 1,000 °C, and H_2 to CO_2 ratios of 1:1 to 3:1 [102]. Chemically, the RWGS process is represented by a main reaction (Equation 5-4) that is thermodynamically favoured at high temperatures. In addition, side reactions (Equation 5-5, Equation 5-6, Equation 5-7, and Equation 5-8) occur and are responsible for the production of methane and soot deposition. In order to eliminate the energy penalty of the pre-FT compression unit, it is generally recommended that the RWGS reactor be operated at the same high operating pressure as the downstream FT reactor [286]. However, it has been observed that high pressure increases the rate of the methanation reaction [122], [286], which has a negative impact on the energy efficiency of the process and outweighs the advantages of a high pressure RWGS reactor. The studies by Adelung et al. [119], [122] used process modelling method to analyse this effect. The ideal operating pressure and temperature ranges that increase de PtL efficiency and the CO_2/H_2 conversion efficiencies have been determined by the authors through a parametric analysis.

$$CO_2 + H_2 \leftrightarrow \ CO + H_2O \quad \Delta H = 41.2 kJ/mol$$

(5-4)

$$CO_2 + 3H_2 \leftrightarrow CH_4 + H_2O \quad \Delta H < 0$$

(5-5)

$$CO_2 + 4H_2 \leftrightarrow CH_4 + 2H_2O \quad \Delta H < 0$$

(5-6)

$$2CO \leftrightarrow C + CO_2 \ \Delta H > 0$$

(5-7)

$$CH_4 \leftrightarrow C + 2H_2 \ \Delta H < 0$$

(5-8)

The recycling of the unreacted syngas from the FT unit to the RWGS is another topic of uncertainty. Although recycling boosts the efficiency, the presence of light hydrocarbons raises the level of operational unpredictability. Various approaches to modelling the decomposition of these light hydrocarbons have been used in previous studies, with a majority assuming an equilibrium conversion inside the RWGS reactor (Equations 5-9, 5-10, 5-11, 5-12, and 5-13). However, there is a lack of kinetic models and experimental data to analyse the effect of the conversion of these components on the selectivity of the RWGS reaction, or whether they can cause any operating problem. The only experimental work analysing the effect of the recycling of hydrocarbons over the performance of the RWGS is the one performed by Wolf et al. [287]. They found that CH_4 was not responsible of any coking up to a CH_4/CO_2 ratio below one. However, replacing CH_4 by C_3H_8, is responsible of thermal and catalytic coking. Catalytic coking increases up to 700 °C and decreases above this temperature. Thermal coking, on the other hand, increases with higher temperatures but can be suppressed by the addition of water [287]. Another approach considers prior reforming of these hydrocarbons with an ATR unit, which may solve the uncertainty problem at the expense of higher CAPEX and lower process efficiencies [102].

$$C_mH_n \rightarrow C_x + zH_2$$

(5-9)

$$C_mH_n \rightarrow C_xH_y + zH_2$$

(5-10)

$$C_mH_n + O_2 \rightarrow CO + H_2$$

(5-11)

$$C_mH_n + H_2O \rightarrow CO + H_2$$

(5-12)

$$C_mH_n + CO_2 \rightarrow CO + H_2$$

(5-13)

Based on the information presented above, the operating conditions selected for this study are 850 °C and 5×10^5 Pa (5 bar) [54] for the "minimization of Gibbs energy modelling" of the RWGS unit, assuming that the operating conditions and reactor geometry are adjusted to reach the equilibrium stage [119], [120]. As a consequence, under these operating conditions, it is assumed that catalytic coking does not occur and due to the presence of moisture in the recycling gas, thermal coking is considered negligible. The same approach as Adelung et al. [122] has been taken in terms of the source of energy for the RWGS reactions. Thus, the RWGS reactor is designed as a steam-reforming reactor, which means that the catalyst is packed inside the tubes, which are then placed inside the furnace, where oxy-combustion provides heat to the system. The RWGS reactor must be made of a high-quality metal or alloy (reactions above 850 °C) that can withstand temperatures as high as 1200 °C [288]. It is also worth noting that following this reactor, the outlet streams are cooled and a biphasic separator is installed to remove water that could deactivate the FT catalyst [119].

2. **Fischer-Tropsch:** There are several approaches for the modelling of the FT reactor, for this study, the kinetic model derived by Marchese et al. [64] has been chosen. The proposed model is a carbide mechanism model which was validated by the authors using experimental data obtained from a tubular fixed-bed reactor filled with Co-Pt/γ-Al_2O_3 catalyst [64], with a length that determines a CO per pass conversion of 75%. This model includes some modifications to account for the main deviations from the Anderson-Schulz-Flory (ASF) distribution including higher methane selectivity, lower ethylene selectivity, and inclusion of olefins production.

   The FT synthesis is modelled through a mechanistic carbide model. The model assumes that CO and H_2 are dissociated on the surface of the catalyst, giving place to the synthesis of CHx, which acts as a building block for long chain hydrocarbons. The model was derived by Marchese et al. [64], and the product synthesis can be estimated through a rate-based approach [64], [120]. The kinetic model can estimate the rate of production of alkanes and alkenes (Table 5-1), which depend on the syngas composition, pressure, temperature and the calculated chain growth probabilities. The deviations from the Anderson-Schulz-Flory model, such as the higher methane

and lower ethylene yield, are accounted in this model. More detail on the model derivation and the equations of Table 5-1 are presented in the publication of Marchese et al. [64].

Table 5-1: Rate of formation for the different species [64].

Methane	$R_{CH_4} = k_{Meth}\alpha_1\sqrt{(K_0 P_{H_2})}P_{H_2}[vac]^*$
Ethylene	$R_{C_2H_4} = k_{Eth}e^{2c}\alpha_1\alpha_2\sqrt{(K_0 P_{H_2})}[vac]^*$
Paraffin	$R_{C_nH_{2n+2}} = k_{Par}\alpha_1\alpha_2\prod_{n=3}^{n}\alpha_n\sqrt{(K_0 P_{H_2})}P_{H_2}[vac]; for\ n \geq 2^*$
Olefin	$R_{C_nH_{2n+2}} = k_{Ol}e^{nc}\alpha_1\alpha_2\prod_{n=3}^{n}\alpha_n\sqrt{(K_0 P_{H_2})}[vac]; for\ n \geq 3^*$

The FT reactor is modelled as a multi-tubular/catalytic reactor, which is sized in order to achieve a CO per pass conversion of 75% [121]. The equation for the synthesis of paraffin could be used until the production of C70 hydrocarbon, and up to C40 for the olefins. In addition to the kinetic equations, the mass balance equation for a catalytic plug flow reactor is considered, by assuming that a cobalt catalyst is used with a bed density of 820 kg/m^3 [118]. These kinetic expressions cannot be directly applied in Aspen Plus; therefore, a "User Model" block is used to represent the FT reactor. The block is connected to Matlab in order to solve the mass balances for each component. The connection is done through excel, which receives and sends information from and to Aspen plus and Matlab [152], [171]. This Aspen Plus-Excel VBA-Matlab interface is represented in Figure 5-3. The resulting size of the reactor for this process configuration was calculated at 150.24 m^3.

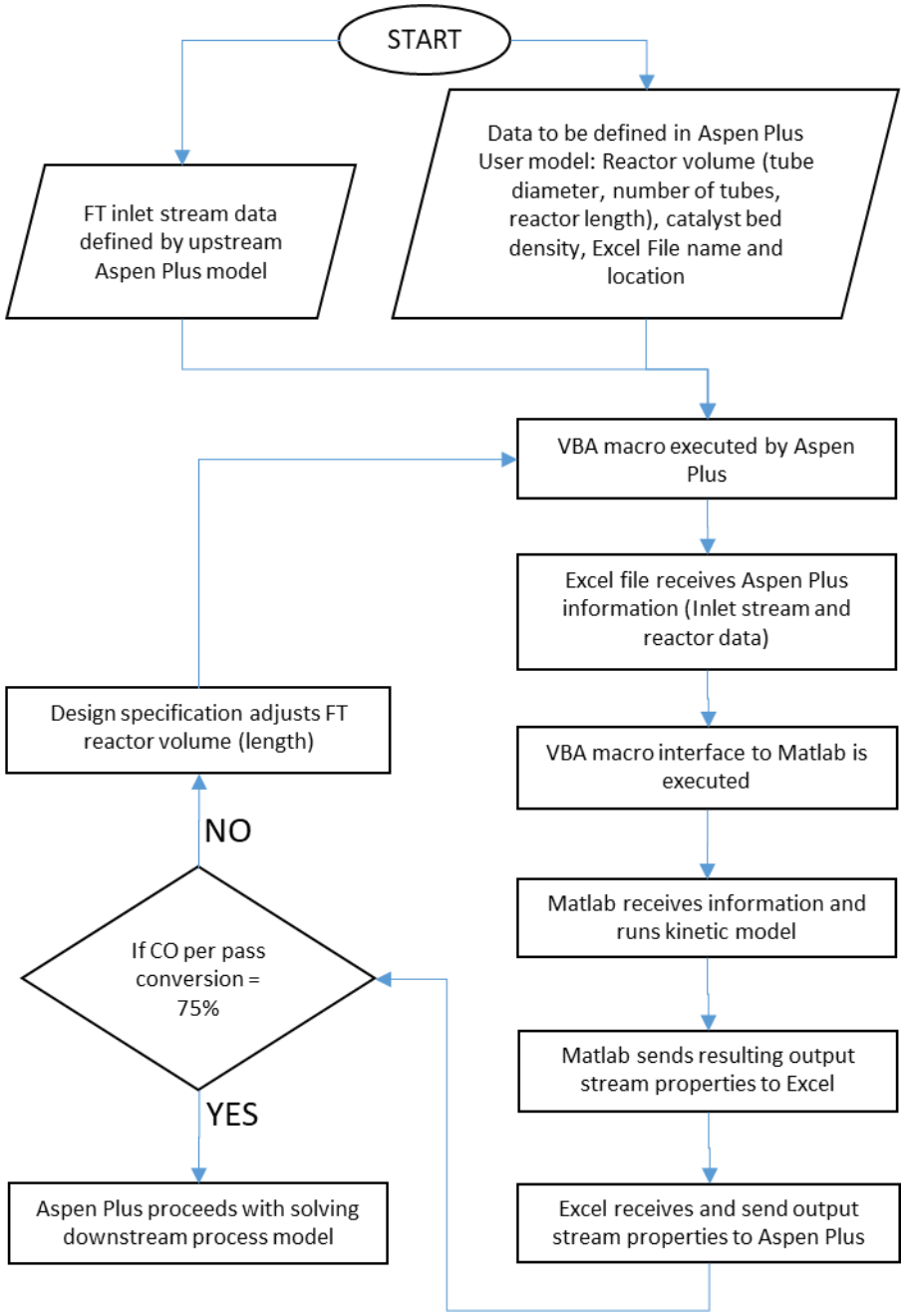

Figure 5-3: Schematic of the pseudo-algorithm of the Aspen Plus-Matlab interface for the mass balance calculations of the FT reactor.

3. **Syncrude upgrading section and unreacted syngas recycling:** The FT reactor's output requires additional processing to yield commercial hydrocarbon fractions, such as naphtha (C_5 to C_7), kerosene (C_8 to C_{16}), and diesel (C_{17} to C_{20}). To accomplish this, a series of cooling and separation stages are used, yielding three phases: 1) unreacted syngas + light hydrocarbons, 2) liquid hydrocarbons, and 3) condensed water. The liquid hydrocarbons are separated in an atmospheric distillation column, and the heavy fraction (C_{21+}) is further processed to increase the final yield of

middle distillates. As a result, the waxes are sent to a hydrocracking reactor, which runs on hydrogen and configured to maximise the jet fuel output [289], [290]. More details about the assumed operating conditions of this reactor can be found in previous work by the authors [171].

To increase efficiency and productivity, the refinery plant must be set up to recycle unreacted gases [118]–[121]. More than one recycling stream can be sent back at various stages of the process and for various purposes, as shown in Figure 5-1: i) One stream is recycled just before the FT reactor to ensure that its inlet has an inert content of 25% for thermal stability inside the reactor [118]. ii) The second stream generates heat for the endothermic RWGS reactions, by its oxy-combustion in the RWGS reactor, which is similar to a steam reformer unit [119]. The oxygen coming from the electrolyser is used in stoichiometric amount($\lambda = 1$), and the resulting flue gas is cooled further for energy recovery before being partially recycled to the oxy-combustor, with the goal of lowering its temperature to 1,200 °C. Finally, the other flue gas fraction is mixed with the fresh CO_2 and H_2, which is then directed to the RWGS reactor after further heating. iii) Finally, the third unreacted gas stream fraction that remains after the split of the required streams mentioned above, is also mixed with the fresh CO_2 and H_2, before the RWGS reactor.

5.2.2.5 Heat integration

The process was heat-integrated to maximise plant energy efficiency while reducing the use of hot and cold utilities. To that end, the software Aspen Energy Analyzer (AEA) was used to perform a Pinch Point analysis. The process and property information of the process streams were sent to the AEA model, while the energy requirements for the DAC and electrolyser were manually entered. The DAC unit requires heat for its operation during the desorption stage. An increase of the bed temperature diminishes the working capacity of the solid sorbent, and therefore, CO_2 and H_2O are released. For the Climeworks DAC unit, desorption occurs at low pressure and moderate temperature. Therefore, a low quality heat source, such as medium or low pressure steam, could be integrated with the DAC system. The latest information provided by Climeworks, shows that the heat requirement is equivalent to 11.9 $MJ_{thermal}$/kg of CO_2 captured [260]; however, Climeworks has also claimed that, due to the continuous improvement and development of the sorbent materials, this heat requirement could be reduced to 5.4 $MJ_{thermal}$/kg of CO_2 [260]. The electrolyser, in contrast, generates heat. The heat released is used for a heat district system in the same manner as in von Hepperger's study [291]. It is assumed that the electrolyser operates at 70 °C [103], and this can be used in a 4th generation or low-temperature district heating system, where the supplied and returned temperatures are 60 °C and 35 °C, respectively [292].

5.2.2.6 Water integration and cooling water system

When it comes to water integration, different parts of the system have the capacity to produce water that could be used to meet the needs of different sections of the system, such as the hydrogen production island. The electrolyser requires to be cooled with cooling water, as indicated in the section above, in order to run at an isothermal temperature of 70 °C. The cooling set-up, however, resembles a dry-cooling system because the heat generated by the electrolyser will be used for district heating. This indicates that the cooling water cycles in a closed loop, never needing make-up water and never creating waste water [283]. As a result, the total ratio of 9.26 kg of H_2O to 1 kg of H_2 remains constant. Furthermore, it is worth noting that the water requirements are primarily derived from the air (captured alongside CO_2 at the DAC unit), and from the RWGS and FT reactors, where it is synthesized as a by-product. In comparison to tap water, the total dissolved solids (TDS) level of air-derived water is roughly ten times lower [293], [294], and as a result, less sewage sludge will be produced. On the contrary, given that the water produced in the PtL process will contain some hydrocarbons, extra treatments may be necessary before its integration.

Moreover, a generic assumption of the amount of water that is lost from the cooling water network of the process plant is not sufficient, and therefore, a more detailed estimation is necessary and it is calculated according to the following equations 5-14:

$$Make\ up\ water = Evaporation\ Loss + Drift\ Loss + Blowdown$$

(5-14)

The evaporation loss is calculated using Equation 5-15 and is caused by water evaporation when cold dry air comes into contact with hot cooling water. Where evaporation is assumed to be 1% of circulation flow for every 10 °F (5.56 °C) rise between the outlet and inlet across the tower. Wind and relative humidity, among other factors, must be corrected. A factor of 0.85 is a reasonable approximation. If the climate is particularly moist, the value may fall to 0.65; if the climate is extremely dry, the value may rise to 1.0 - 1.2 [295].

$$Evaporation\ Loss = \left(0.85 * \left(\frac{1}{100}\right) * \Delta T\right) * \left(\frac{1}{10}\right) * Circulation\ Flow$$

(5-15)

Drift loss is water entrained in the tower discharge vapours, and can range between 0.1 to 0.2% of the circulation flow. For a conservative scenario, 0.2% is assumed. Finally, in order to reduce the system solids concentration, blowdown discards a portion of the concentrated (due to evaporation) circulating water. The number of concentration cycles required to limit scale formation can be used

to calculate the blowdown, as indicated in Equation 5-16 [295]. For a conservative scenario, we assumed four cycles [296].

$$Blowdown\ Loss = \frac{Evaporation\ Loss}{Cycles\ of\ concentration - 1} \quad \textbf{(5-16)}$$

5.2.2.7 Performance indicators

To quantify the performance of the proposed process configuration, the mass and energy performance indicators that are calculated are the carbon conversion efficiency, hydrogen conversion efficiency, and power to liquids efficiency. The equations that describe the mathematical correlations were introduced in Section 3.1.3.

5.2.3 Economic Evaluation

The goal of the economic assessment is to estimate economic indicators, such as CAPEX, OPEX and MJSP. A typical discounted cash flow analysis (DCFA) is used to determine the MJSP, whose financial parameters and assumptions are detailed in Table 5-2. The methodology followed for the economic assessment is described in more detail in Section 3.2. The PEC for the components of the process plant are detailed in Table 5-3. Similarly, the variable costs for the OPEX estimation are presented in Table 5-4:

Table 5-2: Parameters for conducting the discounted cash flow analysis [70], [196].

Location	United Kingdom
Plant life	20 years
Currency	£
Base year	2020
Plant capacity	2,500 kg SAF/h
Discount rate	10%
Tax rate	30%
Construction period	3 years
First 12 months' expenditures	10% of FCI
Next 12 months' expenditure	50% of FCI
Last 12 months' expenditures	40% of FCI
Depreciation method	Straight line
Depreciation period	10 years
Working capital	5% of FCI
Start-up time	6 months
*FCI = Fixed Capital Investment	

Table 5-3: Purchased equipment cost data.

Equipment	Base cost [MM £]	Base capacity	Unit	Scaling factor	Base year	Reference
Compressor	0.40	413	$kW_{electricity}$	0.68	2014	[218]
Cooling tower	2.42	4,530.3	kg_{water}/s	0.78	2014	[215]
Electrolyser	22.79[a]	100	MW_{DC}(for the stack)	0.88[b]	2020	[103]
FT-reactor	6.42[c]	2.52	MMcf/h inlet stream (STP)	0.72	2003	[216]
Hydrocracker reactor	6.23	1.13	kg/s (feed mass flow)	0.70	2014	[218]
Isomerization reactor	0.0042	1	$tonnes_{product}$/year	0.62	2015	[219]
Pump	0.08	10	m^3_{wax}/s	0.36	2014	[218]
RWGS-reactor	4.61	23.89	kg/s reactor output	0.65	2019	[122]

[a]Base cost is back calculated from the CAPEX that is provided by the reference (using a factor of 3.26). [b]Scaling factor is calculated based on the 5MW and 100MW electrolysers studied for 2020. [c]Value back calculated from installed cost provided by source (using a installing factor of 3.6)

MM=Million; cf=cubic feet

Table 5-4: Estimation of the Fixed Operating and Maintenance Cost, and Variable Cost.

Variable Cost (VC)			
A) Products			
	Price		Reference
Naphtha	0.53 £/kg		[297]
Diesel	0.44 £/kg		[297]
Oxygen	0.060 £/kg		[298]
District Heating	0.026 £/kWh		[122]
LP Steam	0.0024 £/kg		[299]
HP Steam	0.0072 £/kg		[299]
B) Utilities			
	Price		Reference
Electricity from wind turbines	0.061 £/kWh		[a]
Electricity from the Grid	0.026 £/kWh		[298]
Waste water treatment	0.415 £/t		[58]
Cooling water	0.025 £/t		[196]
Feed boiler water	0.784 £/t		[58]
Refrigerant (-25 °C)	0.0072 £/kWh		[b]
C) Catalysts			
	Price	Lifetime [years]	Reference
FT synthesis	20.70 £/kg	3	[221]
RWGS reactor	24.95 £/kg	4	[122]
Wax hydrocracking	23.28 £/kg	3	[221]
VC		A+B+C	
OPEX		FOM+VC	

[a] Value calculated from SAM [b] Aspen Plus V10 2016

Different cost estimations for low TRL technologies, such as DAC, come with more uncertainty and direct, indirect costs, as well as operating and maintenance costs, should not be estimated by using the factors applied in cost estimation of nth plant technologies.

1. **Alkaline electrolyser:** Researchers at Germany's Fraunhofer ISE have estimated the costs for both AE and PEM electrolysers, finding that the former has bigger margins for cost reduction. According to this report, the costs of a large scale AE with a capacity of 100MW could drop from 663€/kW in 2020 to 444€ in 2030 [103]. Herein, we have used the 2020 value for the cost estimation of the AE.

2. **Direct air capture cost:** There is a great deal of uncertainty surrounding the present and future costs of DAC units. Among the various assessments developed for DAC cost estimation, the National Academies of Science [300] and Young et al. [301] are the only assessments that thoroughly describe the breakdown of the capital and operating expenditures for relatively high TRL DAC technologies; solid sorbents by Climeworks among them. In this sense, the methodology adopted by Young et al. [301] was considered for the present study. Young et al. [301] determined that long-term Gt CO_2-scale DAC plants would result in lower costs than first-of-a-kind. The approach taken into account by the authors considers a first-of-a-kind (FOAK) solid sorbent DAC unit, the CAPEX and OPEX of which were estimated for a 0.96 ktonneCO_2/y unit (identical capture rate with the Hinwil plant operated by Climeworks). Then, CAPEX, fixed operating and maintenance costs (fixed OPEX costs), and variable costs (variable OPEX costs) are scaled up to the required plant capacity by using learning rates. Since the main intention of this study is to estimate costs for CO_2 capture, transport and storage, the CO_2 capture was recalculated by using the approach proposed by the original source [301]. More details on the calculations could be found in APPENDIX B-2.
3. **Reverse Water Gas Shift reactor:** Due to the novelty of this technology it is challenging to find a reliable equipment price. The considered PEC was taken from the work of Adelung et al. [122]. They developed an approach that is sensible to the operating conditions of the RWGS system. Since the operating conditions of our system are closer to the ones used by these authors, the same cost of the RWGS reactor was considered; nevertheless, the capacity was adjusted to the required for this system, by assuming a generic scaling factor of 0.65 due to the lack of relevant data (Table 5-3).

The levelised cost of the offshore wind electricity is calculated by the SAM software, following the calculations of the power generation curve. Because continuous supply of electricity via wind turbines is not possible, the grid is used as a "virtual storage" of electricity. Policies regulating this dynamic wind farm-grid interaction were not clearly found for the UK. Assuming a similar scheme as in existing net-metering policies (generally applied for small/medium scale generators of renewable energy connected to the grid), the generation costs of the electricity going and coming from the grid are offset. Given the private nature of the companies that own and operate transmission and distribution networks, a fee for network costs, must be paid for electricity drawn from the grid [298]. According to Eurostat [302], this fee is equal to 0.009 £/kWh for a UK-non-household consumer with electricity consumption above 150,000 MWh in 2019. In UK, the network costs are generally passed to the consumers [303], [304], and therefore no charges for injecting energy to the wind farm are considered.

It is important to mention that the OPEX of the DAC unit is not calculated according to this conventional methodology. Instead, the approach followed by Young et al. [301] is adopted as explained for the DAC-CAPEX section. The methodology followed by these authors calculates the OPEX in two stages. The energy requirements are considered from the values stated from Climeworks in the study of Deutz et al. [260]. The DAC unit does not necessitate external heating since the amount of heat that is necessary for the process is provided by the steam produced at the FT reactor. On the other hand, the DAC electricity is considered in the economic calculations. APPENDIX B-2 provides more information of the adopted approach. Additionally, for the estimation of the OPEX, it is important to mention that for the AE, it is necessary to change the stack every ten years, and therefore this cost is as well considered and calculated according to the following Equation 5-17 [305]

$$Alk_{repl.}[£/kW] = \frac{2}{3} * 0.4 * Alk_{CAPEX} \quad \textbf{(5-17)}$$

5.2.4 Life Cycle Assessment (LCA)

The Life Cycle Assessment (LCA) is performed according to the standardised approach outlined in ISO 14040 and 14044 [168]:

5.2.4.1 Goal and scope definition, functional unit

The goal of this LCA is to find the environmental performance of the integrated system, which represents a CO_2 utilisation scenario under the Power-to-aviation concept. The system boundaries are placed in a way that the LCA analyses the whole supply chain until the combustion of the produced SAF, which is known as the Well-to-Wake (WtWa) analysis, as depicted in Figure 5-4. Among the various environmental impacts, the global warming potential (GWP) is mainly assessed, which allows a comparison with existing SAF production pathways, as well as with regulating standards, such as the U.S. Renewable Fuels Standard (RFS) and the European Renewable Energy Directive II (RED II). These standards establish the required threshold for CO_{2eq} emissions reduction compared to those of conventional jet fuel, which is equal to 89 gCO_{2eq}/MJ and 94 gCO_{2eq}/MJ, for the RFS and the RED II, respectively [174], [175]. Synthesized jet fuel can be considered as SAF when its inherent GWP achieves at least 50% and 70% GHG emissions savings when compared to fossil jet fuel, in compliance with the RFS [176] and the RED II [175], respectively. On the other hand, the UK government is planning that for SAF to receive credits under the SAF mandate, it will be required to achieve a 50% GHG saving compared to a fossil fuel benchmark of 89 gCO_{2e}/MJ [17]. In addition, the water footprint is estimated, although there is currently no regulation towards this specific environmental impact.

The functional unit is selected on an energy basis, and therefore it is equal to 1 MJ of SAF while considering that the LHV of the SAF is equal to 42.8 MJ/kg [98] . This choice is made for ease of comparison of fuels with different origin when they have the same end use (e.g. combustion in the same aircraft) [81]. Additionally, SimaPro V.9.3.0.3 is used to conduct the LCA together with its built-in databases, such as Ecoinvent 3.6, which is a reliable source of background information.

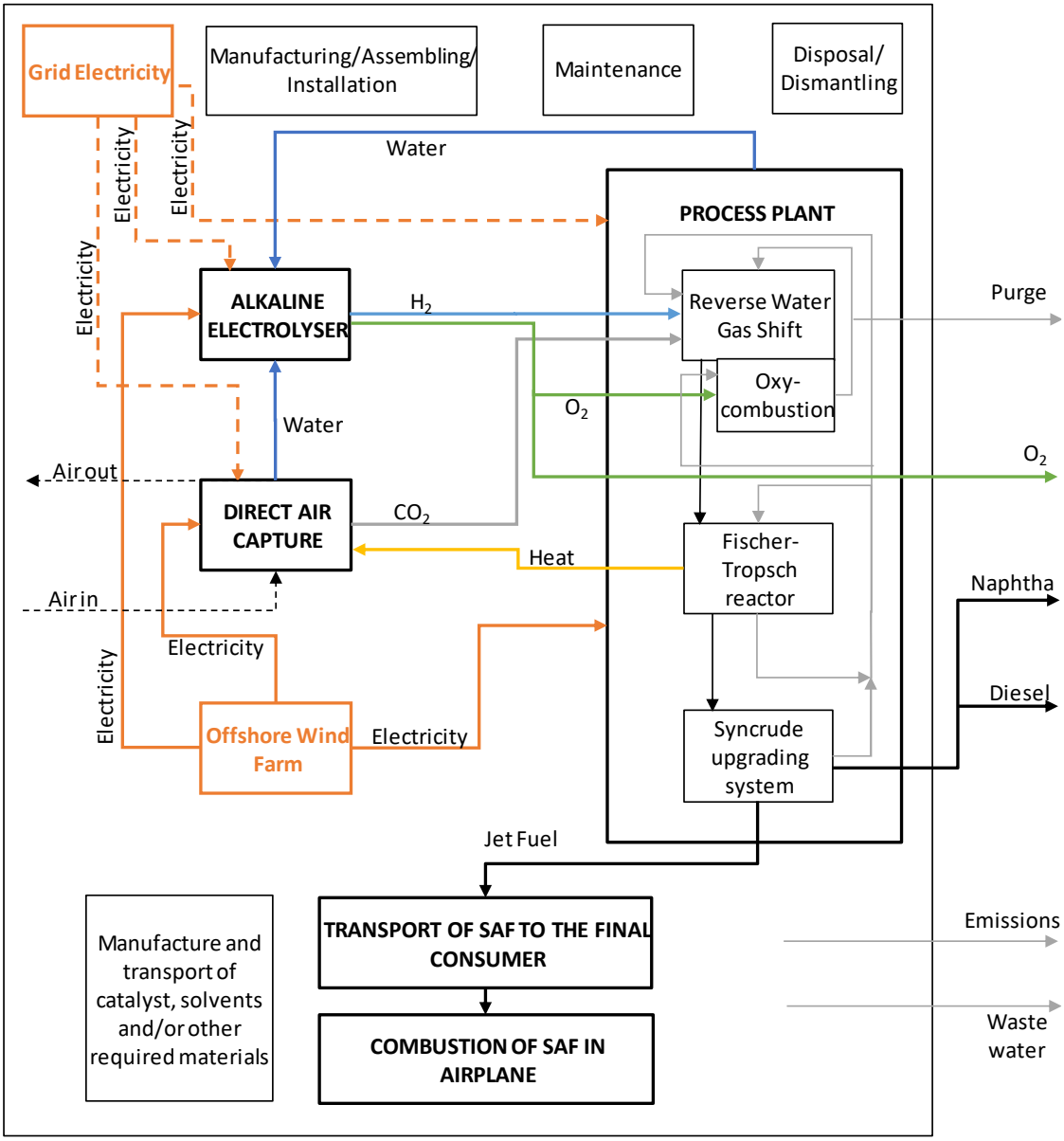

Figure 5-4: The system boundaries for the LCA of the investigated SAF route.

5.2.4.2 Multi-functionality

The selected methods for the multifunctional systems of this study was the energy, as well as the exergy allocation, due to the energy content of the produced SAF and the by-products (naphtha,

diesel) [79], [83]. The base scenario is defined as the exergy allocation, which uses an exergy allocation at the refinery level, however, no allocation is applied in the electrolyser due to the reasons that are further explained in the following sections. The allocation approach based on system expansion is not further explored since this method is prone to calculate lower GHG emissions for substituted products with larger carbon intensities than the studied system [171] [80].

5.2.4.3 Life cycle inventory (LCI) and description of the life cycle stages

The LCI for the described system is elaborated based on two primary data sources: The mass and energy balances produced through the process modelling in Aspen Plus, as well as from the literature-derived data. This information covers the normalised figures, as per the functional unit, for the DAC process, the electrolyser, as well as for the refinery plant. Moreover, the data includes information about the various waste streams and emissions produced throughout the indicated processes. The second data source is comprised of the required background data, which is mainly found in the Ecoinvent 3.6 database, as well as in the literature. The different stages of the system are depicted in Figure 5-4, while more details about the establishment of their associated LCI are explained in the following sections, and can be found in APPENDIX B-3.

1. **Off-shore wind farm:** All phases of the life cycle should be taken into account when evaluating the environmental impact of the electricity produced by the offshore wind farm. Beginning with the production of the various parts, their installation, use, and maintenance, and concluding with the decommissioning and disposal of the buildings and machinery. Previous studies have performed the LCA of different off-shore wind turbine models, while also testing the effect of the operation and maintenance strategy [306], [307], leading to different results in terms of GWP. However, the results obtained are not dramatically different and therefore, for this assessment, a generic inventory is used to represent the production of electricity from an off-shore wind turbine. This LCI is found in the Ecoinvent database, which is available in the SimaPro software, and comes under the name of “electricity production, wind, 1-3MW turbine, offshore, GB”. The database provides information of the high voltage electricity generated in 2012 at UK offshore wind farms connected to the grid. It covers infrastructure inputs as well as operating and maintenance costs. It is worth noting that the database does not account for the use of grid electricity during periods when the wind farm is not in operation. This is because the wind farm has been designed in a way that the electricity taken from the grid equals the electricity injected into it, thereby negating any environmental issues associated with the grid electricity.
2. **Alkaline electrolyser:** For this section, the LCI for the AE is taken from the work provided by Koj et al. [308]. This database provides a thorough inventory for the construction of a Zirfon alkaline

electrolyser of 6MW of capacity. At the same time, this database is combined with the comprehensive mass and energy balances produced in the current work based on [103]. All these data are accordingly arranged, normalized, and introduced in the software SimaPro, where a new inventory is created to represent AE construction and operation (maintenance is not considered due to the absence of data representing this activity). Concerning the AE's operation, no papers or studies have been found that analyse the effect of multi-functionality inherent to it, since an electrolyser not only produces hydrogen, but also by-products, such as oxygen and excess heat. Despite the opportunity of reducing emissions burden to the hydrogen (allocation) or gaining credits due to the displacement of industrial oxygen and heat for district heating production (system expansion), these options have not yet been considered due to some technical challenges and lack of technical and operational expertise, associated to the lack of commercial scale PtL plants [309]. In this sense, different scenarios for the allocation of the emissions in the AE operation are analysed, as explained in Table 6. The main assessment (AA1) assigns 100% of the environmental impacts to hydrogen. The second approach (AA2) assumes an energy allocation, with no emissions attributed to oxygen, while the heat generated from the isothermal operation of the electrolyser is now considered a by-product. Finally, the third approach (AA3) considers both oxygen and district heating as by-products, by using exergy allocation.

3. **Direct Air Capture:** The inventories for the DAC technology is based on two studies found for the Climeworks technology [260], [310]. Deutz et al. [260] and Terlouw et al. [310] provided for the first time complete LCA of a VTSA DAC unit at industrial scale, based on proprietary and confidential information provided by Climeworks, in which refers to the construction of the DAC unit. Despite the fact that the authors did not share this LCI, Terlouw et al. [310] provided a rough inventory based on freely accessible databases that could replicate their obtained findings. Consequently, these inventories were applied to represent the construction of the studied DAC technology. As for the operation, the LCI is also based on the data provided by [260], [310]; however, some numbers are adjusted to reflect the energy and water integration of the DAC system, to the other sections of the plant.
4. **Refinery Plant:** The inventory of the refinery plant is based on the generated mass and energy balances from Aspen Plus, which are normalized for 1 MJ (LHV based) of SAF. The inventory for the construction of the infrastructure is based on the existing inventory for "Chemical factory, organics {GLO}| market for | Cut-off, U" available in Ecoinvent.
5. **Transport of jet fuel:** The Ecoinvent database for "Kerosene {Europe without Switzerland}| market for kerosene | Cut-off, U" [239] is selected to represent this stage. This inventory includes information on the transport of the fuel from the process plant to the final consumer, which

includes data for the operation of storage tanks, and the emissions attributable to the SAF's evaporation, as well as to the effluent treatment.

6. **End use (combustion):** Utilizing jet fuel in an airplane is the final phase of the life cycle. The emissions for the combustion of SAF are obtained from the Ecoinvent database for "Transport, passengers, aircraft, medium haul | Cut-off, U". Since SAF's chemical characteristics closely resemble those of jet fuel, this supposition is considered accurate [80]. In this stage, it is also important to mention that carbon neutrality [240] is assumed for the CO_2 emissions derived from combustion of SAF, since the main building block of the SAF is atmospheric CO_2.

5.2.4.4 Impact assessment: Global Warming Potential and water consumption

Among the midpoint impact categories available in SimaPro, the "Recipe 2016 midpoint (H)" is selected due to its popularity among LCA practitioners, as well as its ability to estimate GWP for a 100-year time horizon. Out of the 18 calculated environmental impacts, the GWP and water consumption are further discussed:

1. **Global Warming Potential:** This effect measures the infrared radiative force caused by GHG emissions, which are given as $kgCO_{2eq}$, and characterisation factors are used for gases other than CO_2. Since the SAF derives from CO_2 drawn from the atmosphere, it is believed that their combustion generate CO_2 with a characterization factor of zero.
2. **Water consumption:** Water is an important resource in the production of hydrogen for the PtL plant. While being the main resource for the process of hydrogen generation, it is also used as a cooling utility. Understanding the water balance is important when it comes to economic and mainly environmental performances of the integrated PtL system. The water utilisation and consumption is accounted in every stage of the process, as mentioned in Section 5.2.2.6. However, the water utilisation of background LCI is detailed in the databases provided by Ecoinvent, alongside the results of Section 5.2.2.6 provide a better accounting of this resource which is as well calculated by ReCiPe Midpoint (H).

5.2.5 Sensitivity and Uncertainty analysis for the TEA and LCA assessments

As shown in Table 5-5 for the TEA, the parameters linked to high uncertainty are modified. According to the classification of the AACE International, for low level of maturity plants, as in the case of the PtL process plant, the CAPEX of the refinery is changed between -30% and + 50% [244]. Analyses of various tax and discount rates values and other significant economic characteristics are also conducted. The risk of investing in a specific project is correlated with the discount rate. For investments in PtL process plants, an optimistic discount rate of 8% is suggested [245], whereas a pessimistic discount rate of

12% is suggested. To reflect a scenario in which the PtL process might qualify for tax exemptions, the optimistic tax rate value is set at 0%, while the higher value is set at 40%. Supporting policies towards renewable energy industries may subsidise the network cost for the grid electricity [303], and therefore a bandwidth between 0 to +50% is considered for this parameter.

For the estimation of the MJSP, the TEA model requires inputs of CAPEX and OPEX estimations of the different sections of the integrated system. However, for ease of interpretation, the TEA model is modified for the sensitivity assessment and, instead of requiring individual CAPEX/OPEX of the CO_2 and H_2 production sections, the cost of capturing CO_2 and producing H_2 are the new inputs; in this way the readers can correlate costs with different technologies for capturing CO_2 and producing H_2. Table 5-5 shows the ranges of these costs using both an optimistic and pessimistic perspective:

Table 5-5: Variables used for the sensitivity and uncertainty analyses of the TEA.

Parameter	Low Value	Nominal	High value	Unit
CO_2 cost	50	359	1000	£/tonne CO_2
H_2 cost	1	3.09	8	£/kg H_2
CAPEX refinery	40.63	58.04	87.06	MM£
Cost of wind electricity	0.030	0.060	0.09	£/kWh
Cost of network use	0	0.009	0.014	£/kWh
TAX rate	0.00	30.00	40.00	%
Discount rate	8.00	10.00	12.00	%

The variables taken into account for the sensitivity analysis of the GWP are listed in Table 5-6. In order to find trustworthy values, the low, nominal, and high values for each parameter were evaluated in the current literature. Given that the system needs a lot of electricity, parameters related to electricity are essential. There are numerous studies that examine the carbon footprint of energy produced by wind; the NREL [307] developed a study that harmonised them, and this analysis took into account both the reported low and high values. Similar to this, several values for the stack efficiency of the AE were identified [284], [311]–[313]; as a result, the low and high values from this review were taken into consideration. The expected reductions of the DAC energy requirements, as a result of the improvements in the Climeworks technology, are used as the low heat and power demands [260]. As there are no reported high-values for DAC energy consumption, a 50% increase over the nominal values is assumed. Likewise, sorbent efficiency, which translates into the sorbent to capture the CO_2 mass ratio, is considered for this sensitivity analysis; for this, the Deutz et al. [260] study provides low, nominal, and high values for it. Finally, three different scenarios are analysed: 1) the UK grid is provided instead of the dedicated renewable energy source. 2) Energy allocation is used for the allocation of the products of the refinery (naphtha, diesel and jet fuel) and electrolyser (hydrogen and

district heating); and 3) 'Excess oxygen, exergy allocation', where exergy allocation is used for the allocation of the products of the refinery (naphtha, diesel and jet fuel), as in the base scenario, however, there is an exergy allocation applied to the electrolyser as well (hydrogen, excess oxygen not used in the refinery, and district heating).

Table 5-6: Variables used for the sensitivity and uncertainty analyses of the LCA.

	Value			References		
	Low	**Nominal**	**High**	**Low**	**Nominal**	**High**
Electricity carbon intensity (gCO_2/kWh)	7	15.25	22.5	[307]	*	[307]
Alkaline Stack efficiency (%)	58	68.81	72.82	[314]	[103]	[103]
Sorbent amount (g/kg CO_2)	3	7.5	11.25	[260]	[260]	-
DAC power requirement [MJ/kgCO_2 captured]	1.8	2.6	3.9	[260]	[260]	-
UK grid (gCO_2/kWh)	-	193.38	-	-	-	-
Excess oxygen, exergy allocation	-	-	-	-	-	-
Energy allocation	-	-	-	-	-	-

* Electricity, high voltage {GB}| electricity production, wind, 1-3MW turbine, offshore | Cut-off, U

Due to the novelty of the 'PtL' concept, the different variables considered for the TEA and LCA assessment are associated with some degree of uncertainty regarding their real value, as reflected in Table 5-5 and Table 5-6. In this sense, the uncertainty analysis is essential to showcase the effect of the uncertain variables on the final results. Thus, Monte Carlo simulations are performed for the MJSP and the GWP based on the same parameters considered for the sensitivity analysis, except for the GWP that uses the first four variables of Table 5-6.

5.3 Results

5.3.1 Process modelling

This section presents the results of the mass and energy balances calculated using the various process models. The FT product distribution is presented in APPENDIX B-4. The DAC models estimate the amount of water that could be captured, and the results are used to explain the water integration and footprint. The process model created in Aspen Plus is critical for presenting mass and energy balances, which are then used for environmental and economic assessments. In addition, the water and heat integration are further discussed.

5.3.1.1 PTL process: mass and energy balance

The mass and energy balances, overall, estimated that 13.3 tonne/h of CO_2 and 3.35 tonne/h of H_2 are required for the production of 0.88 tonne/h of naphtha, 2.52 tonne/h of jet fuel, and 0.81 tonne/h of diesel. Figure 5-5 presents the carbon molar flow and distribution along the process and the products. Carbon is only lost to the atmosphere at the DAC unit and the purge gas, where 1.48 tonne/h and 0.29 tonne/h of CO_2 are emitted, respectively.

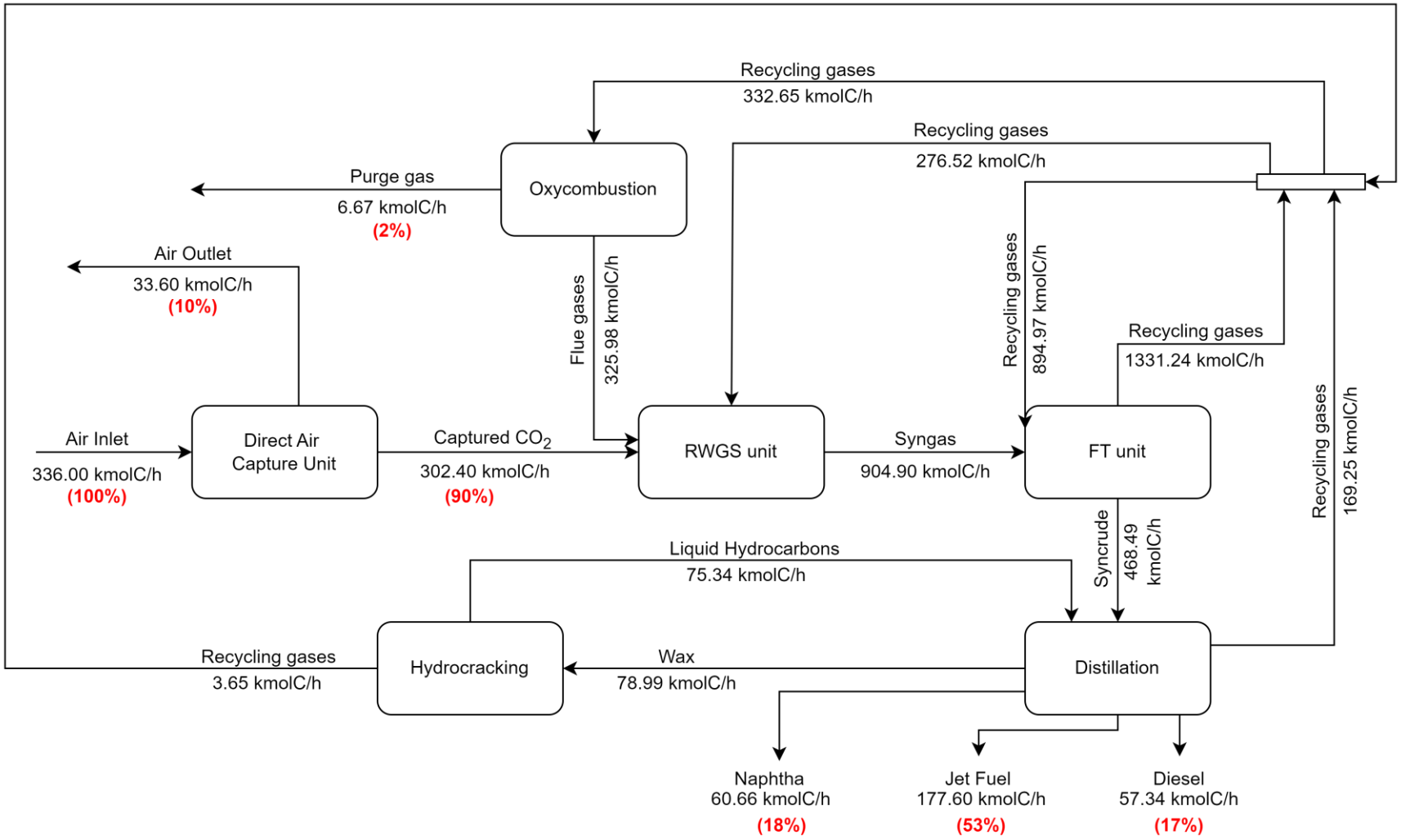

Figure 5-5: The carbon mole flow of the investigated SAF route.

Based on these overall balances, efficiencies such as carbon conversion, hydrogen conversion, and PtL, equal to 88.0%, 39.16%, and 25.6%, respectively. Table 5-7 lists the findings from similar research that examined the synthesis of electrofuels using PtL/FT. It can be seen that the carbon conversion efficiency estimated for this study is in line with previous studies. High carbon efficiencies are highly linked to high CO_2 capture fractions and most studies assume capture of more than 90%. The presence of appropriate recycling streams of the unreacted syngas to the synthesis sections is another crucial factor to take into account. In this sense, a combination of DAC with high CO_2 capture efficiency, as well as the existence of proper recycling streams (as in the present study), enhances the productivity of the products.

Due to the water synthesis that occurs at the RWGS and FT reactors, PtL systems have generally low hydrogen efficiency. One mole of water is synthesised for every mole of CO produced in the RWGS reactor, while at the FT reactor, the amount of produced water is greater (mole basis) than the hydrocarbons generated [315].The estimated hydrogen conversion efficiency of this study is higher than previous research and this is attributed to variations in the process configurations, such as the existence of several recycling streams as well as the employment of a comprehensive FT kinetic model.

Although the PtL efficiency is lower compared to other studies that are contrasted in Table 5-7, it is within the bounds reported in Marchese et al. [121]. The main reason for this is the utilisation of the kinetic approach for the FT reactor. As previously stated, the lumped kinetic model can predict the ASF model's deviations and predicts higher levels of CH_4 production of, which lead to lower production levels of liquid hydrocarbons and, thus, lower PtL efficiency.

Table 5-7: Literature review on technical performance of PtL studies for e-fuel production.

	Main Product	**Carbon efficiency**	**Hydrogen efficiency**	**PtL efficiency**
This study	Jet Fuel	88%	39.16%	28.06%
Adelung et al. [119]	FT liquid fuels	88.00%	28.00%	38.70%
Vidal-Vazquez et al. [117]	Oil and Wax	59.50%	30.80%	N/A
Vidal-Vazquez et al. [117]	Oil and Wax	94.00%	32.00%	47.00%
Zang et al. [316]		45.53%	24.35%	52.20%
König et al.[106]	FT liquid fuels	73.00%	---	45%
Hannula et al. [286]	FT liquid fuels	65%-89%	----	37%-41%
Hannula et al. [286]	FT liquid fuels	50%-55%	----	34%-36%
Marchese et al. [121]	FT liquid fuels	58.1%-73.78%	----	22.6%-36.5%

5.3.1.2 DAC working capacities

Section APPENDIX B-5 illustrates, at atmospheric pressure, the influence of the RH over the CO_2 working capacity. These results [270] confirm the impact of temperature and relative humidity on the CO_2 working capacity: the latter increases with an increase in RH, with the impact being more pronounced at low temperatures. At the operating weather conditions that are taken from the data provided by Merra-2 for Teeside [276] (hourly temperature, pressure and relative humidity conditions for 2020), and considering temperature and pressure of desorption equal to 110 °C and 1×10^4 Pa (0.1 bar) [270], [317], the resulting working capacities for the CO_2 and the H_2O equal 2.82 molCO_2/kg and 9.61 molH_2O/kg of sorbent, respectively. In other words, for 1 kg of CO_2, 1.4 kg of water is produced. When compared with the literature, these results are in agreement with previous studies [270], [317]–[319], for instance, DLR et al. found a value of 1 kg of extracted water per kg of captured CO_2 [319]. Based on the mass balance, this water can cover 60% of the electrolyser's water demand.

5.3.1.3 Heat and water integration

Figure 5-6 illustrates the hot and cold streams taken into account for the Pinch Point analysis as a starting point for the heat integration. The streams that need cooling are shown in red on the diagram, whilst those needing heating are shown in blue. Since the heat released by the syngas combustion is integrated to the RWGS reactor and its inlet stream preheating, they are not taken into account for this diagram or the subsequent analysis. The hot and cold composite curves clearly show that the system's heat integration is a "threshold problem" rather than a "pinch point problem," which means that only one thermal utility is needed, and there is no pinch point temperature. As the process itself provides the necessary heating, no external hot utility is needed in this particular instance.

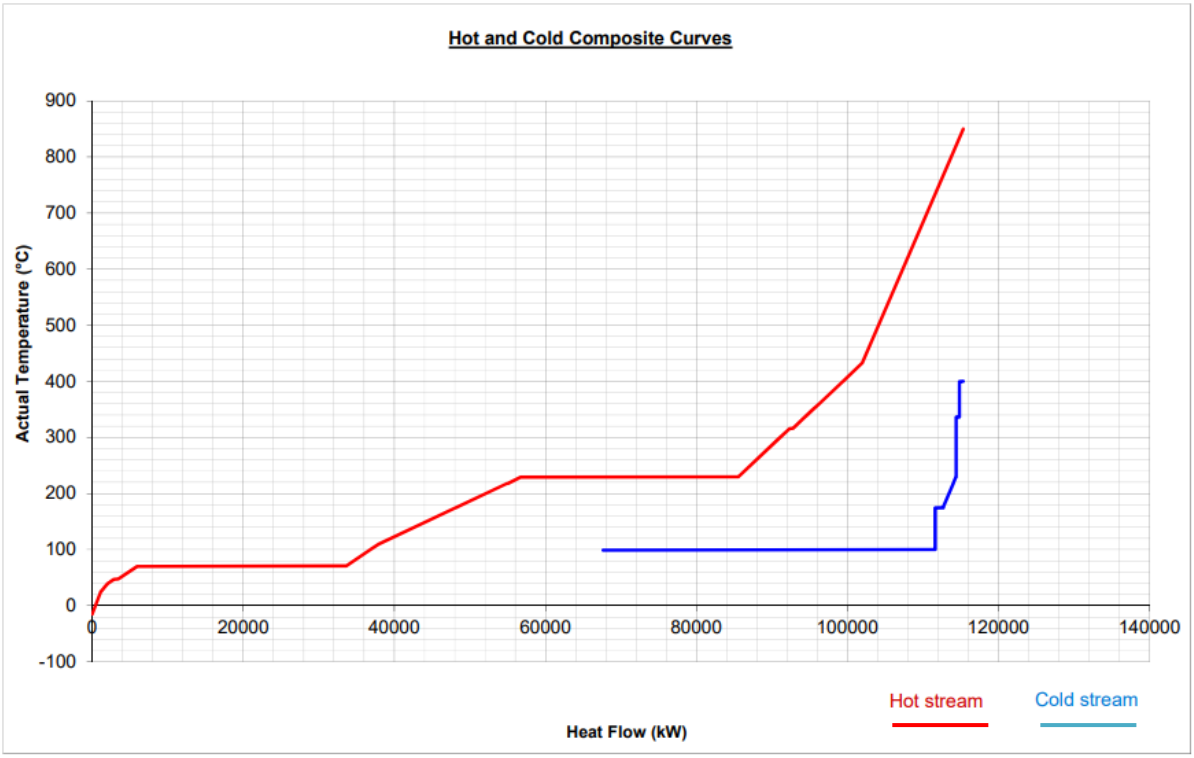

Figure 5-6: The composite curves of the PtL system.

The streams that were taken into consideration for this heat integration, exchange heat when it is possible, but because the process requires more heat than it does cooling, the excess heat is used to produce steam at different qualities, as shown in APPENDIX B-6. As a result, the cooling needs are met by the production of LP and HP steam, cooling water, and a refrigerant. There is no need to install an additional external heat source because the system itself completely meets the heating requirements. There is a synergy between the DAC unit and the process plant because the LP steam generated at the FT reactor is integrated with the DAC for the regeneration of the sorbent. Surplus LP and HP are produced at rates of 7.85 and 26.28 tonne/hr, respectively, which are considered as products with a positive economic input for the system.

The water integration is important for the hydrogen generation, which totally derives from water electrolysis. In total, 30.98 tonnes/h of water is required, from which 17.35 tonnes/h are potentially produced at the DAC unit, while the remaining requirement is considered to be provided by the process. The synthesis reactions occurring at the RWGS and the FT reactors are responsible of the production of 24.84 tonnes/h of water, from which 11.21 tonnes/h are sent to the electrolyser for the hydrogen generation. It is crucial to note that the water produced by the process may contain trace amounts of a variety of substances, including alcohols, ketones, aldehydes, carboxylic acids, and inorganic compounds [315]. As a result, it is crucial that industrial setups choose the best technology

for treating the water. In terms of this study, a typical waste water treatment is taken into account. Although the selection of an adequate water treatment is outside the scope of this study, it is important to mention that if more rigorous purification techniques are needed, this could have an impact on the economic performance of the system.

5.3.1.4 Electricity Requirements and Wind Farm Electricity Generation

The power demand for the various sections of the system are presented in Table 5-8. The dedicated off shore wind farm is designed in order to produce the requirements for the plant. Thus, 103 wind turbines can generate 199.69 MW based on the weather data and the wind farm's technical design. The annual hourly profile of energy generation, as represented in Figure 5-7, reveals that there are times when the wind farm cannot produce the necessary energy. To tackle this, grid electricity is supplied to the system as part of the constant energy supply strategy explained before. In contrast, when the system generates more electricity than what is necessary, the excess is delivered to the grid. Overall, 660 MWh per year are exchanged between the wind farm and the grid.

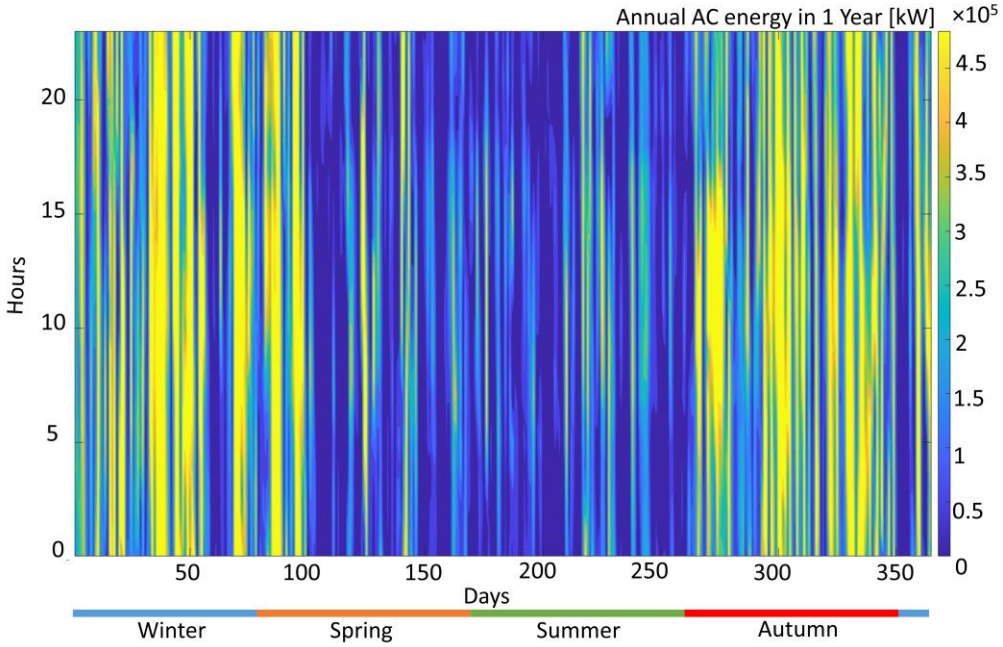

Figure 5-7: Power curve for the designed wind farm.

Table 5-8: The electricity demand of the integrated PtL system.

Process sections	Electricity demand [MW]
Refinery	5.57
Electrolyser	181.15
Direct Air capture	9.61
Overall electricity demand [MW]	
196.33	

5.3.2 Economic performance

Initially, the CAPEX of the system was evaluated, and it is estimated to be 331.55 MM£ (or 1.93 £/kg of SAF). The CAPEX breakdown of the process is 31%, 18% and 51% for the electrolyser, the refinery plant and the DAC respectively. The DAC unit is the dominating expense, and due to its early stage of development, the estimated DAC CAPEX is associated with significant uncertainty [320]. It is difficult to compare the predicted CAPEX with past PtL research because most of them used CO_2 capture costs as inputs for their economic assessment. A similar process configuration was studied by Comidy et al. [102], who found that the cost of the AE+RWGS reactor accounts for 59% of the overall CAPEX. Similarly, Marchese et al. [305], analysed several scenarios for the production of FT-derived wax, finding CAPEX dominated by the cost of the DAC unit, which was based on a liquid sorbent (Carbon Engineering) technology.

The MJSP has been estimated as 5.16 £/kg of SAF (or 0.12 £/MJ). The process is OPEX intensive and the OPEX accounts for around 73% of the MJSP, i.e., 3.76 £/kg; the OPEX breakdown is detailed in Figure 5-8. This figure details the contribution of each component to the OPEX normalised per 1 kg of SAF. Based on these findings, it is possible to conclude that the cost of electricity (grid and wind-derived) accounts for the majority of the OPEX and, as a result, the MJSP. The annualised CAPEX is also a small proportion of the total MJSP, making the uncertainty created by certain equipment costs less significant when compared to the importance of the OPEX. Previous PtL based on FT studies found a variety of levelised costs of the analysed products, probably due to the differences in process configurations, plant capacities and equipment cost data; however, even under the most optimistic scenarios, all the estimated costs are much higher than the fossil-derived fuels. For example Hombach et al. [125] estimated a figure of 4.25 £/kg for the levelised cost of e-diesel in 2015, and a cost reduction to 3.37£/kg for 2030, for DAC-derived CO_2 costs. Adelung et al. [122] calculated minimum selling costs ranging from 1.59 to 4.79 £/kg, for optimistic and pessimistic electrolysis-derived hydrogen scenarios, using CO_2 captured from a cement plant. In another study, Marchese et al. [305], estimated wax production costs ranging from 4.43 to 24.04 £/kg, based on liquid sorbent DAC technology for the capture of CO_2. Comidy et al. [102], assessed a system using nuclear energy and

sea water acidification for CO_2 capture, and for the scenario operating with a dedicated nuclear power plant, the minimum production costs or aircraft carrier's fuel were found ranging from 2.52 to 3.28 £/L. Furthermore, existing research targeting jet fuel production is scarce, and for a similar process configuration as the one of this study, some reports were found in the open literature [38], [127], [128]. In the report of Batteiger et al. [127] a figure of 2.00-2.57 £/kg of SAF are presented for the near-term estimation of the MJSP. Long term (2050) estimations predict that the MJSP could drop to figures of 1.54-1.94 £/kg [38], [127]. Similarly, Fasihi et al. [128] found values for the MJSP ranging between 1.20-1.43, 0.86-1.09 and 0.68-0.80 £/kg for 2030, 2040 and 2050, respectively.

The main conclusion of the analysed scenarios is that the economic performance of the SAF is attributed primarily to the high power requirements associated with green hydrogen generation. Another important point to discuss is that the studies that source their CO_2 requirements from a DAC unit, similar to this study, estimate larger minimum production costs for their PtL products, compared to other configurations with different CO_2 sources (e.g. concentrated sources); therefore, reducing CAPEX and OPEX costs of the various DAC technologies available in the market can play an important role on the reduction of production costs of e-fuels, alongside carbon credits that can be earned due to the utilisation of atmospheric CO_2.

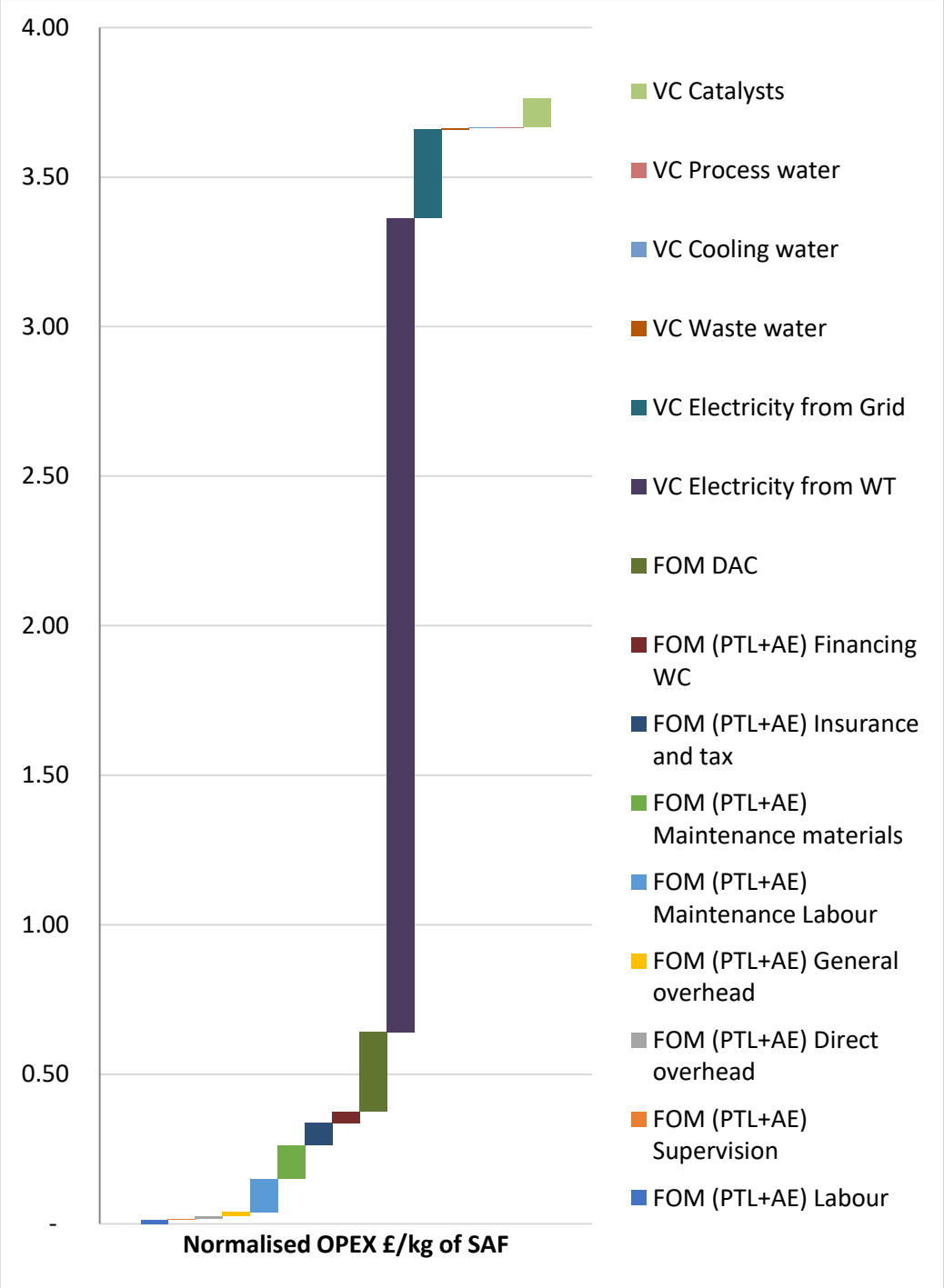

Figure 5-8: The normalised OPEX of the investigated SAF route.

5.3.2.1 Sensitivity analysis and economies of scale

The outputs of the sensitivity of the calculated MJSP are presented in Figure 5-9; the blue and grey bars represent a reduction or increase in the baseline MJSP value, respectively. The largest variations are observed for the cost of producing H_2 and cost of capturing CO_2. Improvements in increasing the efficiency and decreasing the cost of the electrolyser is essential for cost reductions. In addition, lower

electricity costs should be sought and ideally expected; in the UK, for example, low offshore wind electricity prices have already been attained in 2022 (0.037£/kWh) [321], which can be seen as an incentive for the development of PtL projects. The MJSP exhibits low sensitivity to the CAPEX of the refinery. Moreover, governments undoubtedly have a significant role to play in formulating tax rates that could help reduce the MJSP; however, even in the most optimistic scenarios, the MJSP never decreases to levels that could make SAF competitive with fossil-derived jet fuel. Therefore, to encourage the production and consumption of SAF, it is crucial for governments to offer carbon credits or other incentives.

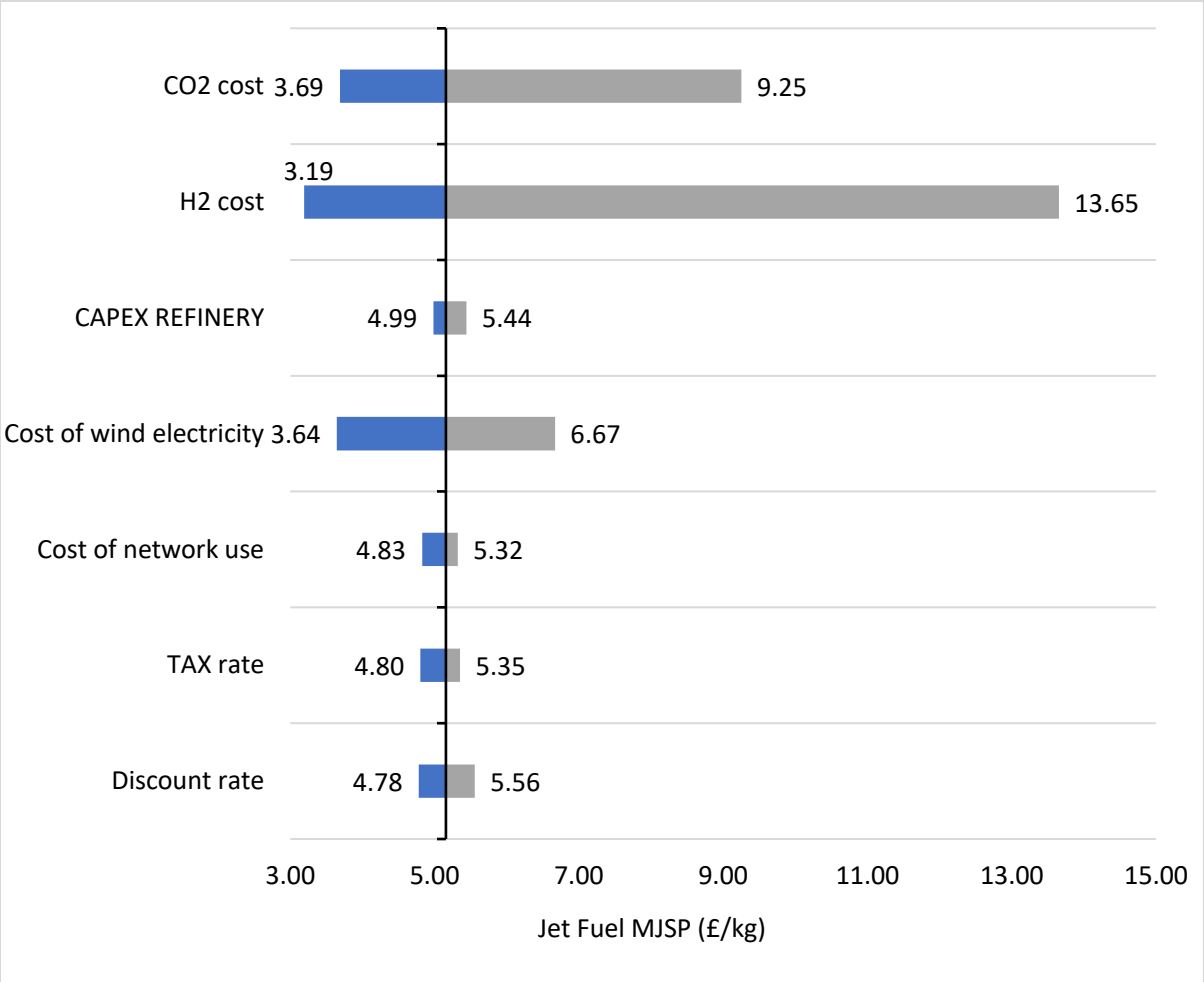

Figure 5-9: Sensitivity of the MJSP to various economic variables.

The effect of economies of scale on the MJSP of the SAF, is shown in Figure 5-10. The CAPEX of each section of the system was adjusted separately for the calculations at different capacities; for the refinery plant, an escalation factor of 0.65 was used; for the AE, a factor of 0.88 (calculated from reference [103]); and for the DAC, the learning rates methodology were applied. On the other hand, a linear adjustment to the capacity of the plant was assumed for all the raw materials, utilities, and

products of the system, as detailed in Rojas et al. [171]. The MJSP can decrease by 15% but the size of the plant should increase by approximately 5 times. When the PtL process is compared to a similar biomass to liquid (BtL) system for the production of SAF, the decline of the MSJP with the increase of the system's capacity is less steep than in the BtL system, as evidenced in the Rojas et al. [171] study. This is explained by the fact that PtL-derived SAF has been shown to be OPEX dependent, whereas BtL-derived SAF has a significant dependence on the CAPEX.

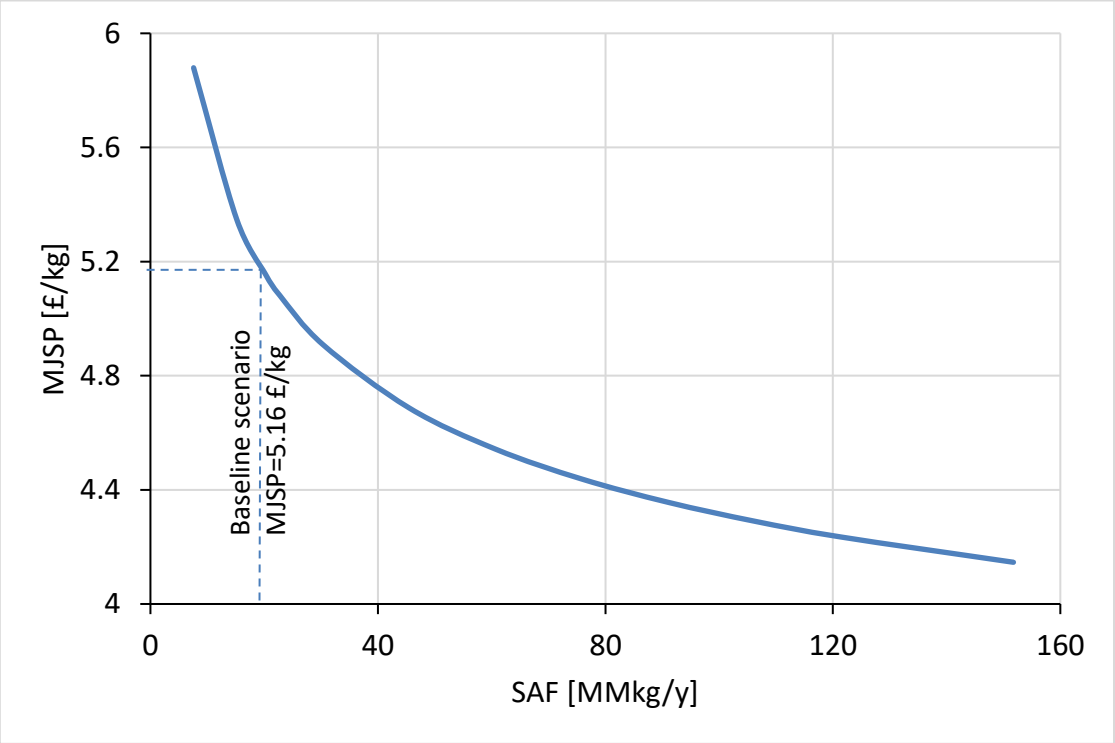

Figure 5-10: Economies of scale for the of the investigated SAF route.

5.3.2.2 Uncertainty analysis

The Monte Carlo analysis yields mean and median MJSPs of 7.68 and 7.47 £/kg of SAF. The similarity of these values demonstrates the uniform distribution of the 10,000 datasets, and this is shown in Figure 5-11. The MJSP could be located anywhere between 2.45 and 12.91 £/kg with a 95% confidence. These findings highlight two points: first, the relatively high value of the standard deviation means that the distribution of the possible MJSP around the mean is very scattered due to the high level of uncertainty that is taken into account for the CO_2 and H_2 costs; and secondly, even in the most optimistic situation, the MJSP is never in a strong position against fossil jet fuel, which further supports the idea that incentives and carbon credits are necessary for PtL-derived SAF.

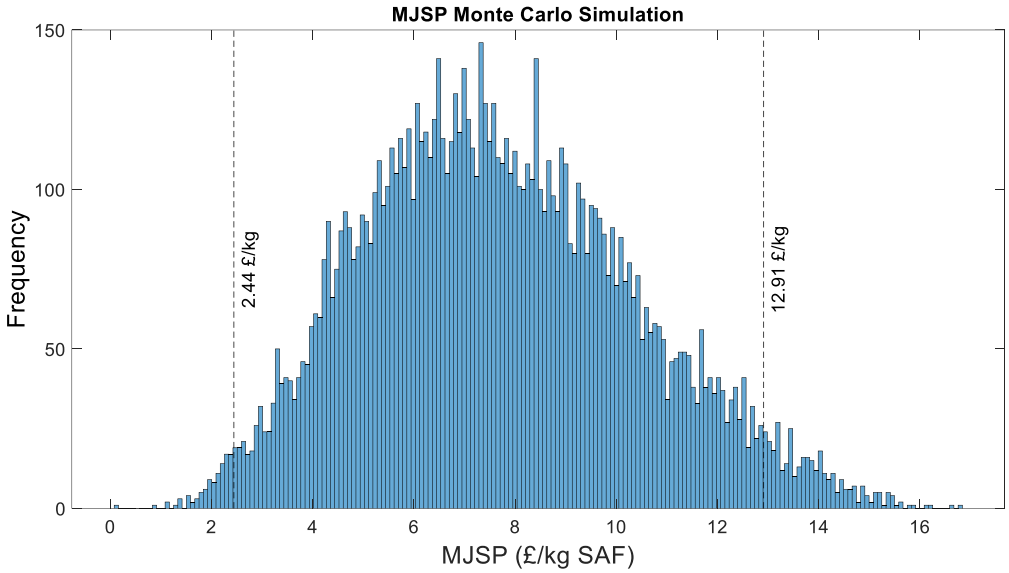

Figure 5-11: Uncertainty analysis of the MJSP.

5.3.3 Environmental performance

The two primary environmental effects examined in the LCA are GWP and water footprint. The discussion of the selected allocation technique is crucial because the subsystems exhibit multifunctional behaviour. As explained before, the chosen allocation methods are based on energy or exergy content, due to the final utilisation of the products. The various factors that have been taken into account for each allocation method are shown in Table 5-9. The primary allocation approach, for which the sensitivity and uncertainty analysis are developed, is the "Exergy allocation process plant, no allocation in the electrolyser," as a result of the facts disclosed about the by-products of the electrolyser. In the following sections, the GWP and water footprint results are widely analysed; however, for a more detailed overview of the other environmental impacts calculated by the ReciPe 2016 Midpoint (H) method, the reader is referred to APPENDIX B-7.

Table 5-9: Description of different allocation methods.

		Products considered for the allocation method		
Subsystem	**Main and by-products**	**Exergy allocation process plant, no allocation in the electrolyser (AA1)**	**Energy allocation (AA2)**	**Exergy allocation (AA3)**
Electrolyser	Hydrogen	Yes	Yes	Yes
	Excess Oxygen	No	No	Yes
	District Heating	No	Yes	Yes
DAC	Carbon Dioxide	Yes	Yes	Yes
	Water	No	No	No
Process plant	Naphtha	Yes	Yes	Yes
	Diesel	Yes	Yes	Yes
	SAF	Yes	Yes	Yes
	Water	No	No	No

5.3.3.1 Global Warming Potential

The GWP is estimated at 21.43 gCO_{2eq}/MJ and the largest contributor is the hydrogen production stage, as shown in Figure 5-12. For more clarity about the role of the offshore-wind electricity, Figure 5-13 provides more specific information about each stage of the WtWa LCA and how the offshore wind electricity contributed to them. Most of the emissions are due to the carbon footprint of the electricity. In this sense, strategies to even further reduce the GWP of the PtL-derived SAF could be considered, such as improvement of the energy efficiency of the system and reduction of the carbon footprint of the electricity source (by improving construction, maintenance, and operation stages). On the other hand, it should be noted that the GWP performance of the SAF complies with the threshold emissions reduction set by the European Renewable Energy Directive II (RED II) [174], the Renewable Fuels Standard (RFS) [175], and the UK SAF mandate [17].

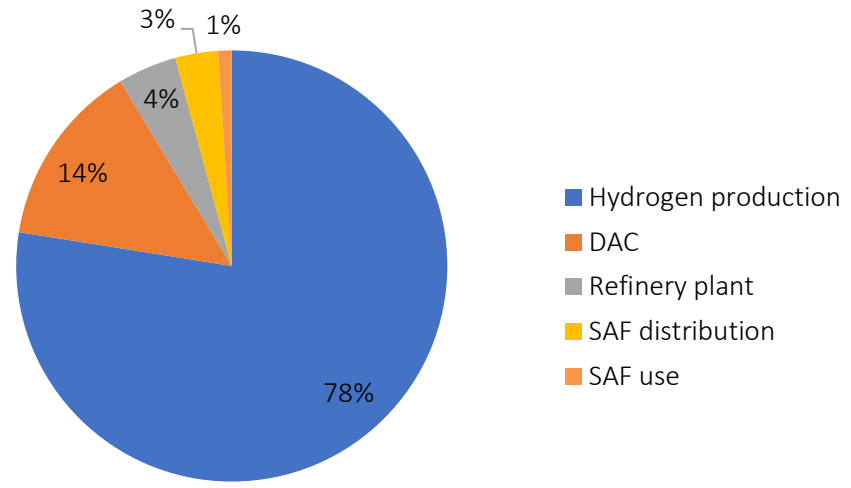

Figure 5-12: The breakdown of the GWP for each process stage.

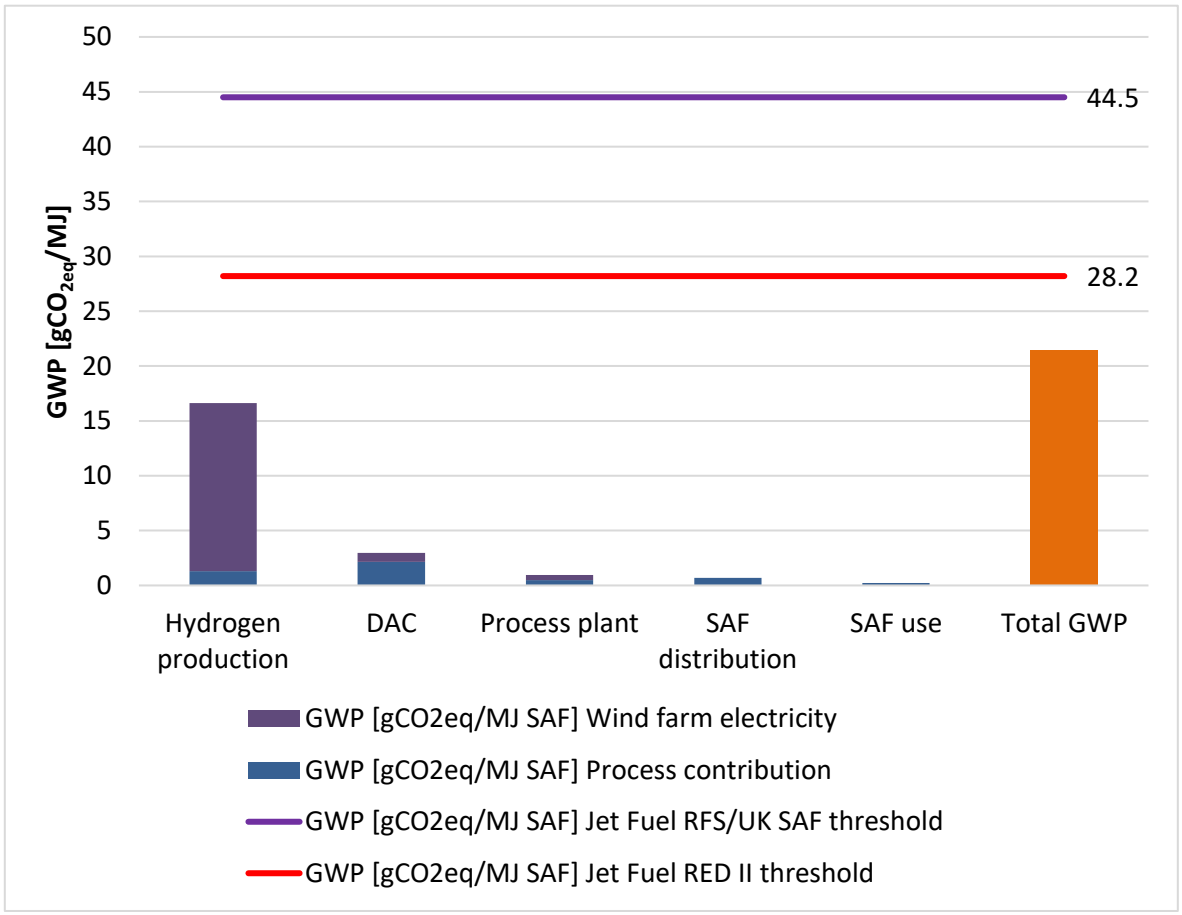

Figure 5-13: The contribution of electricity for each process stage, the overall GWP and comparison with existing sustainability standards.

Some LCA studies have assessed the GWP of FT/PtL for liquid fuels synthesis [102], [125], [322], and some the specific scenario of jet fuel production [38], [124], [127], [136]. The carbon footprint performance of SAF production was found as 13.88 gCO_{2eq}/MJ, 5-10 gCO_{2eq}/MJ and 1 gCO_{2eq}/MJ, by Falter et al. [124], Batteiger et al. [127], and Schmidt et al. [38], respectively. The GWP value estimated herein, i.e. 21.43 gCO_{2eq}/MJ, is of the same order of magnitude, but still significantly higher. These discrepancies may be attributed to factors such as the choice of the DAC technology, the process configuration of the refinery (no FT off-gas recirculation), assumptions for the refinery's mass/energy balance (use of simplified models instead of detailed models), as well as the use of various energy sources to provide electricity. Further, recent studies such as Micheli et al. [136] display a value of 13.4 g CO_{2eq}/MJ for a similar system, while the Royal Society report [323] displays a range of 17-27 gCO_{2eq}/MJ for PtL SAF. It is important to point out that none of these studies or reports have examined synergies between the main components (CO_2 capture, H_2 production and refinery) of the PtL systems as we did in the current research such as the water and heat integration previously discussed.

5.3.3.2 Sensitivity analysis on the GWP

The outputs of the sensitivity analysis of the GWP are presented in Figure 5-14, with the blue and grey bars representing a reduction or increase in the baseline GWP value. The GWP exhibits great sensitivity to the electricity carbon intensity. Furthermore, as shown in Figure 5-14, increasing the energy efficiency of the AE and the DAC, which are the two largest electricity consumers of the system, barely affects the GWP. Some scenarios were evaluated by taking into account various allocation strategies or a different energy supply, such as electricity from the UK grid. Regarding the system's multi-functionality, the GWPs for the energy (AA2) and exergy allocation (AA3) decrease by 13.15% and 7.59%, respectively, when compared with the baseline allocation scenario (AA1). This decrease can be explained by the fact that AA2 and AA3 considered that the electrolyser-related emissions are distributed upstream among its by-products (oxygen, heat), reducing the burden on the H_2 and, consequently, the GWP of the final SAF. Nevertheless, it appears that the different allocation methods do not have a great effect on the GWP. The same cannot be said for the scenario using the current UK grid electricity mix. As it can be seen, using grid energy rather than a dedicated offshore wind farm increases the GWP by almost ten times. Based on these findings (except for the grid electricity scenario), the SAF synthesised under any low/high bounds of the examined parameters will always comply with the most stringent emissions reduction threshold (RED II).

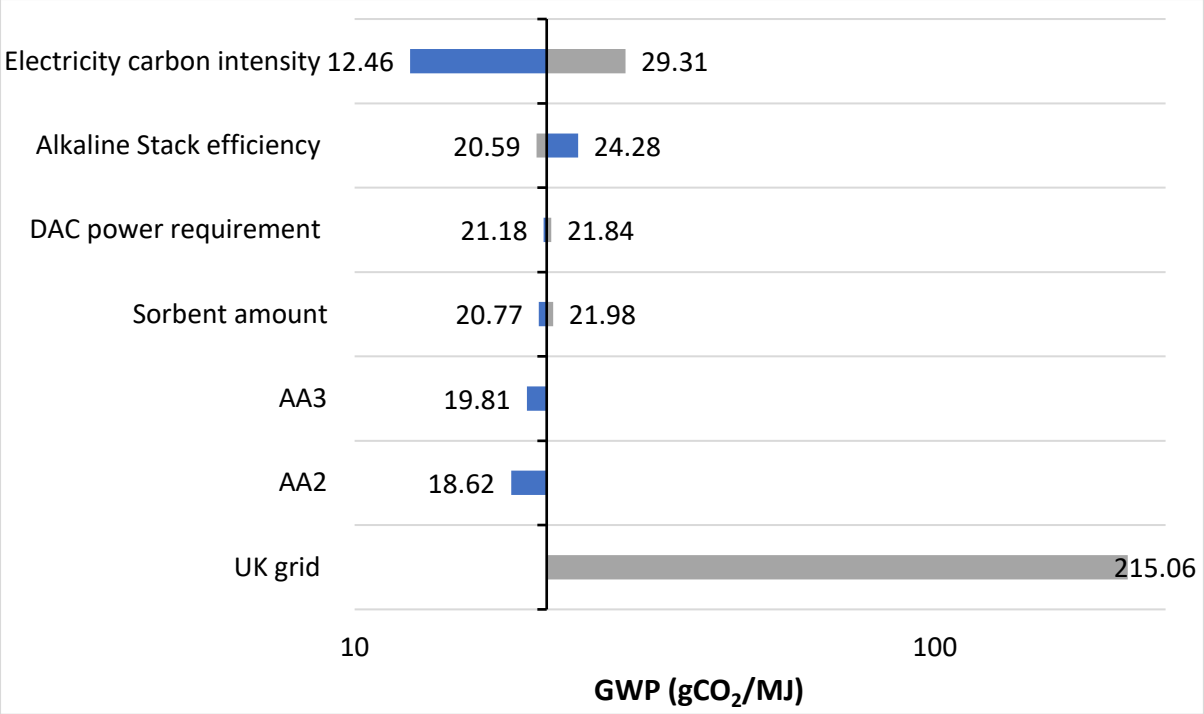

Figure 5-14: Sensitivity analysis on the GWP, and scenario analysis for other allocation methods (AA1 and AA2) and UK grid electricity.

Further, the sensitivity of the GWP is assessed for different electricity sources at different total power requirements as depicted in Figure 5-15. The range for the carbon footprint of the electricity is chosen according to the existing options that are part of the UK grid [324], [325]; however, because the carbon footprint of the fossil-derived sources is very high, only low GWP sources are included. The range for the electricity consumption is based on the efficiency ranges considered for the electrolyser and DAC; the electricity requirement of the refinery plant is assumed unchanged). The GWP potential is recalculated at different conditions as shown in Figure 5-15. The horizontal lines represent the various electricity sources. Clearly, high carbon footprint electricity sources increase the GWP of the SAF. In the bottom of the diagram, Wind, Nuclear and Norwegian import (named in decreasing order) are able to produce SAF with GWP below the SAF mandate threshold at any system power consumption. Moreover, changes in the amount of required electricity does not have a big impact on the GWP, especially for low carbon footprint electricity sources. Thus, achieving low GWP SAF should rely in electricity sources such as wind or nuclear.

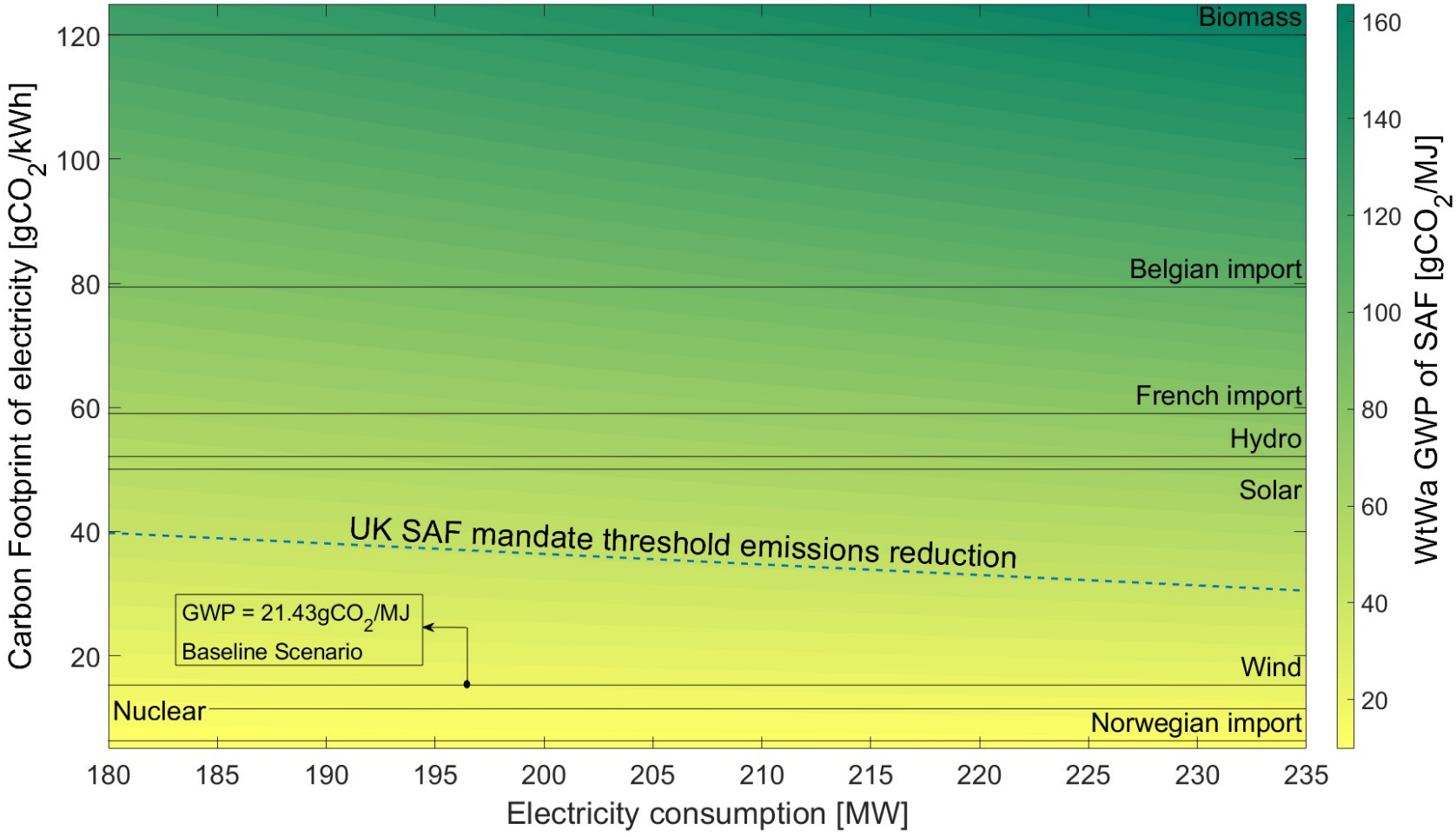

Figure 5-15: The GWP of the WtWa life cycle of SAF for different electricity sources at different PtL electricity consumption.

5.3.3.3 Uncertainty analysis on the GWP

Figure 5-16 depicts the results for the Monte Carlo analysis on the GWP. Further the mean and median GWP values equal to 21.05 and 21.13 gCO_{2eq}/MJ of SAF, respectively. Their similarity is attributed to the symmetric probability distribution. The standard deviation equals 3.54 gCO_{2eq}/MJ which translates into a 95% interval of confidence between 14.10 gCO_{2eq}/MJ to 28.00 gCO_{2eq}/MJ. Based on these results, it is clear that regardless of the uncertainty associated, the GWP of the WtWa study will always result in a SAF that complies with all the emissions reduction thresholds for sustainable aviation fuels. It is expected that the standard deviation will become smaller as the involved technologies become more mature.

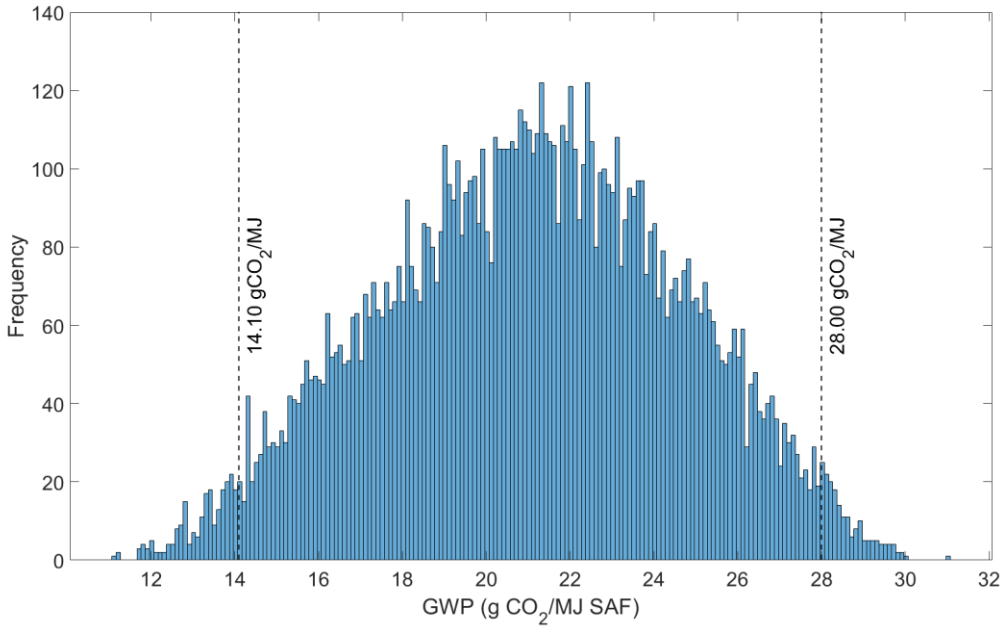

Figure 5-16: Uncertainty analysis of the GWP.

5.3.3.4 Water footprint

It is worth noting that the global warming potential is just one aspect of the environmental impact of SAF production from PtL, and other factors such as water footprint and land use should also be considered. However, reducing the water footprint of SAF production from PtL can help to reduce the overall environmental impact and improve the sustainability of aviation. The resulting water footprint for the analysed scenario equals 0.480 l/MJ of SAF and this is further detailed in Figure 5-17. It is obvious that the stage of hydrogen production accounts for almost 50% of the overall water footprint of the WtWa analysis for SAF derived from PtL. Additionally, Figure 5-18 show the precise impact of the different shares of the various steps for the three stages of the analysis that use the most water:

the production of H_2, CO_2, and SAF. Figure 5-18A shows the water footprint of H_2 production via AE, with negligible contributions from chemicals production (nitrogen, potassium hydroxide). The water requirement for the electrolysis reaction is covered by water produced in the DAC and the refinery, and thus not accounted for the water footprint calculations. It is thus evident that electricity generation has the greatest influence on the water footprint of hydrogen production, while the construction of the electrolyser is almost negligible.

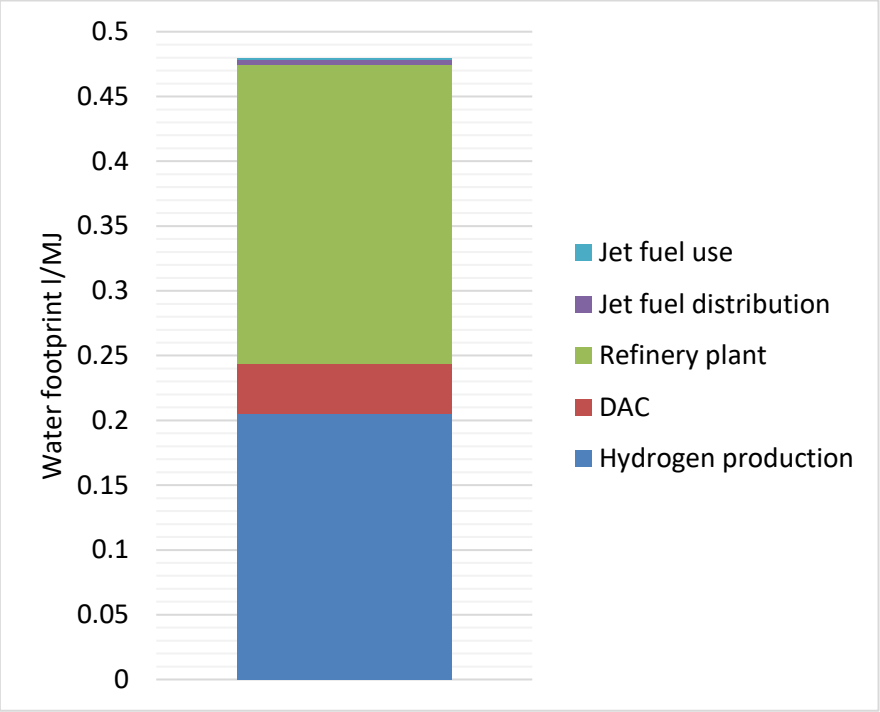

Figure 5-17: The WtWa Water Footprint of the investigated SAF route.

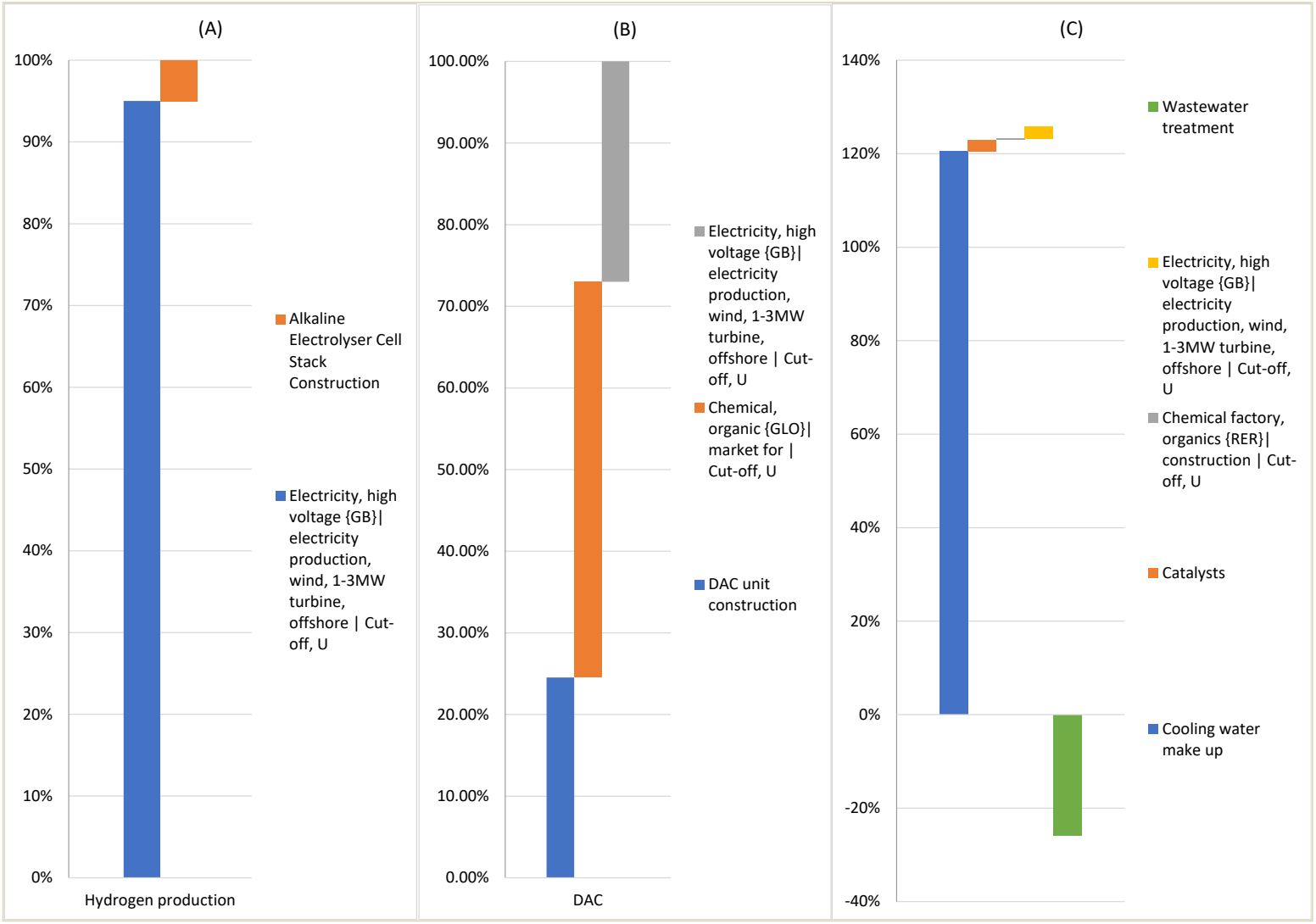

Figure 5-18: The breakdown of the Water Footprint: A) hydrogen production stage. B) Direct Air Capture. C) Refinery plant.

Similarly to the AE, the DAC unit's water footprint does not account for the positive credit of water generated from the air because the electrolyser uses all of it, and therefore is not represented in Figure 5-18B. In contrast to the generation of hydrogen, the phases of construction and chemical production (sorbent) are important for the water footprint calculations of this stage. The inventories used to represent the construction of the DAC unit, as well as the production of the sorbent, are taken from earlier research [260], [310] that are available from Climeworks. It is crucial to note that the inventory provided for the construction phase was an adaptation of the original inventory, which was withheld from publication because it contained proprietary company data. Hence no details regarding the reliability of the water footprint of the adapted inventory are offered. In regards to the sorbent production, which is the main contributor to this stage, the inventory used for this analysis is derived from Terlouw et al. [310]. This inventory is a generic proxy that could represent any sorbent material. As a result of the importance of these two stages, the uncertainty associated with the water footprint of construction and sorbent production should be further investigated.

As depicted in Figure 5-18C, it is clear that the water losses from the cooling water network have a great effect on the final water footprint. The design of the cooling water network estimates the amount of makeup water to replace cooling water losses; these losses will depend on the design operating parameters, as well as on the atmospheric conditions of the plant location. In this sense, an optimised design that targets heat integration, and/or the choice of air cooling system, could play an important role in the reduction of water footprint of this specific stage. Overall, it is found that the water footprint of SAF produced from PtL technology highly depends on the cooling water network design as well as on the water intensity of the electricity used to produce the fuel. Furthermore, the refinery stage benefits from a negative balance in the final water footprint, since the amount of waste water goes to treatment, and after that, it can be utilized for other purposes such as agriculture.

According to a study published by Micheli et al. [136], the water footprint of SAF produced from PtL technology ranges from 6.19×10^{-3} to 0.182 l/MJ of SAF produced, when wind electricity is used, and the variation depends on the technology adopted for the DAC (High or low temperature) and the FT reactor (high or low temperature). For example, SAF produced using wind energy, LT DAC and LT FT reactor, has a water footprint of 0.113 l/MJ. The main difference with the value obtained by this work could be attributed that the former study considered that the manufacturing and end of life of the associated equipment was negligible, while in this study it is seen that this affirmation is not exactly negligible for the DAC stage; another major difference is that the cooling water network was not considered, while this study shows that it has an important contribution, and therefore should be included in future LCA analysis of SAF studies. Other studies analysing the water footprint of SAF from

PtL were elaborated by Batteiger et al. [127] and Schmidt et al. [38], who estimated 0.12 and 0.040 l/MJ of SAF, respectively; however, these analyses do not display the detailed assumptions behind the presented figures.

Scenario analysis is performed considering some of the electricity sources used for the UK grid electricity. The water footprint of the considered sources was taken from Simapro-Ecoinvent Databases, as well as the water footprint of the fossil jet fuel. The results are depicted in Figure 5-19. Among the represented energy sources, the off-shore wind farm shows a better performance compared to the other analysed sources, from which the hydropower has the biggest water footprint. It is evident that this environmental impact puts PtL-derived SAF in disadvantage against fossil jet fuel, regardless of the electricity source linked to the system. However, when compared against biomass-derived aviation fuels, the PtL-SAF has a water footprint 100 or 1000 times lower (as per the values displayed in the report of Schmidt et al. [15]).

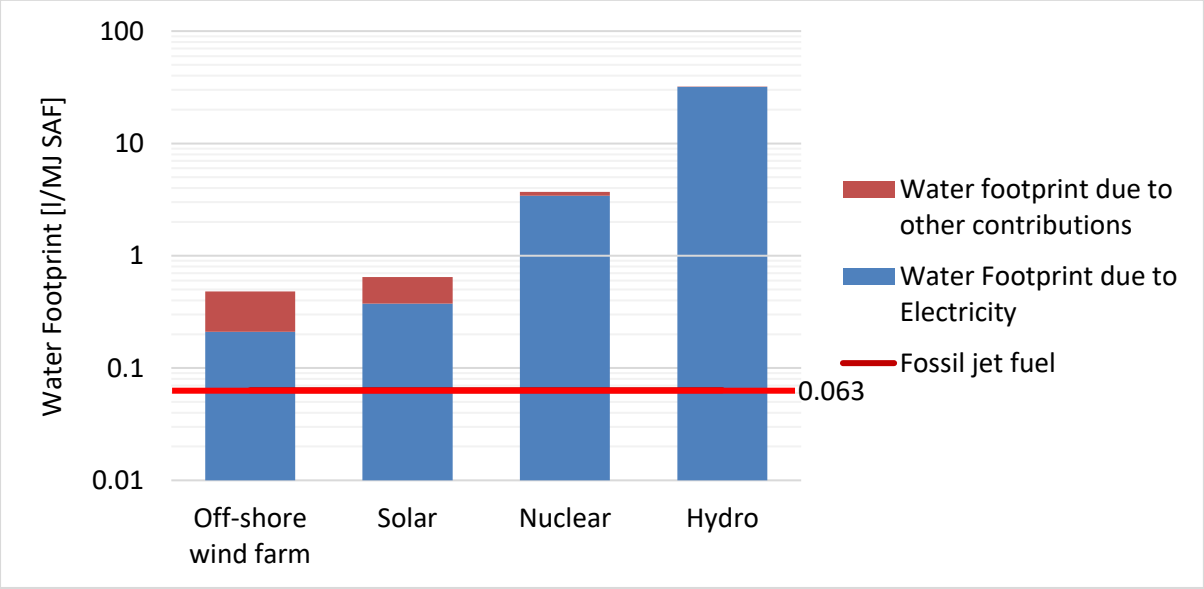

Figure 5-19: Water footprint of the PtL-SAF when connected to different electricity sources.

5.4 Policy analysis: UK SAF Mandate

It is evident that SAF achieves GHG emissions reduction, and that better environmental and economic performance could be achieved by increasing the production and use of SAF. As outlined by the ICAO [326], a range of policy options can be used to promote SAF, including financial incentives, regulations, mandates, and market-based mechanisms. Government subsidies and/or tax credits for companies producing SAF could help offset their expensive production, promoting their more widespread adoption. Similarly, carbon offset programs could be offered by governments or organizations, so companies can invest in SAF production projects in order to neutralize their environmental impact

[327]. Moreover, the creation of guaranteed markets for SAF producers, through the establishment of mandates or targets, could drive investment and innovation to the industry.

The UK government has set a mandate for the use of sustainable aviation fuels (SAF) in commercial aviation. By 2030, all UK airlines must use fuel blends that contain a minimum of 10% SAF, while this will be increased to 50% by 2050. The mandate is a part of a broader government strategy to attain net-zero emissions by 2050 and to promote the growth of a sustainable aviation industry. The mandate includes a number of actions to aid in the creation and application of SAF, such as the establishment of a stakeholder engagement process, the development of a SAF clearinghouse to aid in the trading of SAF certificates, and the provision of financial incentives for SAF production and application [17], [20].

The SAF certificate scheme is applied to simulate various scenarios and calculate the certificate price at which the SAF breaks-even with the fossil jet fuel (gate cost assumed at 0.56 £/kg [256]), for different CO_2 capture, and H_2 production costs. The number of certificates is estimated according to the second consultation of the SAF mandate [19]. Under this approach, the number of certificates is a function of the energy content of the produced SAF ($m \times LHV_i$) (Equation 5-18). However, to promote the use of SAF with larger GHG emissions savings, the number of certificates is also a function of the carbon intensity of the fuel. For the calculation of the carbon intensity factor (CI_{factor}) of the SAF (Equation 5-19), it is assumed that the average CI of SAF (CI_b) is 26.7 gCO_{2e}/MJ for a baseline scenario (which considers a SAF with a GWP reduction of 70% compared to fossil jet fuel), that is compared with the emissions of fossil jet fuel (CI_F) which is taken as 89 gCO_{2e}/MJ [19]. The carbon intensity of the SAF, CI_{SAF}, is the estimated GWP, which is equal to 21.43 gCO_{2eq}/MJ.

$$Certificates = m \times LHV_i \times CI_{factor}$$

(5-18)

$$CI_{factor} = \frac{CI_F - CI_{SAF}}{CI_F - CI_b}$$

(5-19)

Figure 5-20 illustrates the price at which the certificates must be purchased for SAF to break even the cost of conventional jet fuel for different H_2 production costs and CO_2 capture costs. For illustration purposes and to account for even the most unfeasible LCOH for blue and green hydrogen, the considered values take into account a cost range of 1 to 8 £/kg. A range of 30 to 1000 £/tonne is taken into account for the CO_2 capture cost to represent even the most expensive situation due to the low TRL of DAC technologies. Furthermore, APPENDIX B-8 presents the same results for the certificate

cost, but for the carbon impact factor calculated when no upstream emissions are considered for the electricity of the wind farm.

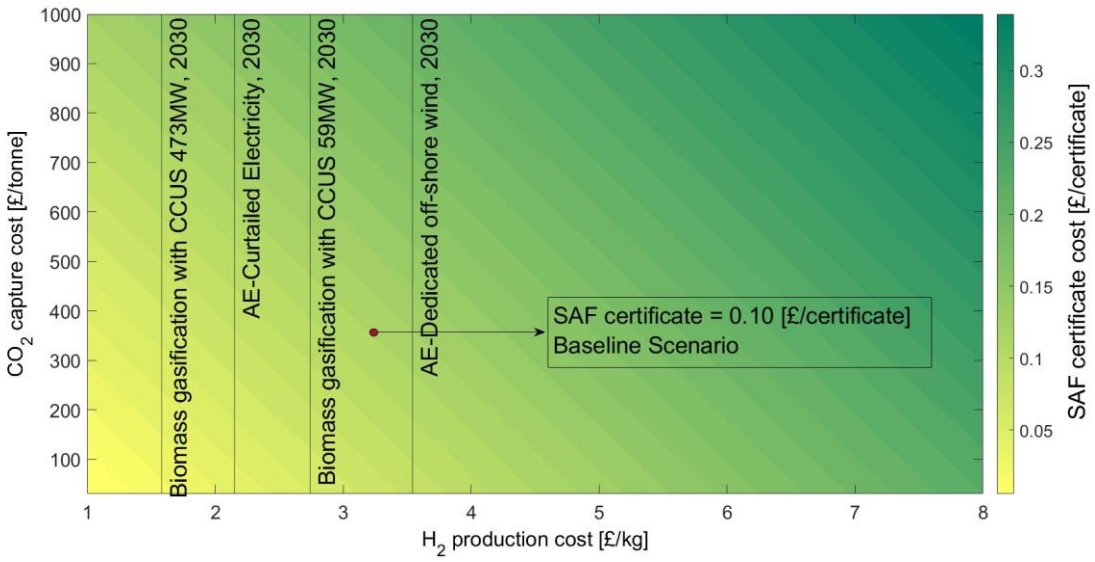

Figure 5-20: The SAF certificate cost for the MJSP to break-even with fossil jet fuel cost (0.56£/kg) for different CO_2 capture and H_2 production costs.

The calculated CI_{factor} is 1.08 and the annual production of SAF is 8.64E+8 MJ/year. The investigated process is eligible for 9.37E+8 certificates per year. According to this figure, the cost of the SAF certificate should be 0.10 £ for the baseline scenario to break-even. Further, the hydrogen produced through biomass gasification with CCU at two distinct scales is presented, along with hydrogen produced by an AE electrolyser from dedicated wind farms and electricity curtailment, at the estimated 2030 cost by BEIS [328]. It is evident that better economic performance is achieved when using hydrogen produced from biomass or curtailed energy. However, limited availability of biomass and of curtailed electricity pose challenges in scaling-up SAF production technologies.

5.5 Conclusions

The aviation industry has set an action plan, in which the development and use of SAF could have the largest impact on decarbonising the sector. The development of such SAF alternatives face technical, economic and environmental issues. Therefore, the development of integrated techno-economic and environmental assessments can provide a better overview on the performance metrics and identify actions that can improve and accelerate their deployment.

Within this context, this research has jointly examined the economic and environmental performance of SAF production through the PtL pathway in the UK. The system has been designed to maximize the

potential benefits of integrating its various components. For example, incorporating the LT DAC unit presents an opportunity to integrate heat from other parts of the process, such as the heat released by the FT reactor. Additionally, the DAC unit produces water and this has been fed to the electrolyser. The economic and environmental evaluations provided significant insights that can be compared to fossil jet fuel. Further, a policy analysis explored ways to support the development of sustainable aviation fuel (SAF). The key findings of these various evaluations can be summarized as follows:

1. The process has a carbon conversion efficiency of 0.88, with PtL and hydrogen conversion efficiencies of 0.26 and 0.39, respectively. Despite modelling efforts to demonstrate this process configuration, there are still several sources of uncertainty, particularly regarding process design. These include the operation of the RWGS reactor, recycling streams to both RWGS and FT reactors, and operating conditions for different sections of the process. As more demonstration and pilot plants become operational, the uncertainties related to these values will decrease.
2. The energy balances indicate that the refinery plant has a lower energy demand compared to the AE and DAC operations. Although the off-shore wind farm has been shown to be a reliable dedicated energy source, ensuring a stable energy supply to the system will require strategies such as utilizing the grid as a virtual storage or designing an effective storage system.
3. The economic evaluation indicates that the cost of SAF produced by this pathway is not competitive with fossil jet fuel. The calculated MJSP stands at 5.16 £/kg and is highly sensitive to electricity and DAC costs. Therefore, technical and economic improvements in CO_2 and H_2 production technologies could lead to cost reductions in MJSP. Lower electricity prices or consumption result in better economic performance. Economies of scale demonstrate that increasing production capacity leads to cost reductions, but not as much as for biomass scenarios, since the PtL system is highly dependent on OPEX. However, it's worth noting that scaling up the PtL system is not limited by feedstock supply and has less location restrictions.
4. The life cycle assessment (LCA) of the system has shown that the global warming potential (GWP) of the SAF produced through this pathway is lower than that of fossil jet fuel and it can meet existing aviation emissions reduction targets, such as the UK SAF mandate. If the source of electricity is an off-shore wind farm (base case scenario), the GWP of the PtL system is 21.43 gCO_{2eq}/MJ. Moreover, the GWP is sensitive to the carbon footprint of the electricity, indicating its dependence on the energy source.
5. The water footprint of the PtL system is 0.48 l/ MJ of SAF and is highly dependent on the water footprint of electricity generation and cooling water requirements. Therefore, a combination of system energy efficiency improvements and an optimal design of the cooling water system are essential for reducing the water consumption. Understanding the appropriate treatment of water

synthesized in the PtL process plant could enable its use in an operating facility. Furthermore, it is important to highlight that the water footprint of PtL-SAF is higher than conventional fossil jet fuel. Nevertheless, compared to other SAF alternatives like biomass-derived fuels, the water footprint of PtL-SAF is significantly lower.

6. The Monte Carlo analysis of the MJSP revealed that it will always remain higher than the gate price of the conventional jet fuel. Therefore, more efforts and government economic incentives are necessary for these fuels to be widely adopted by the aviation industry. On the other hand, for the GWP, the uncertainty analysis showed that the SAF GWP will remain lower than the established UK SAF mandate threshold and other existing thresholds such as the RED II, or the RFS.
7. A policy analysis indicated that the SAF mandate certificate cost should be between 0.009 to 0.35 £/certificate depending on the CO_2 capture and H_2 production costs. For the base case scenario, the SAF mandate certificate should be equal to 0.10 £/certificate of SAF.

These conclusions are part of the growing body of research on power to liquids process configurations, with a particular focus on creating sustainable aviation fuels. It is pivotal that more demonstration and pilot plants should become operational, so that the uncertainties related to the technical, economic and environmental metrics will decrease. Based on the assumptions made in this study, it has been demonstrated that the Power to liquids has the potential to greatly decrease greenhouse gas emissions and thereby aiding the decarbonisation of the aviation industry. However, supporting policies are needed for further development and eventually deployment at large scale. Further research and data gathering for pilot/demo plants will support future investigations and applications.

6. A combined techno-economic and life cycle assessment of a new Power and Biomass to Liquids (PBtL) configuration with negative emissions for the production of Sustainable Aviation Fuel (SAF)

Abstract

A novel configuration of the hybrid Power-and-Biomass to Liquids (PBtL) pathway for producing sustainable aviation fuels (SAF) has been developed and assessed from a techno-economic and environmental perspective. The proposed configuration can achieve negative emissions and hence create a new bioenergy with carbon capture and storage (BECCS) route. The amount of CO_2 that is captured within the process and that is sent for storage ranges from 0% to 100%, defining the various PBtL-CCS scenarios that are evaluated in this study. The outcomes of the economic assessment reflect minimum jet fuel selling prices (MJSP) that range from 0.0651 to 0.0673 £/MJ for the proposed configurations. The calculated MJSPs are OPEX dependent and the major contributor are the electricity consumption, followed by the price of the feedstock, i.e. forest residues chips. Costs for CO_2 compression, transport, and storage have a small contribution to the MJSPs of all the proposed scenarios. The global warming potentials (GWP) range from -105.33 to 13.9°3 gCO_2eq/MJ. Negative emissions have been calculated for the PBtL-CCS scenarios, which demonstrate compliance with emissions reductions thresholds and aligns with the aviation industry's net-zero ambition for 2050. The estimated water footprints range from 0.52 to 0.40 l/MJ. Primary responsible for these values are the water requirements for the operation of the alkaline electrolyser (AE) and refinery, followed by the water footprint of the wind farm electricity. Across all the scenarios, the resulting water footprints are bigger than that of the fossil jet fuel. Based on the economic and environmental estimations of this study, the resulting SAF could benefit of the support proposed by the UK SAF mandate, which could boost their economic performance by awarding certificates with monetary value. Estimates indicate that the cost of certificates that breakeven the fossil jet fuel price could reduce if negative emissions are also rewarded under this scheme.

Keywords: Biomass gasification, Fischer-Tropsch, Power-and-Biomass-to-Liquids, Bioenergy with Carbon Capture and Storage, Techno-economic assessment, Life cycle assessment.

6.1 Introduction

The aviation industry aims to achieve net-zero emissions by 2050, but no SAF production pathway can achieve 100% reduction. Combining BECCS with SAF could lead to fuels with negative emissions, which could be benefited from higher subsidies. Biomass to Liquid (BtL) and Power-to-Liquids (PtL) technologies are essential for sustainable fuel production, but their deployment is limited due to their

early development stages. Furthermore, SAF production from biomass may have a limited production in regions lacking this resource. The PBtL is a hybrid configuration that combines BtL and PtL technologies, producing drop-in SAF through integrated stages like water electrolysis, biomass gasification, and liquid fuel synthesis. The process typically involves a Fischer-Tropsch reactor for hydrocarbon synthesis, with syngas production via reverse water gas shift or direct injection of H_2. Studies show that the PBtL process enhances BtL carbon conversion efficiency, increases fuel productivity, and requires less energy per unit of fuel compared to the PtL configuration.

As explained in Chapter 2, research on TEA for BtL and PtL for SAF production is increasing, but for the PBtL for SAF production remains limited. Habermeyer et al. [147] evaluated a PBtL small-scale experimental facility for FT fuel production with an integrated TEA and LCA approach, however without including FT post-treatment stages. Similarly, few studies have focused on the LCA of PBtL configurations, with a primary focus on the estimation of the GWP. Habermeyer et al. [147] performed the only PBtL SAF-oriented LCA. However, due to the missing syncrude separation section, the estimated environmental impacts would differ from that of a WtWa scenario.

Although a considerable reduction of emissions with respect to fossil jet fuel can be achieved through the PBtL process, a PBtL configuration that can achieve negative emissions was never explored. Recently, there has been a growing interest in CDR technologies as a strategy to constrain global warming to 1.5 °C [5]. BECCS and direct air capture (DAC) are CDR methods that could be applied to the aviation industry. Given that the aviation industry aims to reach net-zero emissions by 2050 and the inherent limitations of SAF technologies to achieve negative emissions, BtL-CCS configurations deserve more consideration. While there is one study for SAF from BtL-CCS in the literature [171], none was found for the PBtL-CCS configuration. This process setup, if properly designed, contains pure CO_2 streams that could be stored, creating potential negative emissions configurations. Further, detailed and combined economic and environmental assessments are required to provide insight into a number of SAF production possibilities on which the aviation industry will rely to meet its 2050 goals.

It is evident that there is still a need for more TEA and LCA studies for the PBtL configuration for SAF, given that none of the existing research has evaluated a Well-to-Wake scenario. Without these LCA boundaries, it is difficult to understand the effect of several parameters on the environmental performance and the interaction of these results with other technical and economic indicators that could be the foundation for the formulation of supporting policies. Furthermore, due to the ambition of a net-zero aviation industry, the assessment of PBtL-CCS configurations capable of achieving negative emissions is deemed crucial, and it is the main focus of this study. To the best of our knowledge, this is the first study of its kind study that analyses the production of SAF through the

PBtL-CCS process configuration from a TEA and LCA approach. Moreover, sensitivity and probabilistic analyses evaluate the degree of uncertainty in the estimated economic and environmental indicators. This study is also significant since it takes a UK-focused approach and provides insightful information about the effect of the preliminary version of the SAF mandate on these SAF production pathways. The SAF mandate is the UK policy scheme to support the development and deployment of SAF technologies.

6.2 Methodology

6.2.1 Goal and scope of the study

The current study evaluates the technical, economic and environmental performance of the SAF production based on the PBtL-CCS process configuration, for various scenarios that differ on the amount of CO_2 that is sent for storage. To this end, a thorough process model is created in Aspen Plus with the goal of establishing the governing mass and energy balances that constitute the foundation for the techno-economic and life cycle assessments. The main TEA key performance indicators (KPIs) are the MJSP, Capital expenditures (CAPEX) and operating expenditures (OPEX), while the LCA quantifies the environmental impacts of the scenarios under consideration; the focus of this study is the GWP and water footprint. Finally, this study combines the resulting technical, economic and environmental KPIs to assess the effect of the UK SAF policy scheme on the viability of the investigated process.

6.2.2 Capacity and location of the plant

The production of SAF from biogenic residues that are not detrimental to normal food provision and/or constitute a danger of deforestation are supported by the UK SAF mandate [19]. As a result, and in addition to their availability in the UK, forest residues (FR) are selected as the source of carbon for the proposed system. A processing capacity of 20 dry-tonnes per hour of FR is considered, as proposed in Section 4.2.2. This value is below the estimated availability of this resource for the production of biofuels in the UK [183]; additionally, even under the most pessimistic scenarios of regional availability, this plant capacity would ensure broader availability of FR for other purposes beyond the demand of the SAF production industry [19].

The operation of PBtL configurations depends on a large supply of low carbon electricity [329]. The UK has a great potential for offshore wind electricity generation, and the UK government has recently declared the goal of achieving an installation capacity of up to 50GW of offshore wind by 2030 as part of its British Energy Security Strategy [330].

Herein, a dedicated off-shore wind farm is connected to the proposed PBtL-CCS scenarios. This study considers that the process plant is located in the Humber area (Teeside), due to its optimal wind profile, and its proximity to Scotland, which contains most forests of public ownership [183]. Furthermore, this choice is supported by the decarbonisation plans of the East Coast Cluster, which is comprised of the Teeside and Humber industrial regions [331]. The Endurance Reservoir, a saline aquifer located 145 kilometres offshore in the North Sea, could be used as the primary CO_2 storage site, based on the cluster's proposal [332].

6.2.3 System description and modelling

This section contains details regarding essential assumptions and specifications used to create the process models of the scenarios. The first section provides a broad overview of the system accompanied with brief descriptions of its key process units and their interaction in terms of mass and energy exchanges. Subsequent sections thoroughly explain these processes and how they are represented in Aspen Plus. Further, additional sections describe the methodology for the heat integration and the sizing of the wind farm. Finally, the main technical performance indicators are defined.

6.2.3.1 System description

Figure 6-1 depicts the main components of the process configuration: 1) The process begins with the grinding and drying of the forest residues chips (***pre-treatment***). Moreover, the water content is reduced from 30% to 10 % [51] through a drier that uses hot air at 120 °C and is implemented in Aspen Plus by following the approach described in Section 4.3.1.2. 2) The processed feedstock is then directed to the ***gasifier***, where it is converted into syngas (more explanation is found in Section 6.2.3.3. 3) The latter then enters the ***syngas cleaning*** section for the mechanical or chemical separation of some impurities. This section includes the ash separator, the tar reformer and the zinc oxide bed for the separation of the sulphur. 4) The cleaned syngas, accompanied by recycled CO_2, and hydrogen are mixed and sent to the ***reverse water gas shift reactor (RWGS)*** to increase the yield of the syngas. 4) The following section is the ***synthesis and separation of hydrocarbons*** in the ***FT reactor*** to convert syngas into syncrude. The latter is separated from the unreacted syngas and short chain hydrocarbons, before being sent to the ***hydrogenation reactor*** for the saturation of olefins, and the final fractionation in the distillation column. The resulting hydrocarbon are naphtha, kerosene, and diesel. A fraction of wax is also produced, but it is sent to the ***hydrocracking reactor***, where large paraffins are cracked into smaller size hydrocarbons, which are sent back to the distillation column for its fractionation. 5) The CO_2 produced by the oxycombustion of unreacted syngas is combined with the CO_2 generated in

the gasifier's combustion chamber; this stream is then split into two distinct streams. The first stream is recycled to the RWGS reactor, for conversion to CO, while the remaining portion is sent to the ***CO_2 compression section***, that involves a series of compressors and intercoolers. This section is responsible to take the gaseous CO_2 to supercritical conditions, enabling its subsequent transport and storage [166], [199]. The fraction of the total CO_2 stream that is sent for storage varies between 0% and 100%, and hence seven different scenarios have been assessed, as presented in Table 6-1. Because there is no gas exiting the refinery plant the 0%TS scenario, a purge (2% of the total CO_2 stream) is included to ensure that inert gases do not accumulate within the system. [119]. More information on the aforementioned process sections can be found in Section 4.3.1.2. 6) Another critical component of the process is the ***alkaline electrolyser*** (AE), which produces H_2 for the hydrocracker, hydrogenation and RWGS reactors. The by-produced oxygen is also valuable for the oxycombustion taking place at three different process sections, the gasifier, tar reformer, and **RWGS reactor** (more about details on the AE and the RWGS can be found in Sections 5.2.2.3 and 5.2.2.4). 7) Depending on the scenario, the oxygen produced in the AE could be in excess, or below the process' requirements. In the first case, excess oxygen is considered as by-product of the total process plant. Otherwise, an ***air separation unit*** (ASU) is annexed to the process for supporting the oxygen provision.

Table 6-1: Description of the investigated scenarios.

Scenario name	Description	Type of process configuration
0%TS	0% of the total CO_2 stream is sent for storage. 2% of the total CO_2 stream is purged.	PBtL
20%TS	20% of the total CO_2 stream is sent for storage. No purge gas.	PBtL-CCS
40%TS	40% of the total CO_2 stream is sent for storage. No purge gas.	PBtL-CCS
50%TS	50% of the total CO_2 stream is sent for storage. No purge gas.	PBtL-CCS
60%TS	60% of the total CO_2 stream is sent for storage. No purge gas.	PBtL-CCS
80%TS	80% of the total CO_2 stream is sent for storage. No purge gas.	PBtL-CCS
100%TS	100% of the total CO_2 stream is sent for storage. No purge gas.	PBtL-CCS

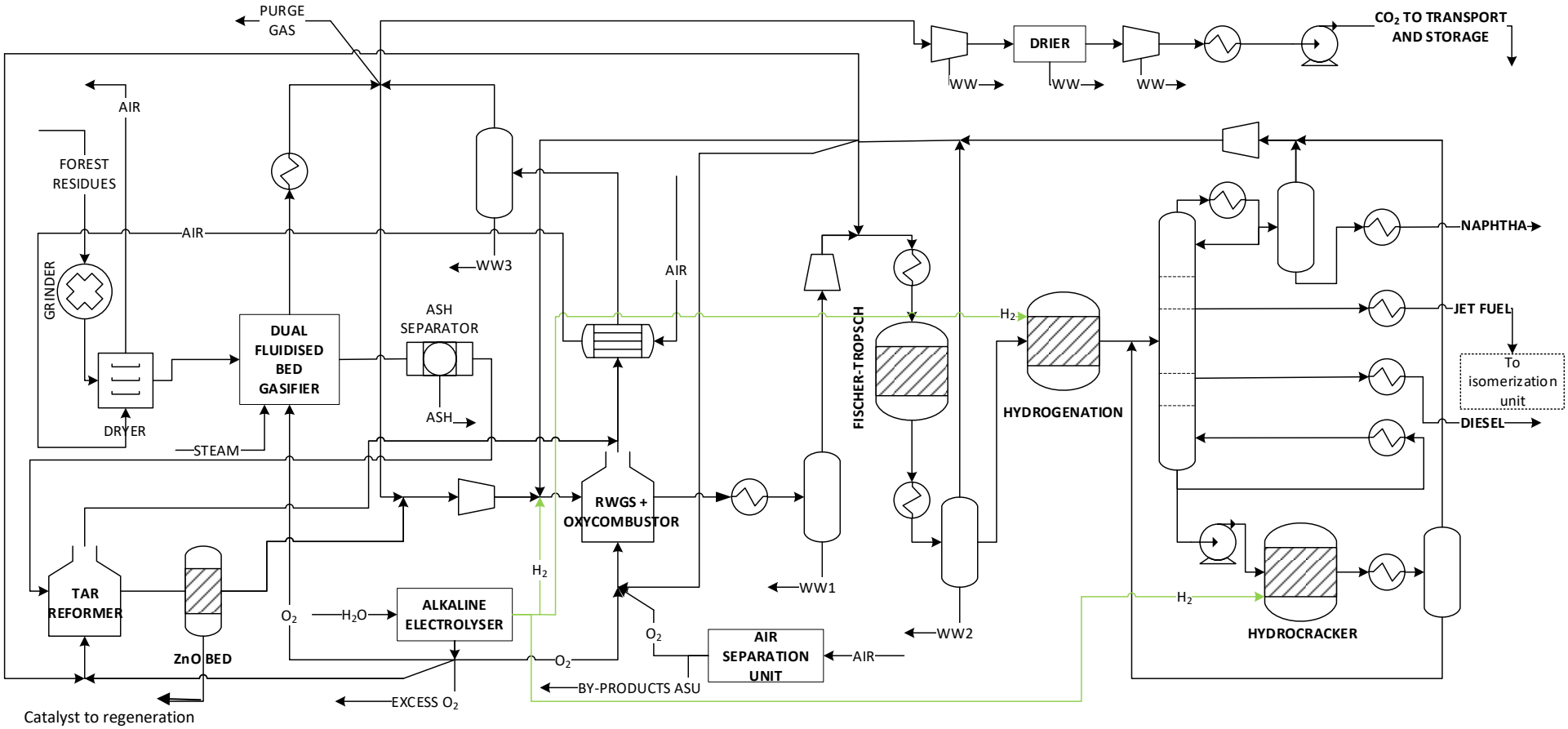

Figure 6-1: Process flow diagram of the investigated PBtL scenarios for SAF production (process plant boundaries).

6.2.3.2 Process modelling

The Aspen Plus V10 software is used to model the refinery plant, with the exception of the ASU and the alkaline electrolyser, for which the mass and energy balances are extracted from the studies of Holst et al. [103] and Young et al. [333], respectively. The "Redlich-Kwong-Soave-Boston-Mathias (RKS-BM)" method is selected for the representation of the thermodynamic and physical-chemical properties, due to its suitability for hydrocarbons processing plants [188]. The approach adopted for dealing with process streams containing solids, such as biomass and ash, is to treat them as non-conventional solids without particle size distribution [171]. The ultimate and proximate composition of the forest residues are presented in Table 6-2. The sections of the refinery as depicted in Figure 6-1, are explained in more detail in Chapter 4 and Chapter 5.

Table 6-2: Proximate and ultimate analysis of forest residues [189].

Proximate analysis (%)	**Forest residues**
Moisture (as received)	30
Fixed carbon (dry basis)	17.16
Volatile matter (dry basis)	82.29
Ash (dry basis)	0.55
Ultimate analysis (mass %)	
Carbon	50.54
Hydrogen	7.08
Nitrogen	0.15
Sulphur	0.57
Oxygen	41.11
Ash	0.55

6.2.3.3 Gasification section

Section 4.3.1.2 discusses the gasifier selection and approach for model development in Aspen Plus; however, this section explains the DFBG design that allows the production of pure CO_2 as flue gas. The DFBG is composed of two separated compartments, one acting as the gasification unit and the other as a combustion chamber [334]. The first compartment uses steam to convert the feedstock into nitrogen-free syngas and char; the latter is sent to the combustion compartment, where it is burnt in the presence of air; the released heat is transported to the gasification compartment through the circulation of the inert bed material, generally sand [201]. A detailed representation of the DFBG and more technical details can be found elsewhere [335]. The advantage of the DFBG is that the separated combustion section allows the use of an inexpensive oxidant such as air. However, more DFBG configurations have been proposed to enhance the carbon recovery, such as the use of pure oxygen

as the oxidant for the combustion chamber [336]. The production of oxygen from an ASU may be similar or even more energy demanding than post combustion CO_2 capture [336]; however, the availability of oxygen from the AE makes the DFBG with oxycombustion configuration suitable, and thereby greater CO_2 availability for storage or for fuel production can be achieved.

6.2.3.4 Recycling of gases and CO_2 and Air separation unit (ASU)

The recycling of the unreacted syngas, and short chain hydrocarbons, that are produced in the FT reactor are recompressed and sent back to various sections of the system as shown in Figure 6-1. Some fractions are recycled back to the synthesis reactors to increase the conversion of the process, while others act as the fuel for oxycombustion [118]–[121]: 1) One fraction is recycled to the FT reactor to increase the inlet inert content to 25% and thus ensure the thermal stability of its operation [118]. 2) Two different streams are utilised as fuel for the oxycombustion of the RWGS and the tar reformer reactors [119]. 3) The remaining fraction is recycled to the RWGS reactor to enhance the syngas production.

The flue gas from the oxycombustion chamber of gasifier contains only CO_2, while the flue gases from tar reformer and RWGS reactor contain also water. Therefore, the hot flue gases from these two latter are first combined and cooled down by heating the air that is used for the drying of the forest residues. Furthermore, some steam is raised and final cooling is achieved by using cooling water. As a result of the cooling process, the water from the flue gas is condensed, and the resultant pure CO_2 stream is mixed with the one coming from the gasifier. The CO_2 stream is split, with one fraction being recycled to the RWGS for enhanced syngas yield, while the other is sent to the compression section for compression, transport and storage. As described in Table 6-1, the choice of the percentage of the total CO_2 stream that is sent to storage creates the different scenarios that are assessed in this study.

The Air Separation Unit is an auxiliary unit that is necessary for meeting the requirements of oxygen of the system for some scenarios, if the oxygen derived from the electrolyser is not enough. The technology selected is the Cryogenic Air Separation, which requires electricity, cooling and heating as the utilities for its operation, while the feedstock is atmospheric air. For simplification, this unit is not modelled within the Aspen Plus system; instead, the mass and energy balances that are found in the study of Young et al. [333] are adjusted according to the needs of each scenario. The advantage of this unit is that is self-sufficient in terms of high-quality cooling utilities, while the heat requirement is provided by the steam produced within the process plant. The electricity consumption, which is equivalent to 0.58 kWh/kg of O_2 [333], is supplied by the wind farm to maintain a low carbon operation.

6.2.3.5 Heat integration and utilities requirements

The scenarios are heat integrated by applying the Pinch Point methodology which optimizes the energy requirements, and results into less cold and hot utilities requirements; within this approach, the cost of the heat exchanger network design is also optimized [337], [338]. The software Aspen Plus Energy Analyser is used for this heat integration. It receives the data of the hot and cold streams from the models created in Aspen Plus, and as output the heat exchanger design and the required utilities are estimated. The selected cold utilities are LP (Low Pressure), MP (Medium Pressure), and HP (High Pressure) steam generation, as well as cooling water and refrigerant. For the steam generation system a 5% of water reposition was assumed [339], meanwhile for the cooling water, the make-up water is calculated in accordance to the environmental conditions of the plant location [295]. The heat that is generated by the electrolyser is used for low temperature district heating, with a supply and return temperature of 60 °C and 35 °C [291], [292], with no reposition water since it is assumed that this cooling water circulates in a closed loop [283].

6.2.3.6 Off-shore wind farm

As proposed in a previous study by the authors [340], the system is connected to a dedicated offshore wind farm. The estimation of the power generation is based on the hourly wind profile that is extracted from the NASA-MERRA 2 website [276], for Teeside (Figure 5-2). Furthermore, the number of turbines for each scenario is adjusted in order that the total injected and total taken electricity are equal during one year of operation of the process plant [282]. Other alternatives such as the annexation of a battery bank [278]–[281] was not analysed, since it has been found to have high capital cost and low energy efficiency [278], [279]. More details on the design of the off-shore wind farm can be found in Section 5.2.2.2

6.2.4 Economic assessment

The economic feasibility of the SAF production scenarios are reflected throughout the estimation of important economic KPIs, such as the CAPEX, OPEX and MJSP, which are calculated based on several assumptions as presented in Table 6-3, and using the discounted cash flow analysis (DCFA). The methodology followed for the economic assessment is described in more detail in Section 3.2. The PEC for the components of the process plant are detailed in Table 6-4. Similarly, the variable costs for the OPEX estimation are presented in Table 6-5. The estimation of the OPEX of the AE and the RWGS, assumptions related to the electricity price, and the AE stack replacement cost are explained in more detail in Section 5.2.3.

Table 6-3: Main adopted assumptions for the economic assessment [70], [196]**.**

Location	United Kingdom
Plant life	20 years
Currency	£
Base year	2022
Plant capacity (based on feedstock input)	20,000 kg FR/h
Discount rate	10%
Federal tax rate	30%
Construction period	3 years
First 12 months' expenditures	10% of FCI
Next 12 months' expenditure	50% of FCI
Last 12 months' expenditures	40% of FCI
Depreciation method	Straight line
Depreciation period	10 years
Working capital	5% of FCI
Start-up time	6 months

*FCI = Fixed Capital Investment

Table 6-4: Purchased equipment cost data.

Equipment	Base cost [MM £]	Base capacity	Unit	Scaling factor	Base year	Reference
Biomass receive and unload	1.751	198.1	Wet tonnes FR/h	0.62	2007	[216]
Biomass storage, preparation, feeding to atmospheric gasifier	1.294	64.6	Wet tonnes FR/h	0.77	1999	[217]
Compressor	0.40	413	$kW_{electricity}$	0.68	2014	[218]
Cooling tower	2.42	4,530.3	kg_{water}/s	0.78	2014	[215]
Cyclone	0.040	1	m^3/s total gas	0.70	2014	[218]
DFBG	9.184	100	$MW_{th,LHV}$ at moisture content of 20%	0.72	2010	[157]
Drier	5.064	1	m^3_{AIR}/s	0.8	2003	[157]
Electrolyser	22.79[a]	100	MW_{DC}(for the stack)	0.88[b]	2020	[103]
FT-reactor	6.42[c]	2.52	MMcf/h inlet stream (STP)	0.72	2003	[216]
Hydrocracker reactor	6.23	1.13	kg/s (feed mass flow)	0.70	2014	[218]
Hydrogenation reactor	1.35	81.9	kg/s (feed mass flow)	0.60	2014	[215]
Isomerization reactor	0.0042	1	$tonnes_{product}$/year	0.62	2015	[219]
Pump	0.08	10	m^3_{wax}/s	0.36	2014	[218]
RWGS-reactor	4.61	23.89	kg/s reactor output	0.65	2019	[122]
Tar reformer	0.68	12	Nm^3/s	0.60	2010	[157]
ZnO guard bed	0.016	8	m^3/s total gas	1.00	2014	[218]

[a]Base cost is back calculated from the CAPEX that is provided by the reference (using a factor of 3.26). [b]Scaling factor is calculated based on the 5MW and 100MW electrolysers studied for 2020. [c]Value back calculated from installed cost provided by source (using a installing factor of 3.6)
MM=Million; cf=cubic feet

Table 6-5: Estimation of the Variable Costs.

Variable Cost (VC)			
Products			
	Price		Reference
Naphtha	0.53 £/kg		[297]
Diesel	0.44 £/kg		[297]
Oxygen	0.060 £/kg		[298]
District Heating	0.026 £/kWh		[122]
LP Steam	0.0024 £/kg		[299]
HP Steam	0.0072 £/kg		[299]
A) Feedstock	Price		Reference
Chips of FR	58.53 £/t		[220]
B) Utilities			
	Price		Reference
Electricity from wind turbines	0.061 £/kWh		[a]
Electricity from the Grid	0.026 £/kWh		[298]
Waste water treatment	0.415 £/t		[58]
Cooling water	0.025 £/t		[196]
Feed boiler water	0.784 £/t		[58]
Refrigerant (-25 °C)	0.0072 £/kWh		[b]
C) Catalysts			
	Price	Lifetime [years]	Reference
FT synthesis	20.70 £/kg	3	[221]
RWGS reactor	24.95 £/kg	4	[122]
Tar Reformer	3% of VC	3	[196]
Wax hydrocracking	18 £/kg	3	[95]
Wax hydrocracking	23.28 £/kg	3	[221]
VC		A+B+C	
OPEX		FOM+VC	

[a] Value calculated from SAM [b] Aspen Plus V10 2016

6.2.5 Life cycle assessment

The environmental impact of the SAF production and utilisation was evaluated according to the methodology of the life cycle assessment on a Well-to-Wake (WtWa) basis. To ensure consistency and transparency of the LCA estimations and assumptions, the standardised approach outlined in the standards ISO 14040 and 14044 was adopted [168]. According to this methodology, the LCA of the scenarios is divided in four main stages: Goal and scope definition, life cycle inventories, environmental impact and interpretation [169]. The following sections will briefly explain the assumptions adopted for the assessment.

6.2.5.1 Goal and scope definition

The aim of this study is to quantify the environmental impacts of SAF production through various PBtL-CCS scenarios, and then compare them against the environmental performance of conventional jet fuel. The analysed scenarios have the same process configuration; however, since the amount of CO_2 that is compressed and sent to storage is different for each one, so are the material and energy balances. Therefore, seven different scenarios are evaluated: 0%TS, 20% TS, 40% TS, 60% TS, 80% TS, and 100%TS. The boundaries of the scenarios start with the extraction of resources and production of raw materials, and finish with the utilisation of the produced SAF, also referred as combustion or end of life, thus a WtWa system, as depicted in Figure 6-2. Given that the SAF is the main product of the system and that this is used for energy purposes, the functional unit is defined as 1 MJ of SAF produced based on its LHV, which is assumed at 42.8 MJ/kg [156]. The location of this assessment is the UK.

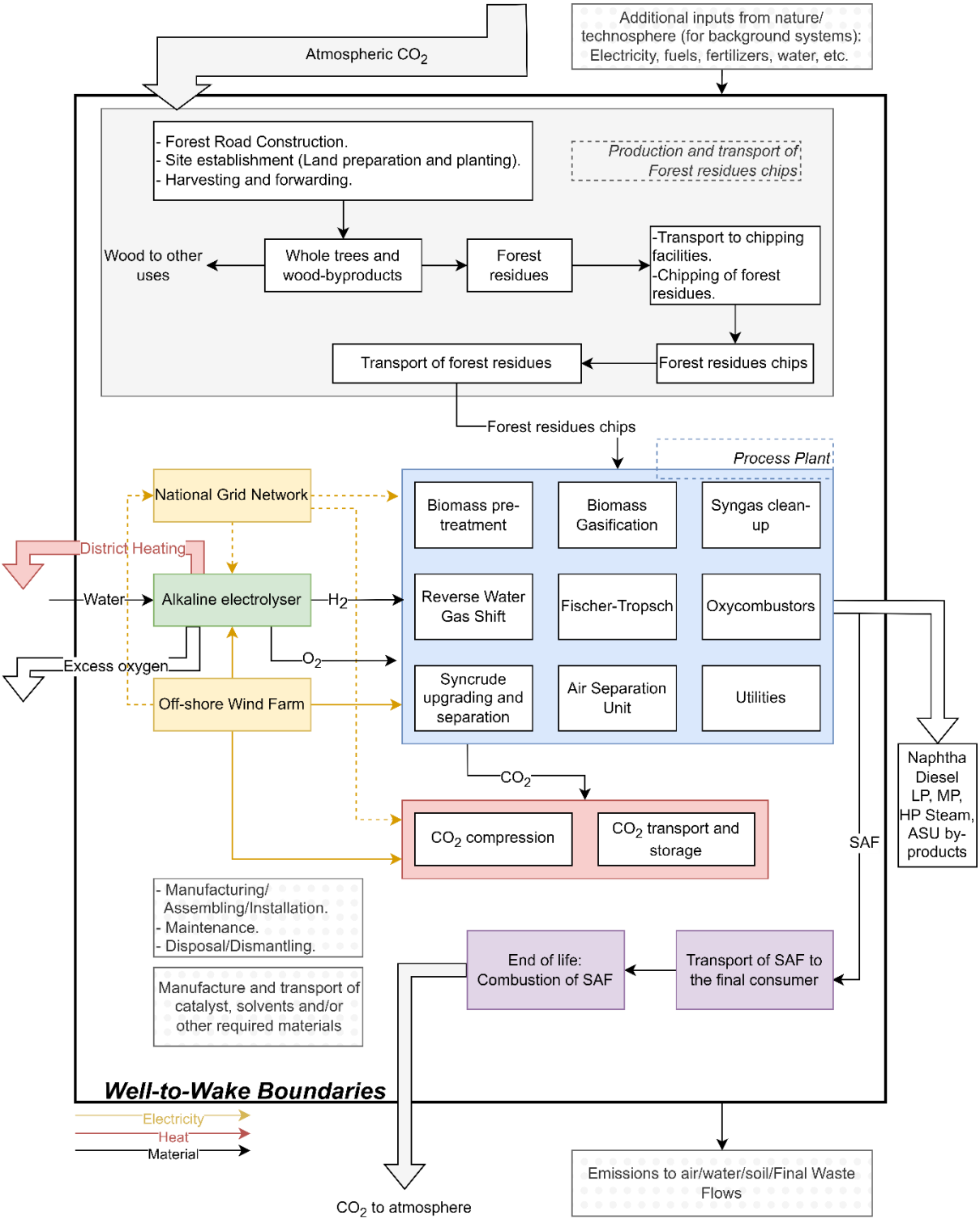

Figure 6-2: Well-to-Wake boundaries of the life cycle assessment of the PBtL-CCS scenarios.

6.2.5.2 Life cycle inventories

This section details the data collection in terms of mass and energy flows interactions within the different stages of the LCA as well as from the interactions of the system with the surroundings. The

data sources are distinguished as foreground and background data. The foreground life cycle inventory (LCI) is mainly built upon the resulting mass and energy balances from the Aspen Plus models. The LCI Ecoinvent 3.6 database, as well as any other external sources are used to generate the LCI of the background data, as well as for completing any information missing for the foreground LCI. The advantage of using Ecoinvent is that it is a very complete database containing a huge variety of LCI for various sectors. From the system models available, the “allocation, cut-off by classification-system” is chosen, as recommended by Ecoinvent [173]. Given the chosen location for the SAF production plant, preferably, UK LCI are chosen, but in the absence of this geographical coverage, Europe, Global, or Rest of the World databases are selected, in order of preference. More insight on the assumptions and data sources of the LCI for the stages inside the system’s boundaries is provided in: i) Forest residues chips production and transport, Section 4.3.3.3; ii) Electrolyser and Wind farm, Section 5.2.4.3; iii) Refinery plant, APPENDIX C-1; iv) CO_2 compression transport and storage, Section 4.3.3.3; v) Transport and final use of jet fuel, Section 4.3.3.3. Additionally, the tables summarizing the inputs and outputs of the LCIs are presented in APPENDIX C-1.

6.2.5.3 Multi-functionality

Initially, ISO 14040 guidelines advice tackling a multifunctional system by applying subdivision or "system expansion." However, in specific situations when this approach is not applicable, the subsequent recommendation is the allocation based on a physical relationship. Lastly, when neither of the approaches is deemed suitable, the economic allocation is advised by the guidelines [170]. Nevertheless, past LCA studies for the production of sustainable fuels observed a tendency of the system expansion approach on calculating lower GWP since in most cases, the co-products were substituting analogous goods with high emissions intensities, such as those of fossil origin [80], [171], [172]. In this sense, the preferred approach for such multifunctional systems is allocation by energy and this approach has been considered herein. The boundaries of the proposed LCA include two multifunctional systems: The alkaline electrolyser and the refinery plant. For the AE or the refinery, allocation means the distribution of the environmental impacts related to its operation, and maintenance, as well as the upstream environmental impacts of all the inputs (energy, or materials), among the outputs of the system. Table 6-6 describes the baseline approach and other complementary approaches. A “YES” means that the related product is considered as a product for the corresponding allocation approach.

Table 6-6: Allocation approaches for the multifunctional system of the WtWa PBtL system.

	PRODUCT/CO-PRODUCT/BY-PRODUCT	APPROACH 1 (Baseline allocation approach)	APPROACH 1B	APPROACH 2	APPROACH 3	APPROACH 4
Alkaline Electrolyser	Allocation	NO*	NO*	EXERGY	NO*	NO*
	Hydrogen	YES	YES	YES	YES	YES
	Oxygen	NO	NO	YES	NO	NO
	District heating	NO	NO	YES	NO	NO
Refinery Plant and upstream inputs	Allocation	ENERGY	ENERGY	ENERGY	EXERGY	ECONOMIC
	SAF	YES	YES	YES	YES	YES
	Naphtha	YES	YES	YES	YES	YES
	Diesel	YES	YES	YES	YES	YES
	LP,MP,HP Steam	NO	NO	NO	YES	YES
	By-products from ASU	NO	NO	NO	YES	YES
CO_2 storage	Allocation	NO**	ENERGY	NO**	NO**	NO**
	SAF	YES	YES	YES	YES	YES
	Naphtha	NO	YES	NO	NO	NO
	Diesel	NO	YES	NO	NO	NO

*Meaning that no allocation is applied, and all the emissions go to the produced hydrogen
**Meaning that the total net negative emissions are substracted only from the WtWa GWP of the SAF

The “baseline approach” is a conservative allocation method recommended in a methodological tool by the UNFCC [341]. Following this approach, emissions are only allocated to the main product of a system. Consequently, for the AE, the emissions from the electrolysis and its upstream activities are solely allocated to the produced hydrogen. For the refinery plant, this translates similarly, and all emissions are allocated to the produced fuels (SAF, diesel, and naphtha) on an energy basis. The choice of this conservative "baseline approach" is supported by the argument that by-products are not produced in significant quantities or that they have little economic or energy significance in comparison to the main products [309], [341]. However, in order to provide more than one set of results, additional allocation approaches are proposed as described in Table 6-6, and relevant results are provided in the results section of the sensitivity analysis.

6.2.5.4 Impact assessment

For the evaluation of the environmental impact as described in the LCIs of the different stages of the system, the ReCiPe midpoint (H) method was chosen. This method is widely applied by LCA practitioners, as it calculates 18 midpoint impact categories, among which the GWP for a 100 years’ time horizon [342]. The accounting of the carbon requires a differentiation between the one of

biogenic or fossil origin due to the storage of CO_2. Biogenic feedstock, such as forest residues requires an uptake of atmospheric CO_2, which is listed as "Carbon dioxide, in air" in the "Inputs from nature" section of the wood chips LCI from Ecoinvent. This carbon experiences a series of physical and chemical transformation until it is released back to the air during the combustion of the SAF; therefore, null GWP characterization factors are assigned to the "Carbon dioxide, in air" and "Carbon dioxide, biogenic" as suggested by the IPCC guidelines [343]. Nevertheless, not all the carbon intake is released through the combustion of the fuel, since some scenarios are coupled to CO_2 storage. For this, the recommended approach is to consider as "negative emissions" when biogenic CO_2 is store [242], therefore a characterization factor of "-1" is applied in these cases.

6.2.6 Sensitivity and uncertainty analysis

Table 6-7 and Table 6-8 summarize the parameters for which the greatest uncertainty is observed and, according to previous studies [171], [340], they are also the ones that contribute the most to the final indicators of economic and environmental performance.

Table 6-7: Parameters considered for the sensitivity and uncertainty analysis of the TEA.

Parameter	Nominal value (for all the scenarios)	Minimum	Maximum
H_2 generation cost [£/kg H_2]	*Different for each scenario, to be presented in results section	1	8
CAPEX refinery [MM£]		-30%[a]	+50%[b]
Cost of wind farm electricity [£/kWh]	0.06	-50%[a]	+50%[b]
Network cost [£/kWh]	0.01	0	-
TAX rate [%]	30	0	40
Discount rate [%]	10	8	12
Feedstock cost [£/kg]	0.06	-50%[a]	+50%[b]
If Naphtha and diesel gate prices same as MJSP of SAF	N/A	-	-

[a] Percentage points lower than the nominal value
[b] Percentage points larger than the nominal value

The selection of the uncertainty range of -30% to + 50% for the CAPEX of the process plant is based on the suggestion by the AACE International [244]. Acknowledging that the CAPEX and OPEX of the AE is also subjected to uncertainty, the cost of H_2 is chosen for ease of representation, instead of analysing the two parameters individually. Therefore, the H_2 production cost is calculated for each scenario. The minimum and maximum discount rates of return represent optimistic and pessimistic scenarios, respectively [245], and the same applies for the tax rate. Moreover, it is also assumed that in an optimistic scenario this type of renewable projects could benefit from the exemption of network cost

payment [303]. For the other parameters a ± 50% range of uncertainty was considered. An additional scenario is also analysed, by considering that the naphtha and diesel are also sold at the same price of the SAF; however, this scenario is not considered for the probabilistic TEA.

Table 6-8: Parameters considered for the sensitivity and uncertainty analysis of the GWP.

Parameter	Nominal value (for all the scenarios)	Minimum	Maximum
Wind electricity carbon intensity [gCO_{2eq}/kWh]	15.25	7	22.5
GWP of FR chips production [gCO_{2eq}/kg wood chips dry basis]	42.35	-30%[b]	+30%[c]
GWP of Transport of FR chips [gCO_{2eq}/kg wood chips dry basis]	18.16	-30%[b]	+200%[c]
GWP of CO_2 compression, T & S [gCO_{2eq}/kg of CO_2 to storage]	3.22[a]	-10%[b]	+10%[c]
Alkaline Stack efficiency (%)	68.81	58.00	73.00
UK grid [gCO_{2eq}/kWh]	193.38	-	-
No upstream emissions wind electricity [gCO_{2eq}/kWh]	0	-	-
Allocation, Approach 2	-	-	-
Allocation, Approach 3	-	-	-
Allocation, Approach 4	-	-	-

[a]For the scenario 0%TS, the nominal value of this parameter is 0
[b]Percentage points lower than the nominal value
[c]Percentage poinst larger than the nominal value

Five main parameters are chosen for the analysis of the sensitivity of the GWP, as presented in Table 6-8. In previous studies, PBtL and PtL configurations were found to be highly affected by the choice of electricity source; therefore, the effect of the GWP of the wind farm electricity is tested for. The selected bandwidth of the carbon intensity for the off-shore wind farm electricity was reported in a National Renewable Energy Laboratory (NREL) report [307], that summarised and harmonised the findings of numerous LCA. Following, the AE efficiency is also tested, for which the chosen range is based on the minimum and maximum values that were found in the literature [284], [311]–[313]. For the GWP of the FR production and transport, and the GWP of CO_2 compression, T & S ranges of ± 30% or ±10% of their nominal values are chosen depending on whether their uncertainty is high or moderate [171]. However, the maximum value for the range for the FR transport is set as +200% of the nominal value, considering a pessimistic scenario where feedstock supply might be covered from forest that are very far. In addition, the effect of the different allocation methods, as described in Table 6-6, was tested.

The probabilistic TEA and LCA are important since they are able to reflect the uncertainty of the estimating parameters [344]. Therefore, this study also performed probabilistic assessment based on

the uncertain parameters presented for the TEA and the LCA, as depicted in Table 6-7 and Table 6-8 respectively. The statistical Monte-Carlo approach changes the uncertain parameters at the same time, choosing arbitrary values between the given uncertain rages for each of them. Assuming a triangular distribution for all the parameters, and executing 10,000 trials, the MJSP and the GWP are recalculated, and estimate mean, median, and standard deviations for each of them.

6.3 Results

6.3.1 Technical results

6.3.1.1 Overall mass and energy balances, and PBtL efficiencies

Table 6-9 summarizes the main inputs and outputs of Aspen Plus simulations for all scenarios. As PBtL configurations are power-intensive processes, the breakdown by process section of the required electricity is also presented. The inlet of forest residues is constant among the different scenarios, while the amount of CO_2 sent for storage gradually increases from the 0%TS to the 100%TS scenario. An increase in the flowrate of CO_2 that is sent for storage is associated with lower carbon circulating throughout the various refinery sections, lower SAF production, and lower hydrogen demand (which is equivalent to a lower electricity requirement). Furthermore, from the 50%TS scenario onwards, the reduced demand for hydrogen makes it necessary to install an ASU to cover the gap between the oxygen requirement of the process and the amount produced in the electrolyser. The PBtL efficiency gradually increases from the 0%TS to the 100%TS scenario and this can be attributed to the reduction of the electricity demand, especially for the electrolyser, where a share of the required electricity is converted into heat.

Table 6-9: Main input/output process streams and electricity requirements for the proposed PBtL scenarios.

	Scenario						
Main inlet/outlet streams [kg/h]	**0%TS**	**20%TS**	**40%TS**	**50%TS**	**60%TS**	**80%TS**	**100%TS**
Forest residues	28571.4	28571.4	28571.4	28571.4	28571.4	28571.4	28571.4
Naphtha	3294.35	2820.01	2493.33	2360.31	2221.73	2019.48	1830.23
SAF	6617.46	5770.66	4984.25	4668.55	4399.18	3909.27	3499.67
Diesel	1951.85	1707.36	1475.64	1382.95	1303.54	1158.97	1037.22
CO_2 to storage	658.69	5478.44	9514.38	11185	12688	15270.9	17494.1
Electricity requirements [MW]							
Electrolyser	286.41	219.68	164.73	142.49	122.98	89.13	61.22
Refinery plant	25.57	23.44	21.76	21.14	20.68	19.79	19.15
ASU	0	0	0	0.3	1.3	3.01	4.48
CO_2 compression	0	0.6	1.04	1.22	1.38	1.66	1.9
PBtL efficiency (%)	**34.05%**	**35.44%**	**36.85%**	**37.55%**	**38.09%**	**39.31%**	**40.41%**

6.3.1.2 Electricity requirements and wind farm design

Table 6-9 exhibits the electricity requirements for the various sections of the analysed scenarios. This information reveals that among all the components for all scenarios, the highest consumption is attributed to the electrolyser, which requires between 71% to 92% of the total power demand. The power demand of the refinery plant represents the second-largest electricity consumption, ranging from 8% (0%TS) to 22% (100%TS). The balance is attributed to the power demand of the ASU and/or the CO_2 compression, depending on which PBtL-CCS scenario is analysed. In brief, the proposed scenarios are energy-intensive, mostly due to H_2 production. Moreover, the energy penalty of coupling a CCS section is almost negligible, even for the scenarios that send large amounts of CO_2 for storage.

To address these substantial electricity requirements, a dedicated offshore wind farm was connected to the PBtL system, which was sized according to the criteria explained in Section 6.2.3.6. Based on the wind speed profile of the plant location and the number of wind turbines, the energy generation profile for all scenarios was calculated using SAM software. Given that the wind profile and the wind turbine model are the same across all scenarios, their energy generation profile only differ in the amount of energy generated. Therefore, only the energy generation profile of the 0%TS scenario is presented in Figure 6-3. This latter highlights the fact that the power supply is not constant and the need for a backup power system, particularly during spring and summer periods.

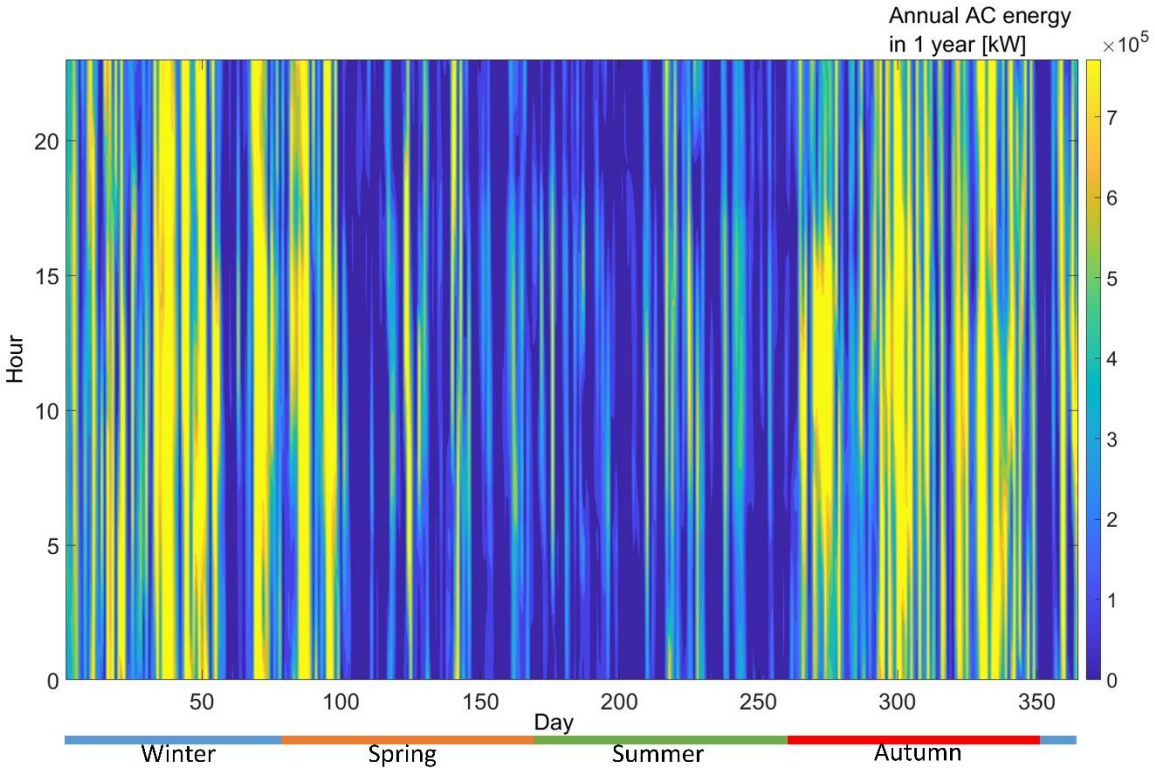

Figure 6-3: Power curve for the wind farm of the 0%TS scenario.

APPENDIX C-3 summarizes the number of wind turbines calculated for each scenario, the total power from the wind farm to the system, the power from the grid to the system, and the excess power from the wind farm to the grid. The estimated number of wind turbines decreases from 164 to 46 for the 0%TS scenario to the 100%TS scenario, as the electricity requirement gradually decreases. Moreover, there is a slight discrepancy between the excess wind electricity sent to the grid and the power received from the grid, but in all cases the former is slightly larger than the latter.

6.3.1.3 Carbon and hydrogen conversion efficiencies

Figure 6-4 and Figure 6-5 depict the flow of the carbon and the hydrogen throughout the main sections of the refinery for all scenarios, while Table 6-10 and Table 6-11 quantitatively describe the molar flows of carbon and hydrogen for the involved streams as depicted in their corresponding figures. Carbon only enters the system as forest residue and after undergoing various transformations, it leaves the refinery plant as gasoline, diesel, SAF, and CO_2. The input of forest residues is constant across the different scenarios, while the amount of CO_2 that is sent to storage varies, and this results in different carbon conversion efficiencies with the 0%TS and 100%TS scenarios having the largest and the lowest values, respectively.

On the other hand, there is more than one input stream of hydrogen: 1) pure hydrogen coming from the AE for the RWGS reactions, the saturation of the olefins produced in the FT reactor and for the hydrocracking reactor; 2) hydrogen contained in the forest residues ; and 3) steam for the gasifier. The hydrogen is either found in the fuels or lost as water since the latter is produced during the RWGS, FT, and combustion reactions. Consequently, the hydrogen conversion efficiency is constrained to values below 23%, which is relatively low when compared to the estimated carbon conversion efficiencies. Furthermore, the amount of pure hydrogen required in the process is determined by the quantity of carbon available in the system as a whole. Given that the conversion of this hydrogen depends on the chemical reactions within the system, the hydrogen conversion efficiencies are very similar across different scenarios (i.e. 21.52% to 22.59%). As a result, the amount of CO_2 sent for storage does not have a substantial impact on them.

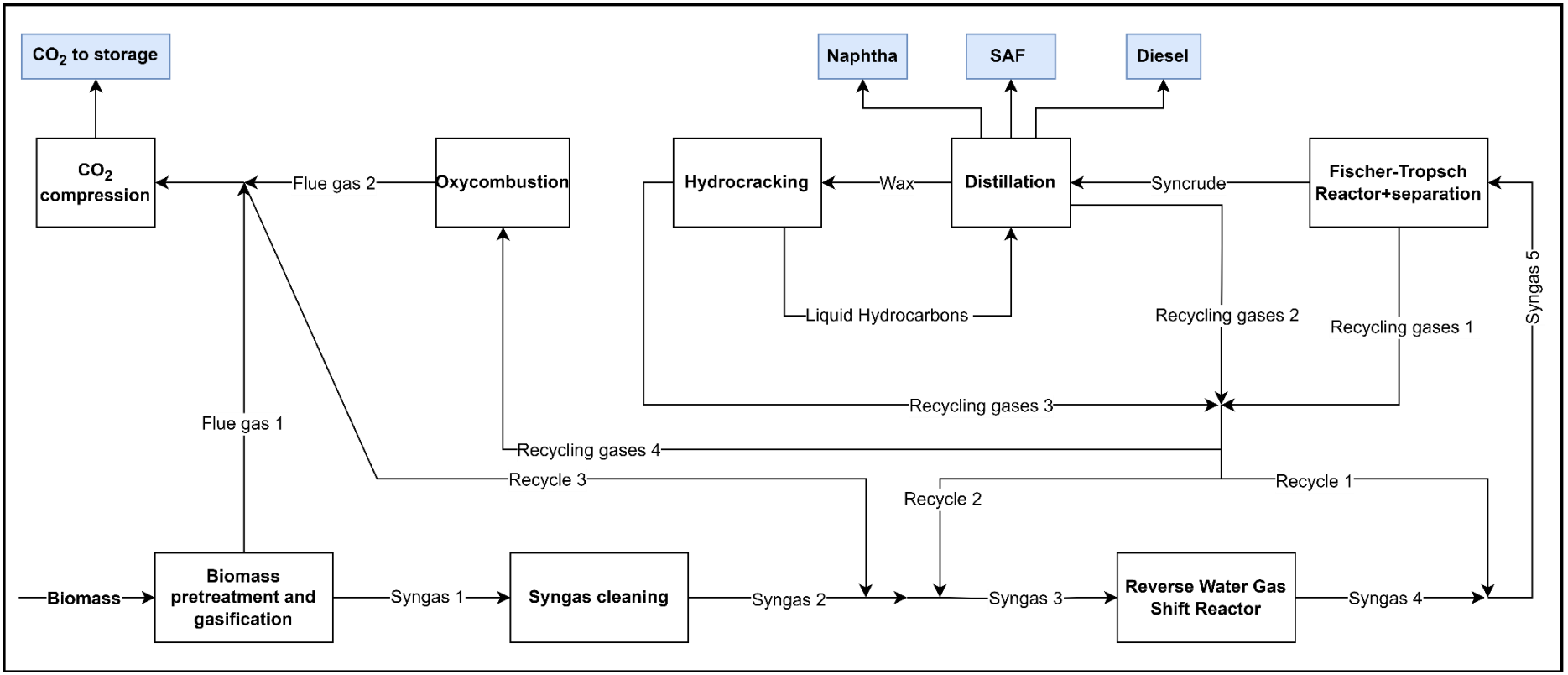

Figure 6-4: Flow of carbon throughout the main process units of the refinery plant.

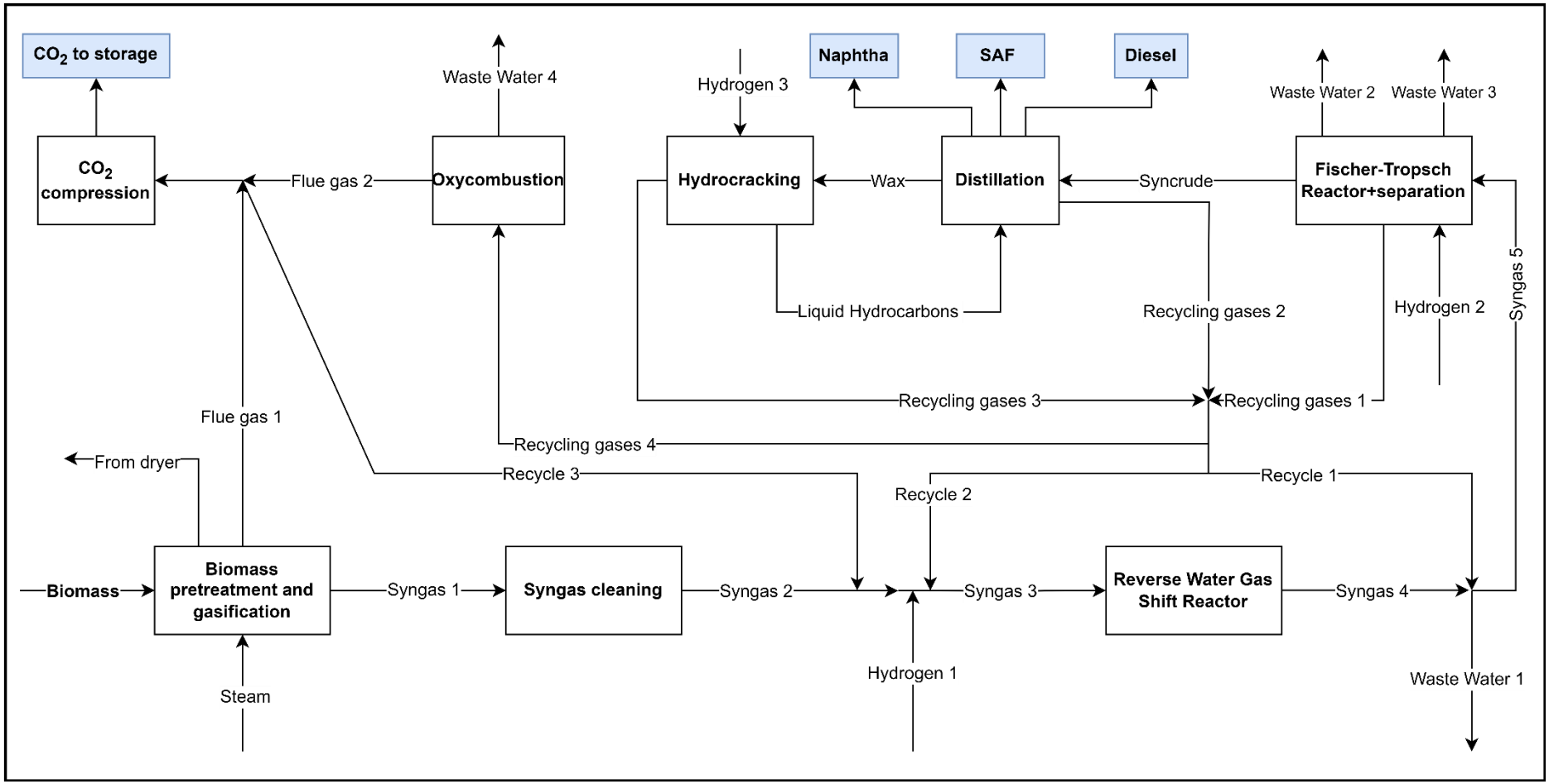

Figure 6-5: Flow of hydrogen throughout the main process units of the refinery plant.

Table 6-10: Molar flowrates of carbon among the various sections of the refinery for the different scenarios.

	Scenarios						
Carbon flow [kmol C/h]	**0%TS**	**20%TS**	**40%TS**	**50%TS**	**60%TS**	**80%TS**	**100%TS**
Biomass	841.56	841.56	841.56	841.56	841.56	841.56	841.56
Syngas 1	634.69	634.69	634.69	634.69	634.69	634.69	634.69
Syngas 2	634.69	634.69	634.69	634.69	634.69	634.69	634.69
Syngas 3	2434.27	2112.84	1843.41	1739.68	1658.03	1517.48	1429.55
Syngas 4	2434.28	2112.84	1843.40	1739.69	1658.04	1517.48	1429.54
Syngas 5	5071.62	4484.73	3856.01	3616.23	3389.55	2986.76	2646.70
Syncrude	1627.66	1191.83	1006.62	932.93	866.37	740.47	630.98
Wax	299.65	255.71	146.97	123.76	203.43	137.26	129.96
Liquid Hydrocarbons	283.22	241.40	137.57	115.58	192.18	128.87	122.15
Recycle 1	2637.34	2371.89	2012.61	1876.55	1731.51	1469.29	1217.15
Recycle 2	1087.72	980.22	885.42	851.51	831.59	796.21	794.86
Recycle 3	709.34	495.41	323.30	253.49	191.76	86.58	0.00
Flue gas 1	206.79	206.79	206.79	206.79	206.79	206.79	206.79
Recycling gases 1	3727.05	3292.78	2849.31	2683.23	2523.12	2246.27	2015.71
Recycling gases 2	498.61	457.50	371.37	336.82	301.34	236.94	178.53
Recycling gases 3	16.43	14.31	9.41	8.18	11.25	8.39	7.81
Recycling gases 4	517.03	412.47	332.06	300.18	272.60	226.10	190.04
Flue gas 2	517.03	412.47	332.05	300.18	272.60	226.10	190.04
Naphtha	225.74	193.23	170.77	161.63	152.05	138.11	125.04
SAF	465.61	406.03	350.70	328.48	309.53	275.06	246.24
Diesel	138.06	120.77	104.38	97.82	92.20	81.98	73.37
CO_2 to storage	14.48*	123.85	215.54	253.49	287.63	346.31	396.83
CARBON CONVERSION EFFICIENCY (%)	**98.56%**	**85.56%**	**74.37%**	**69.86%**	**65.80%**	**58.84%**	**52.84%**

* This is a purge stream, to avoid accumulation of inert gases

The green highlights denote that the streams are inlets or outlets of the system

Table 6-11: Molar flowrates of hydrogen among the various sections of the refinery for the different scenarios.

	Scenario						
Hydrogen flow [kmol H/h]	**0%TS**	**20%TS**	**40%TS**	**50%TS**	**60%TS**	**80%TS**	**100%TS**
Biomass	2356.56	2356.56	2356.56	2356.56	2356.56	2356.56	2356.56
Steam	888.13	888.13	888.13	888.13	888.13	888.13	888.13
Hydrogen 1	5130.44	3914.60	2934.42	2533.22	2160.74	1557.77	1051.37
Hydrogen 2	128.03	113.27	95.26	88.09	81.60	69.42	58.87
Hydrogen 3	62.74	53.54	30.82	25.97	42.59	28.76	27.23
Syngas 1	2554.22	2544.09	2544.09	2544.09	2544.09	2544.09	2544.09
Syngas 2	2547.08	2547.08	2536.99	2536.99	2536.99	2536.99	2536.99
Syngas 3	10747.25	9309.01	8106.88	7637.80	7248.95	6605.03	6175.35
Syngas 4	9738.18	8548.86	7539.69	7149.56	6835.08	6307.90	5976.55
Syngas 5	17180.34	15438.14	13529.93	12807.79	12146.99	10940.14	9937.98
Syncrude	3085.53	2746.12	2320.23	2150.67	1997.06	1704.69	1449.37
Wax	611.82	522.37	303.42	256.41	415.22	281.96	266.58
Liquid Hydrocarbons	593.15	506.19	296.40	251.35	402.12	274.09	258.82
Recycle 1	7442.13	6889.27	5990.26	5658.20	5311.91	4632.25	3961.43
Recycle 2	3069.35	2847.10	2635.33	2567.48	2551.14	2510.24	2587.00
Recycle 3	0.36	0.22	0.13	0.10	0.07	0.03	0.00
Flue gas 1	0.00	0.00	0.00	0.00	0.00	0.00	0.00
Recycling gases 1	10665.88	9734.67	8654.33	8261.64	7891.40	7223.85	6680.34
Recycling gases 2	1223.19	1130.02	921.76	838.10	752.25	594.86	451.60
Recycling gases 3	81.41	69.73	37.84	31.03	55.69	36.62	34.98
Recycling gases 4	1458.98	1198.03	988.34	905.11	836.28	712.83	618.51
Flue gas 2	0.37	0.28	0.22	0.21	0.18	0.15	0.13
CO_2 to storage	0.01	0.06	0.09	0.10	0.11	0.12	0.13
Waste Water 1	1009.10	760.16	567.13	488.22	413.85	297.14	198.80
Waste Water 2	2865.75	2492.78	2153.39	2016.76	1901.40	1691.17	1517.31
Waste Water 3	691.68	578.18	497.57	467.08	438.99	390.14	350.03
Waste Water 4	1458.59	1197.76	988.18	904.91	836.09	712.69	618.38
From Dryer	704.87	704.87	704.87	704.87	704.87	704.87	704.87
Naphtha	535.37	458.28	405.26	383.68	361.12	328.26	297.43
SAF	1016.99	886.82	765.96	717.44	676.03	600.74	537.79
Diesel	291.30	254.82	220.23	206.40	194.55	172.97	154.80
HYDROGEN CONVERSION EFFICIENCY (%)	**21.52%**	**21.84%**	**22.07%**	**22.19%**	**22.27%**	**22.49%**	**22.59%**

The green highlights denote that the streams are inlets or outlets of the system

Discussion and validation of the technical results of the PBtL scenarios: A literature review evidences a variety of PBtL configurations for the production of FT-syncrude that were evaluated; they differ

from each other by the choice of technologies/operating conditions, such as the type of gasifier, gasification agent, type of electrolyser, use of oxygen for fired heaters etc. As a consequence, a wide range of carbon conversion efficiencies are reported, ranging from 33.8% to 97.7%. Most of these studies concluded that PBtL processes have higher carbon conversion efficiencies than BtL [39], [138], [142], [147], and that they have lower or even achieve similar efficiencies compared to PtL scenarios, depending on the process configuration choices. In this study, regardless of the amount of CO_2 that is sent to storage, the estimated carbon conversion efficiencies of the various PBtL scenarios are higher than that of an analogous BtL scenario that was evaluated by the authors [171]. When compared against a similar PtL system (also evaluated by the authors) [340], the 0%TS and 20%TS PBtL scenarios achieve comparable carbon conversion efficiencies. Further, in the literature, the reported PBtL efficiencies range from 32.1% to 54.8% [39], [147], and these are in good agreement with those calculated herein, i.e. 34.05% to 40.41%. The hydrogen conversion efficiency has not been discussed in other PBtL studies, but when compared to the PtL literature, it is evident that for both configurations the efficiency is constrained to low values due to the water production in the FT and RWGS reactors. It should be mentioned that, the gasification model utilised was previously validated in [171], while the FT model was developed and adjusted to experimental values by Marchese et al. [64].

6.3.1.4 Heat integration

Another important output of the process modelling is the estimation of the heating and cooling requirements. These heat interactions were translated into hot and cold composite curves, which are presented in Figure 6-6 for the 0%TS, 50%TS, and 100%TS scenarios (the results for the other scenarios are found in the APPENDIX C-2). The figures show the streams that require cooling in red and those that require heating in blue. The high-temperature heat requirements of the tar reforming and RGWS reactions are met by the oxycombustion of a fraction of the recycling gas, and therefore these units were not considered for the heat integration. Similarly, the ASU was not considered for this integration since the cooling requirements are internally supplied while the heating is met by internally generated MP steam. The hot and cold composite curves exhibit that there is no pinch point temperature and that the system's heat integration is a "threshold problem", meaning that one single thermal utility is required. All the scenarios are self-sufficient in terms of heat requirements, and only external cold utilities are needed. After the heat integration of the process streams, more excess heat at moderate temperatures was available, therefore LP, MP and HP steam are generated. Some of this steam is used within the process (e.g., gasifier, ASU); the mass flows of available steam for sale is detailed in

Table 6-12. Other cooling utilities that were used were cooling water and refrigerant (only for one process stream).

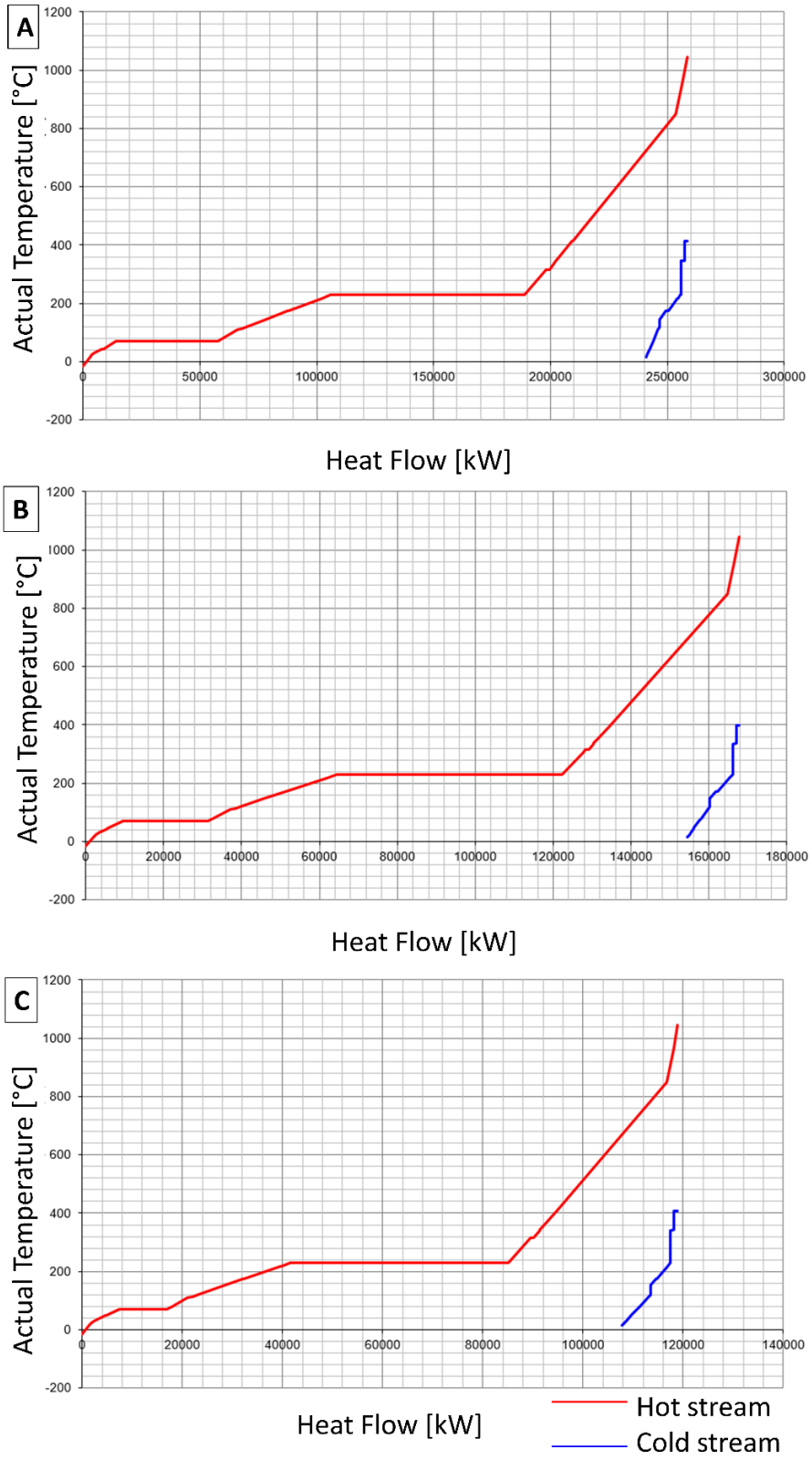

Figure 6-6: Composite curves of the A) 0%TS scenario, B) 50%TS scenario, and C) 100%TS scenario.

Table 6-12: Net steam production for the various scenarios.

	Scenario						
Steam available for sale	**0%TS**	**20%TS**	**40%TS**	**50%TS**	**60%TS**	**80%TS**	**100%TS**
HP Steam [kg/h]	73,202	58,039	48,411	43,714	39,309	35,902	31,946
MP Steam [kg/h]	172,050	148,244	127,842	119,483	112,084	98,791	86,182
LP Steam [kg/h]	6,643	5,555	4,820	4,480	4,192	4,087	2,900

6.3.2 Economic performance

Figure 6-7 presents the summary of the CAPEX and the breakout for all scenarios. For the 0%TS and 20%TS scenarios, the dominant element of the CAPEX is the electrolyser, which represents a share of 48% and 44%. As the amount of CO_2 sent to storage increases, the CAPEX decreases due to the reduction of the plant's productivity (and hence equipment size). The reduction is not linear, since at 50%TS, the ASU CAPEX appears (as the oxygen generated in the electrolyser is no longer enough for the gasifier and the oxycombustors) and this additional equipment slows down the pace of the overall CAPEX reduction. For the scenarios 40%TS, 60%TS, 80%TS, and 100%TS, the CAPEX of the "RWGS, FT, and upgrading" takes over as the primary CAPEX contributor. Further, the CAPEX of the "CO_2 compression" section, even for the scenarios with large amounts of CO_2 sent for storage, is very small; thus, the addition of the CCS supply chain is not expensive.

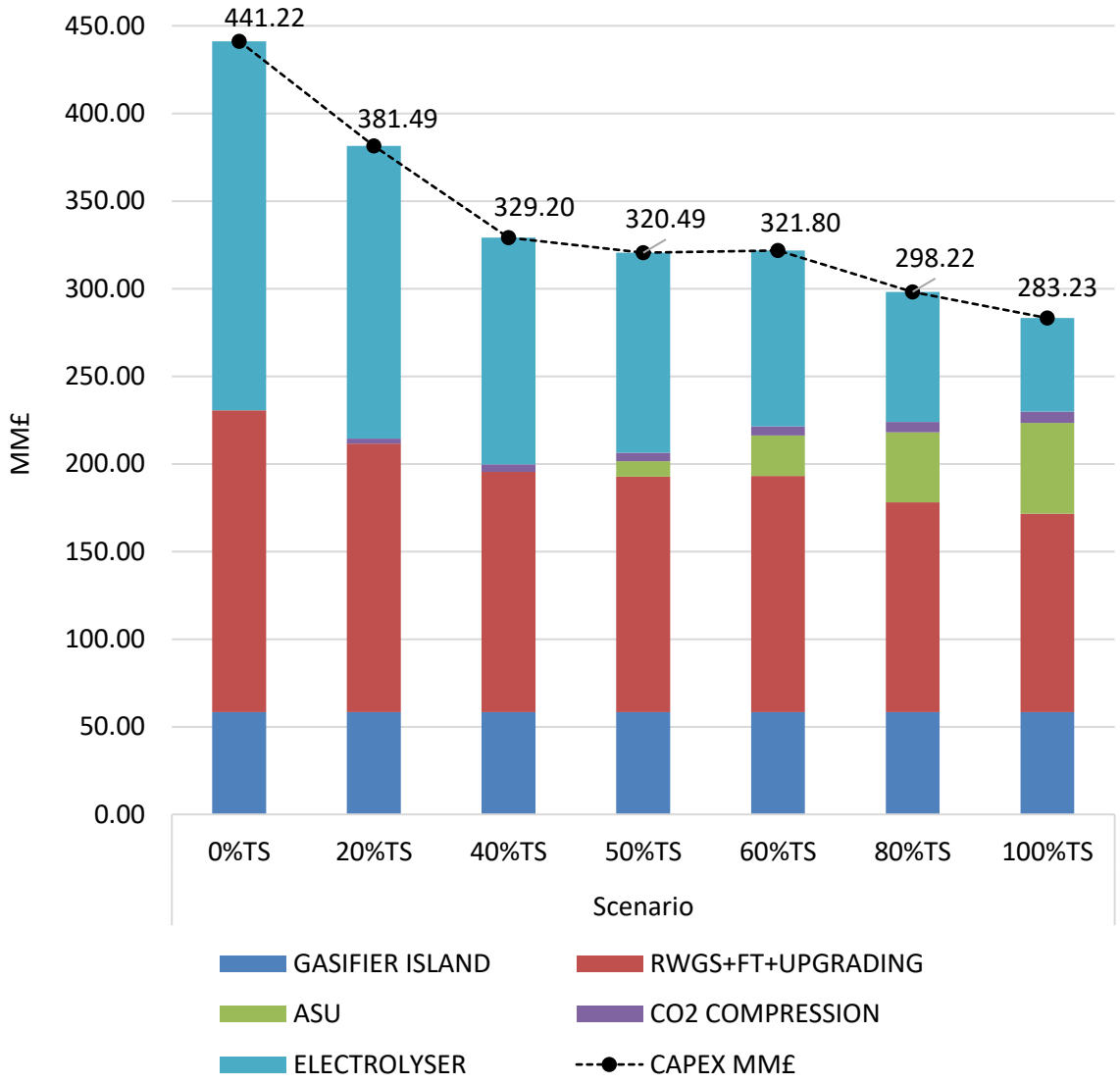

Figure 6-7: CAPEX breakdown for the different scenarios.

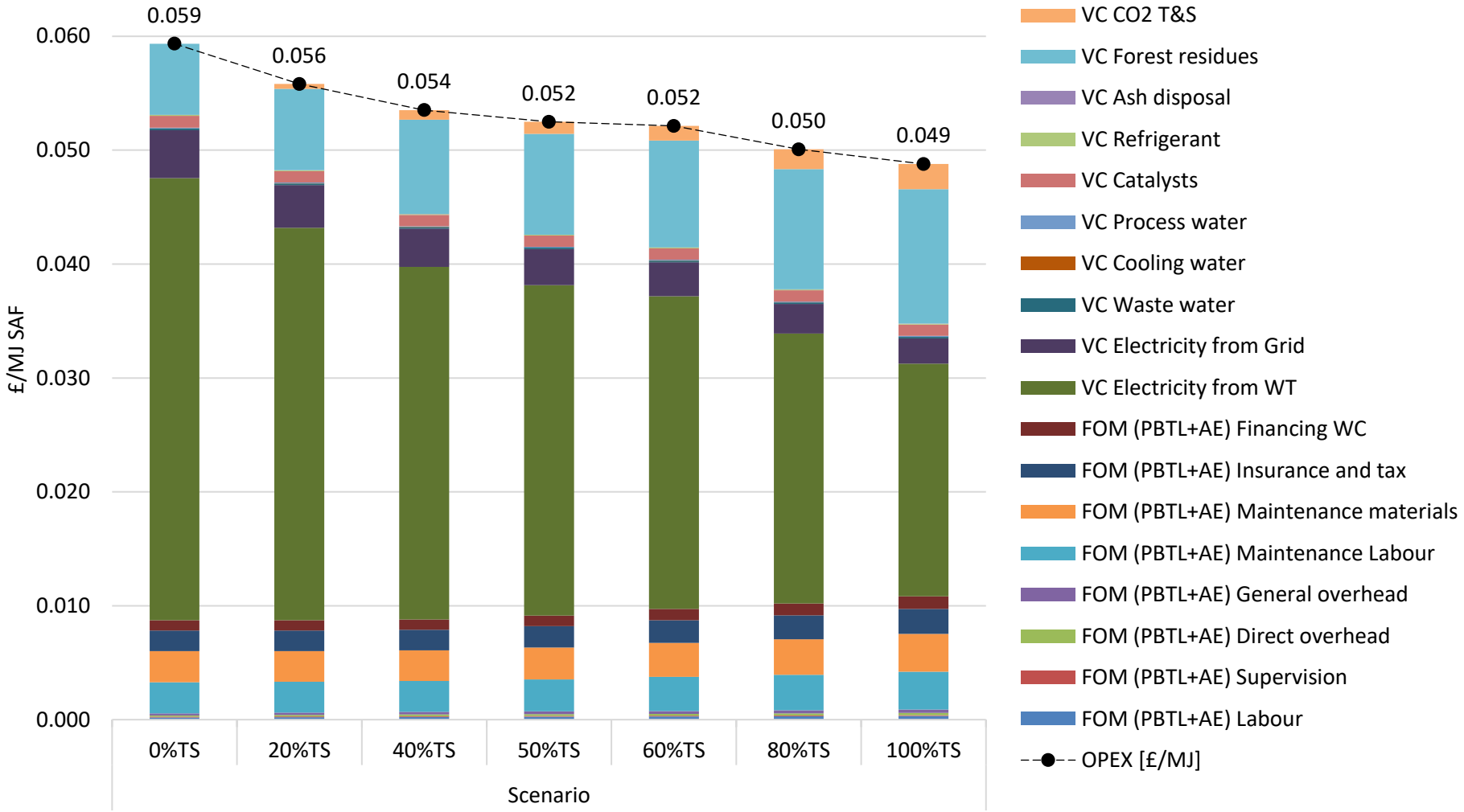

Figure 6-8: OPEX breakdown for the different scenarios, in £/MJ of SAF.

The normalised OPEX per MJ of SAF and its breakdown across all scenarios is presented in Figure 6-8. The largest OPEX was calculated for the 0%TS scenario, while the lowest was found for the 100%TS scenario. As more CO_2 is sent for storage, the OPEX decreases since less hydrogen is required for the process. Across all scenarios, the cost of wind electricity dominates the OPEX, with shares ranging from 65% for the 0%TS scenario to 47% for the 100%TS scenario. The second most significant component is the cost of the forest residue chips, which accounts for 11% and 21% for the 0%TS and the 100%TS scenarios, respectively. Notably, the 100%TS scenario incurs the highest cost for "transport and storage of CO_2," yet this expense only represents 3% of its overall OPEX. In conclusion, the OPEX of the proposed SAF production scenarios are electricity-dependent, and the annexation of CCS does not significantly increase their operational expenditures. Therefore, substantial OPEX reductions rely on lowering the cost of the electricity source.

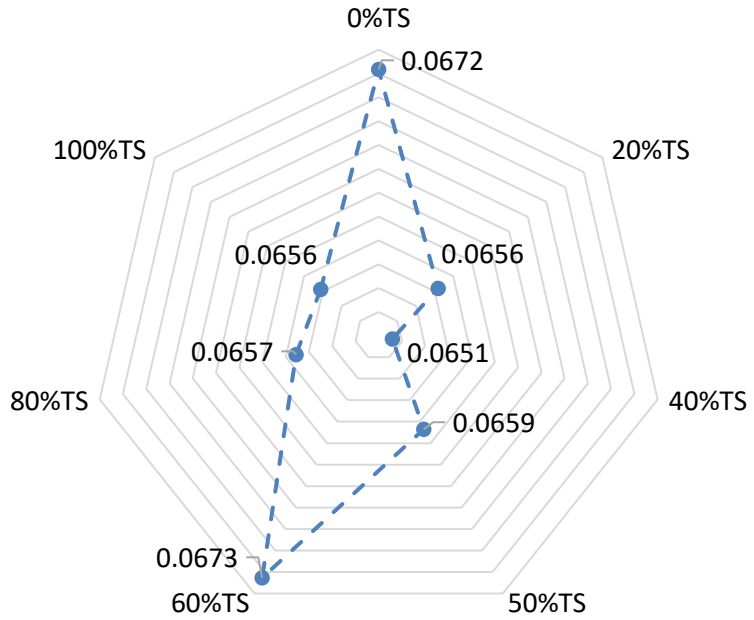

Figure 6-9: MJSP for the scenarios in £/MJ of SAF.

Despite the varying productivity of the scenarios, their MJSPs are not significantly different, as depicted in Figure 6-9. There is no defined trend for these variations since, in some scenarios, the CAPEX changes significantly due to the addition of the ASU. From the information provided in Figure 6-8 and Figure 6-9, it is clear that the MJSP for all cases is OPEX-intensive (e.g., 74% to 88% of the MJSP) and therefore electricity-dependent. None of the scenarios could break even the gate price of the fossil jet fuel, which is equal to 0.0131 £/MJ [256]; however, the estimated MJSPs show a clear reduction when compared to a PtL scenario for SAF production [340]. Finally, it is important to

highlight that the cost of adding CCS does not highly affect the final MJSP, and therefore these PBtL-CCS configurations show their potential as negative emissions technologies (PBtL-CCS).

Comparison of the economic performance of the PBtL scenarios with previous research: Previous studies on PBtL configuration show a wide range of economic performance indicators due to differences in technology selection, process configuration, and final product. Summarizing those studies that assessed PBtL for SAF production, the selling price ranges between 0.0290 £/MJ and 0.0636 £/MJ [39], [147], [345]. The MJSPs of this study are in the upper range of the reported values. Furthermore, these studies also found that the driver for the MJSP value is the OPEX, which is mainly dominated by the cost of the electricity and the feedstock.

6.3.2.1 MJSP sensitivity and uncertainty analyses

Figure 6-10 presents the results of the sensitivity analysis on the MJSP. The production cost of H_2, the electricity cost, and the refinery's CAPEX are responsible for the largest variations of the MJSP for all the analysed scenarios. Considering that the production of H_2 is the biggest electricity consumer, it could be summarised that the MJSP is highly sensitive to the electricity price. This affirmation becomes more noticeable for the 0%TS scenario since it has the largest power requirement among all scenarios. Furthermore, if naphtha and diesel are sold at the same price as the SAF's MJSP, this latter considerably drops. As long as there is a desire to encourage the use of renewable naphtha and diesel, this strategy presents a chance to lower the cost of SAF production.

Furthermore, Figure 6-11 represents the sensitivity of the MJSP at different H_2 and forest residues costs for the 0%TS, 50%TS, and 100%TS scenarios (for the other scenarios, please refer to APPENDIX C-4). While the cost of forest residues may not have a significant impact on the MJSP, their limited availability and resource competition can introduce FR cost volatility, which can potentially impact the economics and feasibility of the proposed SAF production scenarios [346]. From the information provided by Figure 6-11, it is again concluded that the wind electricity cost is the main driver for the MJSP value; especially for the 0%TS, where the effect of the FR cost in the considered window of prices, is smaller. The MJSP becomes more sensitive to the FR cost for the 100%TS scenario.

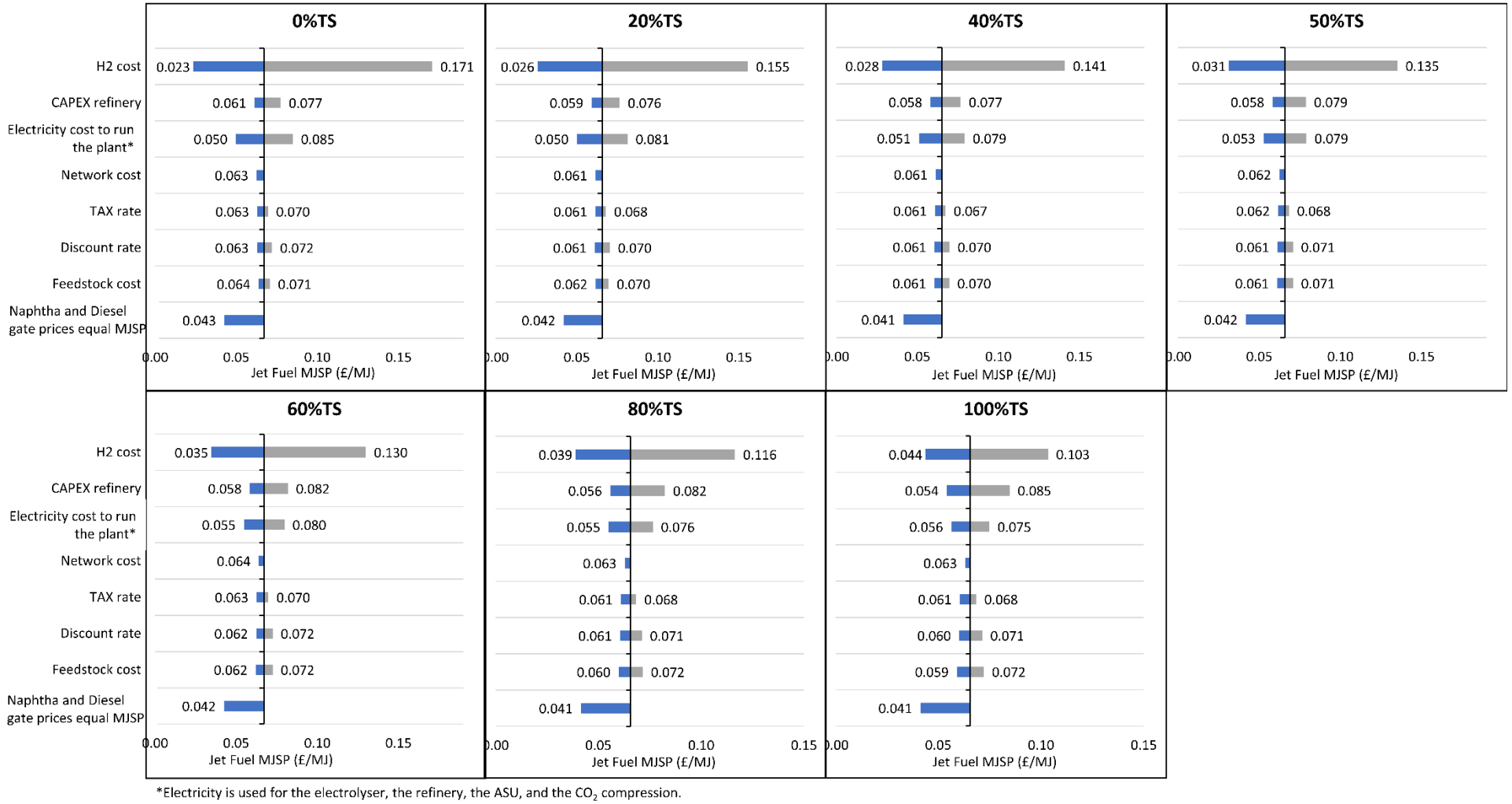

*Electricity is used for the electrolyser, the refinery, the ASU, and the CO_2 compression.

Figure 6-10: Sensitivity analysis on the MJSP for the various scenarios.

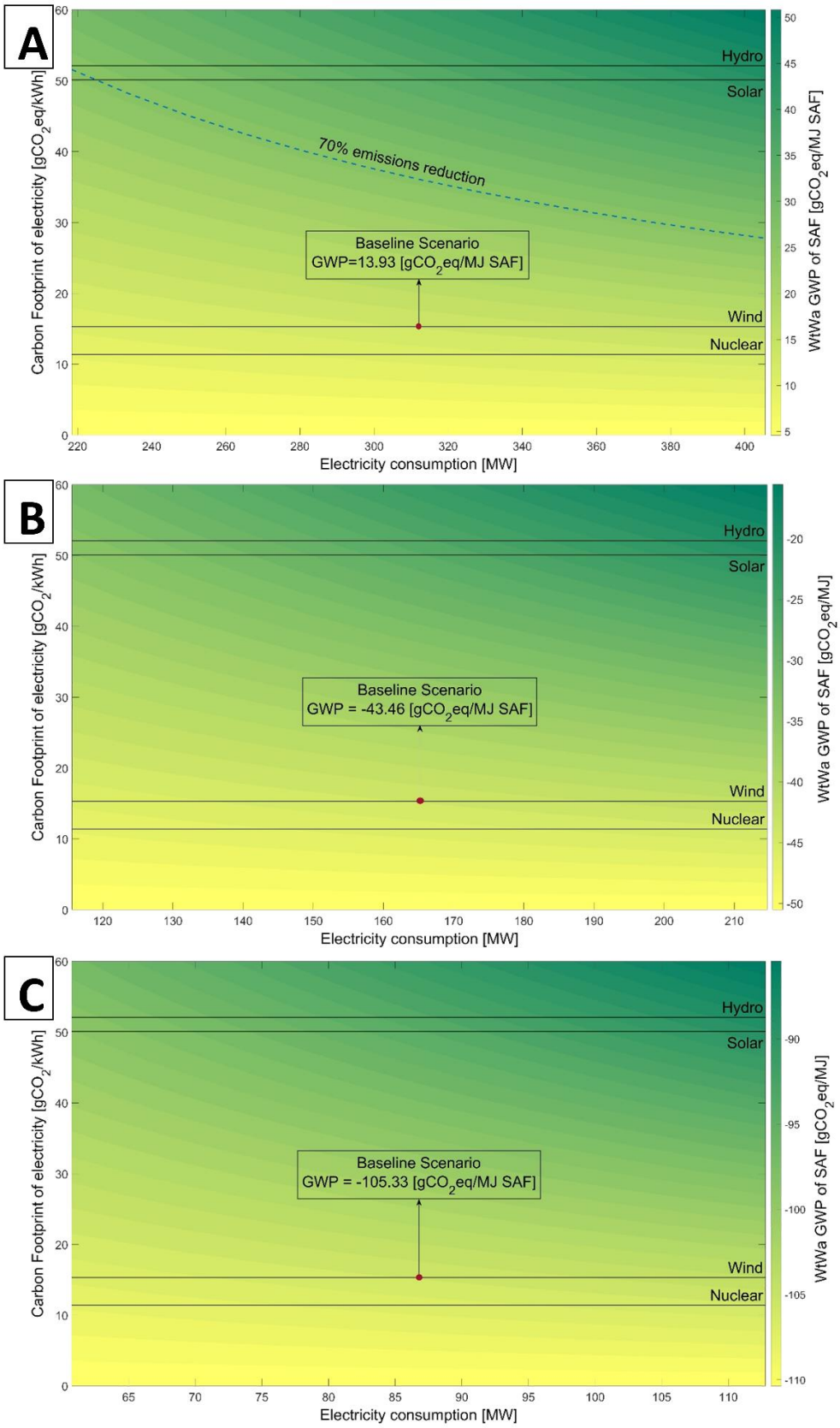

Figure 6-11: Sensitivity of the MJSP of the SAF produced at various feedstock cost and H_2 production cost for: A) 0%TS scenario, B) 50%TS scenario, and C) 100%TS scenario.

Further, a probabilistic estimation of the MJSP is presented in Table 6-13. Given the wide range that was assigned for the cost of production of H_2, the standard deviations are relatively high, and therefore, a wide range of possible values for the MJSP are estimated. Moreover, it should be noticed that the effect of the uncertainty of the H_2 cost is reflected in the mean values, which are higher than those estimated from the deterministic economic assessment. In addition, the lower range of the confidence intervals shows that even in the most optimistic conditions, the PBtL-CCS scenarios are not feasible.

Table 6-13: Monte Carlo results for the estimation of the MJSP.

Scenario	Mean	Median	Standard Deviation	95% Confidence Interval	Units
0%TS	0.087	0.084	0.032	0.025 to 0.149	£/MJ of SAF
20%TS	0.083	0.080	0.028	0.028 to 0.137	
40%TS	0.079	0.077	0.024	0.031 to 0.126	
50%TS	0.078	0.076	0.023	0.034 to 0.122	
60%TS	0.078	0.077	0.021	0.037 to 0.119	
80%TS	0.075	0.074	0.018	0.040 to 0.109	
100%TS	0.072	0.072	0.015	0.044 to 0.101	

6.3.3 Environmental performance

The Recipe Midpoint (H) method calculated 18 environmental impacts, from which two are discussed in the main manuscript, while the others are presented in APPENDIX C-5, calculated under the "baseline allocation approach".

6.3.3.1 Global warming potential (GWP)

Figure 6-12 depicts the results of the GWP for the different scenarios, following two different allocation approaches, as explained in Table 6-6. The "baseline allocation approach," denoted as Approach 1 and represented by orange points, attributes the net negative emissions of CO_2 storage solely to SAF, resulting in a more negative WtWa GWP for each scenario. On the other hand, Approach 1B, represented by blue points, distributes the negative emissions among the SAF, naphtha, and diesel based on their energy content. Considering that the utmost interest of the system is the production of SAF, and that the aviation industry has set the target of "Net-zero" by 2050, the outputs of Approach 1 are considered the **main WtWa GWP results.** Furthermore, they serve as the foundation for sensitivity analyses and for discussions on GWP results in the subsequent sections. It should be noted, regardless the allocation approach used, the amount of net negative CO2eq stored permanently remains the same and this equals to 17,464 tCO_2/y for the 20%TS and 126,214 tCO_2/y for the 100%TS.

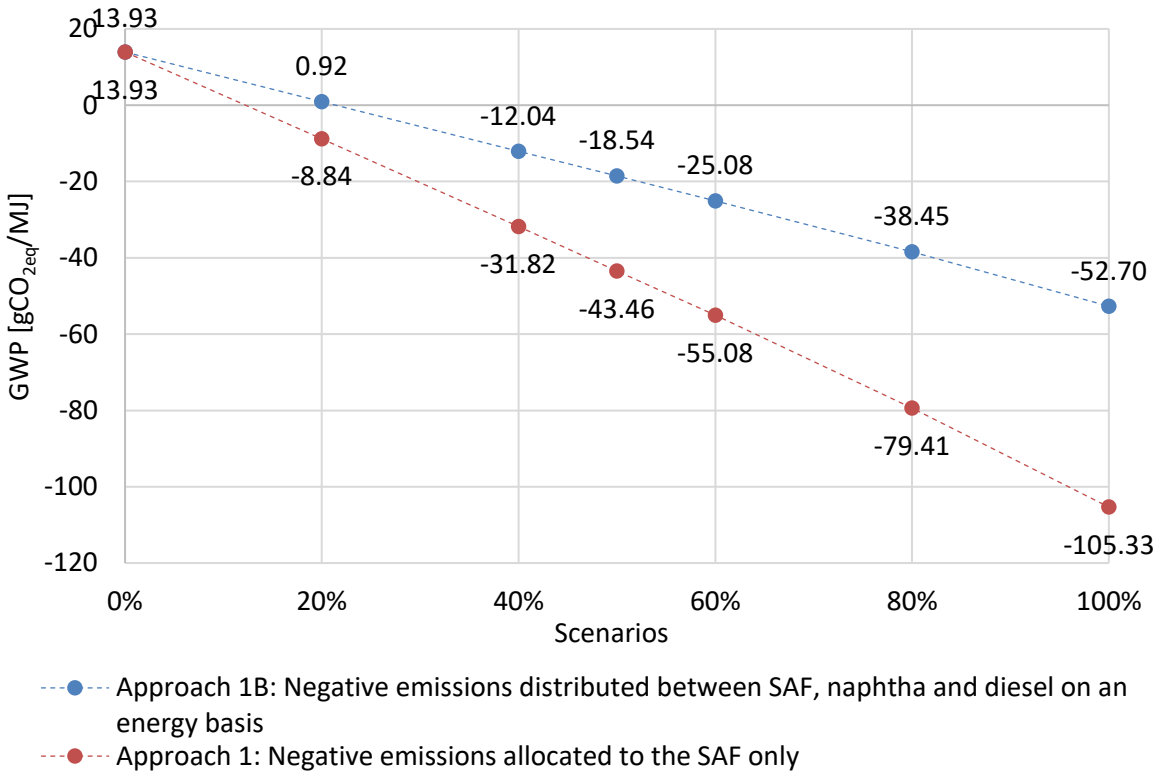

Figure 6-12: GWP as a result of the main and second approach for the attribution of negative emissions, upon the "baseline scenario" (as defined in Table 6-6) allocation method.

The estimation of the GWP results in negative emissions even at 20%TS scenario. Figure 6-13 presents the breakdown of the GWP by LCA stages for each scenario, which are on its turn differentiated between emissions originated from the wind farm electricity and those unrelated to it. Without considering the negative contribution of the CO_2 storage, the major drivers for the GWP of each scenario are the wood chips production and transport, and the wind electricity that is used for the AE operation. Despite the absence of CO_2 storage, the 0%TS scenario achieved a notably low GWP (13.93 gCO_{2eq}/MJ) when compared to the estimated value for a PtL SAF scenario [340] and relatively close to the GWP of a BtL SAF scenario [171]. Furthermore, all the scenarios meet the threshold for emissions reductions specified in existing normative, such as the European Renewable Energy Directive II (RED II) [175], the Renewable Fuels Standard (RFS) [176], and the UK SAF mandate [19]. The estimation of the GWP was addressed by previous research for the PBtL scenario; however, specific LCAs for the SAF production from a PBtL-CCS configuration were not found. Habermeyer et al. [137], [147] have performed a carbon accounting considering the most important stages of the WtWa boundaries, from which they found that green electricity plays an important role on the final specific fuel emissions, which agrees with the results for the 0%TS scenario.

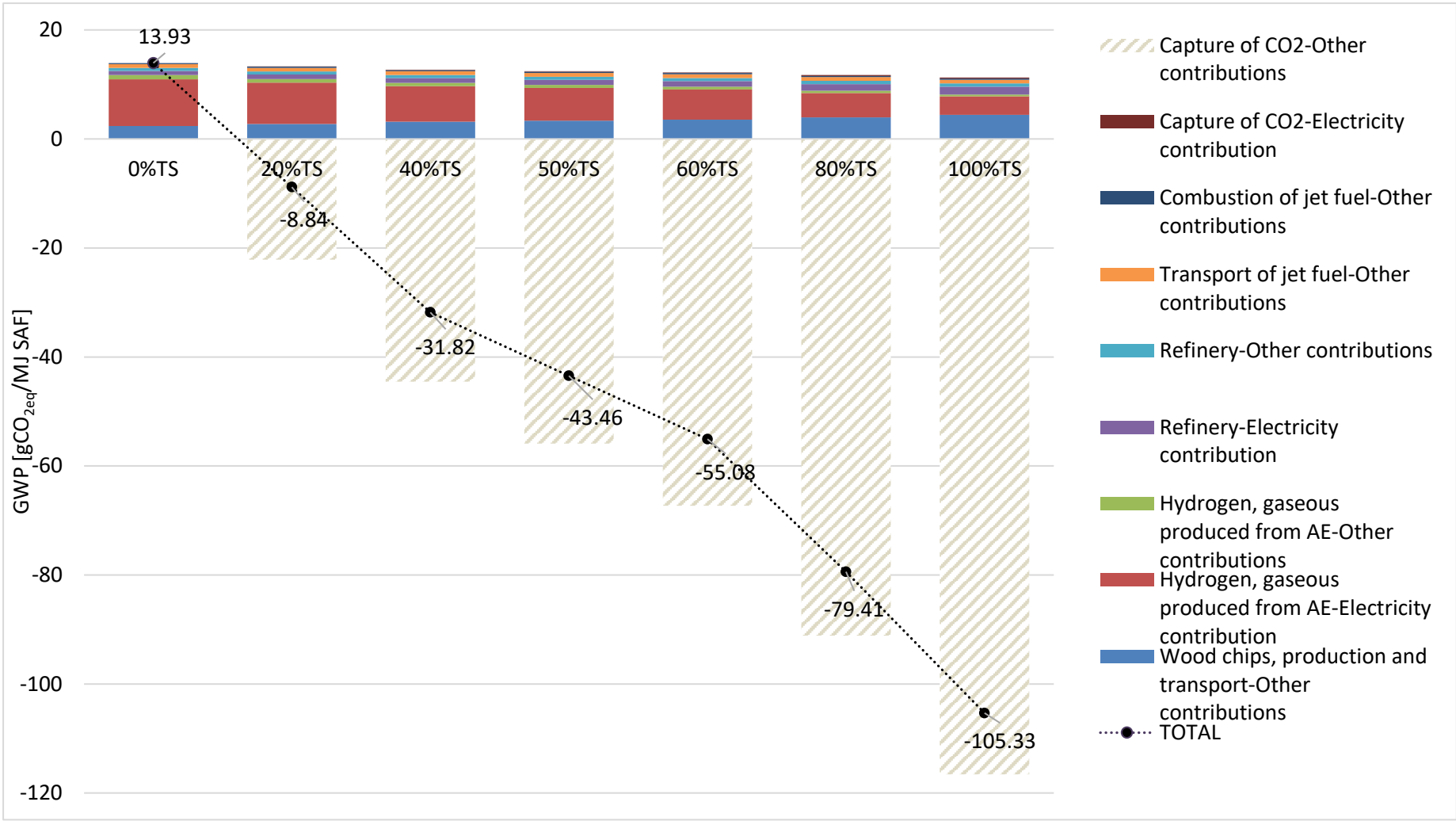

Figure 6-13: Breakdown of GWP for the various scenarios.

6.3.3.2 Sensitivity analysis on the GWP

Figure 6-14 presents the results of the sensitivity analysis on the GWP. A change in the carbon footprint of wind farm electricity (referred to as "electricity carbon intensity") causes the largest variation. Additionally, Figure 6-14 presents the GWP of the alternative scenarios that were proposed based on: 1) various allocation approaches (as described in Table 6-6: Allocation approaches for the multifunctional system of the WtWa PBtL system.Table 6-6), and 2) the use of other electricity sources. The choice of the allocation method slightly affects the results, with approach 4 (economic allocation in the refinery plant) being the one that induces the largest variation. On the other hand, the use of a different electricity source has a high impact on the GWP. For example, when grid electricity is used, the GWP of all the configurations considerably increases; despite this, for scenarios such as 50%TS, 60%TS, 80%TS, and 100%TS, the produced SAF still complies with the 50% emissions reduction threshold of the SAF mandate. Furthermore, if upstream emissions of wind electricity are neglected (as suggested by the SAF mandate), the carbon accounting leads to low GWP for all the scenarios.

Given that it was determined that the main contributor to the GWP is the electricity consumption, the sensitivity of the WtWa GWP under different electricity sources and system's power requirements is presented in Figure 6-15 for the 0%TS, 50%TS, and 100%TS scenarios. The UK SAF mandate defines that a SAF should demonstrate a 70% reduction on the GWP in the most strict threshold, or a 50% reduction in a most reliant case, with respect to the emissions of fossil jet fuel (GWP equal to 89 gCO_{2eq}/MJ) [17], [19]. For the 0%TS scenario, despite the absence of CO_2 storage, the WtWa emissions comply with the SAF mandate restrictions under the considered electricity carbon footprint and consumption ranges proposed in Figure 6-15, while for the 100%TS scenario, the GWP of the SAF is always negative. The figures representing the results for the other scenarios are presented in APPENDIX C-6.

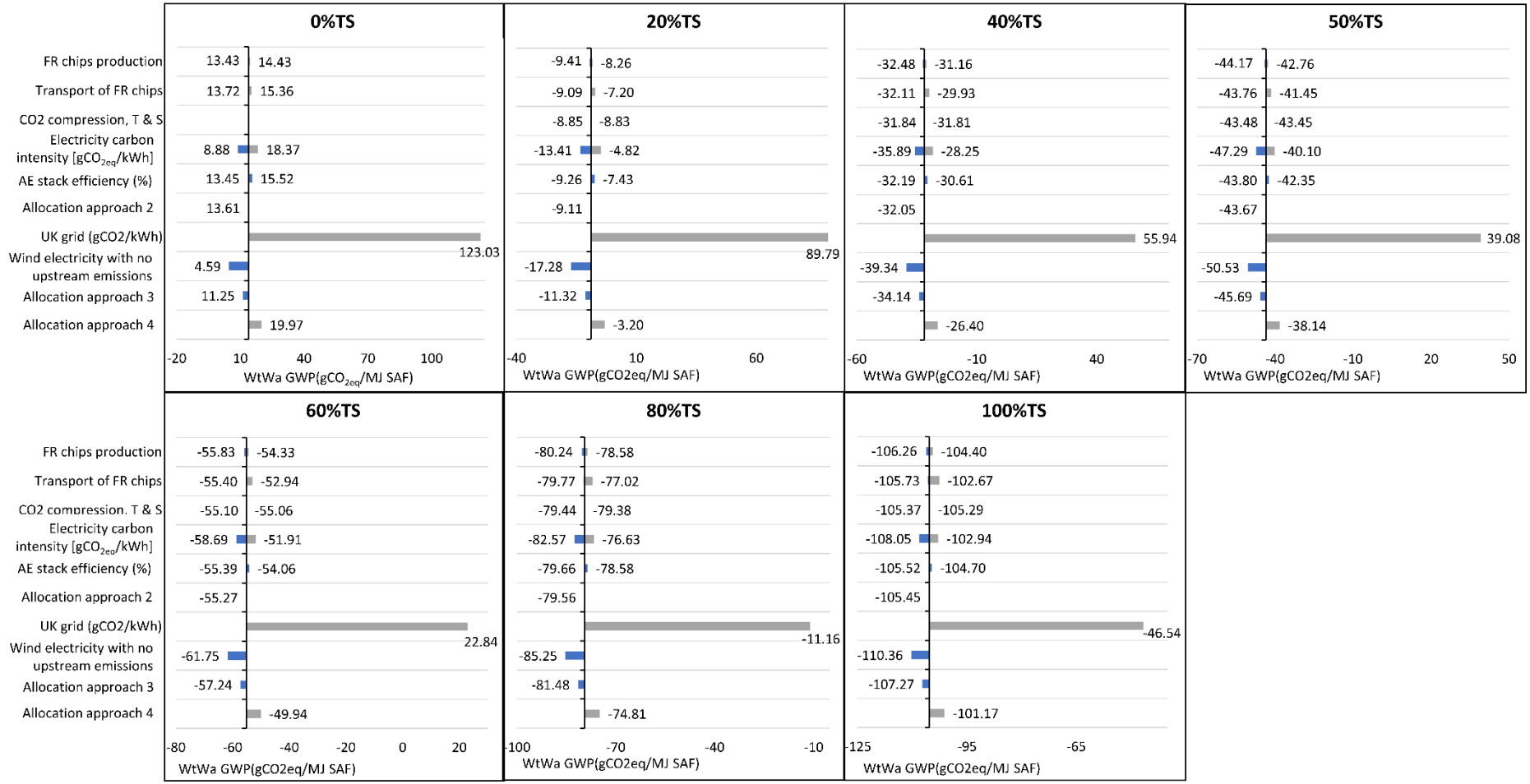

Figure 6-14: Sensitivity analysis on the GWP for the various scenarios.

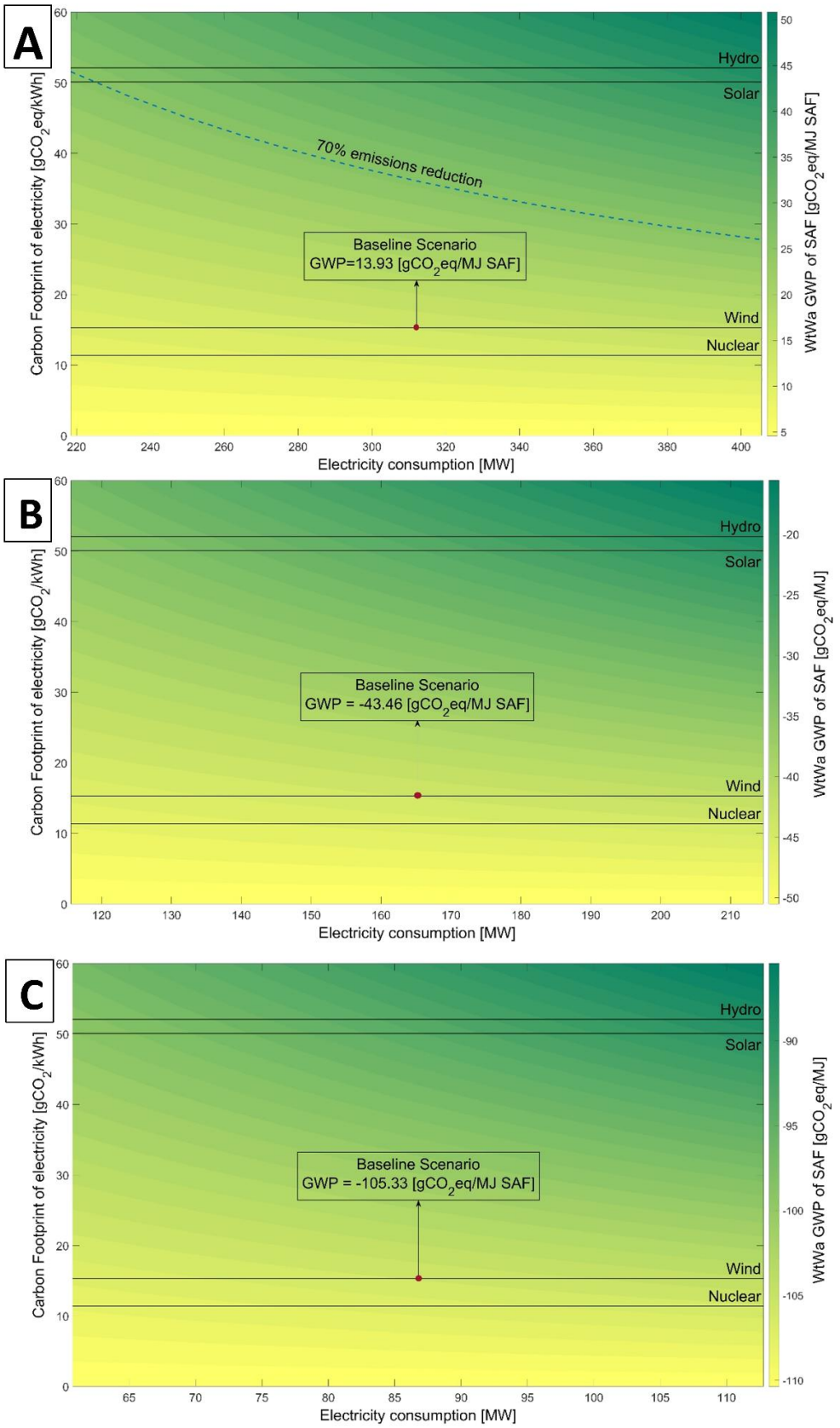

Figure 6-15: The GWP of the WtWa life cycle of SAF for different electricity sources and different electricity consumption for the: A) 0%TS scenario, B) 50%TS scenario, and C) 100%TS scenario.

Table 6-14: Monte Carlo results for the estimation of the GWP.

Scenario	Mean	Median	Standard Deviation	95% Confidence Interval	Units
0%TS	14.43	14.47	2.02	10.47 to 18.40	gCO_{2eq}/MJ
20%TS	-8.24	-8.22	1.85	-11.86 to -4.62	
40%TS	-31.17	-31.15	1.68	-34.47 to -27.88	
50%TS	-42.79	-42.78	1.60	-45.93 to -39.65	
60%TS	-54.39	-54.38	1.54	-57.40 to -51.37	
80%TS	-78.67	-78.68	1.41	-81.44 to -75.90	
100%TS	-104.54	-104.55	1.31	-107.11 to -101.97	

Furthermore, a probabilistic estimation of the GWP derive in the results of Table 6-14. Despite the uncertainty of the selected parameters, the estimated mean is similar to the estimated values from the deterministic assessments for all the scenarios. Moreover, the resulting standard deviations lead to the conclusion that in a 95% confidence interval, the range of estimated GWPs are always negative, except for the 0%TS, that despite possessing a positive GWP, the resulting probabilistic estimations shows that it will always comply even with the most restrictive emissions reduction threshold of the SAF mandate proposal.

6.3.3.3 Water footprint

Figure 6-16 depicts the water footprint, where the contribution of wind electricity is distinguished from the contribution of other parameters for each stage in each scenario. Across all the scenarios, the majority of water consumption occurs in the refinery and the AE, accounting for more than 90% of the total. In the case of the AE, both the electricity consumption and the “other contributions” (which are mainly linked to the water required for the electrolysis) are equally responsible for the total water footprint value. In the case of the refinery plant, the water footprint of the electricity consumption is almost negligible, while the “other contributions” of the refinery plant, which refer to the make-up water for the steam and cooling cycles, account for 97% and 94% in the 0%TS and 100%TS scenarios, respectively. The forest residues production and transport stages have an insignificant effect on the final water footprint value, but it may become more important with other biogenic feedstock source. As an example, it was found that the water footprint of some crops, such as maize or wheat, could have a ten-fold higher value [347] than that of the forest residues. The lowest water footprint is found for the 100%TS scenario, which has the lowest hydrogen requirement and therefore lower electricity consumption.

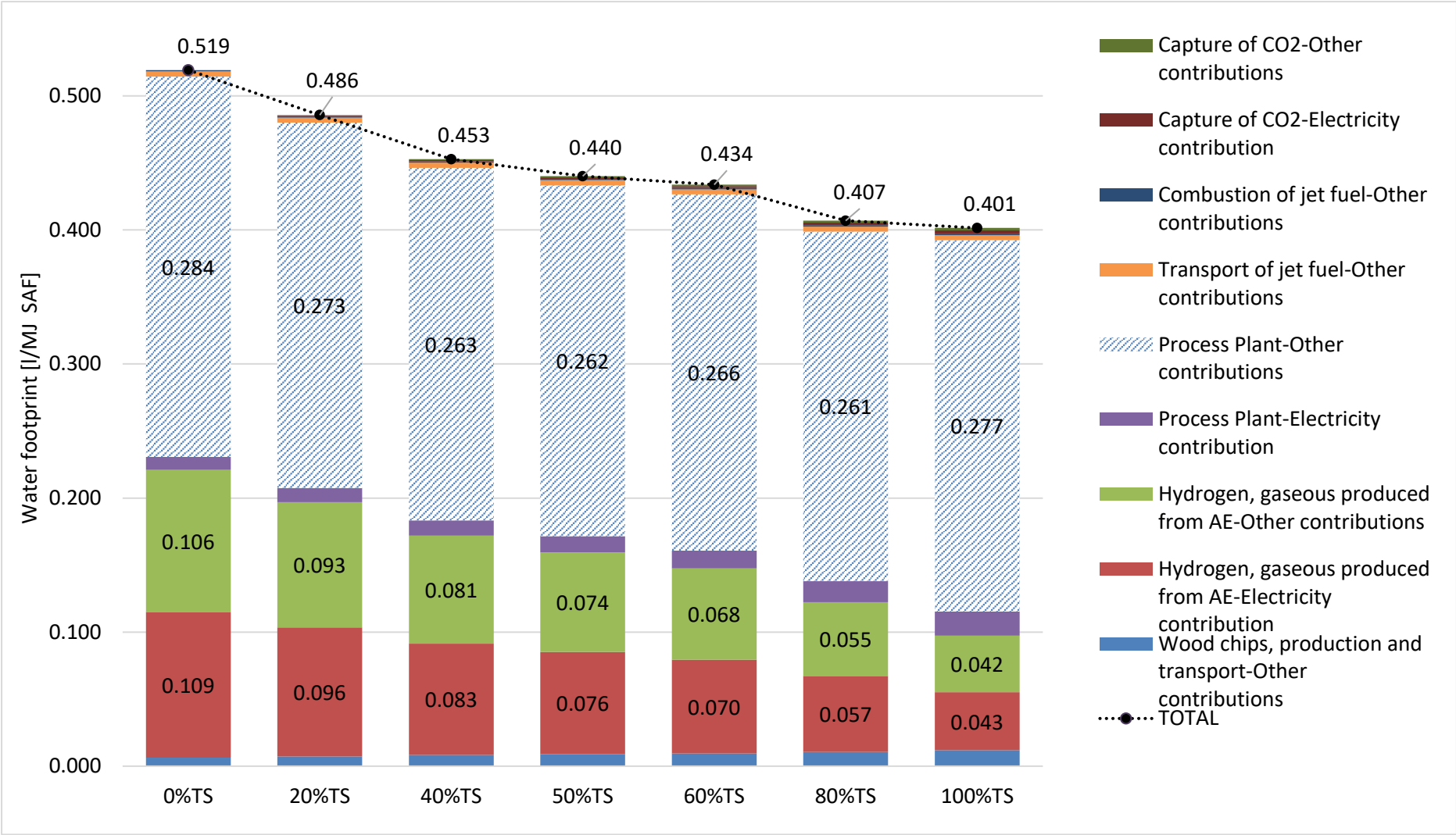

Figure 6-16: Water footprint breakdown for the different scenarios

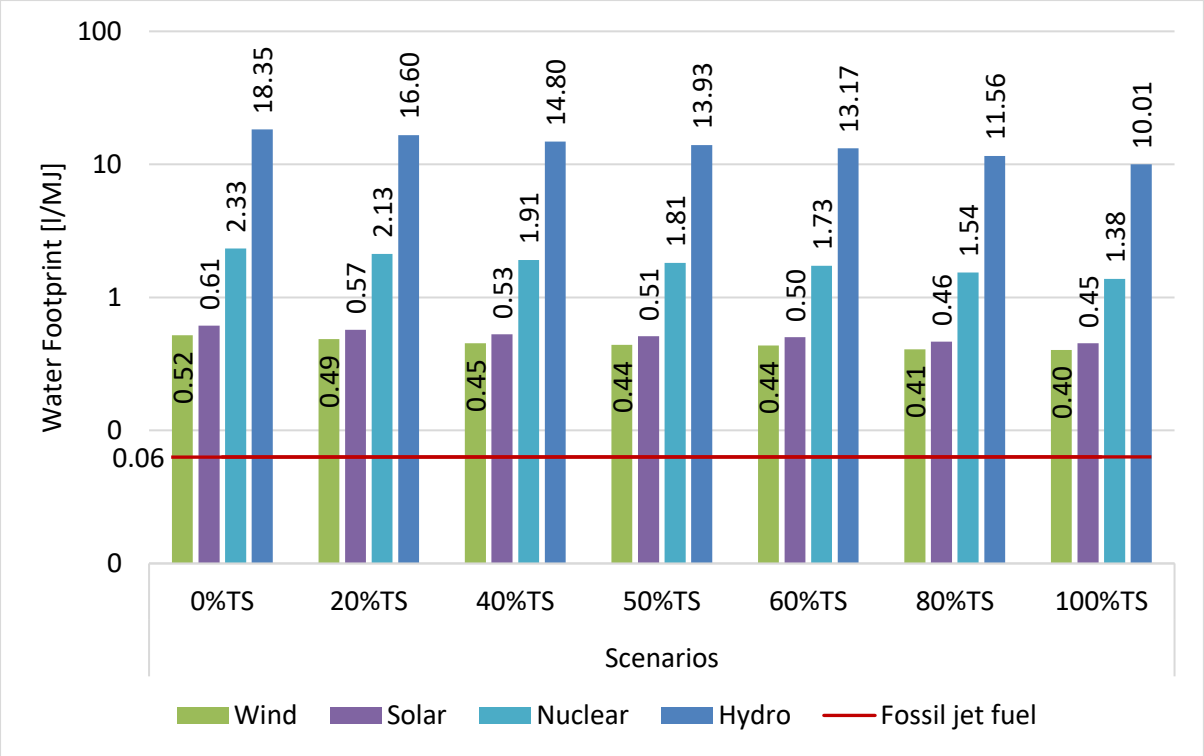

Figure 6-17: Water footprint of the PBtL-CCS scenarios when connected to different electricity sources.

Since the operation of the refinery plant is the main contributor to the water footprint, some strategies, such as the use of air coolers, could reduce it. However, a drawback of dry cooling technologies is that their operating performance is highly sensitive to the humidity and ambient temperatures [348]. Another reduction strategy is that the water synthesized in the process plant could cover the water requirements of the electrolyser. Although the use of waste water does not lower the system's water requirements, it does lessen the removal of water from body sources, and as a result leaving good-quality water for direct consumption [348]. Nevertheless, the use of waste water would require stringent treatment to reduce its hydrocarbon content. Additionally, given the importance of the electricity source on this environmental impact, Figure 6-17 presents the estimated water footprint with other electricity sources. The results show that the best choice is the wind electricity, which results in lower water footprint compared to solar, nuclear, or hydropower. None of these cases achieved a low water footprint when compared with the one associated to fossil jet fuel (0.0632 l/MJ).

6.4 Policy analysis: SAF mandate and negative emissions trading system

The effect of the UK SAF mandate on the economic performance of the SAF production scenarios is assessed in this section. The SAF mandate is still under consultation, with a finalised version expected

by 2025; nevertheless, guidelines for the so called "second consultation" [19] are already available, and these are used herein. The SAF mandate was conceived with the intention of supporting the UK's Net-zero Strategy by achieving net-zero emissions for the aviation industry by 2050 [18]. To accomplish this target, the Jet Zero Strategy was launched by the UK government, from which one of the proposed action plans is to replace 10% of the fossil jet fuel by 2030 with the intention of achieving a 50% SAF uptake by 2050 [19]. The SAF mandate defines SAF as a drop-in fuel that could be used in existing aircraft without modification, while exhibiting a 50% reduction in the life cycle emissions compared to conventional jet fuel. Furthermore, these SAFs must be obtained from sustainable feedstocks that are non-competitive with human consumption and that do not create deforestation [17], [19], [20]. The last statement translates into the use of all kinds of waste, residues, and low-carbon footprint energy, and therefore, since the scenarios analysed on this study rely on forest residues, they qualify for the incentives offered by the SAF mandate guidelines.

The economic support offered by the SAF mandate could benefit SAF producers through a scheme of tradable certificates that will have a monetary value. The value of these certificates will be determined by the market in order to close the gap between SAF and jet fuel prices [19]. Equation 6-1 [19] describes the methodology for the calculation of the amount of certificates; this is proportional to the energy content of the SAF, represented by the term $m_{SAF} \times LHV_{SAF}$ (where m_{SAF} is the mass of the SAF produced and LHV_{SAF} the SAF low heating value, which is fixed at 42.8 MJ/kg [156]). Moreover, to promote the use of SAF with large GHG savings, the number of certificates is proportional to a carbon intensity factor, (CI_{factor}), which in turn is a function of the carbon intensity of the fuel (CI_{SAF}), as depicted in Equation 6-2). The CI_b is the carbon intensity of a benchmark SAF that achieves 70% emission reduction, i.e. 26.7 gCO_{2eq}/MJ, and the CI_F is the carbon intensity of the fossil jet fuel, i.e. 89 gCO_{2eq}/MJ [19].

Under the current stage of the SAF mandate, there is not yet any provision to account for net negative emissions. It is still under discussion whether these negative emissions should be recognized and awarded under the same SAF mandate or another additional policy should reward these BECCS-SAF scenarios [19]. Therefore, to align with this statement, for the six investigated scenarios with negative emissions, the CI_{factor} could be also calculated by assuming that the GWP is zero, as shown in Equation 9. In this sense, two sets of results are presented: 1) Recognising the negative emissions of the scenarios and using Equation 6-2, 2) Disregarding the negative emissions and using Equation 6-3 instead.

$$Number\ of\ certificates = m_{SAF} \times LHV_{SAF} \times CI_{factor} \quad \textbf{(6-1)}$$

$$CI_{factor} = \frac{CI_F - CI_{SAF}}{CI_F - CI_b} \quad \textbf{(6-2)}$$

$$CI_{factor} = \frac{CI_F - If\ (CI_{SAF} \geq 0, CI_{SAF}, 0)}{CI_F - CI_b} \quad \textbf{(6-3)}$$

Only the results representing the extreme and middle scenarios are displayed in the main document, while the reader is referred to APPENDIX C-7, for those of the other scenarios. Instead of estimating one specific value, the figures below intend to show the variability of the price of the certificates under various electricity costs and carbon footprints of the electricity, given that both parameters dominate the MJSP and GWP values. The advantage of this representation is that the effect of using other electricity sources is also represented. Figure 6-18 displays the results for the scenario 0%TS. For a specific electricity cost, the cost of the SAF certificate increases when the GWP of the electricity increases, which highlights the importance of affordable and low-GHG electricity.

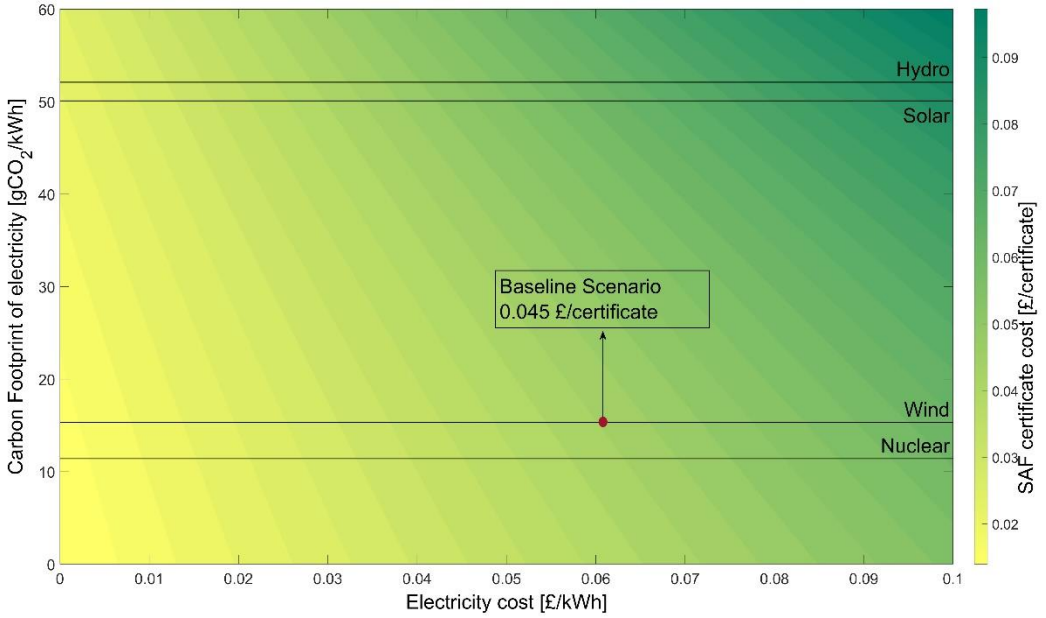

Figure 6-18: The SAF certificate cost for the MJSP to break-even with fossil jet fuel gate price (0.56£/kg) for different electricity costs and electricity carbon footprint, for the 0%TS scenario

The aforementioned explanation could be used to understand the outputs of Figure 6-19 for the scenarios 50%TS and 100%TS, which have much lower SAF certificate costs due to their negative GWP. In what concerns Figures 6-19A and 6-19B, the cost of the SAF certificate is constant for each electricity

cost, regardless of the GWP of the electricity source, since a CI_{factor} of 0 is assigned by Equation 6-3. Therefore, acknowledging the negative emissions from BECCS configurations for the production of SAF could enhance the economic performance of these processes by breaking-even the gate price of fossil jet fuel at lower certificate prices.

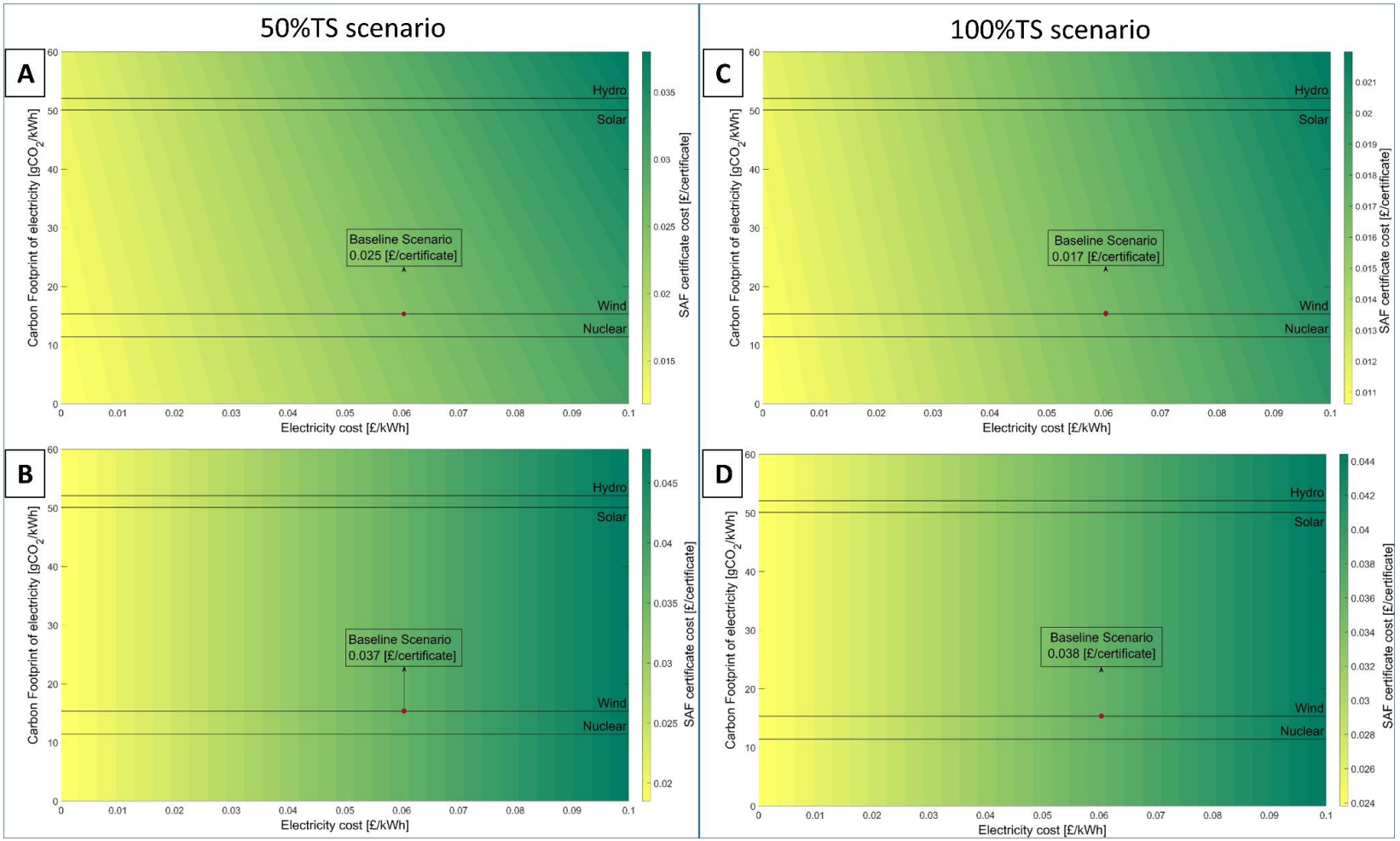

Figure 6-19: The SAF certificate cost for the MJSP to break-even with fossil jet fuel gate price (0.56£/kg) for different electricity costs and electricity carbon footprint, for the: A) 50%TS scenario, acknowledging the negative GWP; B) 50%TS scenario, without acknowledging the negative GWP; C) 100%TS scenario, acknowledging the negative GWP; and D) 100%TS scenario, without acknowledging the negative GWP.

In the second consultation of the SAF mandate, it was put under consideration whether upstream emissions of the electricity source should be taken into account for the carbon accounting of the SAF, meaning that the emissions of renewable energy at the point of delivery could be equal to zero. The only energy source for which potentially upstream emissions will be considered is nuclear energy [19]. If this were confirmed, then the number of certificates estimated for each scenario would be higher for each scenario and therefore the price of the certificates would be lower.

6.5 Conclusions

As proposed by IATA, the achievement of a net-zero aviation industry by 2050 implies several activities, such as the use of SAF. Furthermore, several technical, economic, and environmental challenges need to be overcome in order to achieve the large implementation of the SAF. As the capacity of production for countries with limited biomass availability could be one remarkable challenge, it has been demonstrated that the SAF production capacity of a BtL configuration can be increased by hybridization with the PtL technology. Findings from previous research stated that SAF production pathways could achieve emission reductions; however, achieving net-zero emissions would be only possible by deploying CDR technologies. The proposed PBtL configuration can achieve negative emissions and hence it can be classified as a CDR option. Even for the scenarios with low amounts of CO_2 that goes for storage, a negative GWP was estimated. The following points summarize the findings of this research:

1. The PBtL-CCS processes for SAF production achieved high carbon conversion efficiencies ranging from 55% to 99%, spanning from the 100%TS scenario to the 0%TS scenario. These efficiencies are greater than the one obtained for an analogous SAF BtL pathway, while being similar to the one of a SAF PtL configuration. For the PBtL-CCS scenarios, the CCS addition negatively affects this efficiency as less SAF is produced. Overall, the estimated hydrogen conversion efficiency for all scenarios is very low (21.5% to 22.6%) due to the unavoidable H_2 conversion to water in several unit operations such as the RWGS and FT reactors.
2. The proposed PBtL and PBtL-CCS configurations have large energy requirements, especially the 0% TS scenario which has the highest hydrogen demand, and hence it attains the lowest PBtL efficiency (34.05%). Furthermore, for the PBtL-CCS scenarios, this efficiency increases when more CO_2 is sent to storage (e.g., 40.41% for the 100%TS scenario). The CO_2 compression, transport and storage section requires relatively small amount of electricity, therefore, the energy efficiency of the PBtL-CCS scenarios depends mainly on the hydrogen production stage.
3. The MJSPs range from 0.0651 to 0.0673 £/MJ and are OPEX intensive, due to high electricity consumption. In addition, it was observed that the contribution of the CO_2 compression, to the

OPEX is small. The MJSP sensitivity analysis showed that a significant reduction in the cost of production could be achieved by using cheap electricity. Furthermore, the Monte Carlo analysis revealed that the MJSP is subject to a high level of uncertainty as wide ranges of 95% confidence interval were estimated.

4. The GWP of PBtL 0%TS equals 13.93 gCO_{2eq}/MJ. In spite of being a positive value, the reduction in emissions compared to fossil jet fuel is considerable and well below the UK reduction threshold (but also European and USA) compared to fossil jet fuel. However, in order for the aviation industry to reach the goal of net-zero, the CCS scenario prove to be more suitable. These scenarios yield GWPs ranging from -8.84 to -105.33 gCO_{2eq}/MJ of SAF, spanning from the 20%TS to the 100%TS scenarios. Furthermore, it is important to highlight that all the evaluated scenarios meet even the most stringent emission reduction thresholds (such as the European Renewable Energy Directive II (RED II) [175], the Renewable Fuels Standard (RFS) [176], and the UK SAF mandate [19]), at a low uncertainty level based on the Monte Carlo simulations.
5. The water footprint is not affected by the storage of CO_2, since it mostly depends on the water footprint of the electricity source, the water requirement for the AE, and the refinery processes. Across the various scenarios, the lowest and highest water footprints were observed for the 100%TS scenario, amounting to 0.40 l/MJ, and the 0%TS scenario, with a value of 0.52 l/MJ, respectively. When compared with different electricity sources such as nuclear, solar or hydro power, the wind energy achieves the lowest water consumption. However, when compared to the fossil jet fuel, the water footprints of the analysed scenarios are approximately ten times higher.
6. The use of policies such as the SAF mandate certificate trading scheme could help on achieving more affordable SAF, especially when the negative emissions are also rewarded, demonstrating the advantage of the CCS scenarios over the normal PBtL configuration.

It has been demonstrated that the addition of the CCS supply chain to this new PBtL system has a small effect on the economics and a positive effect on the environmental footprint of the process. Further, such a CDR process that is capable of producing SAF can offset emissions and help the aviation sector to meet its net-zero targets.

7. CONCLUSIONS AND FUTURE WORK

In an effort to reduce its environmental impact, the aviation industry has set a net-zero target to be achieved by 2050. Some major strategies that need to be undertaken to achieve this goal have been identified. It is expected that SAF could be responsible for a significant portion of the emissions reduction efforts in the aviation industry. While SAFs offer lower GWP when compared to fossil fuels, they alone cannot achieve emissions neutrality. Therefore, the aviation industry has integrated CDR technologies into their action plans to achieve the net-zero emissions target by 2050. In addition to the industry's individual efforts, governments must develop their own aviation emissions reduction strategies, supported by robust policies, to facilitate the deployment of SAF, particularly given their current economic challenges.

In this context, this thesis evaluated some process configurations for the production of SAF based on the FT technology that was selected due to its high TRL and adaptability to various feedstocks. The evaluation adopted a holistic approach by including technical, economic, and environmental assessments. This comprehensive examination allowed the identification of trade-offs among the estimated performance indicators and emphasised the importance of supportive policies to improve the economic viability of SAF production routes. In this sense, this chapter outlines the key findings of this research by providing specific insights into each of the main research chapters and presenting an overall perspective on the entire research. Furthermore, the chapter highlights some limitations of the study and identifies knowledge gaps that need further exploration to enhance the understanding of SAF production for a more sustainable aviation industry.

7.1 Importance and contribution of the research

The importance and main contributions of this thesis can be summarised as follows:

1. The study in Chapter 4 provides valuable information for the field of SAF production with negative emissions. The detailed mass and energy balances are useful insights into the effect of adding the CCS to the well-studied BtL process for SAF production, which is also reflected in the economic and environmental performances. This is a pioneering study since it assessed the production of SAF from a BtL-CCS process with a combined TEA and LCA approach. Additionally, it provides insights on the effects of policies that reward SAF production and negative emissions, all within the UK context, but similar policies can be applied elsewhere.
2. The study conducted in Chapter 5 represents an important contribution to the field of SAF production through the PtL pathway. In this study, a detailed model of an integrated DAC, AE, and refinery plant based on the RGWS and FT processes was created in Aspen Plus. This

comprehensive modelling approach allowed the identification of mass and energy integration opportunities among the various sections of the process, something that has not been addressed in the scarce research available for PtL-SAF. In this sense, this study is a first attempt of a comprehensive and combined TEA and LCA assessment of SAF production from the PtL pathway. Another significant contribution is that it is the first study to evaluate how the UK SAF mandate could impact the feasibility of SAF produced from the PtL pathway.

3. The assessments in Chapter 6 represent an important contribution to the research on SAF production within a combined PBtL and BECCS system. The study is the first comprehensive and combined TEA and LCA evaluation of the PBtL and PBtL-CCS scenarios for SAF production. Furthermore, this is the first study proposing a novel process configuration, PBtL-CCS, which can potentially achieve negative emissions. Like the previously mentioned study, another notable contribution of this research is its exploration of the UK SAF mandate and how it aligns with supporting SAF production with negative emissions.

7.2 Scenario-specific and general conclusions

This thesis has investigated several SAF production pathways based on the FT process, which include BtL, BtL-CCS, PtL, PBtL, and PBtL-CCS. The results of these assessments emphasize the critical role of SAF in achieving the aviation emission reduction target, as well as the supportive role of CCS toward the achievement of a net-zero emissions aviation industry.

The conclusions of the study for BtL and BtL-CCS for SAF production can be summarized as follows:

1. The addition of CCS to the BtL process had minimal impact in the technical performance indicators. For instance, the carbon conversion efficiency was the same, while the energy efficiency of the BtL-CCS was slightly lower due to the additional electricity requirement of the CCS section.
2. The integration of the CCS resulted in higher CAPEX and OPEX, which increased the MJSP (£3.27/kg for BtL-CCS vs. £3.03/kg for BtL). None of the scenarios is feasible when compared to the gate price of fossil jet fuel. Nevertheless, as aviation should invest in CDR the proposed negative emissions refineries offer a much cheaper solution than other CDR options such as DAC.
3. Lower feedstock price and reduction in the CAPEX of both scenarios lead to substantial reductions on the MJSP. Additionally, economies of scale can achieve considerable production cost reductions.
4. The LCA estimated a GWP of the BtL-CCS scenario equal to -121.83 gCO2eq/MJ. This result highlights the potential of this SAF production pathway as a CDR strategy.
5. The GWP of the BtL scenario depends on feedstock production and transport, but for the BtL-CCS this can be offset by the CCS chain.

The conclusions for the PtL for SAF production are summarised as follows:

1. The PtL process achieved a good carbon conversion efficiency (e.g., 88%); on the other hand, hydrogen efficiency (e.g., 39%) and PtL efficiency (e.g., 26%) were low due to water synthesis and electricity losses as heat, respectively.
2. The PtL process for SAF production is power-intensive, due to the electrolyser high electricity consumption.
3. The MJSP of the PtL process was estimated at 5.16 £/kg, which is mainly OPEX-intensive. Considerable cost reductions could be achieved with CO_2 and H_2 cost reductions.
4. The GWP (21.43 g CO_{2eq}/MJ) of the SAF from PtL met several aviation emissions reduction thresholds (such as the European Renewable Energy Directive II (RED II) [175], the Renewable Fuels Standard (RFS) [176], and the UK SAF mandate [19]). This is heavily influenced by the electricity source.
5. The water footprint is mainly due to the cooling water requirements and the electricity source, which highlights the need for appropriate process design and selection of the electricity source. In addition, the estimated value was bigger than the one of fossil jet fuel.
6. The SAF produced through PtL qualifies for the economic incentives of the UK SAF mandate because of its GHG emissions reductions. However, in the present context, the economic support must be very high for this fuel to be feasible.

The conclusions for the PBtL and PBtL-CCS for SAF production are the following:

1. PBtL-CCS processes achieved high carbon conversion efficiencies (ranging from 53% to 99%), and the largest was estimated for the PBtL scenario without CCS.
2. High energy requirements were observed, especially for the 0% TS scenario (PBtL only), which had the lowest PBtL efficiency (34.05%). This efficiency improved when more CO_2 was sent to storage, given that the electrolyser was smaller and less electricity was required.
3. The estimated MJSPs were dominated by the OPEX, which heavily depends on electricity consumption. Therefore, the reduction in electricity costs has a significant impact on the MJSP.
4. The estimated GWPs ranged from 13.93 gCO_{2eq}/MJ for PBtL 0%TS to negative values (-105.33 gCO_{2eq}/MJ) for scenarios with CCS. Regardless of the scenario, the analysed process configurations meet the most stringent GHG emission reduction thresholds and show the potential of the PBtL-CCS as a CDR strategy.
5. The water footprint was dominated by the electricity source, the water requirements for AE, and the cooling water requirements of the refinery plant. The estimations lead to values varying from 0.40 l/MJ to 0.52 l/MJ for the different scenarios; these values are higher than the water footprint of fossil jet fuel.

6. The analysed scenarios qualify for the economic incentives of the UK SAF mandate. However, there is a need for clarification if negative emissions are to be rewarded under this scheme.

Based on these scenario-specific outputs, some comprehensive conclusions for this research can be listed:

1. The study is a theoretical one and provides designs that can improve operations. Nevertheless, as in any modelling study, uncertainties exist and these can be decreased when more operational data will be available from demonstration plants.
2. When comparing the various process configurations investigated in this study, it is evident that they exhibit different technical performance indicators. A comparison of the BtL scenarios to the PBtL ones, highlights that the former (BtL and BtL-CCS) result in the lowest SAF production. However, the BtL process stands out for its lower energy requirements, followed by PBtL, and PtL, with the latter being the more energy-intensive. While PtL offers scalability, it could certainly benefit from technical improvements to enhance its energy efficiency. On the other hand, the scalability of BtL and PBtL processes is restricted by the limited availability of biomass in the UK.
3. The FT pathway for the production of SAF under either, the BtL, PtL, or PBtL configurations is not economic feasible against fossil jet fuel. For each scenario several opportunities of economic performance improvement were identified. In common, all these processes for SAF production could become feasible with economic incentives such as the UK SAF mandate.
4. Conduction of sensitivity and uncertainty analysis is crucial to tackle cost uncertainties associated with the low maturity of some critical process stages, e.g., RWGS and FT reactors, the biomass feedstock cost and the energy prices..
5. All the analysed FT production pathways demonstrated to achieve GHG emissions reductions that in most cases are below the thresholds for aviation emission reductions, such as the RED II, or the UK SAF mandate. On the other hand, water footprints of the processes were greater than that of fossil jet fuel. This highlights the trade-offs between various environmental impacts and emphasises the importance of evaluating all environmental aspects, not just the GWP.
6. Overall, the SAF production scenarios without BECCS demonstrated the need for CDR technologies to achieve the net-zero target of the aviation industry. BECCS scenarios demonstrated suitability for the production of negative emissions scenarios, which highlights its suitability as a CDR strategy. The economic impacts of adding CCS were considered negligible, but they resulted in lower fuel productivity in the case of PBtL-CCS configurations. In any case, the proposed CDR refineries appear to be a much more cost-effective solution than other CDR such as DAC.

7.3 Limitations of the study and future work

Based on the findings of this study and the challenges encountered during its elaboration, various recommendations emerge to enhance the work presented in this thesis and address more research gaps within the field of SAF. These recommendations highlight the need for the continued research towards a more comprehensive understanding of SAFs, their production pathways, and their broader technical, economic, and environmental implications.

Various feedstock sources:

- A comprehensive evaluation of non-crop biomass feedstock options available in the UK for SAF production is needed. Initially, it is important to estimate potential availability and assess competing interest for their use in SAF production.
- It is essential to assess the suitability of different syngas cleaning technologies since these new types of feedstocks, e.g., MSW, may contain higher levels of contaminants compared to forest residues. This is particularly relevant because the quality of the raw material directly impacts the composition of the syngas produced, and therefore a more exhaustive cleaning process may be needed.

Different process configurations:

- In scenarios including biomass gasification, it is recommended to explore other types of gasifiers. Technological improvements are continually emerging, which leads to enhanced gasification technologies with better efficiencies, syngas with fewer pollutants, and higher hydrogen yields.
- Different CO_2 sources and electrolyser technologies can be investigated for the PtL-SAF production pathway. This is particularly relevant for the energy requirements, since research is mainly dedicated to more efficient technologies, which can enhance the efficiency of the whole PtL system.
- It is recommended to perform a technical and critical review of studies assessing various process configurations of the BtL, PtL, and PBtL for SAF production. A harmonization of the economic and environmental outputs from these studies could give a better understanding of the benefits and drawbacks of different process configurations that are increasingly diverse.
- The inclusion of a battery bank for the storage of intermittent electricity supply should be analysed for the PtL and PBtL scenarios, and the impact that this would have on the TEA and environmental performance should also be estimated.

Other SAF production routes:

- As the ASTM D7566 standard continues to approve SAF production pathways, there is an increasing requirement for integrated techno-economic and life cycle assessment studies. These research would provide a more complete understanding of the numerous benefits and drawbacks connected with various SAF production processes.
- Other promising processes that have not yet been certified by the aforementioned standard, such as the Power-to-methanol-to-SAF pathway, should also be explored. Furthermore, advances in catalyst research, particularly in the PtL pathway, where single catalytic conversions are being studied as opposed to typical two-step processes, should also be assessed.

Experimental or demonstration plants data:

- More experimental campaigns could provide real data for the validation of the models in this and other research. Particularly, more certitude is needed for the catalytic processes, whose performances are generally measured with an ideal and "clean" feedstock. The performance under real conditions could enhance the process design, which will reflect on the technical, economic, and environmental performance of the whole process configuration.

Techno-economic and life cycle assessments:

- More TEAs are needed as the price of equipment available for low TRL technologies is still uncertain. As there is more technological progress, there is more clarity regarding the prices of this equipment, therefore this data could improve economic estimates.
- It is important to have supply chain and mapping studies of SAF considering more robust models for the UK performance on SAF production, for a realistic metric of production potential.
- Life cycle assessments could be improved by introducing more accurate life cycle inventories for the different foreground and background stages. While GWP can be easily estimated from the available databases, her environmental impacts are reliant on additional data, such as materials used in the construction of these technologies, which is not display by the technology owners. This could be hiding some environmental impacts that might surpass those associated with fossil jet fuel.
- More experimental studies that predict the accurate emissions performance of specific SAF in aircraft engines are crucial. In this thesis, the performance of the combustion of fossil jet fuel was used; however, considering the different properties of this new SAF, this could result in slightly different emissions and therefore different GWP estimations.

- In terms of other contributors to GWP, the associated problems with the large amounts of heat being ejected into the atmosphere as a component of the exhaust efflux are not accounted for in the LCA methodology framework. More research is needed on its contribution to GWP and how it could be taken into account in the assessment of LCA.

Tools for combined techno-economic and life cycle assessment evaluations:

- The approach of combined TEA-LCA evaluation requires the sharing of data between distinct softwares. Developing an interface that could make this process less cumbersome could be of help by reducing the time for the calculations and improving the accuracy of the transfer of data. Furthermore, such a tool could help in developing multi-objective optimisation studies for the whole system while considering technical, economic, and environmental performance indicators in a more straightforward way.

Supporting policies:

- As proposed above, other technologies, process configurations, feedstock inputs, and SAF production pathways should be assessed, in the context of the UK, and other geographic locations, especially in countries with the largest GHG emissions due to international aviation. In this context, the formulation of support policies that help in the implementation of SAF fuels is considered crucial.
- Other policies that reward the negative emissions of SAF-BECCS production pathways are needed. Within the UK framework, the SAF mandate rewards the production of SAF; however, there is still a need for more clarity in whether or not it will include the counting of negative emissions.

The effects of excluding cradle-to-grave emissions from renewable electricity should be thoroughly discussed within the UK SAF mandate. This is especially crucial given that renewable energies still contribute to greenhouse gas emissions in the current context.

REFERENCES

[1] Air Transport Action Group, “Powering global economic growth, employment, trade links, tourism and support for sustainable development through air transport,” Geneva, 2018.

[2] ICAO, “2019 Environmental Report, aviation and climate change,” 2019.

[3] European Environmental Agency, EASA, and EUROCONTROL, “European Aviation Environmental Report 2019,” 2019. doi: 10.20289/eüzfd.59424.

[4] ICAO, “Environmental Report 2016, aviation and climate change,” 2016. doi: 10.1016/j.jval.2012.11.010.

[5] IPCC, “Global warming of 1.5°C: An IPCC Special Report on the impacts of global warming of 1.5°C above pre-industrial levels and related global greenhouse gas emission pathways, in the context of strengthening the global response to the threat of climate change,” 2018. doi: 10.1002/9780470996621.ch50.

[6] B. Graver, K. Zhang, and D. Rutherford, “CO2 emissions from commercial aviation, 2018,” 2019. [Online]. Available: www.theicct.org

[7] Mission Possible, “Making Net-Zero Aviation Possible,” 2022. Accessed: May 19, 2023. [Online]. Available: https://missionpossiblepartnership.org/wp-content/uploads/2023/01/Making-Net-Zero-Aviation-possible.pdf

[8] Department for Business Energy & Industrial Strategy, “2017 UK Greenhouse Gas Emissions, Final Figures,” 2019.

[9] IRENA, “Biofuels for Aviation: Technology brief,” 2017. doi: 10.1016/b978-0-12-809806-6.00012-2.

[10] IATA, “Our Commitment to Fly Net Zero by 2050,” Jul. 19, 2023. https://www.iata.org/en/programs/environment/flynetzero/ (accessed Jul. 19, 2023).

[11] Aviation Environment Federation, “IATA announces net zero emissions by 2050 target for global air transport industry,” Jul. 19, 2023.

[12] IATA, “Fact sheet CORSIA-June 2023,” 2023.

[13] European Union Aviation Safety Agency, “European aviation environmental report 2022.”

[14] GOV.UK, “UK becomes first major economy to pass net zero emissions law,” 2019. https://www.gov.uk/government/news/uk-becomes-first-major-economy-to-pass-net-zero-emissions-law (accessed Jun. 03, 2020).

[15] Secretary of State for Transport, “Aviation Policy Framework,” 2013.

[16] Sustainable Aviation, “Decarbonisation road-map : A path to net zero,” 2020.

[17] Department for Transport, “Sustainable aviation fuels mandate: Summary of consultation responses and government response,” no. July 2022, 2022, [Online]. Available: www.gov.uk/government/organisations/

[18] E. and I. S. Department for Business, “Net Zero Strategy: Build Back Greener,” 2021.

[19] Department for Transport, “Pathway to net zero aviation: Developing the UK sustainable aviation fuel mandate A second consultation on reducing the greenhouse gas emissions of aviation fuel in the UK,” 2023. [Online]. Available: www.nationalarchives.gov.uk/doc/opengovernment-licence/version/3/

[20] Department For Transport, “Sustainable aviation fuels mandate: A consultation on reducing the greenhouse gas emissions of A consultation on reducing the greenhouse gas emissions of aviation fuels in the UK greenhouse gas emissions of aviation fuels in the UK,” no. July, 2021, [Online]. Available: https://assets.publishing.service.gov.uk/government/uploads/system/uploads/attachment_data/file/1005382/sustainable-aviation-fuels-mandate-consultation-on-reducing-the-greenhouse-gas-emissions-of-aviation-fuels-in-the-uk.pdf

[21] Air Transport Action Group, “Beginner’s Guide to Sustainable Aviation Fuel,” 2017.

[22] Air Transport Action Group, “Powering the future of flight. The six easy steps to growing a viable aviation biofuels industry,” 2012.

[23] International Air Transport Association, “Annual Review 2018,” 2018.

[24] U.S. Department of Energy, “Alternative Aviation Fuels: Overview of Challenges, Opportunities, and Next Steps,” 2017.

[25] Fraunhofer Institute for Solar Energy Systems ISE, “Power-to-Liquids,” *Fraunhofer ISE*, 2022. https://www.ise.fraunhofer.de/en/business-areas/hydrogen-technologies-and-electrical-energy-storage/thermochemical-processes/power-to-liquids.html (accessed Jan. 10, 2022).

[26] Ricardo, “Targeted Aviation Advanced Biofuels Demonstration Competition-Feasibility Study Final report,” 2020.

[27] Sustainable Aviation, “Sustainable Aviation Fuels Road-Map,” 2020.

[28] American Standard for Testing and Materials, “Standard Specification for Aviation Turbine Fuel Containing Synthesized Hydrocarbons,” 2022. doi: 10.1520/D7566-22A.

[29] C. J. Chuck, *Biofuels for Aviation: Feedstocks, Technology and Implementation*. 2016. doi: 10.1017/CBO9781107415324.004.

[30] P. Basu, *Biomass Gasification, Pyrolysis and Torrefaction: Practical Design and Theory*. 2013. doi: 10.1016/C2011-0-07564-6.

[31] E. G. Pereira, J. N. Da Silva, J. L. De Oliveira, and C. S. MacHado, “Sustainable energy: A review of gasification technologies,” *Renewable and Sustainable Energy Reviews*, vol. 16, no. 7, pp. 4753–4762, 2012, doi: 10.1016/j.rser.2012.04.023.

[32] M. Puig-Arnavat, J. C. Bruno, and A. Coronas, “Review and analysis of biomass gasification models,” *Renewable and Sustainable Energy Reviews*, vol. 14, no. 9, pp. 2841–2851, 2010, doi: 10.1016/j.rser.2010.07.030.

[33] C. Gutiérrez-Antonio, F. I. Gómez-Castro, J. A. de Lira-Flores, and S. Hernández, “A review on the production processes of renewable jet fuel,” *Renewable and Sustainable Energy Reviews*, vol. 79, no. May, pp. 709–729, 2017, doi: 10.1016/j.rser.2017.05.108.

[34] R. G. dos Santos and A. C. Alencar, “Biomass-derived syngas production via gasification process and its catalytic conversion into fuels by Fischer Tropsch synthesis: A review,” *Int J Hydrogen Energy*, vol. 45, pp. 1–19, 2019, doi: 10.1016/j.ijhydene.2019.07.133.

[35] G. W. Diederichs, M. Ali Mandegari, S. Farzad, and J. F. Görgens, “Techno-economic comparison of biojet fuel production from lignocellulose, vegetable oil and sugar cane juice,” *Bioresour Technol*, vol. 216, pp. 331–339, 2016, doi: 10.1016/j.biortech.2016.05.090.

[36] G. Liu, B. Yan, and G. Chen, “Technical review on jet fuel production,” *Renewable and Sustainable Energy Reviews*, vol. 25, pp. 59–70, 2013, doi: 10.1016/j.rser.2013.03.025.

[37] German Environment Agency, “Integration of Power to Gas/Power to Liquids into the ongoing,” no. june, p. 18, 2016.

[38] P. Schmidt and W. Weindorf, “Power-to-Liquids: Potentials and Perspectives for the Future Supply of Renewable Aviation Fuel,” *Dessau-Roßlau*, no. september, pp. 1–36, 2016, [Online]. Available: https://www.umweltbundesamt.de/en/publikationen/power-to-liquids-potential-perspectives-for-the

[39] R. U. Dietrich, F. G. Albrecht, S. Maier, D. H. König, S. Estelmann, S. Adelung, Z. Bealu, and A. Seitz, “Cost calculations for three different approaches of biofuel production using biomass, electricity and CO2,” *Biomass Bioenergy*, vol. 111, pp. 165–173, Apr. 2018, doi: 10.1016/j.biombioe.2017.07.006.

[40] R. Mahmud, S. M. Moni, K. High, and M. Carbajales-Dale, “Integration of techno-economic analysis and life cycle assessment for sustainable process design – A review,” *J Clean Prod*, vol. 317, Oct. 2021, doi: 10.1016/j.jclepro.2021.128247.

[41] S. Farzad, M. A. Mandegari, and J. F. Görgens, “A critical review on biomass gasification, co-gasification, and their environmental assessments,” *Biofuel Research Journal*, vol. 3, no. 4, pp. 483–495, 2016, doi: 10.18331/BRJ2016.3.4.3.

[42] R. C. Brown and T. R. Brown, *Biorenewable Resources: Engineering New Products from Agriculture: Second Edition*. 2014. doi: 10.1002/9781118524985.

[43] P. Suresh, R. Malina, M. D. Staples, S. Lizin, H. Olcay, D. Blazy, M. N. Pearlson, and S. R. H. Barrett, “Life Cycle Greenhouse Gas Emissions and Costs of Production of Diesel and Jet Fuel from Municipal Solid Waste,” *Environ Sci Technol*, vol. 52, no. 21, pp. 12055–12065, 2018, doi: 10.1021/acs.est.7b04277.

[44] H. Knoef, “Handbook of Biomass Gasification,” *BTG Group*, 2005.

[45] E. R. Widjaya, G. Chen, L. Bowtell, and C. Hills, “Gasification of non-woody biomass: A literature review,” *Renewable and Sustainable Energy Reviews*, vol. 89, no. September 2016, pp. 184–193, 2018, doi: 10.1016/j.rser.2018.03.023.

[46] A. Anukam, S. Mamphweli, P. Reddy, E. Meyer, and O. Okoh, “Pre-processing of sugarcane bagasse for gasification in a downdraft biomass gasifier system: A comprehensive review,” *Renewable and Sustainable Energy Reviews*, vol. 66, pp. 775–801, 2016, doi: 10.1016/j.rser.2016.08.046.

[47] S. K. Sansaniwal, K. Pal, M. A. Rosen, and S. K. Tyagi, “Recent advances in the development of biomass gasification technology: A comprehensive review,” *Renewable and Sustainable Energy Reviews*, vol. 72, no. January, pp. 363–384, 2017, doi: 10.1016/j.rser.2017.01.038.

[48] A. Molino, V. Larocca, S. Chianese, and D. Musmarra, “Biofuels production by biomass gasification: A review,” *Energies (Basel)*, vol. 11, no. 4, pp. 1–31, 2018, doi: 10.3390/en11040811.

[49] A. Molino, S. Chianese, and D. Musmarra, “Biomass gasification technology: The state of the art overview,” *Journal of Energy Chemistry*, vol. 25, no. 1, pp. 10–25, 2016, doi: 10.1016/j.jechem.2015.11.005.

[50] D. Baruah and D. C. Baruah, “Modeling of biomass gasification: A review,” *Renewable and Sustainable Energy Reviews*, vol. 39, pp. 806–815, 2014, doi: 10.1016/j.rser.2014.07.129.

[51] M. Siedlecki, W. de Jong, and A. H. M. Verkooijen, “Fluidized bed gasification as a mature and reliable technology for the production of bio-syngas and applied in the production of liquid

transportation fuels-a review," *Energies (Basel)*, vol. 4, no. 3, pp. 389–434, 2011, doi: 10.3390/en4030389.

[52] M. Materazzi and A. Holt, "Experimental analysis and preliminary assessment of an integrated thermochemical process for production of low-molecular weight biofuels from municipal solid waste (MSW)," *Renew Energy*, vol. 143, pp. 663–678, 2019, doi: 10.1016/j.renene.2019.05.027.

[53] P. Arora, A. F. A. Hoadley, S. M. Mahajani, and A. Ganesh, "Compartment model for a dual fluidized bed biomass gasifier," *Chemical Engineering Research and Design*, vol. 117, pp. 274–286, 2017, doi: 10.1016/j.cherd.2016.10.025.

[54] S. S. Ail and S. Dasappa, "Biomass to liquid transportation fuel via Fischer Tropsch synthesis - Technology review and current scenario," *Renewable and Sustainable Energy Reviews*, vol. 58, pp. 267–286, 2016, doi: 10.1016/j.rser.2015.12.143.

[55] P. M. Maitlis and A. de Klerk, *Greener Fischer-Tropsch Processes for Fuels and Feedstocks*. 2013. doi: 10.1002/9783527656837.

[56] M. N. Hassankiadeh, A. Khajehfard, and M. Golmohammadi, "Kinetic and Product Distribution Modeling of Fischer-Tropsch Synthesis in a Fluidized Bed Reactor," *International Journal of Chemical Engineering and Applications*, vol. 3, no. 6, pp. 400–403, 2012, doi: 10.7763/ijcea.2012.v3.227.

[57] A.M. Subiranas, "Combining Fischer-Tropsch Synthesis (FTS) and Hydrocarbon Reactions in one Reactor. Dissertation, Universität Karlsruhe (TH)," 2009.

[58] S. Michailos and A. Bridgwater, "A comparative techno-economic assessment of three bio-oil upgrading routes for aviation biofuel production," *Int J Energy Res*, vol. 43, no. 13, pp. 7206–7228, 2019, doi: 10.1002/er.4745.

[59] D. H. König, F. G. Albrecht, and R. U. Dietrich, "Power and biomass-to-liquid (PBTL): A promising approach to produce biofuels using electricity," *European Biomass Conference and Exhibition Proceedings*, vol. 2016, no. 24thEUBCE, pp. 1074–1078, 2016.

[60] U. Neuling and M. Kaltschmitt, "Techno-economic and environmental analysis of aviation biofuels," *Fuel Processing Technology*, vol. 171, no. September 2017, pp. 54–69, 2018, doi: 10.1016/j.fuproc.2017.09.022.

[61] H. Mahmoudi, M. Mahmoudi, O. Doustdar, H. Jahangiri, A. Tsolakis, S. Gu, and M. LechWyszynski, "A review of Fischer Tropsch synthesis process, mechanism, surface chemistry and catalyst formulation," *Biofuels Engineering*, vol. 2, no. 1, pp. 11–31, Dec. 2017, doi: 10.1515/bfuel-2017-0002.

[62] U. Pandey, A. Runningen, L. Gavrilović, E. A. Jørgensen, K. R. Putta, K. R. Rout, E. Rytter, E. A. Blekkan, and M. Hillestad, "Modeling Fischer–Tropsch kinetics and product distribution over a cobalt catalyst," *AIChE Journal*, vol. 67, no. 7, pp. 1–15, 2021, doi: 10.1002/aic.17234.

[63] M. Ostadi, E. Rytter, and M. Hillestad, "Evaluation of kinetic models for Fischer–Tropsch cobalt catalysts in a plug flow reactor," *Chemical Engineering Research and Design*, vol. 114, no. 3, pp. 236–246, 2016, doi: 10.1016/j.cherd.2016.08.026.

[64] M. Marchese, N. Heikkinen, E. Giglio, A. Lanzini, J. Lehtonen, and M. Reinikainen, "Kinetic study based on the carbide mechanism of a co-pt/γ-al2 o3 fischer–tropsch catalyst tested in a laboratory-scale tubular reactor," *Catalysts*, vol. 9, no. 9, pp. 1–25, 2019, doi: 10.3390/catal9090717.

[65] H. Wei, W. Liu, X. Chen, Q. Yang, J. Li, and H. Chen, “Renewable bio-jet fuel production for aviation: A review,” *Fuel*, vol. 254, no. June, 2019, doi: 10.1016/j.fuel.2019.06.007.

[66] I. Kurucz, Adorjan;Bencik, *Syngas : Production Methods, Post Treatment and Economics*. New York: Nova Science Publishers, Incorporated, 2009.

[67] W.-C. Wang, L. Tao, J. Markham, Y. Zhang, E. Tan, L. Batan, M. Biddy, W.-C. Wang, L. Tao, Y. Zhang, E. Tan, E. Warner, and M. Biddy, “Review of Biojet Fuel Conversion Technologies,” no. July, p. 98, 2016.

[68] R. Davis, L. Tao, E. C. D. Tan, M. J. Biddy, G. T. Beckham, C. Scarlata, J. Jacobson, K. Cafferty, J. Ross, J. Lukas, D. Knorr, and P. Schoen, “Process Design and Economics for the Conversion of Lignocellulosic Biomass to Hydrocarbons: Dilute-Acid and Enzymatic Deconstruction of Biomass to Sugars and Biological Conversion of Sugars to Hydrocarbons,” *National Renewable Energy Laboratory-NREL*, no. October 2013, p. 147, 2013, doi: 10.2172/1107470.

[69] M. J. A. Tijmensen, A. P. C. Faaij, C. N. Hamelinck, and M. R. M. Van Hardeveld, “Exploration of the possibilities for production of Fischer Tropsch liquids and power via biomass gasification,” *Biomass Bioenergy*, vol. 23, no. 2, pp. 129–152, 2002, doi: 10.1016/S0961-9534(02)00037-5.

[70] R. M. Swanson, A. Platon, J. A. Satrio, and R. C. Brown, “Techno-economic analysis of biomass-to-liquids production based on gasification scenarios,” *ACS National Meeting Book of Abstracts*, no. November, 2009.

[71] R. P. Anex, A. Aden, F. K. Kazi, J. Fortman, R. M. Swanson, M. M. Wright, J. A. Satrio, R. C. Brown, D. E. Daugaard, A. Platon, G. Kothandaraman, D. D. Hsu, and A. Dutta, “Techno-economic comparison of biomass-to-transportation fuels via pyrolysis, gasification, and biochemical pathways,” *Fuel*, vol. 89, no. 1, pp. S29–S35, 2010, doi: 10.1016/j.fuel.2010.07.015.

[72] K. Atsonios, M. A. Kougioumtzis, K. D. Panopoulos, and E. Kakaras, “Alternative thermochemical routes for aviation biofuels via alcohols synthesis: Process modeling, techno-economic assessment and comparison,” *Appl Energy*, vol. 138, pp. 346–366, 2015, doi: 10.1016/j.apenergy.2014.10.056.

[73] IEA, “Implementation of bio-CCS in biofuels production,” 2018. [Online]. Available: https://www.ieabioenergy.com

[74] J. I. Hileman, D. S. Ortiz, J. T. Bartis, H. M. Wong, E. Donohoo, Pearl, M. A. Weiss, and I. A. Waitz, “Near-Term Feasibility of Alternative Jet Fuels -Technical Report,” *RAND Corporation and MIT*, pp. 1–152, 2009.

[75] J. Marano and J. Ciferno, “Life-cycle greenhouse-gas emissions inventory for Fischer-Tropsch fuels,” *Report Prepared for the US Department of …*, no. June, p. 186, 2001.

[76] G. S. Forman, T. E. Hahn, and S. D. Jensen, “Greenhouse gas emission evaluation of the GTL pathway,” *Environ Sci Technol*, vol. 45, no. 20, pp. 9084–9092, 2011, doi: 10.1021/es202101b.

[77] D. T. Allen, C. F. Murphy, K. S. Rosselot, and R. Denton, “Alternative Energy Fuels Analysis Support to AFRL/RZPF,” Austin, Texas, 2011.

[78] J. D. Kinder and T. Rahmes, “Evaluation of Bio-derived Sythetic Paraffinic Kerosene (Bio-SPK),” 2009. doi: 10.1016/j.apsusc.2010.04.018.

[79] S. Unnasch, B. Riffel, V. N. T. S. Center, L. L. C. Life Cycle Associates, and F. A. Administration, “Review of Jet Fuel Life Cycle Assessment Methods and Sustainability Metrics,” vol. 298, no. 0704, p. 123p, 2015.

[80] S. De Jong, K. Antonissen, R. Hoefnagels, L. Lonza, M. Wang, A. Faaij, and M. Junginger, “Life-cycle analysis of greenhouse gas emissions from renewable jet fuel production,” *Biotechnol Biofuels*, vol. 10, no. 1, pp. 1–18, 2017, doi: 10.1186/s13068-017-0739-7.

[81] Argonne National Laboratory, “Life Cycle Analysis of Alternative Aviation Fuels in GREET,” Chicago, 2012.

[82] D. B. Agusdinata, F. Zhao, K. Ileleji, and D. Delaurentis, “Life cycle assessment of potential biojet fuel production in the United States,” *Environ Sci Technol*, vol. 45, no. 21, pp. 9133–9143, 2011, doi: 10.1021/es202148g.

[83] B. W. Kolosz, Y. Luo, B. Xu, M. M. Maroto-Valer, and J. M. Andresen, “Life cycle environmental analysis of ‘drop in’ alternative aviation fuels: A review,” *Sustain Energy Fuels*, vol. 4, no. 7, pp. 3229–3263, 2020, doi: 10.1039/c9se00788a.

[84] D. T. Allen, C. Allport, K. Atkins, J. S. Cooper, R. M. Dilmore, L. C. Draucker, K. E. Eickmann, J. C. Gillen, and W. Gillette, “Framework and Guidance for Estimating Greenhouse Gas Footprints of Aviation Fuels,” 2009.

[85] S. Fuss and F. Johnsson, “The BECCS Implementation Gap – A Swedish Case Study,” vol. 8, no. February, pp. 1–18, 2021, doi: 10.3389/fenrg.2020.553400.

[86] M. Fajardy, A. Köberle, N. M. A. C. Dowell, and A. Fantuzzi, “Briefing paper No 28 BECCS deployment : a reality check,” no. 28, 2019.

[87] M. Fajardy and N. Mac Dowell, “Can BECCS deliver sustainable and resource efficient negative emissions?,” *Energy Environ Sci*, vol. 10, no. 6, pp. 1389–1426, 2017, doi: 10.1039/c7ee00465f.

[88] M. Bui, M. Fajardy, and N. Mac Dowell, “Bio-Energy with CCS (BECCS) performance evaluation: Efficiency enhancement and emissions reduction,” *Appl Energy*, vol. 195, pp. 289–302, 2017, doi: 10.1016/j.apenergy.2017.03.063.

[89] N. Mac Dowell and M. Fajardy, “Inefficient power generation as an optimal route to negative emissions via BECCS?,” *Environmental Research Letters*, vol. 12, no. 4, 2017, doi: 10.1088/1748-9326/aa67a5.

[90] M. Bui, M. Fajardy, and N. Mac Dowell, “Bio-energy with carbon capture and storage (BECCS): Opportunities for performance improvement,” *Fuel*, vol. 213, no. October 2017, pp. 164–175, 2018, doi: 10.1016/j.fuel.2017.10.100.

[91] N. Mac Dowell and M. Fajardy, “On the potential for BECCS efficiency improvement through heat recovery from both post-combustion and oxy-combustion facilities,” *Faraday Discuss*, vol. 192, pp. 241–250, 2016, doi: 10.1039/c6fd00051g.

[92] D. Zhang, M. Bui, M. Fajardy, P. Patrizio, F. Kraxner, and N. Mac Dowell, “Unlocking the potential of BECCS with indigenous sources of biomass at a national scale,” *Sustain Energy Fuels*, vol. 4, no. 1, pp. 226–253, 2019, doi: 10.1039/c9se00609e.

[93] M. Bui, D. Zhang, M. Fajardy, and N. Mac Dowell, “Delivering carbon negative electricity, heat and hydrogen with BECCS – Comparing the options,” *Int J Hydrogen Energy*, vol. 46, no. 29, pp. 15298–15321, 2021, doi: 10.1016/j.ijhydene.2021.02.042.

[94] I. S. Tagomori, P. R. R. Rochedo, and A. Szklo, “Techno-economic and georeferenced analysis of forestry residues-based Fischer-Tropsch diesel with carbon capture in Brazil,” *Biomass Bioenergy*, vol. 123, no. March, pp. 134–148, 2019, doi: 10.1016/j.biombioe.2019.02.018.

[95] A. Rafiee, K. Rajab Khalilpour, D. Milani, and M. Panahi, “Trends in CO2 conversion and utilization: A review from process systems perspective,” *J Environ Chem Eng*, vol. 6, no. 5, pp. 5771–5794, 2018, doi: 10.1016/j.jece.2018.08.065.

[96] P. Schmidt, V. Batteiger, A. Roth, W. Weindorf, and T. Raksha, “Power-to-Liquids as Renewable Fuel Option for Aviation: A Review,” *Chem Ing Tech*, vol. 90, no. 1, pp. 127–140, 2018, doi: 10.1002/cite.201700129.

[97] B. R. de Vasconcelos and J. M. Lavoie, “Recent advances in power-to-X technology for the production of fuels and chemicals,” *Front Chem*, vol. 7, no. JUN, pp. 1–24, 2019, doi: 10.3389/fchem.2019.00392.

[98] ASTM, “Standard Specification for Aviation Turbine Fuel Containing Synthesized Hydrocarbons,” 2019 doi: 10.1520/D1655-10.2.

[99] I. Dincer and C. Acar, “Review and evaluation of hydrogen production methods for better sustainability,” *Int J Hydrogen Energy*, vol. 40, no. 34, pp. 11094–11111, 2014, doi: 10.1016/j.ijhydene.2014.12.035.

[100] O. Schmidt, A. Gambhir, I. Staffell, A. Hawkes, J. Nelson, and S. Few, “Future cost and performance of water electrolysis: An expert elicitation study,” *Int J Hydrogen Energy*, vol. 42, no. 52, pp. 30470–30492, 2017, doi: 10.1016/j.ijhydene.2017.10.045.

[101] J. Chi and H. Yu, “Water electrolysis based on renewable energy for hydrogen production,” *Cuihua Xuebao/Chinese Journal of Catalysis*, vol. 39, no. 3, pp. 390–394, 2018, doi: 10.1016/S1872-2067(17)62949-8.

[102] L. J. F. Comidy, M. D. Staples, and S. R. H. Barrett, “Technical, economic, and environmental assessment of liquid fuel production on aircraft carriers,” *Appl Energy*, vol. 256, no. June, p. 113810, 2019, doi: 10.1016/j.apenergy.2019.113810.

[103] M. Holst, S. Aschbrenner, T. Smolinka, C. Voglstätter, and G. Grimm, “Cost Forecast for Low Temperature Electrolysis - Technology Driven Bottom-up Prognosis for PEM and Alkaline Water Electrolysis Systems,” p. 79, 2021.

[104] P. R. Schmidt, W. Zittel, W. Weindorf, and T. Raksha, “Empowering a sustainable mobility future with zero emission fuels from renewable electricity,” p. 203, 2016, [Online]. Available: www.fvv-net.de

[105] F. G. Albrecht, D. H. Konig, and R. U. Dietrich, “The potential of using power-to-liquid plants for power storage purposes,” *International Conference on the European Energy Market, EEM*, vol. 2016-July, 2016, doi: 10.1109/EEM.2016.7521203.

[106] D. H. König, M. Freiberg, R. U. Dietrich, and A. Wörner, “Techno-economic study of the storage of fluctuating renewable energy in liquid hydrocarbons,” *Fuel*, vol. 159, pp. 289–297, 2015, doi: 10.1016/j.fuel.2015.06.085.

[107] A. König, K. Ulonska, A. Mitsos, and J. Viell, “Optimal Applications and Combinations of Renewable Fuel Production from Biomass and Electricity,” *Energy and Fuels*, vol. 33, no. 2, pp. 1659–1672, 2019, doi: 10.1021/acs.energyfuels.8b03790.

[108] A. Tremel, P. Wasserscheid, M. Baldauf, and T. Hammer, “Techno-economic analysis for the synthesis of liquid and gaseous fuels based on hydrogen production via electrolysis,” *Int J Hydrogen Energy*, vol. 40, no. 35, pp. 11457–11464, 2015, doi: 10.1016/j.ijhydene.2015.01.097.

[109] P. Kaiser, R. B. Unde, C. Kern, and A. Jess, “Production of liquid hydrocarbons with CO2 as carbon source based on reverse water-gas shift and fischer-tropsch synthesis,” *Chem Ing Tech*, vol. 85, no. 4, pp. 489–499, 2013, doi: 10.1002/cite.201200179.

[110] D. H. König, N. Baucks, R. U. Dietrich, and A. Wörner, “Simulation and evaluation of a process concept for the generation of synthetic fuel from CO2 and H2,” *Energy*, vol. 91, pp. 833–841, 2015, doi: 10.1016/j.energy.2015.08.099.

[111] S. Brynolf, M. Taljegard, M. Grahn, and J. Hansson, “Electrofuels for the transport sector: A review of production costs,” *Renewable and Sustainable Energy Reviews*, vol. 81, no. February 2017, pp. 1887–1905, 2018, doi: 10.1016/j.rser.2017.05.288.

[112] F. Ausfelder and K. Wagemann, “Power-to-Fuels: E-Fuels as an Important Option for a Climate-Friendly Mobility of the Future,” *Chem Ing Tech*, vol. 92, no. 1–2, pp. 21–30, 2020, doi: 10.1002/cite.201900180.

[113] J. Bekkering, K. Zwart, G. Martinus, J. Langerak, J. Tideman, T. van der Meij, K. Alberts, M. van Steenis, and J. P. Nap, “Farm-scale bio-power-to-methane: Comparative analyses of economic and environmental feasibility,” *Int J Energy Res*, vol. 44, no. 3, pp. 2264–2277, 2020, doi: 10.1002/er.5093.

[114] X. Zhang, J. Witte, T. Schildhauer, and C. Bauer, “Life cycle assessment of power-to-gas with biogas as the carbon source,” *Sustain Energy Fuels*, vol. 4, no. 3, pp. 1427–1436, 2020, doi: 10.1039/c9se00986h.

[115] C. Wulf, J. Linßen, and P. Zapp, “Review of power-to-gas projects in Europe,” *Energy Procedia*, vol. 155, pp. 367–378, 2018, doi: 10.1016/j.egypro.2018.11.041.

[116] R. Schäppi, D. Rutz, F. Dähler, A. Muroyama, P. Haueter, J. Lilliestam, A. Patt, P. Furler, and A. Steinfeld, “Drop-in fuels from sunlight and air,” *Nature*, vol. 601, no. 7891, pp. 63–68, 2022, doi: 10.1038/s41586-021-04174-y.

[117] F. Vidal, J. Koponen, V. Ruuskanen, C. Bajamundi, A. Kosonen, P. Simell, J. Ahola, C. Frilund, J. Elfving, M. Reinikainen, N. Heikkinen, J. Kauppinen, and P. Piermartini, “Power-to-X technology using renewable electricity and carbon dioxide from ambient air : SOLETAIR proof-of-concept and improved process concept,” *Journal of CO2 Utilization*, vol. 28, no. September, pp. 235–246, 2018, doi: 10.1016/j.jcou.2018.09.026.

[118] P. Kaiser and A. Jess, “Modeling of Multitubular Reactors for Iron- and Cobalt-Catalyzed Fischer-Tropsch Syntheses for Application in a Power-to-Liquid Process,” *Energy Technology*, vol. 2, no. 5, pp. 486–497, 2014, doi: 10.1002/ente.201300189.

[119] S. Adelung, S. Maier, and R. U. Dietrich, “Impact of the reverse water-gas shift operating conditions on the Power-to-Liquid process efficiency,” *Sustainable Energy Technologies and Assessments*, vol. 43, no. November 2020, p. 100897, 2021, doi: 10.1016/j.seta.2020.100897.

[120] M. Marchese, E. Giglio, M. Santarelli, and A. Lanzini, “Energy performance of Power-to-Liquid applications integrating biogas upgrading, reverse water gas shift, solid oxide electrolysis and Fischer-Tropsch technologies,” *Energy Convers Manag*, vol. 6, no. January, p. 100041, 2020, doi: 10.1016/j.ecmx.2020.100041.

[121] M. Marchese, G. Buffo, M. Santarelli, and A. Lanzini, “CO2from direct air capture as carbon feedstock for Fischer-Tropsch chemicals and fuels: Energy and economic analysis,” *Journal of CO2 Utilization*, vol. 46, p. 101487, 2021, doi: 10.1016/j.jcou.2021.101487.

[122] S. Adelung and R.-U. Dietrich, “Impact of the reverse water-gas shift operating conditions on the Power-to-Liquid fuel production cost,” *Fuel*, vol. 317, p. 123440, 2022, doi: 10.1016/j.fuel.2022.123440.

[123] C. van der Giesen, R. Kleijn, and G. J. Kramer, “Energy and climate impacts of producing synthetic hydrocarbon fuels from CO2,” *Environ Sci Technol*, vol. 48, no. 12, pp. 7111–7121, 2014, doi: 10.1021/es500191g.

[124] C. Falter, V. Batteiger, and A. Sizmann, “Climate Impact and Economic Feasibility of Solar Thermochemical Jet Fuel Production,” *Environ Sci Technol*, vol. 50, pp. 470–477, 2016, doi: 10.1021/acs.est.5b03515.

[125] K. Heidgen, H. Maas, L. E. Hombach, L. Dor, T. J. Wallington, and G. Walther, “Economic and environmental assessment of current (2015) and future (2030) use of E-fuels in light-duty vehicles in Germany,” vol. 207, pp. 153–162, 2019, doi: 10.1016/j.jclepro.2018.09.261.

[126] F. Pöhlmann and A. Jess, “Influence of Syngas Composition on the Kinetics of Fischer-Tropsch Synthesis of using Cobalt as Catalyst,” *Energy Technology*, vol. 4, no. 1, pp. 55–64, 2016, doi: 10.1002/ente.201500216.

[127] V. Batteiger, K. Ebner, A. Habersetzer, L. Moser, P. Schmidt, W. Weindorf, and T. Rakscha, “Power-to-Liquids – A scalable and sustainable fuel supply perspective for aviation,” 2022. [Online]. Available: https://www.umweltbundesamt.de/en/publications

[128] M. Fasihi and O. A. Solomon, “E-Kerosene for Commercial Aviation From Green Hydrogen and CO 2 from Direct Air Capture – Volumes , Cost ,” no. September, 2022.

[129] J. C. Koj, C. Wulf, and P. Zapp, “Environmental impacts of power-to-X systems - A review of technological and methodological choices in Life Cycle Assessments,” *Renewable and Sustainable Energy Reviews*, vol. 112, no. November 2018, pp. 865–879, 2019, doi: 10.1016/j.rser.2019.06.029.

[130] N. Von Der Assen, J. Jung, and A. Bardow, “Life-cycle assessment of carbon dioxide capture and utilization: Avoiding the pitfalls,” *Energy Environ Sci*, 2013, doi: 10.1039/c3ee41151f.

[131] N. Von Der Assen, P. Voll, M. Peters, and A. Bardow, “Life cycle assessment of CO2 capture and utilization: A tutorial review,” *Chemical Society Reviews*. 2014. doi: 10.1039/c3cs60373c.

[132] A. Zimmermann, J. Wunderlich, G. Buchner, S. Michailos, A. Marxen, and H. Naims, “Techno-Economic Assessment Guidelines for CO 2 Utilisation,” vol. 8, no. January, pp. 1–23, 2018, doi: 10.3389/fenrg.2020.00005.

[133] A. Zimmerman, J. Wunderlich, G. Buchner, L. Müller, K. Armstrong, S. Michailos, A. Marxen, H. Naims, F. Mason, G. Stokes, and E. Williams, “Techno-Economic Assessment & Life-Cycle Assessment Guidelines for CO2 Utilization,” 2018. doi: 10.3998/2027.42/145436.

[134] T. Wich, W. Lueke, G. Deerberg, and M. Oles, “Carbon2Chem®-CCU as a Step Toward a Circular Economy,” *Front Energy Res*, vol. 7, no. January, pp. 1–14, 2020, doi: 10.3389/fenrg.2019.00162.

[135] X. Zhang, C. Bauer, C. L. Mutel, and K. Volkart, “Life Cycle Assessment of Power-to-Gas: Approaches, system variations and their environmental implications,” *Appl Energy*, vol. 190, pp. 326–338, 2017, doi: 10.1016/j.apenergy.2016.12.098.

[136] M. Micheli, D. Moore, V. Bach, and M. Finkbeiner, “Life-Cycle Assessment of Power-to-Liquid Kerosene Produced from Renewable Electricity and CO2 from Direct Air Capture in Germany,” *Sustainability (Switzerland)*, vol. 14, no. 17, Sep. 2022, doi: 10.3390/su141710658.

[137] F. Habermeyer, V. Papantoni, U. Brand-Daniels, and R. U. Dietrich, “Sustainable aviation fuel from forestry residue and hydrogen - a techno-economic and environmental analysis for an immediate deployment of the PBtL process in Europe,” *Sustain Energy Fuels*, 2023, doi: 10.1039/d3se00358b.

[138] M. Hillestad, M. Ostadi, G. D. Alamo Serrano, E. Rytter, B. Austbø, J. G. Pharoah, and O. S. Burheim, "Improving carbon efficiency and profitability of the biomass to liquid process with hydrogen from renewable power," *Fuel*, vol. 234, pp. 1431–1451, Dec. 2018, doi: 10.1016/j.fuel.2018.08.004.

[139] S. Mesfun, K. Engvall, and A. Toffolo, "Electrolysis Assisted Biomass Gasification for Liquid Fuels Production," *Front Energy Res*, vol. 10, Jun. 2022, doi: 10.3389/fenrg.2022.799553.

[140] T. Schulzke, "Synergies from Direct Coupling of Biomass-to-Liquid and Power-to-Liquid Plants," *Chem Eng Technol*, vol. 40, no. 2, pp. 254–259, Feb. 2017, doi: 10.1002/ceat.201600179.

[141] M. Ostadi, B. Austbø, and M. Hillestad, "Parametric Optimization of a Power and Biomass to Liquid Process," in *Computer Aided Chemical Engineering*, Elsevier B.V., 2019, pp. 287–292. doi: 10.1016/B978-0-12-818597-1.50045-X.

[142] M. Ostadi, E. Rytter, and M. Hillestad, "Boosting carbon efficiency of the biomass to liquid process with hydrogen from power: The effect of H2/CO ratio to the Fischer-Tropsch reactors on the production and power consumption," *Biomass Bioenergy*, vol. 127, Aug. 2019, doi: 10.1016/j.biombioe.2019.105282.

[143] M. Ostadi, B. Austbø, and M. Hillestad, "Exergy analysis of a process converting power and biomass to a liquid fuel," *Chem Eng Trans*, vol. 76, pp. 205–210, 2019, doi: 10.3303/CET1976035.

[144] A. S. Nielsen, M. Ostadi, B. Austbø, M. Hillestad, G. del Alamo, and O. Burheim, "Enhancing the efficiency of power- and biomass-to-liquid fuel processes using fuel-assisted solid oxide electrolysis cells," *Fuel*, vol. 321, Aug. 2022, doi: 10.1016/j.fuel.2022.123987.

[145] M. Ostadi, K. G. Paso, S. Rodriguez-Fabia, L. E. Øi, F. Manenti, and M. Hillestad, "Process integration of green hydrogen: Decarbonization of chemical industries," *Energies (Basel)*, vol. 13, no. 18, Sep. 2020, doi: 10.3390/en13184859.

[146] J. Weyand, F. Habermeyer, and R. U. Dietrich, "Process design analysis of a hybrid power-and-biomass-to-liquid process – An approach combining life cycle and techno-economic assessment," *Fuel*, vol. 342, Jun. 2023, doi: 10.1016/j.fuel.2023.127763.

[147] F. Habermeyer, J. Weyand, S. Maier, E. Kurkela, and R. U. Dietrich, "Power Biomass to Liquid — an option for Europe's sustainable and independent aviation fuel production," *Biomass Convers Biorefin*, 2023, doi: 10.1007/s13399-022-03671-y.

[148] M. Dossow, V. Dieterich, A. Hanel, H. Spliethoff, and S. Fendt, "Improving carbon efficiency for an advanced Biomass-to-Liquid process using hydrogen and oxygen from electrolysis," *Renewable and Sustainable Energy Reviews*, vol. 152, Dec. 2021, doi: 10.1016/j.rser.2021.111670.

[149] S. A. Isaacs, M. D. Staples, F. Allroggen, D. S. Mallapragada, C. P. Falter, and S. R. H. Barrett, "Environmental and Economic Performance of Hybrid Power-to-Liquid and Biomass-to-Liquid Fuel Production in the United States," *Environ Sci Technol*, vol. 55, no. 12, pp. 8247–8257, 2021, doi: 10.1021/acs.est.0c07674.

[150] T. E. Casavant and R. P. Côté, "Using chemical process simulation to design industrial ecosystems," *J Clean Prod*, vol. 12, no. 8–10, pp. 901–908, Oct. 2004, doi: 10.1016/j.jclepro.2004.02.034.

[151] AspenTech, "Building and Running a Process Model Aspen Plus 7," 2007.

[152] J. Fontalvo, “Usando modelos de usuario en Matlab® en la interfaz de Aspen plus® con Excel® como puente,” *Ingenieria e Investigacion*, vol. 34, no. 2, pp. 39–43, 2014, doi: 10.15446/ing.investig.v34n2.41621.

[153] J. Q. Albarelli, S. Onorati, P. Caliandro, E. Peduzzi, M. A. A. Meireles, F. Marechal, and A. V. Ensinas, “Multi-objective optimization of a sugarcane biorefinery for integrated ethanol and methanol production,” *Energy*, vol. 138, pp. 1281–1290, 2017, doi: 10.1016/j.energy.2015.06.104.

[154] M. Marchese, S. Chesta, M. Santarelli, and A. Lanzini, “Techno-economic feasibility of a biomass-to-X plant: Fischer-Tropsch wax synthesis from digestate gasification,” *Energy*, vol. 228, p. 120581, 2021, doi: 10.1016/j.energy.2021.120581.

[155] Engineering Toolbox, “Fuels - Higher and Lower Calorific Values,” 2023. https://www.engineeringtoolbox.com/fuels-higher-calorific-values-d_169.html (accessed Aug. 07, 2023).

[156] ASTM, “Standard Specification for Aviation Turbine Fuel Containing Synthesized Hydrocarbons (ASTM D7566-21),” *Annual Book of ASTM Standards*, pp. 1–38, 2021, doi: 10.1520/D7566-21.operated.

[157] S. Heyne and S. Harvey, “Impact of choice of CO 2 separation technology on thermo-economic performance of Bio-SNG production processes,” no. April 2013, pp. 299–318, 2014, doi: 10.1002/er.

[158] D. Humbird, R. Davis, L. Tao, C. Kinchin, D. Hsu, A. Aden, P. Schoen, J. Lukas, B. Olthof, M. Worley, D. Sexton, and D. Dudgeon, “Process Design and Economics for Biochemical Conversion of Lignocellulosic Biomass to Ethanol: Dilute-Acid Pretreatment and Enzymatic Hydrolysis of Corn Stover,” *National Renewable Energy Laboratory*, no. May, pp. 1–147, 2011, doi: 10.2172/1107470.

[159] S. Michailos, D. Parker, and C. Webb, “A multicriteria comparison of utilizing sugar cane bagasse for methanol to gasoline and butanol production,” *Biomass Bioenergy*, vol. 95, pp. 436–448, 2016, doi: 10.1016/j.biombioe.2016.06.019.

[160] Chemical Engineering, “Chemical Engineering Plant Cost Index.” https://www.chemengonline.com/ (accessed Aug. 07, 2023).

[161] M. S. Peters, K. D. Timmerhaus, and R. E. West, *Plant Design and Economics for Chemical Engineers 5th edition*. 2003.

[162] I. Dimitriou, H. Goldingay, and A. V. Bridgwater, “Techno-economic and uncertainty analysis of Biomass to Liquid (BTL) systems for transport fuel production,” *Renewable and Sustainable Energy Reviews*, vol. 88, no. February, pp. 160–175, 2018, doi: 10.1016/j.rser.2018.02.023.

[163] G. Towler and R. Sinnott, “Capital Cost Estimating,” in *Chemical Engineering Design*, Elsevier, 2013, pp. 307–354. doi: 10.1016/B978-0-08-096659-5.00007-9.

[164] P. Haro, F. Johnsson, and H. Thunman, “Improved syngas processing for enhanced Bio-SNG production: A techno-economic assessment,” *Energy*, vol. 101, pp. 380–389, 2016, doi: 10.1016/j.energy.2016.02.037.

[165] M. S. Peters and K. D. Timmerhaus, *Plant Design and Economics for Chemical Engineers*. 1991. doi: 10.1080/00137915908965075.

[166] S. Michailos, M. Walker, A. Moody, D. Poggio, and M. Pourkashanian, “Biomethane production using an integrated anaerobic digestion, gasification and CO2 biomethanation process in a real waste water treatment plant: A techno-economic assessment,” *Energy*

Convers Manag, vol. 209, no. February, p. 112663, 2020, doi: 10.1016/j.enconman.2020.112663.

[167] Office for National Statistics, "A01: Summary of labour market statistics - Office for National Statistics." https://www.ons.gov.uk/employmentandlabourmarket/peopleinwork/employmentandemployeetypes/datasets/summaryoflabourmarketstatistics (accessed May 12, 2021).

[168] H. Baumann and A.-M. Tillman, *The Hitch Hiker's Guide to LCA*. 2004.

[169] R. Heijungs, K. Allacker, E. Benetto, M. Brandão, J. Guinée, S. Schaubroeck, T. Schaubroeck, and A. Zamagni, "System Expansion and Substitution in LCA: A Lost Opportunity of ISO 14044 Amendment 2," *Frontiers in Sustainability*, vol. 2, no. June, pp. 1–3, 2021, doi: 10.3389/frsus.2021.692055.

[170] International Organization for Standardization, "Environmental Management - Life Cycle Assessment - Principles and Framework (ISO 14040:2006)," 2006 doi: 10.1016/j.ecolind.2011.01.007.

[171] M. F. Rojas Michaga, S. Michailos, M. Akram, E. Cardozo, K. J. Hughes, D. Ingham, and M. Pourkashanian, "Bioenergy with carbon capture and storage (BECCS) potential in jet fuel production from forestry residues: A combined Techno-Economic and Life Cycle Assessment approach," *Energy Convers Manag*, vol. 255, no. November 2021, p. 115346, 2022, doi: 10.1016/j.enconman.2022.115346.

[172] Royal Academy of Engineering, "Sustainability of liquid biofuels," 2017.

[173] Ecoinvent, "System Models," Jul. 26, 2023. https://ecoinvent.org/the-ecoinvent-database/system-models/ (accessed Jul. 26, 2023).

[174] N. Pavlenko and S. Searle, "ICCT working paper: Assessing the sustainability implications of alternative aviation fuels," 2021.

[175] S. Majer, K. Oehmichen, D. Moosmann, H. S. Dbfz, K. Sailer, M. Matosic, T. Reinholz, M. Decorte, S. P. Eba, S. Königsberger, A. Wolf, L. Maggioni, M. Edel, F. Belin, E. Anna, L. L. Fluxys, and C. Mariusse, "D5 . 1 Assessment of integrated concepts and identification of key factors and drivers," 2021.

[176] TransportPolicy.net, "US: Fuels: Renewable Fuel Standard | Transport Policy." https://www.transportpolicy.net/standard/us-fuels-renewable-fuel-standard/ (accessed Dec. 20, 2021).

[177] W.-C. Wang, "Techno-economic analysis for evaluating the potential feedstocks for producing hydro-processed renewable jet fuel in Taiwan," *Energy*, vol. 179, pp. 771–783, 2019, doi: 10.1016/j.energy.2019.04.181.

[178] T. R. Brown and R. C. Brown, "A review of cellulosic biofuel commercial-scale projects in the United States," *Biofuels, Bioproducts and Biorefining*, vol. 7, pp. 235–245, 2013, doi: 10.1002/bbb.

[179] N. Yilmaz and A. Atmanli, "Sustainable alternative fuels in aviation," *Energy*, vol. 140, pp. 1378–1386, 2017, doi: 10.1016/j.energy.2017.07.077.

[180] C. Whittaker, N. Mortimer, R. Murphy, and R. Matthews, "Energy and greenhouse gas balance of the use of forest residues for bioenergy production in the UK," *Biomass Bioenergy*, vol. 35, no. 11, pp. 4581–4594, 2011, doi: 10.1016/j.biombioe.2011.07.001.

[181] Defra, "Dti DfT. Defra, UK Biomass Strategy," 2007.

[182] S. Searle and C. Malins, “National case studies on potential waste and residue availability for cellulosic biofuel production in the EU,” pp. 1–38, 2013.

[183] E4tech, “Advanced drop-in biofuels: UK production capacity outlook to 2030,” no. February, p. 83, 2017.

[184] Energy Technologies Institute, “Taking stock of UK CO2 storage,” 2017.

[185] Energy Technologies Institute, “Carbon Capture and Storage Potential for CCS in the UK.” doi: 10.1002/ghg3.11.

[186] Sccs, “Opportunities for CO2 Storage around Scotland: An Integrated Strategic Research Study,” *Text*, 2009.

[187] C. Wildbolz, “Life Cycle Assessment of Selected Technologies for CO2 Transport and Sequestration,” *Environmental Engineering*, 2007.

[188] Aspen Technology Inc. and Aspen Plus V 8.4, “Aspen Physical Property System: Physical Property Methods,” *Methods*, pp. 1–234, 2013, [Online]. Available: http://profsite.um.ac.ir/~fanaei/_private/Property Methods 8_4.pdf

[189] J. Xie, W. Zhong, B. Jin, Y. Shao, and H. Liu, “Simulation on gasification of forestry residues in fluidized beds by Eulerian-Lagrangian approach,” *Bioresour Technol*, vol. 121, pp. 36–46, 2012, doi: 10.1016/j.biortech.2012.06.080.

[190] M. M. Wright, J. A. Satrio, R. C. Brown, D. E. Daugaard, and D. D. Hsu, “Techno-economic analysis of biomass fast pyrolysis to transportation fuels. Technical Report NREL/TP-6A20-46586,” *Nrel*, vol. 89, no. November, pp. 463–469, 2010, [Online]. Available: https://doi.org/10.1016/j.fuel.2010.07.029

[191] AspenPlus, *Aspen Plus 2004.1: Getting Started Modeling Processes with Solids*. 2004.

[192] L. Abdelouahed, O. Authier, G. Mauviel, J. P. Corriou, G. Verdier, and A. Dufour, “Detailed modeling of biomass gasification in dual fluidized bed reactors under aspen plus,” *Energy and Fuels*, vol. 26, no. 6, pp. 3840–3855, 2012, doi: 10.1021/ef300411k.

[193] A. Dufour, P. Girods, E. Masson, Y. Rogaume, and A. Zoulalian, “Synthesis gas production by biomass pyrolysis: Effect of reactor temperature on product distribution,” *Int J Hydrogen Energy*, vol. 34, no. 4, pp. 1726–1734, 2009, doi: 10.1016/j.ijhydene.2008.11.075.

[194] M. Cortazar, L. Santamaria, G. Lopez, J. Alvarez, L. Zhang, R. Wang, X. Bi, and M. Olazar, “A comprehensive review of primary strategies for tar removal in biomass gasification,” *Energy Conversion and Management*, vol. 276. Elsevier Ltd, Jan. 15, 2023. doi: 10.1016/j.enconman.2022.116496.

[195] M. L. Matthias Binder, Michael Kraussler, Matthias Kuba, K. Nath, D. Das, M. Binder, M. Kraussler, M. Kuba, M. Luisser, International Environmental Agency, M. L. Matthias Binder, Michael Kraussler, Matthias Kuba, International Environmental Agency, M. Binder, M. Kraussler, M. Kuba, M. Luisser, International Environmental Agency, and M. L. Matthias Binder, Michael Kraussler, Matthias Kuba, “Hydrogen from Biomass Gasification,” 2018.

[196] S. Michailos, O. Emenike, D. Ingham, K. J. Hughes, and M. Pourkashanian, “Methane production via syngas fermentation within the bio-CCS concept: A techno-economic assessment,” *Biochem Eng J*, vol. 150, no. May, p. 107290, 2019, doi: 10.1016/j.bej.2019.107290.

[197] S. D. Phillips, J. K. Tarud, and M. J. Biddy, “Gasoline from Wood via Integrated Gasification , Synthesis , and Methanol-to- Gasoline Technologies,” *Energy*, no. January, 2011, doi: NREL/TP-5100-47594.

[198] H. F. Garces, H. M. Galindo, L. J. Garces, J. Hunt, A. Morey, and S. L. Suib, “Low temperature H2S dry-desulfurization with zinc oxide,” *Microporous and Mesoporous Materials*, vol. 127, no. 3, pp. 190–197, 2010, doi: 10.1016/j.micromeso.2009.07.022.

[199] J. A. Scott and T. A. Adams, “Biomass-Gas-and-Nuclear-To-Liquids (BGNTL) Processes Part I: Model Development and Simulation,” *Canadian Journal of Chemical Engineering*, vol. 96, no. 9, pp. 1853–1871, 2018, doi: 10.1002/cjce.23231.

[200] IEA Bioenergy and L. Waldheim, *Gasification of waste for energy carriers. A review.*, vol. Task 33. 2018.

[201] IRENA, “Innovation Technology Outlook for Advanced Liquid Biofuels,” *International Renewable Energy Agency (IRENA)*, p. 132, 2016, [Online]. Available: http://www.irena.org/-/media/Files/IRENA/Agency/Publication/2016/IRENA_Innovation_Outlook_Advanced_Liquid_Biofuels_2016.pdf

[202] T. A. Adams, Y. K. Salkuyeh, and J. Nease, “Processes and simulations for solvent-based CO2 capture and syngas cleanup,” in *Reactor and Process Design in Sustainable Energy Technology*, 2014. doi: 10.1016/B978-0-444-59566-9.00006-5.

[203] J. Stanislowski and T. Snyder, “Modeling and Cost Evaluation of CO2 Capture Processes,” no. May. 2012.

[204] L. Tock, M. Gassner, and F. Maréchal, “Thermochemical production of liquid fuels from biomass: Thermo-economic modeling, process design and process integration analysis,” *Biomass Bioenergy*, vol. 34, no. 12, pp. 1838–1854, 2010, doi: 10.1016/j.biombioe.2010.07.018.

[205] D. Clark, H. Stuart, T. Cabot, P. J. Freeman, E. K. Berens, T. Cabot, M. Milton, T. Hopkins, J. Staines, and R. Henson, “VERFAHREN ZUR CO2- ABSCHEIDUNG UND -SPEICHERUNG,” vol. 923, no. August, pp. 920–923, 2006.

[206] K. Im-orb, L. Simasatitkul, and A. Arpornwichanop, “Techno-economic analysis of the biomass gasification and Fischer-Tropsch integrated process with off-gas recirculation,” *Energy*, vol. 94, pp. 483–496, 2016, doi: 10.1016/j.energy.2015.11.012.

[207] U. M. Teles and F. A. N. Fernandes, “Hydrocracking of Fischer-Tropsch products. Optimization of diesel and naphtha cuts,” *Chem Biochem Eng Q*, vol. 22, no. 2, pp. 227–231, 2008.

[208] M. Sudiro and A. Bertucco, “Production of synthetic gasoline and diesel fuel by alternative processes using natural gas and coal: Process simulation and optimization,” *Energy*, vol. 34, no. 12, pp. 2206–2214, 2009, doi: 10.1016/j.energy.2008.12.009.

[209] V. Marcantonio, M. De Falco, M. Capocelli, E. Bocci, A. Colantoni, and M. Villarini, “Process analysis of hydrogen production from biomass gasification in fluidized bed reactor with different separation systems,” *Int J Hydrogen Energy*, vol. 44, no. 21, pp. 10350–10360, 2019, doi: 10.1016/j.ijhydene.2019.02.121.

[210] C. N. Hamelinck, A. P. C. Faaij, H. den Uil, and H. Boerrigter, “Production of FT transportation fuels from biomass; technical options, process analysis and optimisation, and development potential,” *Energy*, vol. 29, no. 11, pp. 1743–1771, 2004, doi: 10.1016/j.energy.2004.01.002.

[211] J. G. Speight, *Gasification processes for syngas and hydrogen production*, no. Chapter 1. Woodhead Publishing Limited, 2015. doi: 10.1016/B978-0-85709-802-3.00006-0.

[212] E. Rubio-Castro, J. Maria, and M. Serna-Gonzalez, “Optimal Design of Cooling Water Systems,” *Energy Management Systems*, no. August 2011, 2011, doi: 10.5772/18894.

[213] T. A. Adams and P. I. Barton, “Combining coal gasification and natural gas reforming for efficient polygeneration,” *Fuel Processing Technology*, vol. 92, no. 3, pp. 639–655, 2011, doi: 10.1016/j.fuproc.2010.11.023.

[214] L. R. Clausen, B. Elmegaard, and N. Houbak, “Technoeconomic analysis of a low CO2 emission dimethyl ether (DME) plant based on gasification of torrefied biomass,” *Energy*, vol. 35, no. 12, pp. 4831–4842, 2010, doi: 10.1016/j.energy.2010.09.004.

[215] O. Onel, A. M. Niziolek, J. A. Elia, R. C. Baliban, and C. A. Floudas, “Biomass and Natural Gas to Liquid Transportation Fuels and Olefins (BGTL + C2 _ C4): Process Synthesis and Global Optimization,” 2015, doi: 10.1021/ie503979b.

[216] K. M. Holmgren, “Investment cost estimates for gasification- based biofuel production systems,” *ivl, Swedish Environmental Research Institute*, no. August, pp. 1–26, 2015.

[217] G. Liu, E. D. Larson, R. H. Williams, T. G. Kreutz, and X. Guo, “Making Fischer-Tropsch fuels and electricity from coal and biomass: Performance and cost analysis,” *Energy and Fuels*, vol. 25, no. 1, pp. 415–437, 2011, doi: 10.1021/ef101184e.

[218] F. G. Albrecht, D. H. König, N. Baucks, and R. U. Dietrich, “A standardized methodology for the techno-economic evaluation of alternative fuels – A case study,” *Fuel*, vol. 194, pp. 511–526, 2017, doi: 10.1016/j.fuel.2016.12.003.

[219] L. P. Lauven, I. Karschin, and J. Geldermann, “Simultaneously optimizing the capacity and configuration of biorefineries,” *Comput Ind Eng*, vol. 124, no. March 2017, pp. 12–23, 2018, doi: 10.1016/j.cie.2018.07.014.

[220] J. L. Carrasco, S. Gunukula, A. A. Boateng, C. A. Mullen, W. J. DeSisto, and M. C. Wheeler, “Pyrolysis of forest residues: An approach to techno-economics for bio-fuel production,” *Fuel*, vol. 193, pp. 477–484, 2017, doi: 10.1016/j.fuel.2016.12.063.

[221] S. Michailos, D. Parker, and C. Webb, “A techno-economic comparison of Fischer–Tropsch and fast pyrolysis as ways of utilizing sugar cane bagasse in transportation fuels production.,” *Chemical Engineering Research and Design*, vol. 118, pp. 206–214, 2017, doi: 10.1016/j.cherd.2017.01.001.

[222] G. Manzolini, E. Macchi, and M. Gazzani, “CO2 capture in natural gas combined cycle with SEWGS. Part B: Economic assessment,” *International Journal of Greenhouse Gas Control*, vol. 12, pp. 502–509, 2013, doi: 10.1016/j.ijggc.2012.06.021.

[223] C. L. Whittaker, N. D. Mortimer, and R. W. Matthews, “Understanding the carbon footprint of timber transport in the United Kingdom,” *North Energy, report*, 2010, [Online]. Available: https://scholar.google.com/scholar?q=whittaker++understand+carbon+footprint+of+timber+transport+in+the+uk&btnG=&hl=en&as_sdt=0%2C5#1

[224] Ecoinvent, “Hardwood forestry, oak, sustainable forest management, RoW EcoQuery - Dataset Details (UPR),” 2017. https://v36.ecoquery.ecoinvent.org/Details/UPR/aaa46c1a-d6a1-4cff-a1dc-b888b8e12598/290c1f85-4cc4-4fa1-b0c8-2cb7f4276dce (accessed Jul. 12, 2021).

[225] Ecoinvent, “Softwood forestry, spruce, sustainable forest management, RoW EcoQuery - Dataset Details (UPR),” 2017. https://v36.ecoquery.ecoinvent.org/Details/UPR/2caee472-c8ff-4cbb-bdd6-ec10bab515c7/290c1f85-4cc4-4fa1-b0c8-2cb7f4276dce (accessed Jul. 12, 2021).

[226] F. Werner, “Background report for the life cycle inventories of wood and wood based products for updates of ecoinvent 2.2,” no. March, 2017.

[227] S. Alberici, G. Toop, and S. Critchley, “Ecofys-A Navigant Company Summary report,” p. 30, 2018.

[228] S. Wittkopf, “Bereitstellung von Hackgut zur thermischen Verwertung durch Forstbetriebe in Bayern,” p. 217, 2004.

[229] S. Albrecht, S. Rüter, J. Welling, M. Knauf, U. Mantau, A. Braune, M. Baitz, H. Weimar, S. Sorgel, J. Kreissig, J. Deimling, and S. Hellwig, “ÖKOLOGISCHE POTENZIALE DURCH HOLZNUTZUNG GEZIELT FÖRDERN,” 2008.

[230] Forestry Commission, “Wood Production (roundwood removals): 1976 to 2018 FINAL - data.gov.uk,” 2019. https://data.gov.uk/dataset/e2443ddd-ccc3-46de-bbce-fcfb719f49d9/wood-production-roundwood-removals-1976-to-2018-final (accessed Jul. 13, 2021).

[231] Forestry Commission and FC, “Forestry Statistics 2018 - Forest Research,” no. September, pp. 1–9, 2018.

[232] E. Le Net, F. Bajric, D. Vötter, and S. Berg, “Identification of existing transport methods and alternative methods or new approaches with data about costs, labour input and energy consumption.,” *European Forest Institute …*, p. 68, 2011.

[233] Ecoinvent, “Market for wood chips, wet, measured as dry mass, GLO EcoQuery - Dataset Details (UPR),” 2017. https://v36.ecoquery.ecoinvent.org/Details/UPR/9327cf8c-90af-4c38-969a-789f0a0e760d/8b738ea0-f89e-4627-8679-433616064e82 (accessed Jul. 13, 2021).

[234] R. Taylor, “Advanced Biofuel Feedstocks – An Assessment of Sustainability,” *E4tech*, vol. 2, pp. 1–82, 2014.

[235] Ecoinvent, “Synthetic gas production, from wood, at fixed bed gasifier, RoW EcoQuery - Dataset Details (UPR),” 2017. https://v36.ecoquery.ecoinvent.org/Details/UPR/b2faac05-ce66-4140-9588-86b69b3d1250/290c1f85-4cc4-4fa1-b0c8-2cb7f4276dce (accessed Jul. 13, 2021).

[236] R. Cuéllar-Franca, P. García-Gutiérrez, I. Dimitriou, R. H. Elder, R. W. K. Allen, and A. Azapagic, “Utilising carbon dioxide for transport fuels: The economic and environmental sustainability of different Fischer-Tropsch process designs,” *Appl Energy*, vol. 253, no. July, p. 113560, 2019, doi: 10.1016/j.apenergy.2019.113560.

[237] Ecoinvent, “Air compressor production, screw-type compressor, 300kW, RER EcoQuery - Dataset Details (UPR),” *2017*. https://v36.ecoquery.ecoinvent.org/Details/UPR/f4dda843-27c0-42af-b8c1-022696e9f3da/290c1f85-4cc4-4fa1-b0c8-2cb7f4276dce (accessed Jul. 14, 2021).

[238] B. Senior, “CO2 Storage in the UK - Industry Potential,” p. 40, 2009.

[239] Ecoinvent, “Market for kerosene EcoQuery - Dataset Details (UPR),” 2017. https://v36.ecoquery.ecoinvent.org/Details/ShowUndefined/edcee36f-755b-49eb-b0c5-802debd94874 (accessed Jul. 15, 2021).

[240] F. Cherubini, N. D. Bird, A. Cowie, G. Jungmeier, B. Schlamadinger, and S. Woess-Gallasch, “Energy- and greenhouse gas-based LCA of biofuel and bioenergy systems: Key issues, ranges and recommendations,” *Resour Conserv Recycl*, vol. 53, no. 8, pp. 434–447, 2009, doi: 10.1016/j.resconrec.2009.03.013.

[241] S. Bello, Á. Galán-Martín, G. Feijoo, M. T. Moreira, and G. Guillén-Gosálbez, “BECCS based on bioethanol from wood residues: Potential towards a carbon-negative transport and side-effects,” *Appl Energy*, vol. 279, 2020, doi: 10.1016/j.apenergy.2020.115884.

[242] IEAGHG, “Biomass and CCS -- Guidance for accounting for negative emissions,” 2014.

[243] International Energy Agency, “Combining Bioenergy with CCS,” 2011.

[244] AACE International, “Recommended Practice No. 18R-97: Cost Estimate Classification System, Rev March 1, 2016,” p. 10, 2016, [Online]. Available: http://www.aacei.org/toc/toc_18R-97.pdf

[245] P. Lamers, E. C. D. Tan, E. M. Searcy, C. J. Scarlata, K. G. Cafferty, and J. J. Jacobson, “Strategic supply system design - a holistic evaluation of operational and production cost for a biorefinery supply chain,” *Biofuels, Bioproducts and Biorefining*, vol. 9, no. 6, pp. 648–660, Nov. 2015, doi: 10.1002/bbb.1575.

[246] DECC, “Electricity Generation Costs and Hurdle Rates Lot 3 : Non-Renewable Technologies,” 2016.

[247] E4Tech, “Review of Technologies for Gasification of Biomass and Wastes Final report,” *NNFCC The Bioeconomy Consultants*, no. June, pp. 1–130, 2009.

[248] S. de Jong, R. Hoefnagels, A. Faaij, R. Slade, R. Mawhood, and M. Junginger, “The feasibility of short-term production strategies for renewable jet fuels - a comprehensive techno-economic comparison,” *Biofuels, Bioproducts and Biorefining*, 2015, doi: 10.1002/bbb.1613.

[249] A. M. Petersen, R. Melamu, J. H. Knoetze, and J. F. Görgens, “Comparison of second-generation processes for the conversion of sugarcane bagasse to liquid biofuels in terms of energy efficiency, pinch point analysis and Life Cycle Analysis,” *Energy Convers Manag*, vol. 91, pp. 292–301, 2015, doi: 10.1016/j.enconman.2014.12.002.

[250] A. M. Petersen, S. Farzad, and J. F. Görgens, “Techno-economic assessment of integrating methanol or Fischer-Tropsch synthesis in a South African sugar mill,” *Bioresour Technol*, 2015, doi: 10.1016/j.biortech.2015.02.007.

[251] W. C. Wang and L. Tao, “Bio-jet fuel conversion technologies,” *Renewable and Sustainable Energy Reviews*, vol. 53, pp. 801–822, 2016, doi: 10.1016/j.rser.2015.09.016.

[252] National Energy Technology Laboratory (NETL), “Development of Baseline Data and Analysis of Life Cycle Greenhouse Gas Emissions of Petroleum-Based Fuels,” pp. 1–310, 2008, doi: DOE/NETL-2009/1346.

[253] J. Han, L. Tao, and M. Wang, “Well-to-wake analysis of ethanol-to-jet and sugar-to-jet pathways,” *Biotechnol Biofuels*, vol. 10, pp. 1–15, 2017, doi: 10.1186/s13068-017-0698-z.

[254] Department for Transport, “RTFO Guidance Part One: Process Guidance,” 2021. Accessed: Apr. 24, 2023. [Online]. Available: https://assets.publishing.service.gov.uk/government/uploads/system/uploads/attachment_data/file/998434/rtfo-guidance-part-1-process-guidance-2021.pdf

[255] Bioenergy Insight Magazine, “Generators of biomethane can claim RHI and RTFO payments,” 2019. https://www.bioenergy-news.com/news/generators-of-biomethane-can-claim-rhi-and-rtfo-payments/ (accessed May 03, 2021).

[256] IATA, “IATA - Fuel Price Monitor,” 2021. https://www.iata.org/en/publications/economics/fuel-monitor/ (accessed Apr. 28, 2021).

[257] R. W. Stratton, H. M. Wong, and J. I. Hileman, “Life Cycle Greenhouse Gas Emissions from Alternative Jet Fuels,” 2010.

[258] P. Schmidt, V. Batteiger, A. Roth, and W. Weindorf, “Power-to-Liquids as Renewable Fuel Option for Aviation : A Review,” no. 1, pp. 127–140, 2018, doi: 10.1002/cite.201700129.

[259] Q. Yu and D. W. F. Brilman, “Design Strategy for CO2 Adsorption from Ambient Air Using a Supported Amine Based Sorbent in a Fixed Bed Reactor,” *Energy Procedia*, vol. 114, no. November 2016, pp. 6102–6114, 2017, doi: 10.1016/j.egypro.2017.03.1747.

[260] S. Deutz and A. Bardow, “Life-cycle assessment of an industrial direct air capture process based on temperature–vacuum swing adsorption,” *Nat Energy*, vol. 6, no. 2, pp. 203–213, 2021, doi: 10.1038/s41560-020-00771-9.

[261] C. Drechsler and D. W. Agar, “Intensified integrated direct air capture - power-to-gas process based on H2O and CO2 from ambient air,” *Appl Energy*, vol. 273, no. April, p. 115076, 2020, doi: 10.1016/j.apenergy.2020.115076.

[262] C. Surgenor, “Europe’s first power-to-liquid demo plant in Norway plans renewable aviation fuel production in 2023,” *One (Only Natural Energy)*, 2020. https://www.onlynaturalenergy.com/europes-first-power-to-liquid-demo-plant-in-norway-plans-renewable-aviation-fuel-production-in-2023/ (accessed Jan. 10, 2022).

[263] Die Bundesregierung, “PtL-Roadmap: Initiativen der Bundeslander,” 2021.

[264] N. Muller and N. King, “Aviation: Germany opens world’s first plant for clean jet fuel,” *DW*, 2021. https://www.dw.com/en/sustainable-aviation-fuel-power-to-liquid/a-59398405 (accessed Jan. 10, 2022).

[265] Department for Transport, “Jet Zero Consultation,” 2021. [Online]. Available: https://assets.publishing.service.gov.uk/government/uploads/system/uploads/attachment_data/file/1002716/jet-zero-consultation-a-consultation-on-our-strategy-for-net-zero-aviation.pdf

[266] M. Grahn, E. Malmgren, A. D. Korberg, M. Taljegard, and J. E. Anderson, “Review of electrofuel feasibility — cost and environmental impact Progress in Energy,” *Progress*, 2022.

[267] G. Goodman and V. Martin, “Wind powered electricity in the UK,” *Offshore Wind Outlook 2019*, no. May 2020, p. 1, 2019, [Online]. Available: www.iea.org/reports/offshore-wind-outlook-2019%0Ahttps://assets.publishing.service.gov.uk/government/uploads/system/uploads/attachment_data/file/875384/Wind_powered_electricity_in_the_UK.pdf

[268] “Onshore vs offshore wind energy: what’s the difference? | National Grid Group.” https://www.nationalgrid.com/stories/energy-explained/onshore-vs-offshore-wind-energy (accessed Apr. 12, 2022).

[269] Department for Transport, “Low carbon fuels strategy Call for ideas,” 2022. Accessed: Apr. 24, 2023. [Online]. Available: https://www.gov.uk/government/consultations/low-carbon-fuel-strategy-call-for-ideas

[270] F. Sabatino, A. Grimm, F. Gallucci, M. van Sint Annaland, G. J. Kramer, and M. Gazzani, “A comparative energy and costs assessment and optimization for direct air capture technologies,” *Joule*, vol. 5, no. 8, pp. 2047–2076, 2021, doi: 10.1016/j.joule.2021.05.023.

[271] M. Fasihi, E. Olga, and C. Breyer, “Techno-economic assessment of CO 2 direct air capture plants,” *J Clean Prod*, vol. 224, pp. 957–980, 2019, doi: 10.1016/j.jclepro.2019.03.086.

[272] N. McQueen, K. V. Gomes, C. McCormick, K. Blumanthal, M. Pisciotta, and J. Wilcox, “A review of direct air capture (DAC): scaling up commercial technologies and innovating for the future,” *Progress in Energy*, vol. 3, no. 3, p. 032001, 2021, doi: 10.1088/2516-1083/abf1ce.

[273] C. Beuttler, L. Charles, and J. Wurzbacher, “The Role of Direct Air Capture in Mitigation of Anthropogenic Greenhouse Gas Emissions.” pp. 1–7, 2019. doi: 10.3389/fclim.2019.00010.

[274] C. Gebald, “Development of amine-functionalized adsorbent for carbon dioxide capture from atmospheric air,” *ETH Zürich*, no. 21853, pp. 1–133, 2014, [Online]. Available: https://www.research-collection.ethz.ch/handle/20.500.11850/97310

[275] J. A. Wurzbacher, C. Gebald, S. Brunner, and A. Steinfeld, “Heat and mass transfer of temperature-vacuum swing desorption for CO2 capture from air,” *Chemical Engineering Journal*, vol. 283, pp. 1329–1338, 2016, doi: 10.1016/j.cej.2015.08.035.

[276] “MERRA-2.” https://gmao.gsfc.nasa.gov/reanalysis/MERRA-2/ (accessed Aug. 29, 2022).

[277] Pacific Green, “Green hydrogen: why batteries are a key part of the picture.” https://www.pacificgreen-energystorage.com/articles/green-hydrogen-why-batteries-are-key-part-picture (accessed Jun. 09, 2022).

[278] H. Tebibel, “Methodology for multi-objective optimization of wind turbine/battery/electrolyzer system for decentralized clean hydrogen production using an adapted power management strategy for low wind speed conditions,” *Energy Convers Manag*, vol. 238, p. 114125, 2021, doi: 10.1016/j.enconman.2021.114125.

[279] B. Olateju, A. Kumar, and M. Secanell, “A techno-economic assessment of large scale wind-hydrogen production with energy storage in Western Canada,” *Int J Hydrogen Energy*, vol. 41, no. 21, pp. 8755–8776, 2016, doi: 10.1016/j.ijhydene.2016.03.177.

[280] M. Gökçek and C. Kale, “Optimal design of a Hydrogen Refuelling Station (HRFS) powered by Hybrid Power System,” *Energy Convers Manag*, vol. 161, no. February, pp. 215–224, 2018, doi: 10.1016/j.enconman.2018.02.007.

[281] A. Ursúa, E. L. Barrios, J. Pascual, I. San Martín, and P. Sanchis, “Integration of commercial alkaline water electrolysers with renewable energies: Limitations and improvements,” *Int J Hydrogen Energy*, vol. 41, no. 30, pp. 12852–12861, 2016, doi: 10.1016/j.ijhydene.2016.06.071.

[282] J. G. García Clúa, R. J. Mantz, and H. De Battista, “Optimal sizing of a grid-assisted wind-hydrogen system,” *Energy Convers Manag*, vol. 166, pp. 402–408, Jun. 2018, doi: 10.1016/j.enconman.2018.04.047.

[283] A. J. Simon, W. Daily, and R. G. White, “Hydrogen and Water : An Engineering , Economic and Environmental Analysis,” 2010.

[284] A. Pietra, M. Gianni, N. Zuliani, S. Malabotti, and R. Taccani, “Experimental characterization of an alkaline electrolyser and a compression system for hydrogen production and storage,” *Energies (Basel)*, vol. 14, no. 17, pp. 1–17, 2021, doi: 10.3390/en14175347.

[285] D. Jang, H. S. Cho, and S. Kang, “Numerical modeling and analysis of the effect of pressure on the performance of an alkaline water electrolysis system,” *Appl Energy*, vol. 287, no. January, p. 116554, 2021, doi: 10.1016/j.apenergy.2021.116554.

[286] I. Hannula, N. Kaisalo, and P. Simell, “Preparation of Synthesis Gas from CO2 for Fischer–Tropsch Synthesis—Comparison of Alternative Process Configurations,” *C—Journal of Carbon Research*, vol. 6, no. 3, p. 55, 2020, doi: 10.3390/c6030055.

[287] A. Wolf, C. Kern, and A. Jess, “Renewable synthesis-gas-production - Do hydrocarbons in the reactant flow of the reverse water-gas shift reaction cause coke formation?,” *DGMK Tagungsbericht*, vol. 2013, no. 2, pp. 215–221, 2013.

[288] J. M. ; Repasky and R. L. Zeller, III, “WO2021062384A1,” 2021

[289] S. Vedachalam, P. Boahene, and A. K. Dalai, “Production of jet fuel by hydrorefining of Fischer-Tropsch wax over Pt/Al-TUD-1 bifunctional catalyst,” *Fuel*, vol. 300, no. February, p. 121008, 2021, doi: 10.1016/j.fuel.2021.121008.

[290] J. Frątczak, H. de Paz Carmona, Z. Tišler, J. M. Hidalgo Herrador, and Z. Gholami, “Hydrocracking of Heavy Fischer–Tropsch Wax Distillation Residues and Its Blends with Vacuum Gas Oil Using Phonolite-Based Catalysts,” *Molecules*, vol. 26, no. 23, p. 7172, Nov. 2021, doi: 10.3390/molecules26237172.

[291] F. von Hepperger, “Implementation of water electrolysis in Växjö’s combined heat and power plant and the use of excess heat . A techno-economic analysis.”

[292] H. Li, S. Svendsen, O. Gudmundsson, M. Kuosa, M. Rämä, K. Sipilä, M. Blesl, M. Broydo, M. Stehle, R. Pesch, D. Pietruschka, H. Huther, M. Grajcar, A. Jentsch, A. Kallert, D. Schmidt, Y. H. Im, and C. Bevilacqua, “Low Temperature District Heating for Future Energy Systems,” 2017. doi: 10.1016/j.egypro.2018.08.224.

[293] Skuma, “Is London tap water safe?-Statistics,” 2021. https://www.skumawater.com/is-london-tap-water-safe (accessed Jul. 21, 2022).

[294] M. E. Aline Noutcha, O. Damiete, M. Johnny Jr, O. Ngozi, C. U. Ezera, and S. N. Okiwelu, “Quantity and Quality of Water Condensate from Air Conditioners and Its Potential Uses at the University of Port Harcourt, Nigeria),” *Pelagia Research Library Advances in Applied Science Research*, vol. 7, no. 6, pp. 45–48, 2016.

[295] CheCalc, “Cooling Tower Makeup Water,” 2023. https://checalc.com/solved/ctmakeup.html (accessed Jan. 03, 2023).

[296] JMP, “Cooling Tower and Condenser Water Design Part 9: Controlling Cycles of Concentration —.” https://jmpcoblog.com/hvac-blog/cooling-tower-and-condenser-water-design-part-9-controlling-cycles-of-concentration (accessed Jan. 04, 2023).

[297] RAC Foundation, “UK pump prices,” 2021. https://www.racfoundation.org/data/uk-daily-fuel-table-with-breakdown (accessed Jun. 02, 2021).

[298] S. Michailos, M. Walker, A. Moody, D. Poggio, and M. Pourkashanian, “A techno-economic assessment of implementing power-to-gas systems based on biomethanation in an operating waste water treatment plant,” *J Environ Chem Eng*, vol. 9, no. 1, p. 104735, 2021, doi: 10.1016/j.jece.2020.104735.

[299] U.S. Department of Energy and Energy Efficiency and Renewable Energy, “How To Calculate The True Cost of Steam,” 2003. Accessed: Apr. 24, 2023. [Online]. Available: https://www.energy.gov/eere/amo/articles/how-calculate-true-cost-steam#:~:text=In%20most%20companies%2C%20the%20reported,total%20amount%20of%20steam%20produced.

[300] National Academies, *Negative Emissions Technologies and Reliable Sequestration*. 2019. doi: 10.17226/25259.

[301] J. Young, N. McQueen, C. Charalambous, S. Foteinis, O. Hawrot, M. Ojeda, H. Pilorgé, J. Andresen, P. Psarras, P. Renforth, S. Garcia, and M. van der Spek, “The cost of direct air capture and storage: the impact of technological learning, regional diversity, and policy.,” *ChemRxiv Preprint*, pp. 1–37, 2022.

[302] Eurostat, “Electricity prices components for non-household consumers - annual data (from 2007 onwards),” 2022. https://ec.europa.eu/eurostat/databrowser/view/NRG_PC_205_C__custom_3590784/default/table?lang=en (accessed Oct. 15, 2022).

[303] GOV.UK, “Energy Security Bill factsheet: Network charging compensation scheme for energy intensive industries (added 9 May 2023),” May 29, 2023. https://www.gov.uk/government/publications/energy-security-bill-factsheets/energy-security-bill-factsheet-network-charging-compensation-scheme-for-energy-intensive-industries (accessed Jun. 14, 2023).

[304] M. Grubb and P. Drummond, “UK industrial electricity prices: Competitiveness in a low carbon world,” 2018. Accessed: Jun. 15, 2023. [Online]. Available: https://www.ucl.ac.uk/bartlett/sustainable/sites/bartlett/files/uk_industrial_electricity_prices_-_competitiveness_in_a_low_carbon_world.pdf

[305] M. Marchese, G. Buffo, M. Santarelli, and A. Lanzini, “CO2 from direct air capture as carbon feedstock for Fischer-Tropsch chemicals and fuels : Energy and economic analysis,” *Journal of CO2 Utilization*, vol. 46, p. 101487, 2021, doi: 10.1016/j.jcou.2021.101487.

[306] A. Garcia-Teruel, G. Rinaldi, P. R. Thies, L. Johanning, and H. Jeffrey, “Life cycle assessment of floating offshore wind farms: An evaluation of operation and maintenance,” *Appl Energy*, vol. 307, no. September 2021, p. 118067, 2022, doi: 10.1016/j.apenergy.2021.118067.

[307] NREL, “Wind LCA Harmonization,” vol. 2012, no. Awea, p. 2, 2013, doi: 10.1111/j.1530-9290.2012.00464.x/pdf.National.

[308] J. C. Koj, C. Wulf, A. Schreiber, and P. Zapp, “Site-dependent environmental impacts of industrial hydrogen production by alkalinewater electrolysis,” *Energies (Basel)*, vol. 10, no. 7, 2017, doi: 10.3390/en10070860.

[309] M. Delpierre, “An ex-ante LCA study on wind-based hydrogen production in the Netherlands,” *TU Delft Technology, Policy and Management*, no. August, 2019, [Online]. Available: https://repository.tudelft.nl/islandora/object/uuid%3Afc89a24e-9ef8-49cf-b5fb-3f3fa1e3051b

[310] T. Terlouw, K. Treyer, C. Bauer, and M. Mazzotti, “Life Cycle Assessment of Direct Air Carbon Capture and Storage with Low-Carbon Energy Sources,” *Environ Sci Technol*, vol. 55, no. 16, pp. 11397–11411, 2021, doi: 10.1021/acs.est.1c03263.

[311] Z. Abdin, C. J. Webb, and E. M. A. Gray, “Modelling and simulation of an alkaline electrolyser cell,” *Energy*, vol. 138, pp. 316–331, 2017, doi: 10.1016/j.energy.2017.07.053.

[312] H. Kojima, T. Matsuda, H. Matsumoto, and T. Tsujimura, “Development of dynamic simulator of alkaline water electrolyzer for optimizing renewable energy systems,” *Journal of International Council on Electrical Engineering*, vol. 8, no. 1, pp. 19–24, 2018, doi: 10.1080/22348972.2018.1436931.

[313] A. S. Tijani, N. A. B. Yusup, and A. H. A. Rahim, “Mathematical Modelling and Simulation Analysis of Advanced Alkaline Electrolyzer System for Hydrogen Production,” *Procedia Technology*, vol. 15, pp. 798–806, 2014, doi: 10.1016/j.protcy.2014.09.053.

[314] M. Sánchez, E. Amores, D. Abad, L. Rodríguez, and C. Clemente-Jul, “Aspen Plus model of an alkaline electrolysis system for hydrogen production,” *Int J Hydrogen Energy*, vol. 45, no. 7, pp. 3916–3929, 2020, doi: 10.1016/j.ijhydene.2019.12.027.

[315] N. A. Rahman, C. Jose Jol, A. A. Linus, D. S. Rozellia Kamel Sharif, and V. Ismail, “Fischer Tropsch water composition study from distillation process in gas to liquid technology with ASPEN simulation,” *Case Studies in Chemical and Environmental Engineering*, vol. 3, Jun. 2021, doi: 10.1016/j.cscee.2021.100106.

[316] G. Zang, P. Sun, A. A. Elgowainy, A. Bafana, and M. Wang, “Performance and cost analysis of liquid fuel production from H2and CO2based on the Fischer-Tropsch process,” *Journal of CO2 Utilization*, vol. 46, no. February, p. 101459, 2021, doi: 10.1016/j.jcou.2021.101459.

[317] M. J. Bos, S. R. A. Kersten, and D. W. F. Brilman, “Wind power to methanol: Renewable methanol production using electricity, electrolysis of water and CO2 air capture,” *Appl Energy*, vol. 264, no. August 2019, p. 114672, 2020, doi: 10.1016/j.apenergy.2020.114672.

[318] J. Elfving, C. Bajamundi, J. Kauppinen, and T. Sainio, “Modelling of equilibrium working capacity of PSA, TSA and TVSA processes for CO2 adsorption under direct air capture conditions,” *Journal of CO2 Utilization*, vol. 22, pp. 270–277, Dec. 2017, doi: 10.1016/j.jcou.2017.10.010.

[319] S. I. für Z. S. S. W. I. für K. U. E. W. Deutsches Zentrum für Luft und Raumfahrt (DLR), “MENA Fuels: Multikriterielle Bewertung von Bereitstellungstechnologien synthetischer Kraftstoffe, Teilbericht Nr. 3 (D2.1),” 2021.

[320] L. Jiang, W. Liu, R. Q. Wang, A. Gonzalez-diaz, M. F. Rojas-michaga, S. Michailos, M. Pourkashanian, X. J. Zhang, and C. Font-palma, “Sorption direct air capture with CO 2 utilization,” *Prog Energy Combust Sci*, vol. 95, no. January, p. 101069, 2023, doi: 10.1016/j.pecs.2022.101069.

[321] “Price of offshore wind power falls to cheapest ever level in UK | Wind power | The Guardian.” https://www.theguardian.com/environment/2022/jul/08/price-offshore-wind-power-falls-cheapest-ever-level-uk (accessed Feb. 22, 2023).

[322] C. M. Liu, N. K. Sandhu, S. T. McCoy, and J. A. Bergerson, “A life cycle assessment of greenhouse gas emissions from direct air capture and Fischer-Tropsch fuel production,” *Sustain Energy Fuels*, vol. 4, no. 6, pp. 3129–3142, 2020, doi: 10.1039/c9se00479c.

[323] The Royal Society, “Net zero aviation fuels: Resource requirements and environmental impacts,” 2023. Accessed: Apr. 24, 2023. [Online]. Available: https://royalsociety.org/-/media/policy/projects/net-zero-aviation/net-zero-aviation-fuels-policy-briefing.pdf

[324] A. Rogers and O. Parson, “GridCarbon: A smartphone app to calculate the carbon intensity of the UK electricity grid,” pp. 2–5, 2017.

[325] ESO, “ESO Data Portal: ESO Carbon Intensity Balancing Actions Methodology - Dataset| National Grid Electricity System Operator.” https://data.nationalgrideso.com/carbon-intensity1/carbon-intensity-of-balancing-actions/r/eso_carbon_intensity_balancing_actions_methodology#next (accessed Mar. 02, 2023).

[326] International Civil Aviation Organization, “Guidance on potential policies and coordinated approaches for the deployment of sustainable aviation fuels,” 2022. Accessed: Apr. 24, 2023. [Online]. Available: https://www.icao.int/environmental-protection/Documents/SAF/Guidance%20on%20SAF%20policies%20-%20Version%201.pdf

[327] AVFUEL, “Avfuel’s Carbon Offset Program.” https://www.avfuel.com/Fuel/Alternative-Fuels/Carbon-Offset (accessed Mar. 01, 2023).

[328] E. & I. S. Department for Business, “Hydrogen production costs 2021,” 2021. Accessed: Apr. 24, 2023. [Online]. Available: https://assets.publishing.service.gov.uk/government/uploads/system/uploads/attachment_data/file/1011506/Hydrogen_Production_Costs_2021.pdf

[329] R. Dahl, “Evaluation of the new Power & Biomass to Liquid (PBtL) concept for production of biofuels from woody biomass,” 2020.

[330] The Crown Estate's Offshore Wind Evidence and Change Programme, "Future Offshore Wind Future offshore wind scenarios: an assessment of deployment drivers," 2022. Accessed: Aug. 03, 2023. [Online]. Available: https://www.marinedataexchange.co.uk/details/3558/summary

[331] Scottish Carbon Capture & Storage, "Global CCS Map." https://www.sccs.org.uk/resources/global-ccs-map (accessed Aug. 03, 2023).

[332] The CCUS Hub, "East Coast Cluster," Jul. 28, 2023. https://ccushub.ogci.com/focus_hubs/east-coast-cluster/ (accessed Jul. 28, 2023).

[333] A. F. Young, H. G. D. Villardi, L. S. Araujo, L. S. C. Raptopoulos, and M. S. Dutra, "Detailed Design and Economic Evaluation of a Cryogenic Air Separation Unit with Recent Literature Solutions," *Ind Eng Chem Res*, vol. 60, no. 41, pp. 14830–14844, Oct. 2021, doi: 10.1021/acs.iecr.1c02818.

[334] R. Thomson, P. Kwong, E. Ahmad, and K. D. P. Nigam, "Clean syngas from small commercial biomass gasifiers; a review of gasifier development, recent advances and performance evaluation," *Int J Hydrogen Energy*, vol. 45, no. 41, pp. 21087–21111, 2020, doi: 10.1016/j.ijhydene.2020.05.160.

[335] N. Hanchate, S. Ramani, C. S. Mathpati, and V. H. Dalvi, "Biomass gasification using dual fluidized bed gasification systems: A review," *Journal of Cleaner Production*, vol. 280. Elsevier Ltd, Jan. 20, 2021. doi: 10.1016/j.jclepro.2020.123148.

[336] S. Pissot, T. B. Vilches, H. Thunman, and M. Seemann, "Dual fluidized bed gasification configurations for carbon recovery from biomass," *Energy and Fuels*, vol. 34, no. 12, pp. 16187–16200, Dec. 2020, doi: 10.1021/acs.energyfuels.0c02781.

[337] A. López-fernández, D. Bolonio, I. Amez, B. Castells, M. F. Ortega, and M. J. García-martínez, "Design and pinch analysis of a gft process for production of biojet fuel from biomass and plastics," *Energies (Basel)*, vol. 14, no. 19, pp. 1–31, 2021, doi: 10.3390/en14196035.

[338] G. Towler and R. Sinnott, *Chemical Engineering Design*. Elsevier, 2013. doi: 10.1016/C2009-0-61216-2.

[339] US Department of Energy, "Minimize Boiler Blowdown." https://www.energy.gov/sites/prod/files/2014/05/f16/steam9_blowdown.pdf (accessed Aug. 06, 2023).

[340] M. F. Rojas-Michaga, S. Michailos, E. Cardozo, M. Akram, K. J. Hughes, D. Ingham, and M. Pourkashanian, "Sustainable aviation fuel (SAF) production through power-to-liquid (PtL): A combined techno-economic and life cycle assessment," *Energy Convers Manag*, vol. 292, p. 117427, Sep. 2023, doi: 10.1016/j.enconman.2023.117427.

[341] United Nations Framework Convention on Climate Change, "Methodological tool Apportioning emissions from production processes between main product and co-and by-product," 2015.

[342] National Institute for Public Health and the Environment, "LCIA: the ReCiPe model | RIVM," 2018. https://www.rivm.nl/en/life-cycle-assessment-lca/recipe (accessed Jun. 01, 2021).

[343] T. Sonderegger and N. Stoikou, "Implementation of life cycle impact assessment methods in the ecoinvent database v3.9 and v3.9.1."

[344] S. Tighe, "Guidelines for Probabilistic Pavement Life Cycle Cost Analysis," *Transportation Research Record: Journal of the Transportation Research Board*, vol. 1769, no. 1, pp. 28–38, Jan. 2001, doi: 10.3141/1769-04.

[345] F. Habermeyer, J. Weyand, S. Maier, E. Kurkela, and R. U. Dietrich, “Power Biomass to Liquid — an option for Europe’s sustainable and independent aviation fuel production,” *Biomass Convers Biorefin*, 2023, doi: 10.1007/s13399-022-03671-y.

[346] 3keel, “Biomass for energy A framework for assessing the role of domestic feedstocks in the UK’s energy transition,” 2022.

[347] J. F. Schyns, M. J. Booij, and A. Y. Hoekstra, “The water footprint of wood for lumber, pulp, paper, fuel and firewood,” *Adv Water Resour*, vol. 107, pp. 490–501, Sep. 2017, doi: 10.1016/j.advwatres.2017.05.013.

[348] S.-Y. Pan, S. W. Snyder, A. I. Packman, Y. J. Lin, and P.-C. Chiang, “Cooling water use in thermoelectric power generation and its associated challenges for addressing water-energy nexus,” *Water-Energy Nexus*, vol. 1, no. 1, pp. 26–41, Jun. 2018, doi: 10.1016/j.wen.2018.04.002.

[349] A. Dufour, S. Valin, P. Castelli, S. Thiery, G. Boissonnet, A. Zoulalian, and P. A. Glaude, “Mechanisms and kinetics of methane thermal conversion in a syngas,” *Ind Eng Chem Res*, vol. 48, no. 14, pp. 6564–6572, 2009, doi: 10.1021/ie900343b.

[350] A. Inayat, A. Murni Melati, M. Ibrahim, A. Mutalib, and M. Khairuddin Yunus, “Kinetic Modeling of Biomass Steam Gasification System for Hydrogen Production with CO2 Adsorption,” in *Proceedings of International Conference for Technical Postgraduates (TECHPOS 2009)*, 2009.

[351] C. Gebald, T. Zimmermann, and P. Tingaut, “Porous adsorbent structure for adsorption of CO2 from a gas mixture,” 2012

[352] Ecoinvent, “Chemical factory construction, RER,” Jul. 26, 2023. https://v391.ecoquery.ecoinvent.org/Details/UPR/ff3bfab4-65c0-4f40-b84c-143fae9177f6/8b738ea0-f89e-4627-8679-433616064e82 (accessed Jul. 26, 2023).

APPENDIX A

A-1. Pyrolysis and gasification correlation parameters and kinetic expressions

Table A-1: Parameters for the correlations of pyrolysis [192], [349]**.**

Product	a	b	c
CH_4	-4.341×10^{-5}	10.12×10^{-2}	-51.08
H_2	1.362×10^{-5}	-2.517×10^{-2}	12.19
CO	-3.524×10^{-5}	9.770×10^{-2}	-24.93
CO_2	3.958×10^{-5}	-9.126×10^{-2}	64.02
C_2H_4	-6.873×10^{-5}	14.94×10^{-2}	-76.89
C_2H_6	8.265×10^{-6}	-2.105×10^{-2}	13.38
C_6H_6	-3.134×10^{-5}	7.544×10^{-2}	-42.72
C_7H_8	-4.539×10^{-6}	0.687×10^{-2}	1.462
C_6H_6O	1.508×10^{-5}	-3.662×10^{-2}	22.19
$C_{10}H_8$	-8.548×10^{-6}	1.882×10^{-2}	-9.851
H_2O	5.157×10^{-5}	11.86×10^{-2}	84.91

Table A-2: Reaction kinetics for homogenous and heterogeneous reactions [53]**.**

Heterogeneous reactions			**References**
1	$C_{10}H_8 \rightarrow 9C + \frac{1}{6}C_6H_6 + \frac{7}{2}H_2$	$r_1 = 21.11exp\left(-\frac{61000}{RT}\right)\frac{\dot{m_{char}}}{\dot{V_{reactor}}}C_{C_{10}H_8}$	[192]
2	$C_6H_6 + H_2O \rightarrow 3C + 2CH_4 + CO$	$r_2 = 21.11exp\left(-\frac{61000}{RT}\right)\frac{\dot{m_{char}}}{\dot{V_{reactor}}}C_{C_6H_6}$	[192]
3	$C_7H_8 + H_2 \rightarrow C_6H_6 + CH_4$	$r_3 = 21.11exp\left(-\frac{61000}{RT}\right)\frac{\dot{m_{char}}}{\dot{V_{reactor}}}C_{C_7H_8}$	[192]
4	$CH_4 \rightarrow C + 2H_2$	$r_4 = 0.01exp\left(-\frac{263000}{RT}\right)\frac{\dot{m_{char}}}{\dot{V_{reactor}}}P_{CH_4}$	[192]
Homogeneous reactions			
5	$CO_2 + H_2 \rightarrow CO + H_2O$	$r_5 = 1.26 \times 10^5 exp\left(-\frac{263000}{RT}\right)C_{CO_2}C_{H_2}$	[30]
6	$CO + H_2O \rightarrow CO_2 + H_2$	$r_6 = 2780exp\left(-\frac{12560}{RT}\right)C_{CO}C_{H_2O}$	[30]
7	$CH_4 + H_2O \rightarrow CO + 3H_2$	$r_7 = 234.14exp\left(-\frac{211000}{RT}\right){P_{CH_4}}^{-1.48}{P_{H_2O}}^{-0.11}{P_{H_2}}^{-0.91}$	[349]
8	$C + H_2O \rightarrow CO + H_2$	$r_8 = 2 \times 10^8 exp\left(-\frac{49884}{RT}\right)C_{H_2O}C_{Char}$	[350]
9	$C + 2H_2 \rightarrow CH_4$	$r_9 = 120exp\left(-\frac{148995}{RT}\right)C_{H_2}C_{Char}$	[350]
10	$C_{10}H_8 \rightarrow 9C + \frac{1}{6}C_6H_6 + \frac{7}{2}H_2$	$r_{10} = 3.4 \times 10^{14} exp\left(-\frac{350000}{RT}\right){C_{C_{10}H_8}}^{1.6}{C_{H_2}}^{-0.5}$	[192]
11	$C_6H_6 + H_2O \rightarrow 3C + 2CH_4 + CO$	$r_{11} = 4 \times 10^{16} exp\left(-\frac{443000}{RT}\right)C_{C_6H_6}{C_{H_2}}^{-0.4}{C_{H_2O}}^{0.2}$	[192]
12	$C_7H_8 + H_2 \rightarrow C_6H_6 + CH_4$	$r_{12} = 1.04 \times 10^{12} exp\left(-\frac{247000}{RT}\right)C_{C_7H_8}{C_{H_2}}^{0.5}$	[192]

A-2. Fortran Statements for the pyrolysis section

```
FACT=(100 - MOIST)/100
ASH=(ULT(1)/100)*FACT
N2=(ULT(4)/100)*FACT
CL2=(ULT(5)/100)*FACT
S=(ULT(6)/100)*FACT
EXT=ASH+N2+CL2+S
FACTT=(100-MOIST-ASH*100)/100
CH4=((-4.341E-5*TEM*TEM+10.12E-2*TEM-51.08)*FACTT)/100
H2=((1.362E-5*TEM*TEM-2.517E-2*TEM+12.19)*FACTT)/100
CO =((-3.524E-5*TEM*TEM+9.970E-2*TEM-24.93)*FACTT)/100
CO2 =((3.958E-5*TEM*TEM-9.126E-2*TEM+64.02)*FACTT)/100
C2H4 =((-6.873E-5*TEM*TEM+14.94E-2*TEM-76.89)*FACTT)/100
C2H6=((0.826E-5*TEM*TEM-2.105E-2*TEM+13.38)*FACTT)/100
C6H6=((-3.134E-5*TEM*TEM+7.544E-2*TEM-42.72)*FACTT)/100
C7H8=((-0.453E-5*TEM*TEM+0.687E-2*TEM+1.462)*FACTT)/100
C6H6O=((1.508E-5*TEM*TEM-3.662E-2*TEM+22.19)*FACTT)/100
C10H8=((-0.854E-5*TEM*TEM+1.882E-2*TEM-9.851)*FACTT)/100
H2O=((5.157E-5*TEM*TEM-11.86E-2*TEM+84.91)*FACTT + MOIST)/100
CHAR=1-CH4-H2-CO-CO2-C2H4-C2H6-C6H6-C7H8-C6H6O-C10H8-H2O-EXT
```

A-3. Matlab Code for the gasification reactions

```
function
[ParEnt,ParReal,CorSal]=user_model(ParEnt,ParReal,CorEnt)
T=CorEnt(27);
P=CorEnt(28);
zf=ParReal(1);
dia=ParReal(2);
z0=0;
a0=CorEnt(1);
b0=CorEnt(7);
c0=CorEnt(15);
d0=CorEnt(6);
e0=CorEnt(3);
f0=CorEnt(2);
g0=CorEnt(23);
h0=CorEnt(14);
l0=CorEnt(16);

zspan = [z0 zf]; % Range for the length of the reactor
y0 = [a0; b0; c0; d0; e0; f0; g0; h0; l0];
```

```
[z, y] =ode45(@(z,y) Designequation(z,y,T,P,dia),zspan,y0);

TA=[z y];
A=(TA(:,2));
B=(TA(:,3));
C=(TA(:,4));
D=(TA(:,5));
E=(TA(:,6));
F=(TA(:,7));
G=(TA(:,8));
H=(TA(:,9));
L=(TA(:,10));

CorSal=CorEnt;
CorSal(1)=A(end);%kmoles of H2O per second at the exit of the
reactor
CorSal(7)=B(end);%kmoles of H2 per second at the exit of the
reactor
CorSal(15)=C(end);%kmoles of C per second at the exit of the
reactor
CorSal(6)=D(end);%kmoles of CH4 per second at the exit of the
reactor
CorSal(3)=E(end);%kmoles of CO per second at the exit of the
reactor
CorSal(2)=F(end);%kmoles of CO2 per second at the exit of the
reactor
CorSal(23)=G(end);%kmoles of C10H8 per second at the exit of the
reactor
CorSal(14)=H(end);%kmoles of C6H6 per second at the exit of the
reactor
CorSal(16)=L(end);%kmoles of C7H8 per second at the exit of the
reactor
CorSal(26)=sum(CorSal(1:25));

function dydz = Designequation(z,y,T,P,dia)
a=y(1);
b=y(2);
c=y(3);
d=y(4);
e=y(5);
f=y(6);
g=y(7);
h=y(8);
l=y(9);
ca=((a*P)/((a+b+d+e+f+g+h+l)*8.314e3*T));
cb=((b*P)/((a+b+d+e+f+g+h+l)*8.314e3*T));
cc=((c*P)/((a+b+d+e+f+g+h+l)*8.314e3*T));
ce=((e*P)/((a+b+d+e+f+g+h+l)*8.314e3*T));
cf=((f*P)/((a+b+d+e+f+g+h+l)*8.314e3*T));
cg=((g*P)/((a+b+d+e+f+g+h+l)*8.314e3*T));
ch=((h*P)/((a+b+d+e+f+g+h+l)*8.314e3*T));
cl=((l*P)/((a+b+d+e+f+g+h+l)*8.314e3*T));
Pd=((d*P)/(a+b+d+e+f+g+h+l));
Pa=((a*P)/(a+b+d+e+f+g+h+l));
Pb=((b*P)/(a+b+d+e+f+g+h+l));
```

```
r1=21.11*(exp(-61000/(8.314*T)))*(cg)*((cc)*12);
r2=21.11*(exp(-61000/(8.314*T)))*(ch)*((cc)*12);
r3=21.11*(exp(-61000/(8.314*T)))*(cl)*((cc)*12);
r4=0.01*(exp(-263000/(8.314*T)))*(Pd)*((cc)*12);
r5=1.26e5*(exp(-263000/(8.314*T)))*(cf)*(cb);
r6=2780*(exp(-12560/(8.314*T)))*(ce)*(ca);
r7=234.136*(exp(-211000/(8.314*T)))*((Pd)^(-1.48))*((Pa)^(-
0.11))*((Pb)^(-0.91));
r8=2e8*(exp(-49884/(8.314*T)))*(cc)*(ca);
r9=120*(exp(-148995/(8.314*T)))*(cc)*(cb);
r10=3.4e14*(exp(-350000/(8.314*T)))*((cg)^(1.6))*((cb)^(-0.5));
r11=4e16*(exp(-443000/(8.314*T)))*((ch)^(1.3))*((cb)^(-
0.4))*((ca)^(0.2));
r12=1.04e12*(exp(-247000/(8.314*T)))*(cl)*((cb)^(0.5));
da=(-(r2)+(r5)-(r6)-(r7)-(r8)-(r11))*(pi*((dia/2)^2));
db=((7/2)*(r1)+2*(r4)-(r5)+(r6)+3*(r7)+(r8)-2*(r9)+(7/2)*(r10)-
(r12)-(r3))*(pi*((dia/2)^2));
dc=(9*r1+3*r2+r4-r8-r9+9*r10+3*r11)*(pi*((dia/2)^2));
dd=(2*(r2)+(r3)-(r4)-(r7)+(r9)+2*(r11)+(r12))*(pi*((dia/2)^2));
de=((r2)+(r5)-(r6)+(r7)+(r8)+(r11))*(pi*((dia/2)^2));
df=(-(r5)+(r6))*(pi*((dia/2)^2));
dg=(-(r1)-(r10))*(pi*((dia/2)^2));
dh=(-(r2)+(r3)+(1/6)*(r10)-
(r11)+(r12)+(1/6)*(r1))*(pi*((dia/2)^2));
dl=(-(r3)-(r12))*(pi*((dia/2)^2));
dydz = [da; db; dc; dd; de; df; dg; dh; dl];
end
end
```

A-4. Life cycle inventories

Table A-3: Transport of wood chips from forest to process plant

PRODUCTS		
Outputs to technosphere: Products and co-products	**Amount**	**Unit**
Wood chips, wet, measured as dry mass {UK}| market for | Cut-off, U	0.24	kg
INPUTS		
Inputs from nature	**Amount**	**Unit**
Inputs from technosphere: materials/fuels	**Amount**	**Unit**
Transport, freight, lorry, unspecified {ZA}| market for transport, freight, lorry, unspecified | Cut-off, U	1.75E-02	tkm
Wood chips, wet, measured as dry mass {RoW}| hardwood forestry, oak, sustainable forest management | Cut-off, U	1.67E-02	kg
Wood chips, wet, measured as dry mass {RoW}| softwood forestry, spruce, sustainable forest management | Cut-off, U	2.28E-01	kg
Inputs from technosphere: electricity/heat	**Amount**	**Unit**

Table A-4: FT process (Displacement method), BECCS Scenario.

Products		
Outputs to technosphere: Products and co-products	**Amount**	**Unit**
Jet fuel production, from synthetic gas, from wood gasification, at DFBG, with CCS	1	MJ
Outputs to technosphere: Avoided products	Amount	**Unit**
Naphtha {Europe without Switzerland}| naphtha production, petroleum refinery operation | Cut-off, U	3.80E-03	kg
Diesel {Europe without Switzerland}| diesel production, petroleum refinery operation | APOS, S	1.14E-02	kg
Electricity, high voltage {GB}| production mix | APOS, S	1.78E-02	kWh
Inputs		
Inputs from nature	Amount	**Unit**
Water, cooling, unspecified natural origin, GB	1.06E+00	l
Water, process and cooling, unspecified natural origin	1.57E-01	l
Inputs from technosphere: materials/fuels	Amount	**Unit**
Wood chips, wet, measured as dry mass {UK}| market for | Cut-off, U	2.45E-01	kg
Monoethanolamine {GLO}| market for | Cut-off,U	2.07E-04	kg
Silica sand {GLO}| market for | Cut-off, U	1.21E-02	kg
Cobalt {GLO}| market for | Cut-off, U	1.96E-05	kg
Zeolite, powder {GLO}| market for | Cut-off, U	2.19E-06	kg
Portafer {GLO}| market for | Cut-off, U	1.91E-07	kg
Aluminium oxide, non-metallurgical {RoW}| market for aluminium oxide, non-metallurgical | Cut-off, U	2.71E-07	kg
Nickel, 99.5% {GLO}| market for | Cut-off, U	3.00E-07	kg
Petroleum refinery {GLO}| market for refinery | Cut-off, U	3.11E-11	p
Inputs from technosphere: electricity/heat	**Amount**	**Unit**

Outputs		
Emissions to air	Amount	**Unit**
Carbon dioxide, biogenic	1.95E-01	kg
Carbon monoxide, biogenic	5.03E-06	kg
Nitrogen oxides	1.49E-03	kg
Sulfur dioxide	2.78E-04	kg
Water/m3	5.82E-02	m3
Monoethanolamine	2.07E-04	kg
Outputs to technosphere: Waste treatment	Amount	**Unit**
Inert waste, for final disposal {RoW}| market for inert waste, for final disposal | Cut-off, U	1.21E-02	kg
Wastewater, from residence {RoW}| market for wastewater, from residence | Cut-off, U	1.94E-04	m3
Wood ash mixture, pure {Europe without Switzerland}| market for wood ash mixture, pure | Cut-off, U	1.35E-03	kg
CO2	1.38E-01	kg

Table A-5: FT process (Displacement method), BE Scenario.

Products		
Outputs to technosphere: Products and co-products	**Amount**	**Unit**
Jet fuel production, from synthetic gas, from wood gasification, at DFBG, with CCS	1	MJ
Outputs to technosphere: Avoided products	Amount	**Unit**
Naphtha {Europe without Switzerland}| naphtha production, petroleum refinery operation | APOS, S	3.80E-03	kg
Diesel {Europe without Switzerland}| diesel production, petroleum refinery operation | APOS, S	1.14E-02	kg
Electricity, high voltage {GB}| production mix | APOS, S	3.00E-02	kWh
Inputs		
Inputs from nature	Amount	**Unit**
Water, cooling, unspecified natural origin, GB	1.06E+00	l
Water, process and cooling, unspecified natural origin	1.57E-01	l
Inputs from technosphere: materials/fuels	Amount	**Unit**
Wood chips, wet, measured as dry mass {UK}| market for | Cut-off, U	2.45E-01	kg
Monoethanolamine {GLO}| market for | APOS, S	2.07E-04	kg
Silica sand {GLO}| market for | Cut-off, U	1.21E-02	kg
Cobalt {GLO}| market for | Cut-off, U	1.96E-05	kg
Zeolite, powder {GLO}| market for | Cut-off, U	2.19E-06	kg
Portafer {GLO}| market for | Cut-off, U	1.91E-07	kg
Aluminium oxide, non-metallurgical {RoW}| market for aluminium oxide, non-metallurgical | Cut-off, U	2.71E-07	kg
Nickel, 99.5% {GLO}| market for | Cut-off, U	3.00E-07	kg
Petroleum refinery {GLO}| market for refinery | Cut-off, U	3.11E-11	p
Inputs from technosphere: electricity/heat	**Amount**	**Unit**

Outputs		
Emissions to air	Amount	**Unit**
Carbon dioxide, biogenic	3.33E-01	kg
Carbon monoxide, biogenic	1.07E-04	kg
Nitrogen oxides	1.49E-03	kg
Sulfur dioxide	2.78E-04	kg
Water/m3	6.00E-02	m3
Monoethanolamine	2.07E-04	kg
Outputs to technosphere: Waste treatment	Amount	**Unit**
Inert waste, for final disposal {RoW}| market for inert waste, for final disposal | Cut-off, U	1.21E-02	kg
Wastewater, from residence {RoW}| market for wastewater, from residence | Cut-off, U	1.94E-04	m3
Wood ash mixture, pure {Europe without Switzerland}| market for wood ash mixture, pure | Cut-off, U	1.35E-03	kg

Table A-6: FT process (Energy allocation), BECCS scenario.

Products			
Outputs to technosphere: Products and co-products	**Amount**	**Unit**	**Allocation %**
Jet fuel production, from synthetic gas, from wood gasification, at DFBG, with CCS	1	MJ	58.35169
Naphtha {Europe without Switzerland}| naphtha production, petroleum refinery operation | Cut-off, U	3.80E-03	kg	9.630282
Diesel {Europe without Switzerland}| diesel production, petroleum refinery operation | APOS, S	1.14E-02	kg	28.2796
Electricity, high voltage {GB}| production mix | APOS, S	1.78E-02	kWh	3.738425
Outputs to technosphere: Avoided products	**Amount**	**Unit**	
Inputs			
Inputs from nature	Amount	**Unit**	
Water, cooling, unspecified natural origin, GB	1.06	l	
Water, process and cooling, unspecified natural origin	0.16	l	
Inputs from technosphere: materials/fuels	Amount	**Unit**	
Wood chips, wet, measured as dry mass {UK}| market for | Cut-off, U	2.45E-01	kg	
Monoethanolamine {GLO}| market for | Cut-off,U	2.07E-04	kg	
Silica sand {GLO}| market for | Cut-off, U	1.21E-02	kg	
Cobalt {GLO}| market for | Cut-off, U	1.96E-05	kg	
Zeolite, powder {GLO}| market for | Cut-off, U	2.19E-06	kg	
Portafer {GLO}| market for | Cut-off, U	1.91E-07	kg	
Aluminium oxide, non-metallurgical {RoW}| market for aluminium oxide, non-metallurgical | Cut-off, U	2.71E-07	kg	
Nickel, 99.5% {GLO}| market for | Cut-off, U	3.00E-07	kg	
Petroleum refinery {GLO}| market for refinery | Cut-off, U	3.11E-11	p	

Inputs from technosphere: electricity/heat	Amount	Unit
Outputs		
Emissions to air	**Amount**	**Unit**
Carbon dioxide, biogenic	1.95E-01	kg
Carbon monoxide, biogenic	5.03E-06	kg
Nitrogen oxides	1.49E-03	kg
Sulfur dioxide	2.78E-04	kg
Water/m3	5.82E-02	m3
Monoethanolamine	2.07E-04	kg
Outputs to technosphere: Waste treatment	**Amount**	**Unit**
Inert waste, for final disposal {RoW}| market for inert waste, for final disposal | Cut-off, U	1.21E-02	kg
Wastewater, from residence {RoW}| market for wastewater, from residence | Cut-off, U	1.94E-04	m3
Wood ash mixture, pure {Europe without Switzerland}| market for wood ash mixture, pure | Cut-off, U	1.35E-03	kg
CO2	1.38E-01	kg

Table A-7: FT process (Energy allocation), BE Scenario.

Products			
Outputs to technosphere: Products and co-products	**Amount**	**Unit**	**Allocation %**
Jet fuel production, from synthetic gas, from wood gasification, at DFBG, with CCS	1	MJ	56.90
Naphtha {Europe without Switzerland}| naphtha production, petroleum refinery operation | Cut-off, U	3.80E-03	kg	9.39
Diesel {Europe without Switzerland}| diesel production, petroleum refinery operation | APOS, S	1.14E-02	kg	27.57
Electricity, high voltage {GB}| production mix | APOS, S	3.00E-02	kWh	6.14
Outputs to technosphere: Avoided products	**Amount**	**Unit**	
Inputs			
Inputs from nature	**Amount**	**Unit**	
Water, cooling, unspecified natural origin, GB	1.06	l	
Water, process and cooling, unspecified natural origin	0.16	l	
Inputs from technosphere: materials/fuels	**Amount**	**Unit**	
Wood chips, wet, measured as dry mass {UK}| market for | Cut-off, U	2.45E-01	kg	
Monoethanolamine {GLO}| market for | Cut-off,U	2.07E-04	kg	
Silica sand {GLO}| market for | Cut-off, U	1.21E-02	kg	
Cobalt {GLO}| market for | Cut-off, U	1.96E-05	kg	
Zeolite, powder {GLO}| market for | Cut-off, U	2.19E-06	kg	
Portafer {GLO}| market for | Cut-off, U	1.91E-07	kg	
Aluminium oxide, non-metallurgical {RoW}| market for aluminium oxide, non-metallurgical | Cut-off, U	2.71E-07	kg	
Nickel, 99.5% {GLO}| market for | Cut-off, U	3.00E-07	kg	
Petroleum refinery {GLO}| market for refinery | Cut-off, U	3.11E-11	p	

Inputs from technosphere: electricity/heat	Amount	Unit
Outputs		
Emissions to air	**Amount**	**Unit**
Carbon dioxide, biogenic	3.33E-01	kg
Carbon monoxide, biogenic	1.07E-04	kg
Nitrogen oxides	1.49E-03	kg
Sulfur dioxide	2.78E-04	kg
Water/m3	6.00E-02	m3
Monoethanolamine	2.07E-04	kg
Outputs to technosphere: Waste treatment	**Amount**	**Unit**
Inert waste, for final disposal {RoW}| market for inert waste, for final disposal | Cut-off, U	1.21E-02	kg
Wastewater, from residence {RoW}| market for wastewater, from residence | Cut-off, U	1.94E-04	m3
Wood ash mixture, pure {Europe without Switzerland}| market for wood ash mixture, pure | Cut-off, U	1.35E-03	kg

A-5. Environmental impacts of SAF and fossil jet fuel

Table A-8. Recipe 2016 Midpoint environmental impact categories.

Symbol	Impact category
A	Global warming
B	Stratospheric ozone depletion
C	Ionizing radiation
D	Ozone formation, Human health
E	Fine particulate matter formation
F	Ozone formation, Terrestrial ecosystems
G	Terrestrial acidification
H	Freshwater eutrophication
I	Marine eutrophication
J	Terrestrial ecotoxicity
K	Freshwater ecotoxicity
L	Marine ecotoxicity
M	Human carcinogenic toxicity
N	Human non-carcinogenic toxicity
O	Land use
P	Mineral resource scarcity
Q	Fossil resource scarcity
R	Water consumption

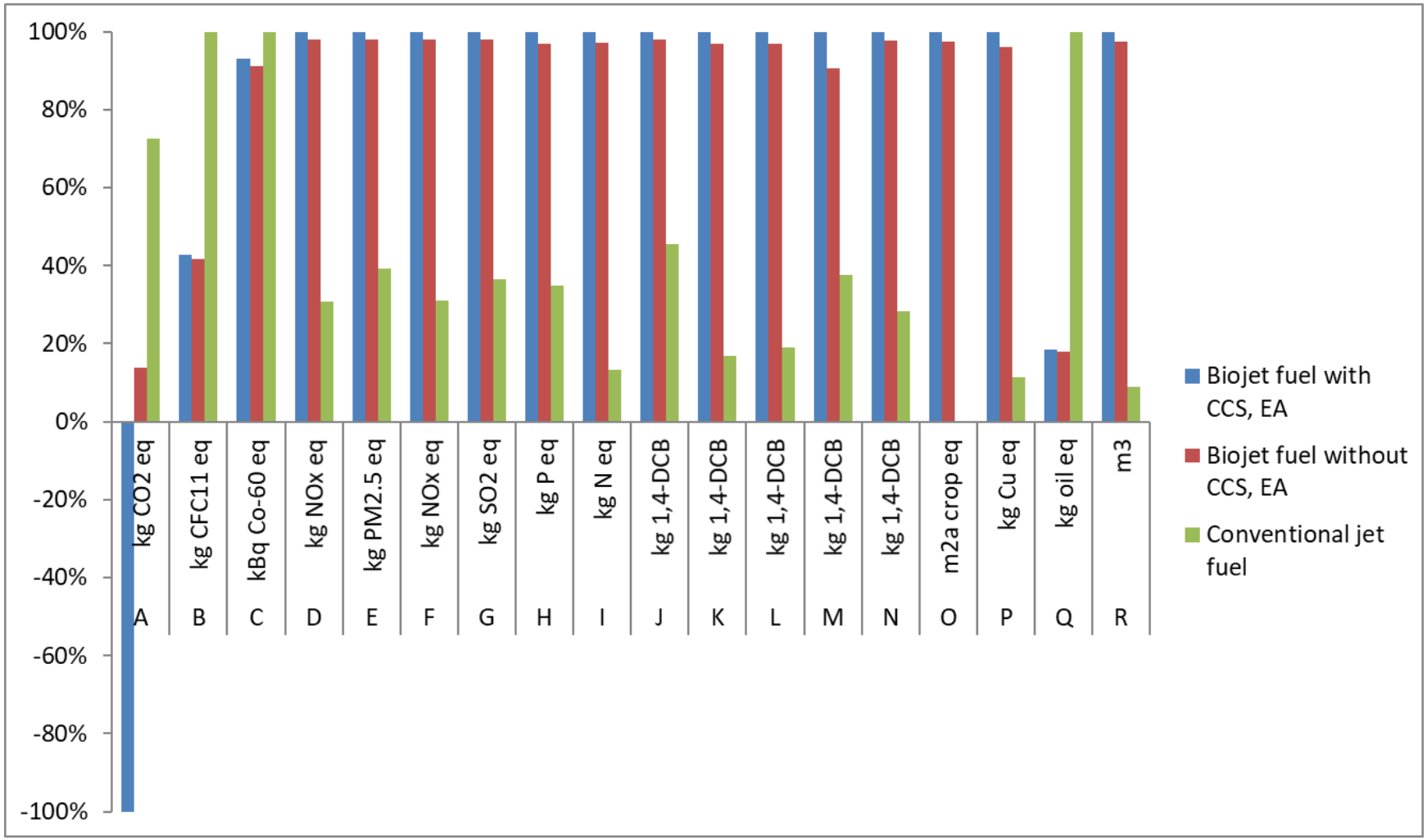

Figure A-1: Recipe 2016 Midpoint environmental impact categories for the Energy-allocation (EA) results of BECCS and BE scenarios, against conventional jet fuel.

APPENDIX B

B-1. Direct Air Capture modelling

A simplified model has been used for the calculation of the working capacities of the adsorbent and obtain an estimate of the amount of CO_2 and H_2O produced in the DAC unit. It is important to highlight that the model takes into account the effect of the relative humidity in the working capacity of CO_2. The energy requirements could be calculated through geometry assumptions; however, due to the modularity of the system, the power and thermal requirements are taken from the literature [260]. As in previous studies, the calculations were based on the sorbent APDES-NFC, which according to Sabatino et al. [270] is supposed to be similar to the one used by Climeworks. The CO_2 equilibrium loading capacity (q_{CO2}) is calculated according to the temperature-dependant Toth equation (Equations B.1, B.2, B.3, B.4). The calculation of an empirical temperature (Equation B.5) also captures the effect of the humidity in the calculation of the CO_2 loading capacity.

$$q_{CO2}(p,T) = \left[\frac{n_s b p_{CO2}}{((1+(bp_{CO2})^t)^{1/t}}\right]_{chem} + \left[\frac{n_s b p_{CO2}}{((1+(bp_{CO2})^t)^{1/t}}\right]_{phys}$$

Equation B.1

$$n_s = n_{s0} exp\left[\chi\left(1-\frac{T}{T_0}\right)\right]$$

Equation B.2

$$b = b_0 exp\left[\frac{\Delta H_0}{RT_0}\left(\frac{T_0}{T}-1\right)\right]$$

Equation B.3

$$t = t_0 + \alpha\left(1-\frac{T_0}{T}\right)$$

Equation B.4

$$T_{eq}(T,H) = T - a\left(\frac{278K}{T}\right)^b RH$$

Equation B.5

In Equation B.1, B.2, B.3 and B.4, ns, b and t are Toth parameters that depend on the temperature. Sabatino et al. adjusted these equations to experimental work available in the open literature, for a group of commercial solid sorbents, from which the values for the sorbent APDES-NFC are considered (Table B.1). In equation B.5, RH is the relative humidity, while 'a' and 'b' are parameters that were adjusted by Sabatino et al. from the humidity-related experimental data provided by Veneman et al. (Table B.1).

The working capacity of the water was calculated by using the Guggenheim-Anderson-de Boer (GAB) model (Equation B.6). Similar to the Toth model, Equations B.7, B.8 and B.9 are used to calculate the temperature-dependant parameters that are applied in the GAB model. The various experimental fitted values are listed in Table B.1.

$$q_{H_2O}(T, p_{H_2O}) = C_m \frac{C_G K_{ads} \frac{p_{H_2O}}{p_0}}{\left(1 - K_{ads} \frac{p_{H_2O}}{p_0}\right)\left(1 + (C_G - 1) K_{ads} \frac{p_{H_2O}}{p_0}\right)}$$

Equation B.6

$$C_G(T) = C_{G,0} \exp\left(\frac{\Delta H_C}{RT}\right)$$

Equation B.7

$$K_{ads}(T) = K_0 \exp\left(\frac{\Delta H_K}{RT}\right)$$

Equation B.8

$$C_m(T) = C_{m,0} \exp\left(\frac{\beta}{T}\right)$$

Equation B.9

Table B-1: Fitted parameters for the empirical equations for the APDES-NFC sorbent.

Parameter	APDES-NFC	Reference
CARBON DIOXIDE		
T0 (K)	296	[270]
PHYSISORPTION		
b0 (1/Mpa)	$5.60\times10^{+05}$	
ΔH (kJ/mol)	50	
t0 (-)	0.368	
α (-)	0.368	
ns0 (mol/kg)	2.31	
χ (-)	2.501	
CHEMISORPTION		
b0 (1/Mpa)	-	
ΔH (kJ/mol)	-	
t0 (-)	-	
α	-	
ns0 (mol/kg)	-	
χ (-)	-	
EMPIRICAL TEMPERATURE (RH EFFECT)		
a (-)	116.87	
b (-)	15	
WATER		
Cg0 (-)	6.86	[351]
ΔHc (kJ/mol)	-4.12	
K0 (-)	2.27	
ΔHk (kJ/mol)	-2.53	
Cm0 (mol/kg)	0.0208	
β [K]	1540	
PROCESS CONDITIONS		
T_{ads} (K)	283	[276]
P_{ads} (Pa)	1×10^{5}	[276]
$y_{CO2,\ ads}$ (-)	0.0004	[270]
RH_{ads} (%)	85	[276]
T_{des}(K)	388	[270]
P_{des}(Pa)	1×10^{4}	[270]
$y_{CO2,\ des}$(-)	To be calculated	-
RH % des	To be calculated	-

The concentration of CO_2 during the desorption stage is calculated by the relation of the working capacities of the CO_2 and H_2O (Equation B-10), which are calculated considering the solid efficiencies of 0.55 and 0.57 for the CO_2 and the H_2O respectively, according to Bos et al. [317].

At the same time, the working capacities depend of the desorption conditions. Therefore, Equation B-10, B-11 and B-12 are solved iteratively.

$$x_{CO2,des} = \frac{\Delta q_{CO2}\eta_{s,CO2}}{\Delta q_{CO2}\eta_{s,CO2} + \Delta q_{H2O}\eta_{s,H2O}}$$

Equation B-10

$$RH_{des} = \frac{P_{des}(1 - x_{CO2,des})}{P_{sat}(T_{des})}$$

Equation B-11

$$\Delta q_i = q_{i,ads} - q_{i,des}$$

Equation B-12

B-2. DAC CO_2 capture cost estimation methodology

The cost estimation of the DAC section is based on the methodology presented by Young et al. [301]. The researchers employed the hybrid costing approach, which combines a bottom-up cost estimation of the First-of-a-Kind (FOAK) project and a top-down approach, leveraging technological learning, to calculate the costs of future, Nth-of-a-Kind (NOAK) projects. The chosen scale for the FOAK plant of the solid sorbent technology is based on the Hinwil plant, operated by Climeworks. The following sections, summarize the approach proposed by Young et al. [301], while pointing out some modifications to better reflect the scenario analysed by this study.

B-2.1 FOAK CAPEX estimation

Initially, Young et al. [301]estimated the direct material costs for the different components of a FOAK plant, which were upgraded to installed costs through installation factors. It is important to note that our research only takes into account the capture and utilisation of CO_2, and hence CO_2 compression, transport and storage are excluded from any analysis. The installation cost (IC) is increased by a factor of 1.15 to become the "installed cost with engineering procurement" (EPC), which is then modified to the UK context by a "Material scaling factor" (x_1). Following, the EPC is escalated to the total project cost (TPC) of the FOAK plant. The TPC is obtained from equation B-13:

$$TPC = EPC * (1 + x_2/100)$$

Equation B-13

For this, the EPC is added with the contingencies (x_2), which are TRL dependant. Then, by using Equation B-14, the total capital requirement (TCR) was calculated by adding the overnight costs, which are composed by the owner's costs, spare parts costs, start-up capital, start-up labour, start-up fuel, and start-up chemicals:

$$TCR = TPC + Overnight\ costs$$

Equation B-14

The following step consists in calculating the capital recovering factor (CRF), by using a discount rate (x_3) specific for the UK, and 20 years as plant life (differently to the 25 years proposed by Young et al. [301]):

$$CRF = \frac{x_3 * [(1 + x_3)^T]}{-1 + (1 + x_3)^T}$$

Equation B-15

Then, the CRF is used to annualise the TCR (ATCR), and by applying a capacity factor of 90%, the CAPEX for the FOAK plant is calculated, as shown in the following Equation B-16:

$$ATCR = 0.9 * AnTCR$$

Equation B-16

The factors marked as 'x_1, x_2, and x_3' are associated to some uncertainty and expressed with a triangular distribution (minimum, mean, and maximum), therefore the CAPEX calculation is tackled with a probabilistic approach, from which the mean value is assumed as the CAPEX for the unit. For more information about the values of the aforementioned factors, please refer to Young et al. [301].

B-2.2 FOAK OPEX estimation

The OPEX estimation is divided into 'Fixed Operating and Maintenance and costs' (FOM) and 'Variable Operating Costs' (VOC). The FOM is constituted by the direct and indirect labour, as well as maintenance, insurance and local taxes. These parameters are calculated based on reasonable assumptions, and some of them are estimated as a percentage of the TPC [301]; then, these parameters are adjusted according to some factors that are location specific, and therefore adjusted to the UK context.

As for the VOC costs, this section of the OPEX is made of energy requirements (heat and power), cooling water and chemical costs (solid sorbent). The energy requirements are considered from the study published by Deutz et al. [260]. Moreover, the VOC estimation does not consider the heat requirement, since the DAC unit of the proposed system is integrated to the process plant, from which it receives low grade heat as required. Furthermore, the cost of the electricity is considered constant and the value calculated by the software SAM is assumed. Finally, the addition of the FOM and VO result in the total OPEX for the FOAK plant.

B-2.3 NOAK cost estimation

The resulting ATCR and OPEX calculated based on the methodology explained in the previous sections can be combined to calculate the cost of CO_2 capture when a FOAK plant is used. The FOAK CO_2 capture cost must then be upgraded to t that of the NOAK plant, the capacity of which is adjusted to the required CO_2 for the refinery plant. The learning rates proposed by Young et al. [301] are applied, as shown in Equation B-17 and B-18.

$$b = -\frac{\ln(1 - Lr)}{ln2}$$

Equation B-17

$$y = ax^{-b}$$

Equation B-18

In equation B-17, b represents the learning exponent, while Lr is the learning rate. The estimated b is then used in Equation B-18, where x represents the ratio of the desired capacity over the FOAK capacity. 'y' is the NOAK CAPEX or OPEX estimated in \$/tonneCO_2. Since the FOM estimation depends on the CAPEX (TPC) value, the same learning rate is applied for both cases. The value of Lr provided inin [301] is again expressed as a range with a minimum, middle and maximum values, and therefore a probabilistic approach is employed for the NOAK cost estimations. As for the VOC estimations, the authors proposed to use different Lr for the NOAK-VOC value. However, this value indirectly implies that the energy consumption of the system will be lower in a NOAK plant; in our study, being more conservative, it is assumed that the NOAK and FOAK VOC costs are the same (energy requirements will stay constant in the next years). Finally, the upgraded CAPEX, FOM and VOC are added, resulting in the NOAK-CO_2 capture cost. The estimations and the approach proposed by Young et al. [301] are based in 2019 in US dollars,

and therefore, they are adjusted accordingly to the set conditions of the economic assessment of this study.

B-3. Life Cycle Inventories

The inventories for the most significant WtWa stages are shown in the following tables. Table B-2 provides the main inventory for the operation of the DAC unit. The background information for the construction section can be found in the study of Terlouw et al. [310]. Tables B-3, B-4, and B-5 describe the mass and energy balance of the operation of the alkaline electrolyser, using different approaches for the multi-functionality of this stage. The background information of the construction can be found in the study of Koj et al. [308], while the operation inventory was formulated based on the information provided by Holst et al. [103]. Similarly, Tables B-6 and B-7, describe the operation of the process plant, by considering energy and exergy allocations. These inventories were constructed based on the models developed in Aspen Plus.

Table B-2: LCI of DAC operation**.**

Products		
Outputs to technosphere: Products and co-products	**Amount**	**Unit**
CO2 captured from air	1000	kg
Outputs to technosphere: Avoided products	**Amount**	**Unit**
Inputs		
Inputs from nature	**Amount**	**Unit**
Inputs from technosphere: materials/fuels	**Amount**	**Unit**
DAC unit construction	1.25E-05	p
Chemical, organic {GLO}| market for | Cut-off, U	7.5	kg
Inputs from technosphere: electricity/heat	**Amount**	**Unit**
Electricity, high voltage {GB}| electricity production, wind, 1-3MW turbine, offshore |	2600	MJ
Outputs		
Emissions to air	**Amount**	**Unit**
Emissions to water	**Amount**	**Unit**
Outputs to technosphere: Waste treatment	**Amount**	**Unit**

Table B-3: LCI of AE operation, without allocation to the by-products.

WITHOUT ALLOCATION		
Products		
Outputs to technosphere: Products and co-products	**Amount**	**Unit**
Hydrogen, gaseous produced from AE	1	kg
Outputs to technosphere: Avoided products	**Amount**	**Unit**
Inputs		
Inputs from nature	**Amount**	**Unit**
Inputs from technosphere: materials/fuels	**Amount**	**Unit**
Nitrogen, liquid {RoW}| market for | Cut-off, U	0.29	g
Potassium hydroxide {GLO}| market for | Cut-off, U	1.9	g
Inputs from technosphere: electricity/heat	**Amount**	**Unit**
Electricity, high voltage {GB}| electricity production, wind, 1-3MW turbine, offshore | Cut-off, U	192.09	MJ
Alkaline Electrolyser Cell Stack Construction	9.63E-08	p
Outputs		
Emissions to air	**Amount**	**Unit**
Emissions to water	**Amount**	**Unit**
Outputs to technosphere: Waste treatment	**Amount**	**Unit**

Table B-4: LCI of AE operation, with exergy allocation.

INVENTORY 2-1 EXERGY ALLOCATION			
Products			
Outputs to technosphere: Products and co-products	**Amount**	**Unit**	**Allocation %**
Hydrogen, gaseous produced from AE	1	kg	90.34%
Heat, district or industrial, natural gas {Europe without Switzerland}| market for he	29254.58	kJ	2.93%
Oxygen	4.33	kg	6.72%
Outputs to technosphere: Avoided products	**Amount**	**Unit**	
Inputs			
Inputs from nature	**Amount**	**Unit**	
Inputs from technosphere: materials/fuels	**Amount**	**Unit**	
Nitrogen, liquid {RoW}| market for | Cut-off, U	0.29	g	
Potassium hydroxide {GLO}| market for | Cut-off, U	1.9	g	
Inputs from technosphere: electricity/heat	**Amount**	**Unit**	
Electricity, high voltage {GB}| electricity production, wind, 1-3MW turbine, offshore | Cut-off,	192.09	MJ	
Alkaline Electrolyser Cell Stack Construction	9.63E-08	p	
Outputs			
Emissions to air	**Amount**	**Unit**	
Emissions to water	**Amount**	**Unit**	
Outputs to technosphere: Waste treatment	**Amount**	**Unit**	

Table B-5: LCI of AE operation, with energy allocation.

INVENTORY 2-1 ENERGY ALLOCATION			
Products			
Outputs to technosphere: Products and co-products	**Amount**	**Unit**	**Allocation %**
Hydrogen, gaseous produced from AE	1	kg	82.90%
Heat, district or industrial, natural gas {Europe without Switzerland}| market for he	2.93E+04	kJ	17.10%
Outputs to technosphere: Avoided products	**Amount**	**Unit**	
Inputs			
Inputs from nature	**Amount**	**Unit**	
Inputs from technosphere: materials/fuels	**Amount**	**Unit**	
Nitrogen, liquid {RoW}| market for | Cut-off, U	0.29	g	
Potassium hydroxide {GLO}| market for | Cut-off, U	1.9	g	
Inputs from technosphere: electricity/heat	**Amount**	**Unit**	
Electricity, high voltage {GB}| electricity production, wind, 1-3MW turbine, offshore | Cut-off,	192.09	MJ	
Alkaline Electrolyser Cell Stack Construction	9.63E-08	p	
Outputs			
Emissions to air	**Amount**	**Unit**	
Emissions to water	**Amount**	**Unit**	
Outputs to technosphere: Waste treatment	**Amount**	**Unit**	

Table B-6: LCI of the process plant operation, with exergy allocation.

Products			
Outputs to technosphere: Products and co-products	**Amount**	**Unit**	**Allocation %**
Jet fuel production, from synthetic gas	1	kg	59.81%
Naphtha {Europe without Switzerland}| naphtha production, petroleum refinery operation | Cut-off, U	0.35	kg	21.09%
Diesel {Europe without Switzerland}| diesel production, petroleum refinery operation | Cut-off, U	0.32	kg	19.10%
Outputs to technosphere: Avoided products	**Amount**	**Unit**	
Inputs			
Inputs from nature	**Amount**	**Unit**	
Water, cooling, unspecified natural origin, GB	17.88	l	
Water, process and cooling, unspecified natural origin	2.10	l	
Inputs from technosphere: materials/fuels	**Amount**	**Unit**	
CO2 from DAC	5.27	kg	
H2 from electrolyser	1.35	kg	
Cobalt {GLO}| market for | Cut-off, U	2.03E-03	kg	
Zeolite, powder {GLO}| market for | Cut-off, U	3.52E-05	kg	
Nickel, 99.5% {GLO}| market for | Cut-off, U	6.45E-05	kg	
Chemical factory, organics {RER}| construction | Cut-off, U	3.11E-11	p	
Inputs from technosphere: electricity/heat	**Amount**	**Unit**	
Electricity, high voltage {GB}| electricity production, wind, 1-3MW turbine, offs	7.94	MJ	
Outputs			
Emissions to air	**Amount**	**Unit**	
Carbon dioxide, atmospheric	1.16E-01	kg	
Water/m3	3.29E-03	m3	
Oxygen	1.61E-15	kg	
Emissions to water	**Amount**	**Unit**	
Outputs to technosphere: Waste treatment	**Amount**	**Unit**	
Wastewater, from residence {RoW}| market for wastewater, from residence |	9.70E-03	m3	

Table B-7: LCI of the process plant operation, with energy allocation.

Products			
Outputs to technosphere: Products and co-products	**Amount**	**Unit**	**Allocation %**
Jet fuel production, from synthetic gas	1	kg	59.83%
Naphtha {Europe without Switzerland}| naphtha production, petroleum refinery operation | Cut-off, U	0.35	kg	21.05%
Diesel {Europe without Switzerland}| diesel production, petroleum refinery operation | Cut-off, U	0.32	kg	19.12%
Outputs to technosphere: Avoided products	**Amount**	**Unit**	
Inputs			
Inputs from nature	**Amount**	**Unit**	
Water, cooling, unspecified natural origin, GB	17.88	l	
Water, process and cooling, unspecified natural origin	2.10	l	
Inputs from technosphere: materials/fuels	**Amount**	**Unit**	
CO2 from DAC	5.27	kg	
H2 from electrolyser	1.35	kg	
Cobalt {GLO}| market for | Cut-off, U	2.03E-03	kg	
Zeolite, powder {GLO}| market for | Cut-off, U	3.52E-05	kg	
Nickel, 99.5% {GLO}| market for | Cut-off, U	6.45E-05	kg	
Chemical factory, organics {RER}| construction | Cut-off, U	3.11E-11	p	
Inputs from technosphere: electricity/heat	**Amount**	**Unit**	
Electricity, high voltage {GB}| electricity production, wind, 1-3MW turbine, offs	7.94	MJ	
Outputs			
Emissions to air	**Amount**	**Unit**	
Carbon dioxide, atmospheric	1.16E-01	kg	
Water/m3	3.29E-03	m3	
Oxygen	1.61E-15	kg	
Emissions to water	**Amount**	**Unit**	
Outputs to technosphere: Waste treatment	**Amount**	**Unit**	
Wastewater, from residence {RoW}| market for wastewater, from residence |	9.70E-03	m3	

B-4 Fischer-Tropsch product distribution

The product distribution at the outlet of the FT reactor, which is modelled by using the carbide mechanism, is presented in Figure B-1. As explained above, this model takes into account the main deviations from the Anderson-Schulz-Flory (ASF) model. This can be observed by three main effects on Figure B-1: 1) the amount of methane produced is much higher than the one predicted by ASF; 2) the amount of ethylene is less than the estimation by ASF, and 3) the model is able to predict the production of paraffin, as well as olefins. These results are validated against the results obtained by Marchese et al. [64], which are presented as rate of formation and validated against experimental values.

It is important to mention that the higher prediction of methane production has an impact in the process design, since it also means that the amount of gaseous streams that are recycled to the different sections of the process is larger, when compared to a process model that follows the ASF distribution. Concerning the olefins, their production is significant until the olefin C15.

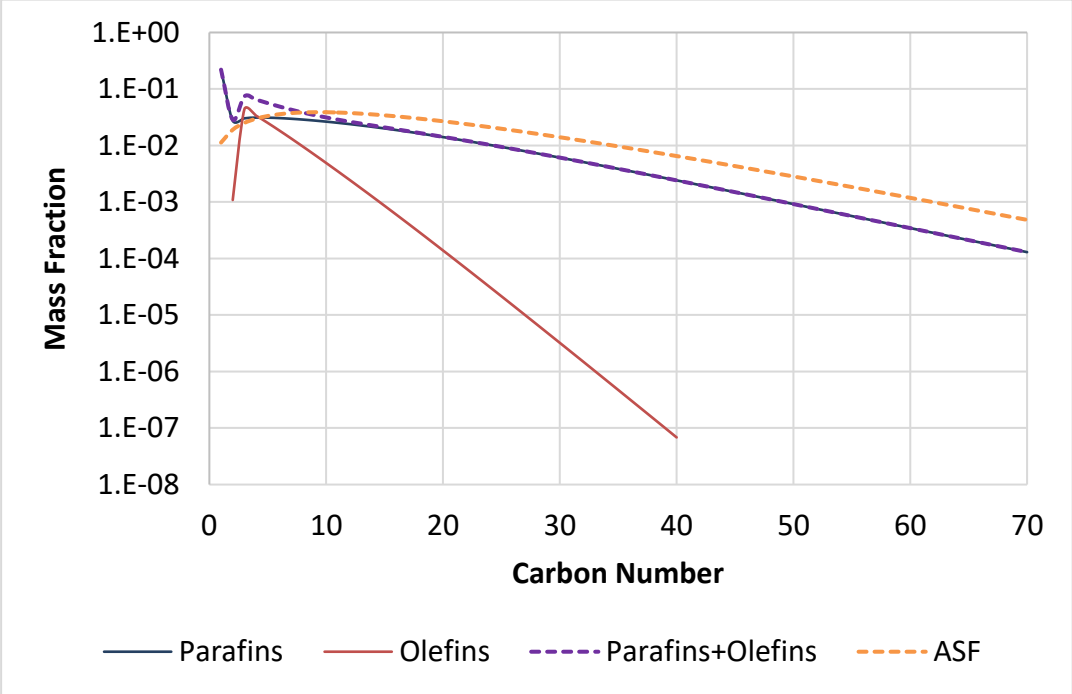

Figure B-1: Hydrocarbon distribution after the FT reactor and comparison with the ASF model.

B-5. DAC humidity influence on the CO_2 working capacity

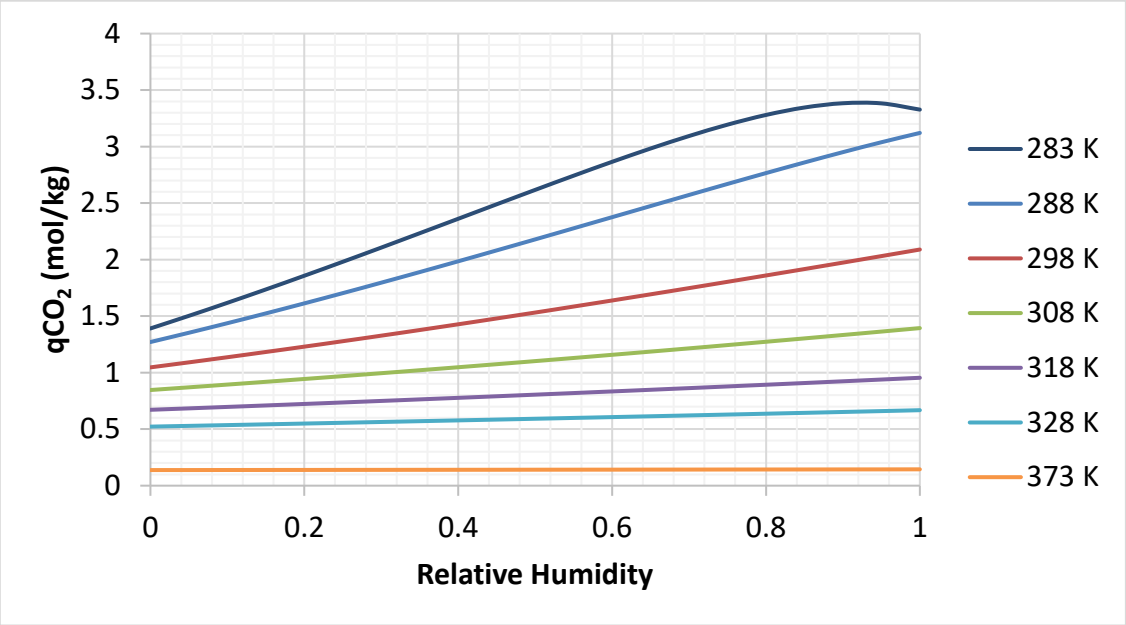

Figure B-2: CO_2 working capacities at different temperatures and relative humidity.

* Model is not very accurate at low temperature (283 K) and high relative humidity (>0.9); however, this is outside the operating conditions of the proposed system).

B-6. Heat integration

Figure B-3 represents the heat exchanger network designed for the refinery plant; the electrolyser and the DAC units have been included. The blue lines at the top represent external cooling utilities corresponding, i.e., from top to bottom, HP Steam Generation, LP Steam Generation, Cooling Water (electrolyser), Cooling water (process), and Refrigerant. The middle red and blue lines represent the process streams needing cooling and heating, respectively. Finally, the bottom red line represents LP steam as heating utility, which is internally generated. Therefore, it can be seen that a proper heat integration results in a system requiring only external cooling utilities.

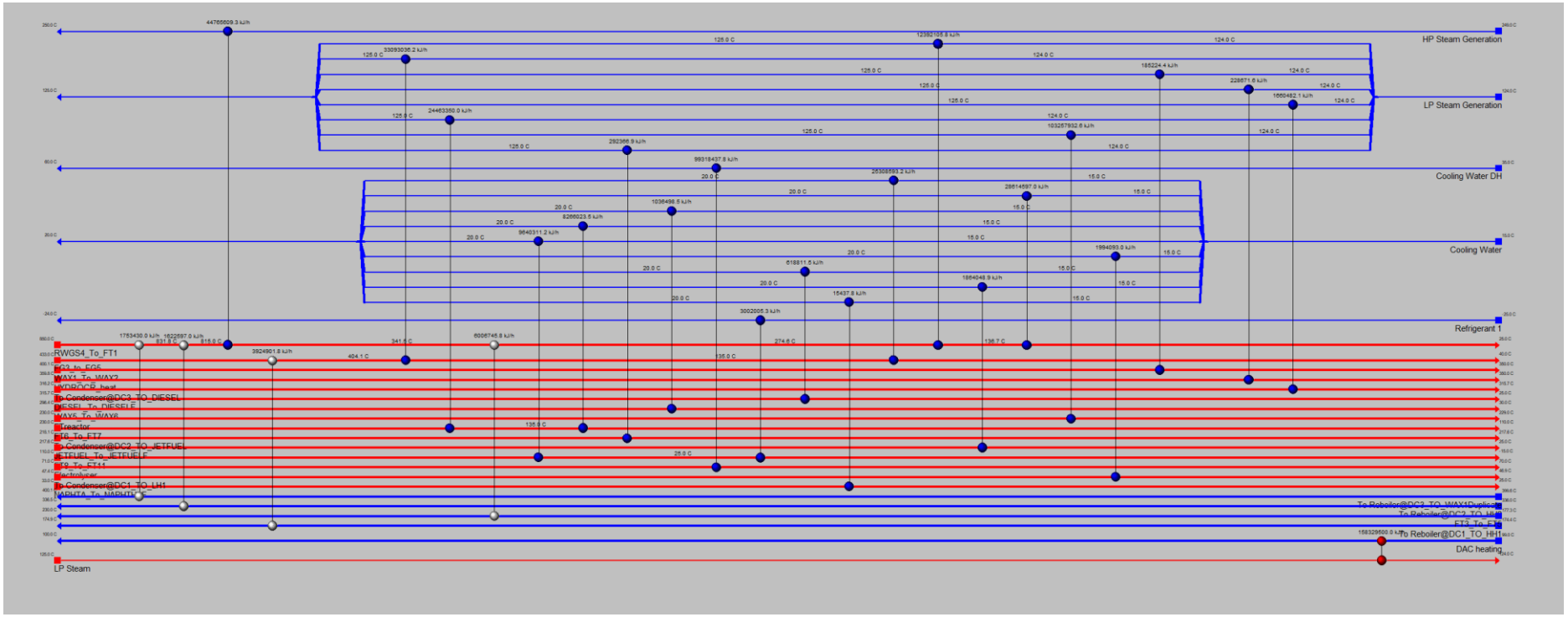

Figure B-3: Heating and cooling network of the PtL system.

B-7. Life Cycle assessment: Midpoint Environmental impacts

Table B-8: Midpoint Environmental Impacts

Impact category	Units	Allocation AA1
Global warming	kg CO_2 eq	2.14E-02
Stratospheric ozone depletion	kg CFC11 eq	1.17E-08
Ionizing radiation	kBq Co-60 eq	9.15E-04
Ozone formation, Human health	kg NOx eq	3.99E-04
Fine particulate matter formation	kg PM2.5 eq	1.25E-04
Ozone formation, Terrestrial ecosystems	kg NOx eq	4.02E-04
Terrestrial acidification	kg SO2 eq	3.33E-04
Freshwater eutrophication	kg P eq	1.23E-05
Marine eutrophication	kg N eq	2.51E-06
Terrestrial ecotoxicity	kg 1,4-DCB	4.83E-01
Freshwater ecotoxicity	kg 1,4-DCB	7.78E-03
Marine ecotoxicity	kg 1,4-DCB	9.84E-03
Human carcinogenic toxicity	kg 1,4-DCB	5.70E-03
Human non-carcinogenic toxicity	kg 1,4-DCB	9.63E-02
Land use	m2a crop eq	5.64E-04
Mineral resource scarcity	kg Cu eq	1.38E-03
Fossil resource scarcity	kg oil eq	5.93E-03
Water consumption	m^3	4.18E-04

B-8. Policy analysis: UK SAF Mandate

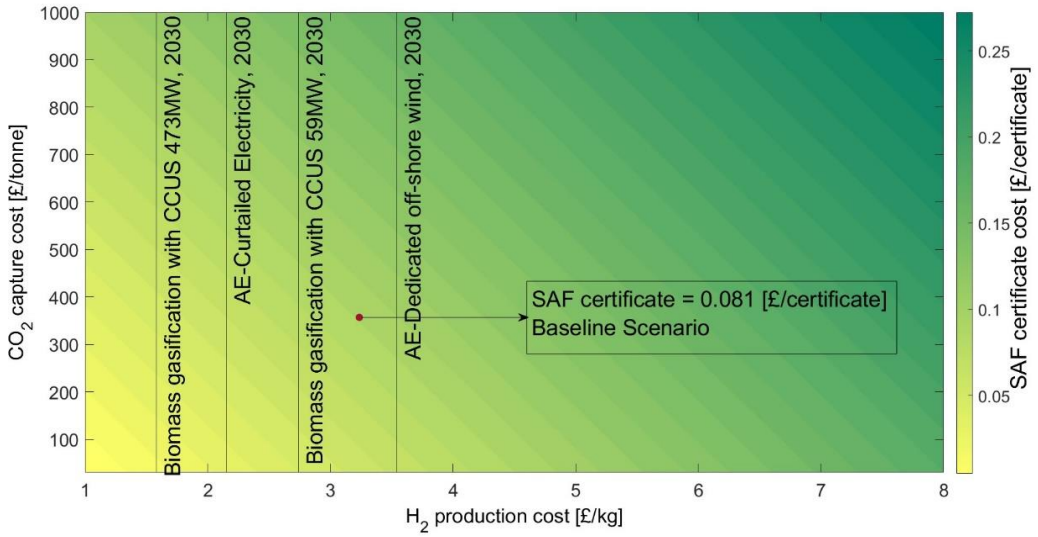

Figure B-4: The SAF certificate cost for the MJSP to break-even with fossil jet fuel cost (0.56£/kg) for different CO_2 capture and H_2 production costs. The upstream emissions for the wind farm electricity are neglected.

APPENDIX C

C-1. Life cycle inventories (LCI)

The following sections present the data for the LCI of some relevant subsystems of the proposed configurations:

Table C-1: LCI of forest residues chips transport.

Products		
Outputs to technosphere: Products and co-products	**Amount**	**Unit**
Wood chips, wet, measured as dry mass {UK}| market for | Cut-off, U	1.000	kg of dry biomass
Inputs		
Inputs from nature	**Amount**	**Unit**
Inputs from technosphere: materials/fuels	**Amount**	**Unit**
Transport, freight, lorry, unspecified {ZA}| market for transport, freight, lorry, unspecified | Cut-off, U	0.143*	tkm
Wood chips, wet, measured as dry mass {RoW}| hardwood forestry, oak, sustainable forest management | Cut-off, U	0.068	kg
Wood chips, wet, measured as dry mass {RoW}| softwood forestry, spruce, sustainable forest management | Cut-off, U	0.932	kg

*Value adjusted from original inventory to represent the transport of FR chips with 30% of water content for 100 km

Table C-2: LCI of alkaline electrolyser operation [308].

Products	0%TS	20%TS	40%TS	50%TS	60%TS	80%TS	100%TS	
Outputs to technosphere: Products and co-products				**Amount**				**Unit**
Hydrogen, gaseous produced from AE	1	1.00	1.00	1.00	1.00	1.00	1.00	kg
Heat, district or industrial, natural gas {Europe without Switzerland}| market for heat, district or industrial, natural gas | Cut-off, U	29254.58	29254.58	29254.58	29254.58	29254.58	29254.58	29254.58	kJ
Oxygen	2.16	1.47	0.45	0.00	0.00	0.00	0.00	kg
Outputs to technosphere: Avoided products				**Amount**				**Unit**
Inputs								
Inputs from nature				**Amount**				**Unit**
Inputs from technosphere: materials/fuels				**Amount**				**Unit**
Water, completely softened {RER}| market for water, completely softened | Cut-off, U	9.26	9.26	9.26	9.26	9.26	9.26	9.26	kg
Nitrogen, liquid {RoW}| market for | Cut-off, U	0.29	0.29	0.29	0.29	0.29	0.29	0.29	g
Potassium hydroxide {GLO}| market for | Cut-off, U	1.90	1.90	1.90	1.90	1.90	1.90	1.90	g
Inputs from technosphere: electricity/heat				**Amount**				**Unit**
Electricity, high voltage {GB}| electricity production, wind, 1-3MW turbine, offshore | Cut-off, U	192	193	194	195	196	197	198	MJ
Alkaline Electrolyser Cell Stack Construction	9.63E-08	9.63E-08	9.63E-08	9.63E-08	9.63E-08	9.63E-08	9.63E-08	p
Outputs								
Emissions to air				**Amount**				**Unit**
Emissions to water				**Amount**				**Unit**
Outputs to technosphere: Waste treatment				**Amount**				**Unit**

C-1.1 Refinery plant: This stage encompasses the gasification island (biomass pre-treatment, gasifier and syngas cleaning sections), the syngas conversion and syncrude upgrading plant (RWGS, FT, hydrogenation, hydrocracking, distillation columns, and isomerization sections), and the ASU. The main inputs to the refinery are electricity, hydrogen and oxygen coming from the electrolyser, forest residues chips, and some other external utilities, such as water and air. On the other hand, the outputs of this section are SAF, naphtha, diesel, and LP/MP/HP steam. Alongside, other materials are needed, such as catalyst, reposition of fluidising media for the gasifier, and make up water for the cooling and steam systems. As some of this data are not calculated in the process model, some rough assumptions/calculations were performed: 1) Catalyst are changed every 3 years, and in the LCI of the refinery, they are represented by their main constituent (in terms of functionality). 2) The amount of fluidising media to be replaced was taken from an existing gasifier LCI from Ecoinvent [235]. 3) The makeup water flows for the cooling water and steam systems were calculated as explained in a previous study by the authors [340], and they are considered as "inputs from nature". Furthermore, for the background data related to the chemical facility (construction, assembling, installation, disassembling, among others) the LCI was taken from Ecoinvent [352] and adjusted to the capacity of the analysed scenario as explained in a previous work by the authors [171]. Table C-3 presents the LCI for the refinery stage:

Table C-3: LCI of the process plant (as shown in Figure 1 of the main manuscript, except by the AE).

Products	0%TS	20%TS	40%TS	50%TS	60%TS	80%TS	100%TS	
Outputs to technosphere: Products and co-products				**Amount**				**Unit**
Jet fuel production, from synthetic gas	1	1	1	1	1	1	1.00	kg
Naphtha production from synthetic gas	0.498	0.489	0.500	0.506	0.505	0.517	0.523	kg
Diesel production from synthetic gas	0.295	0.296	0.296	0.296	0.296	0.296	0.296	kg
HP Steam	11.062	10.058	9.713	9.364	8.936	9.184	9.128	kg
MP Steam	25.999	25.689	25.649	25.593	25.478	25.271	24.626	kg
LP Steam	1.004	0.963	0.967	0.960	0.953	1.045	0.829	kg
Gaseous N2	0.000	0.000	0.000	0.108	0.498	1.301	2.165	kg
Liquid O2	0.000	0.000	0.000	0.020	0.091	0.239	0.398	kg
Liquid N2	0.000	0.000	0.000	0.011	0.051	0.133	0.221	kg
Liquid Ar	0.000	0.000	0.000	0.002	0.010	0.027	0.044	kg
Outputs to technosphere: Avoided products				**Amount**				**Unit**
Inputs								
Inputs from nature				**Amount**				**Unit**
Water, process and cooling, unspecified natural origin	28.674	27.406	26.567	26.410	26.602	26.130	27.262	l
Inputs from technosphere: materials/fuels				**Amount**				**Unit**
Wood chips, wet, measured as dry mass {UK}| market for | Cut-off, U	3.022	3.466	4.013	4.284	4.546	5.116	5.715	kg
H2 from electrolyser	0.811	0.713	0.619	0.572	0.524	0.427	0.328	kg
Silica sand {GLO}| market for | Cut-off, U	0.150	0.172	0.199	0.212	0.225	0.254	0.283	kg
Cobalt {GLO}| market for | Cut-off, U	1.94E-03	1.84E-03	1.84E-03	1.85E-03	1.84E-03	1.84E-03	1.85E-03	kg
Nickel, 99.5% {GLO}| market for | Cut-off, U	3.50E-05	3.59E-05	3.77E-05	3.86E-05	3.94E-05	4.12E-05	4.32E-05	kg
Zeolite, powder {GLO}| market for | Cut-off, U	9.17E-05	8.99E-05	5.44E-05	4.71E-05	9.49E-05	6.80E-05	7.30E-05	kg
Chemical factory, organics {RER}| construction | Cut-off, U	3.11E-11	3.11E-11	3.11E-11	3.11E-11	3.11E-11	3.11E-11	3.11E-11	p
Inputs from technosphere: electricity/heat				**Amount**				**Unit**

Electricity, high voltage {GB}| electricity production, wind, 1-3MW turbine, offshore | Cut-off, U	13.911	14.993	16.468	17.474	19.113	22.522	26.270	MJ
Outputs								
Emissions to air				**Amount**				**Unit**
Carbon dioxide, biogenic	0.0963	0	0	0	0	0	0	kg
Outputs to technosphere: Waste treatment							**Amount**	**Unit**
Inert waste, for final disposal {RoW}| market for inert waste, for final disposal | Cut-off, U	0.150	0.172	0.199	0.212	0.225	0.254	0.283	kg
Wastewater, from residence {RoW}| market for wastewater, from residence | Cut-off, U	8.20E-03	7.85E-03	7.60E-03	7.48E-03	7.35E-03	7.12E-03	6.91E-03	m3
Wood ash mixture, pure {Europe without Switzerland}| market for wood ash mixture, pure | Cut-off, U	0.0166	0.0191	0.0221	0.0236	0.0250	0.0281	0.0314	kg
CO_2	0.000	0.949	1.909	2.396	2.884	3.906	4.998	kg

Table C-4: LCI of the CO_2 compression, transport and storage.

ZProducts	0%TS	20%TS	40%TS	50%TS	60%TS	80%TS	100%TS	
Outputs to technosphere: Products and co-products				Amount				Unit
Storage, CO2, aquifer, 100 km pipeline	0	1	1	1	1	1	1	kg
Inputs								
Inputs from nature				Amount				Unit
Inputs from technosphere: materials/fuels				Amount				Unit
Well, double aquifer	0	2.54E-11	2.54E-11	2.54E-11	2.54E-11	2.54E-11	2.54E-11	p
Transport, pipeline, supercritical CO2, w/o recompression	0	0.2	0.2	0.2	0.2	0.2	0.2	tkm
Air compressor, screw-type compressor, 300kW {RER}| production | Cut-off, U	0.00E+00	1.14E-09	6.57E-10	5.59E-10	4.93E-10	4.09E-10	3.57E-10	p
Inputs from technosphere: electricity/heat				Amount				Unit
Electricity, high voltage {GB}| electricity production, wind, 1-3MW turbine, offshore | Cut-off, U	0.00E+00	1.09E-01	1.09E-01	1.09E-01	1.09E-01	1.09E-01	1.09E-01	kWh
Outputs								
Emissions to air				Amount				Unit
Carbon dioxide, fossil	0	-1	-1	-1	-1	-1	-1	kg
Emissions to water				Amount				Unit
Outputs to technosphere: Waste treatment				Amount				Unit

C-2. Heat integration results: Composite curves of the intermediate scenarios

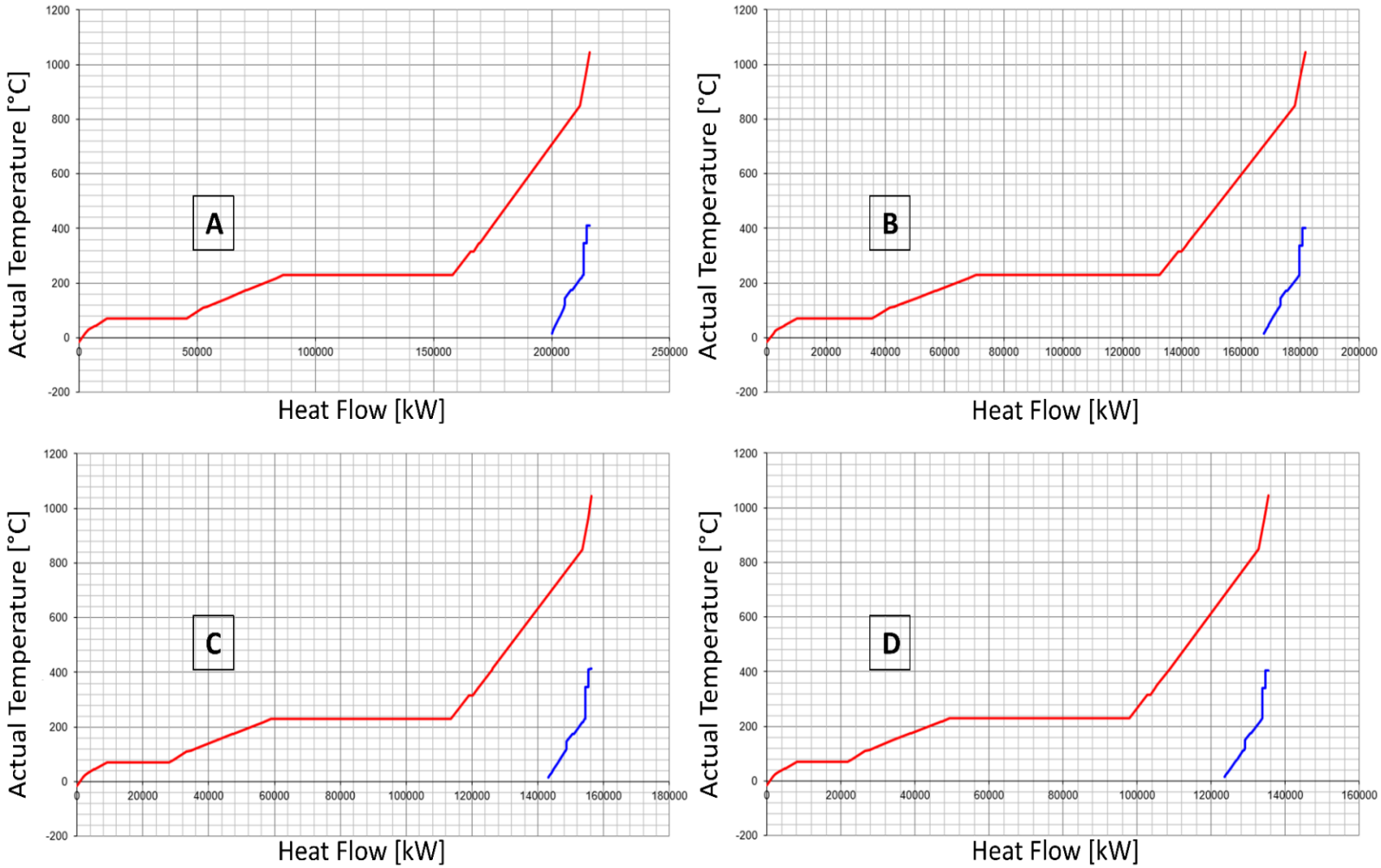

Figure C-1: Composite curves of the A) 20%TS scenario, B) 40%TS scenario, C) 60%TS scenario, and D) 80%TS scenario.

C-3. Power curves of the proposed scenarios

Table C-5: Wind farm size and output of electricity.

Scenario	0%TS	20%TS	40%TS	50%TS	60%TS	80%TS	100%TS
Number of turbines	164	127	98	86	77	59	46
Average hourly power generation [MW]	314.46	246.23	187.53	165.59	147.30	114.36	88.53
Total annual power from wind farm to the system [MWh]	1,438,265.82	1,128,210.58	861,705.47	761,039.48	673,811.68	525,179.56	402,023.95
Total annual Power from the grid [MWh]	1,057,565.28	821,489.23	638,517.91	560,143.16	496,910.46	383,517.95	292,061.32
Total annual Power to the grid [MWh]	1,316,434.92	1,028,768.42	781,078.84	689,514.93	616,579.18	476,603.18	373,523.77

C-4. Sensitivity analysis on the MJSP

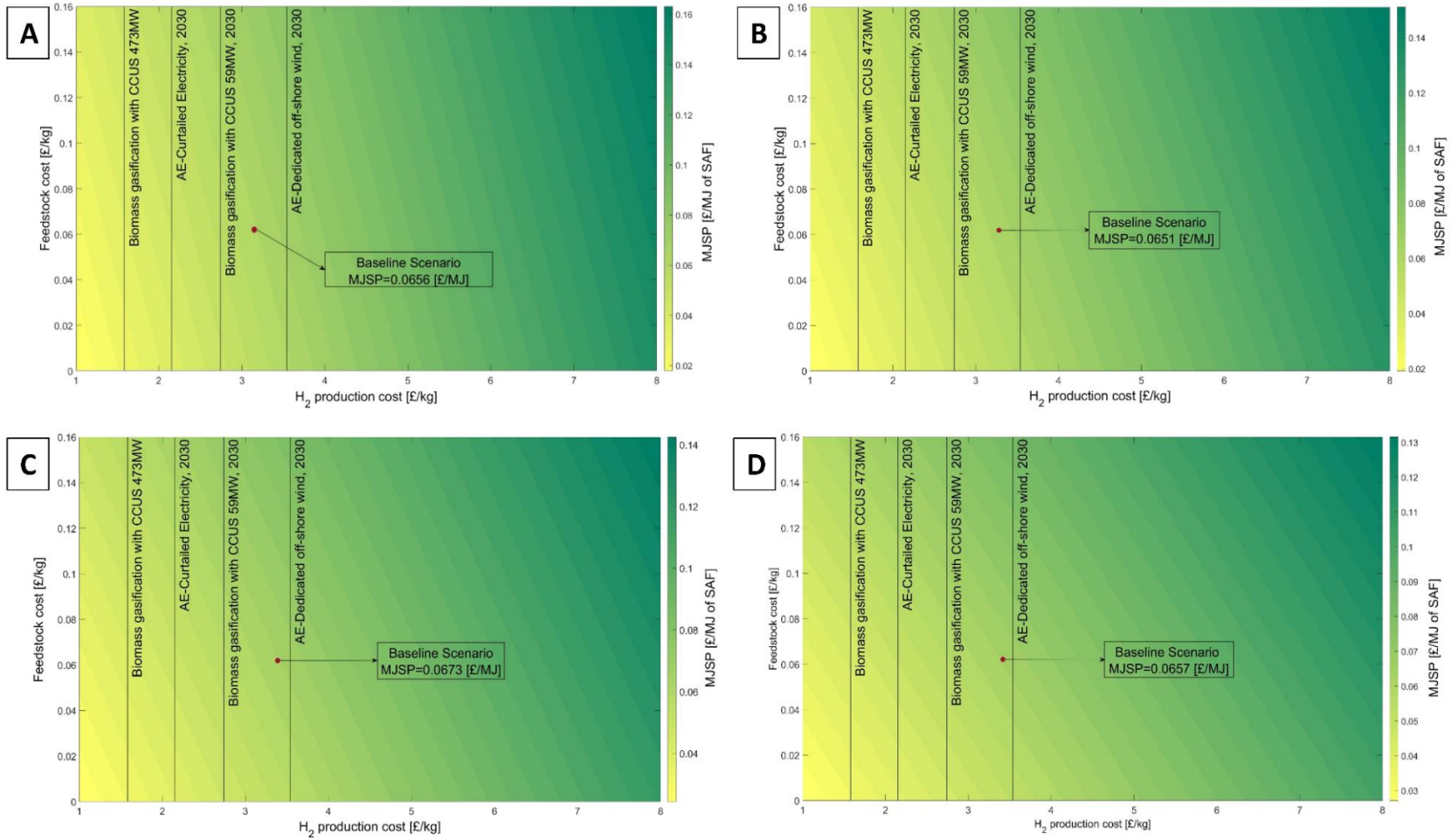

Figure C-2: Sensitivity of the MJSP of the SAF produced at various feedstock cost and H_2 production cost for: A) 20%TS scenario, B) 40%TS scenario, C) 60%TS scenario, and D) 80%TS scenario.

C-5. Life Cycle assessment: Midpoint Environmental impacts

Impact category	Units	0%TS	20%TS	40%TS	50%TS	60%TS	80%TS	100%TS
Global warming	kg CO_2 eq	1.39E-02	-8.84E-03	-3.18E-02	-4.35E-02	-5.51E-02	-7.94E-02	-1.05E-01
Stratospheric ozone depletion	kg CFC11 eq	8.24E-09	7.93E-09	7.64E-09	7.51E-09	7.41E-09	7.18E-09	6.99E-09
Ionizing radiation	kBq Co-60 eq	5.92E-04	5.60E-04	5.29E-04	5.14E-04	5.01E-04	4.74E-04	4.48E-04
Ozone formation, Human health	kg NOx eq	3.84E-04	3.84E-04	3.83E-04	3.83E-04	3.83E-04	3.83E-04	3.83E-04
Fine particulate matter formation	kg PM2.5 eq	9.37E-05	9.01E-05	8.65E-05	8.48E-05	8.32E-05	7.99E-05	7.67E-05
Ozone formation, Terrestrial ecosystems	kg NOx eq	3.87E-04	3.86E-04	3.86E-04	3.86E-04	3.86E-04	3.86E-04	3.86E-04
Terrestrial acidification	kg SO2 eq	2.56E-04	2.47E-04	2.37E-04	2.33E-04	2.29E-04	2.20E-04	2.11E-04
Freshwater eutrophication	kg P eq	7.31E-06	6.80E-06	6.29E-06	6.04E-06	5.83E-06	5.38E-06	4.95E-06
Marine eutrophication	kg N eq	1.62E-06	1.52E-06	1.42E-06	1.37E-06	1.33E-06	1.24E-06	1.15E-06
Terrestrial ecotoxicity	kg 1,4-DCB	3.35E-01	3.18E-01	3.01E-01	2.93E-01	2.86E-01	2.70E-01	2.56E-01
Freshwater ecotoxicity	kg 1,4-DCB	4.33E-03	3.95E-03	3.56E-03	3.37E-03	3.21E-03	2.85E-03	2.51E-03
Marine ecotoxicity	kg 1,4-DCB	5.52E-03	5.05E-03	4.56E-03	4.32E-03	4.11E-03	3.68E-03	3.25E-03
Human carcinogenic toxicity	kg 1,4-DCB	3.16E-03	2.90E-03	2.62E-03	2.49E-03	2.37E-03	2.13E-03	1.90E-03
Human non-carcinogenic toxicity	kg 1,4-DCB	6.74E-02	6.45E-02	6.16E-02	6.03E-02	5.92E-02	5.68E-02	5.45E-02
Land use	m2a crop eq	4.06E-02	4.67E-02	5.37E-02	5.71E-02	6.06E-02	6.77E-02	7.53E-02
Mineral resource scarcity	kg Cu eq	8.76E-04	8.10E-04	7.51E-04	7.25E-04	7.01E-04	6.49E-04	6.00E-04
Fossil resource scarcity	kg oil eq	3.82E-03	3.70E-03	3.59E-03	3.54E-03	3.51E-03	3.43E-03	3.37E-03
Water consumption	m^3	5.19E-04	4.86E-04	4.53E-04	4.40E-04	4.34E-04	4.07E-04	4.01E-04

C-6. Sensitivity analysis of the GWP

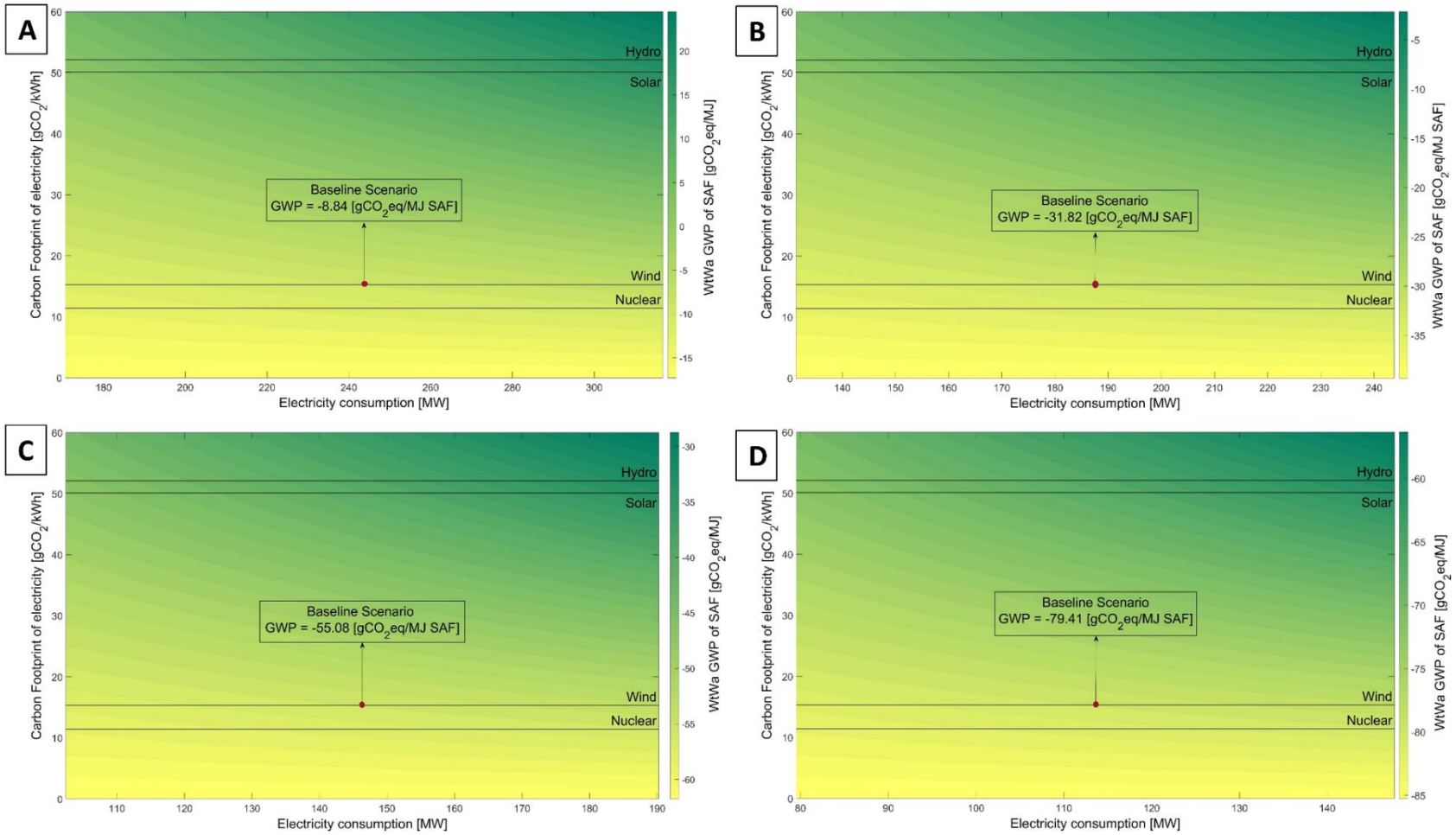

Figure C-3: The GWP of the WtWa life cycle of SAF for different electricity sources and different electricity consumption for the: A) 20%TS scenario, B) 40%TS scenario, C) 60%TS scenario, and D) 80%TS scenario.

C-7. Policy analysis: SAF mandate

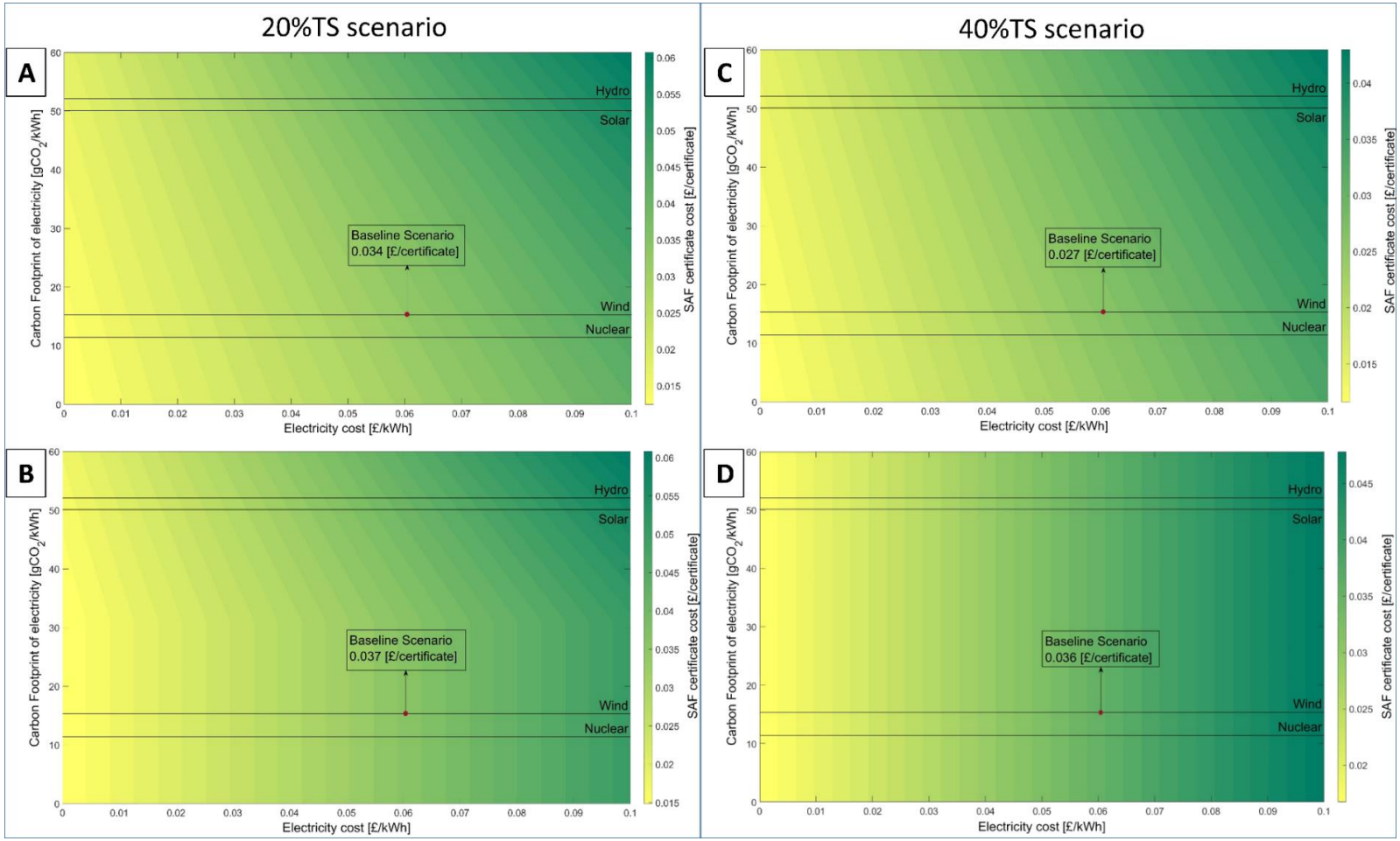

Figure C-4: The SAF certificate cost for the MJSP to break-even with fossil jet fuel gate price (0.56£/kg) for different electricity costs and electricity carbon footprint, for the: A) 20%TS scenario, acknowledging the negative GWP; B) 20%TS scenario, without acknowledging the negative GWP; C) 40%TS scenario, acknowledging the negative GWP; and D) 40%TS scenario, without acknowledging the negative GWP.

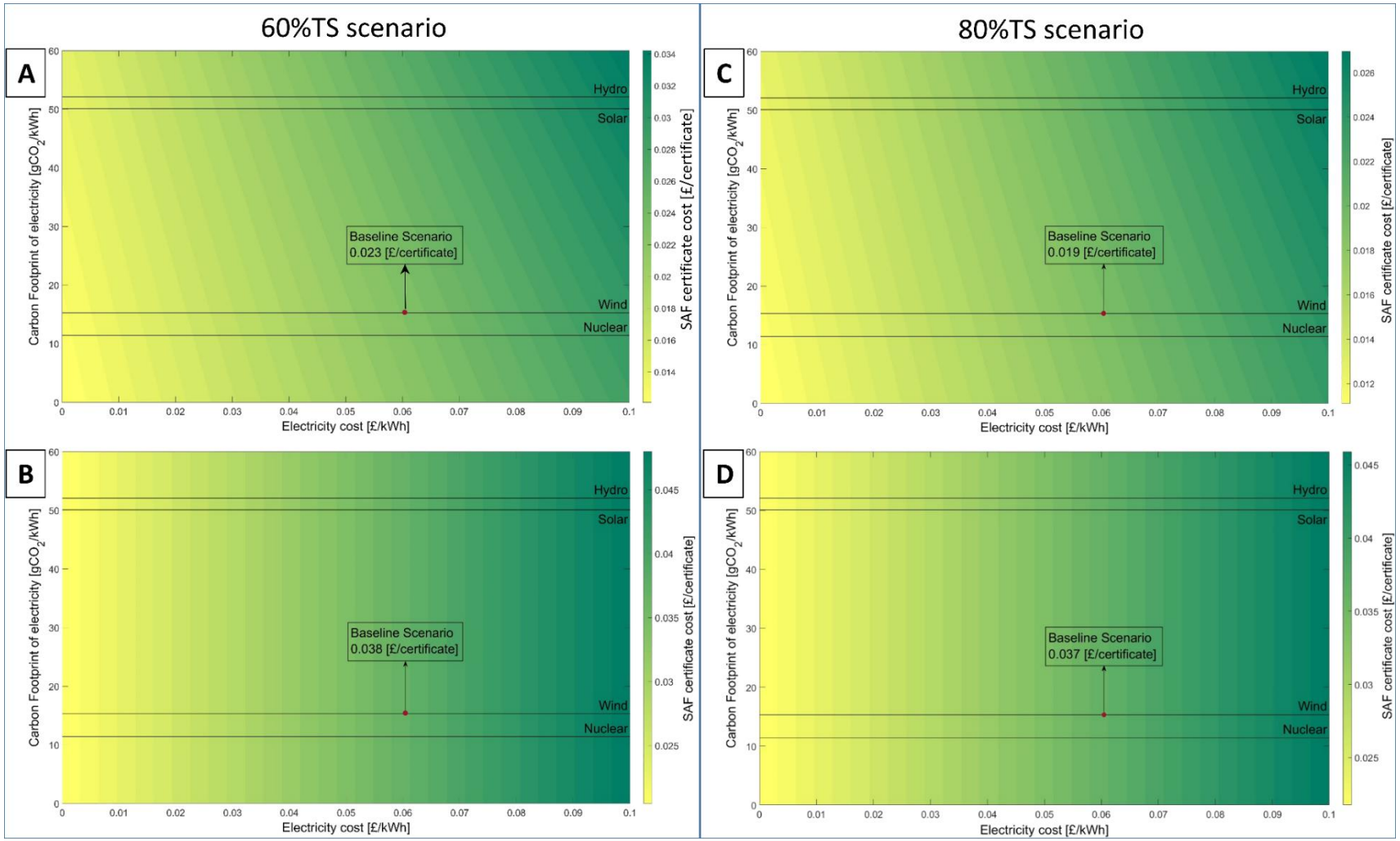

Figure C-5: The SAF certificate cost for the MJSP to break-even with fossil jet fuel gate price (0.56£/kg) for different electricity costs and electricity carbon footprint, for the: A) 60%TS scenario, acknowledging the negative GWP; B) 60%TS scenario, without acknowledging the negative GWP; C) 80%TS scenario, acknowledging the negative GWP; and D) 80%TS scenario, without acknowledging the negative GWP.